APPENDIX A. TUTORIAL ON USING AMPLITUDE PROBABILITY DISTRIBUTIONS TO CHARACTERIZE THE INTERFERENCE OF ULTRAWIDEBAND TRANSMITTERS TO NARROWBAND RECEIVERS

Robert J. Achatz[1]

A.1 Introduction

The *amplitude probability distribution function* (APD) is used in radio engineering to describe signal amplitude *statistics*. The APD and its corresponding graph, shown in Figure A.1, succinctly express the probability that a signal amplitude exceeds a threshold. For example, the APD in Figure A.1 shows that the signal amplitude rarely exceeds high voltages. Statistics such as percentiles, deciles, and the median can be read directly from the APD. Other statistics such as average power can be computed with the APD.

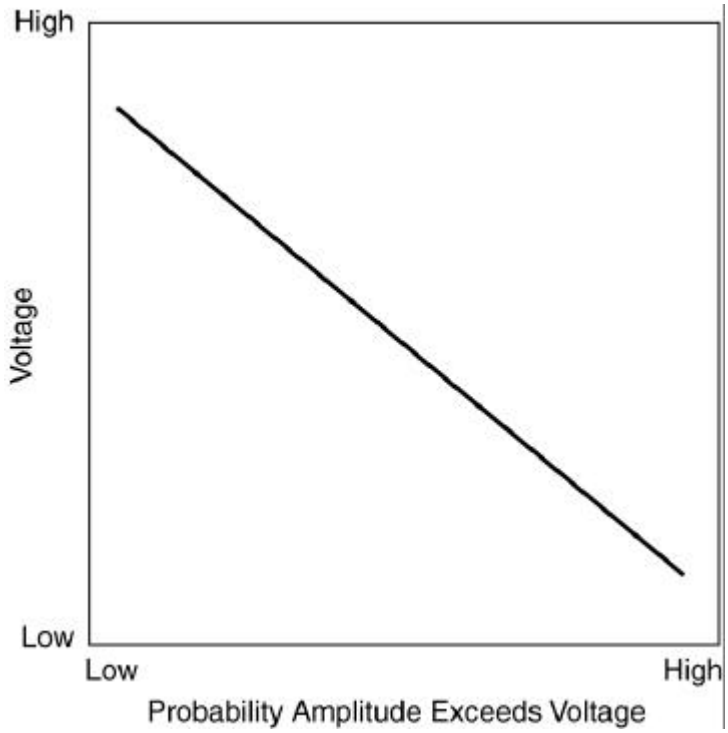

Figure A.1. Amplitude probability distribution.

The "signal" the APD characterizes is often noise or interference. For example, APDs are commonly used to characterize the amplitude statistics of *non-Gaussian* noise produced by

[1]The author is with the Institute for Telecommunication Sciences, National Telecommunications and Information Administration, U.S. Department of Commerce, Boulder, CO 80305.

lightning or unintentional emissions from man-made electrical or electronic devices. Numerous studies have shown that average noise power alone cannot predict the performance of receivers operating in non-Gaussian noise. APD statistics are needed for accurate predictions.

Today, many radio engineers are unfamiliar with the APD and its applications. This is because most modern receivers are designed to operate in bands with (zero-mean) *Gaussian* noise which is completely characterized by the average noise power statistic alone. Consequently, APD statistics are not needed for more accurate predictions.

Recently, federal spectrum regulators have been asked to allow emissions from *ultrawideband* (UWB) transmitters to overlay bands licensed to services that use *narrowband* receivers. Critics have charged that UWB transmitters may cause interference to 'victim' narrowband receivers. The amplitude statistics of this potential interference are dependent upon the specifications of the UWB signal and the band limiting filter in the narrowband receiver. The APD can be used to characterize this interference and correlate UWB signal and band limiting filter specifications to narrowband receiver performance.

The purpose of this tutorial is to introduce basic APD concepts to radio engineers and spectrum regulators who have not previously used the APD. It is hoped that these concepts will provide a firm basis for discussions on regulation of UWB transmitters. Emphasis is placed on understanding features likely to be found in band limited UWB signal APDs. These features are demonstrated with "tutorial" APDs of Gaussian noise, sinusoid (continuous wave) signals, and periodically pulsed sinusoid signals. Although the audience is intended to be broad, a limited number of mathematic expressions are used to avoid the ambiguity found in everyday language.

A.2 Signal Amplitude Characterization

A.2.1 APD Fundamentals

A *bandpass signal* is a signal whose bandwidth is much less than the *center frequency*. Bandpass signals are expressed mathematically as

$$s(t) = A(t)\cos(2\pi f_c + \phi(t)) ,$$

where A(t) is the baseband amplitude, $\phi(t)$ is the baseband phase, and f_c is the center frequency. The amplitude and phase define the *complex baseband signal*, $A(t)e^{j\phi(t)}$, whose spectrum is centered about 0 Hz.

The amplitude is always positive and is considered to be a *random variable*, A, when characterized by an APD. Formally, a new random variable, $\underline{A}_n$, is present at each sampling instant. The set $\{A_1, A_2, \ldots A_N\}$ is called the *random sample* of the random variable A if each

random variable is independent and identically distributed. Realizations or values of the random sample are denoted by the set $\{a_1, a_2, \ldots a_N\}$.

Associated with every random variable is a *probability density function* (PDF). The discrete PDF expresses the *probability* that a random variable "*A*" will have a realization equal to "a_i":

$$p(a_i) = P(A=a_i) ,$$

where *P*() is the probability of its argument. PDF values are positive and the area under a PDF is equal to 1.0.

The *cumulative distribution function* CDF expresses the probability that a random variable "*A*" will have a realization less than or equal to "*a*":

$$c(a) = P(A \# a) .$$

The discrete CDF is obtained by integrating the discrete PDF

$$c(a) = \sum_i p(a_i) ,$$

for all a_i less than or equal to *a*. CDF values range from 0.0 to 1.0.

Radio engineers are generally more concerned about how often a noise or interference amplitude exceeds a threshold. Thus they often prefer to use the complement of the CDF (CCDF) or APD. The APD function expresses the probability that a random variable "*A*" will have a realization greater than "*a*":

$$cc(a) = P(A>a) .$$

The discrete APD is obtained by subtracting the discrete CDF from 1.0.

$$cc(a) = 1.0\text{-}c(a) .$$

For clarification, Figure A.2 shows graphs of the discrete PDF, CDF, and APD for the random sample realizations:

$$\{a_1, a_2, \ldots a_{10}\} = \{1,2,3,3,1,4,4,3,4,3\} \text{ volts.}$$

The discrete PDF is estimated from the histogram. By convention, the axes of the APD are oriented differently from the axes of the CDF and PDF.

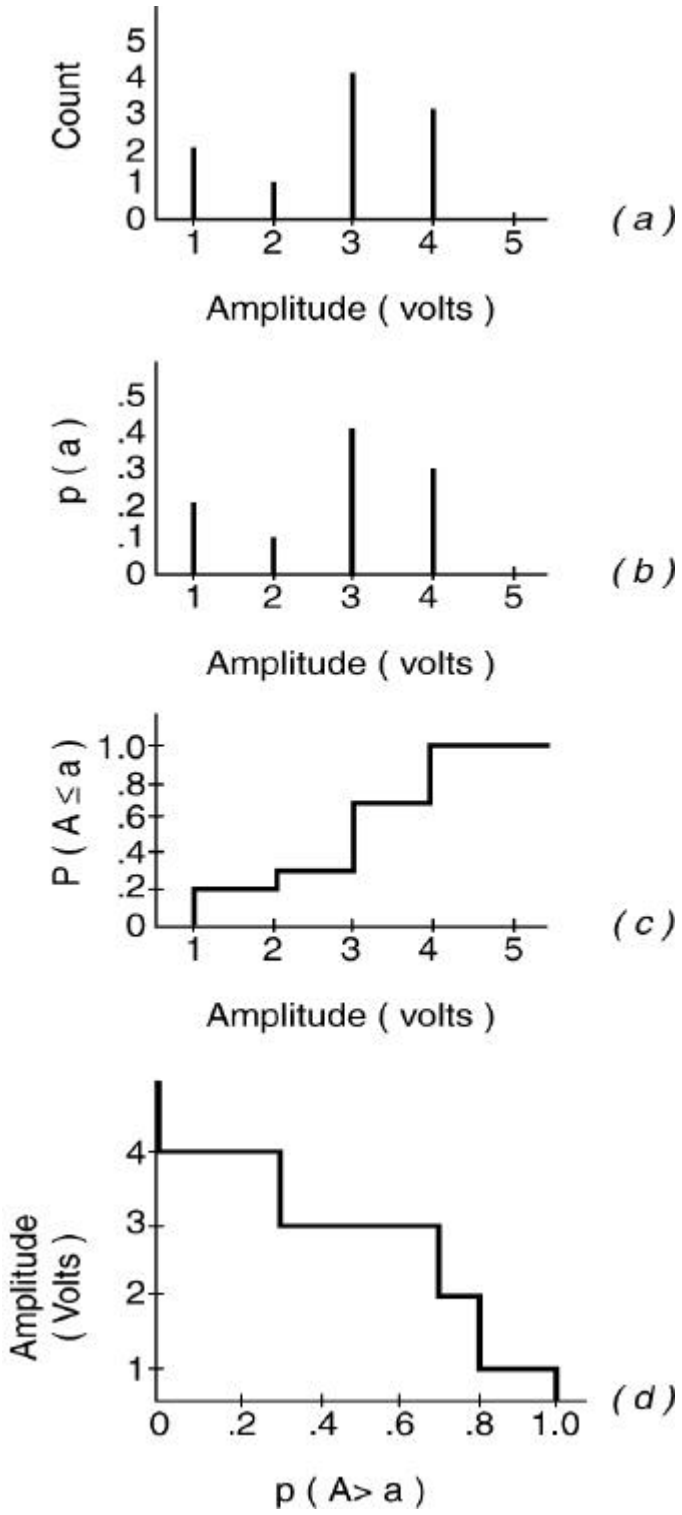

Figure A.2. Example histogram (a), probability density function (b), cumulative distribution function (c), and amplitude probability distribution function (d).

A.2.2 Statistic fundamentals

Statistics are functions that operate on the random sample. The *statistic value* is the result of a statistic operating on *random sample values*. Figure A.3 illustrates these relationships. Common statistical functions are percentile, mean or average, and root mean square (RMS). *First-order* statistics, addressed in this tutorial, assume the random variables are independent and identically distributed. *Second-order* statistics, not addressed in this tutorial, measure the correlation between these random variables. *Stationary* statistics are independent of time whereas *non-stationary* statistics are functions of time. Noise and interference amplitude statistics are non-stationary in many cases. Thus radio engineers sometimes measure the statistics of the amplitude statistics such as the median average noise power.

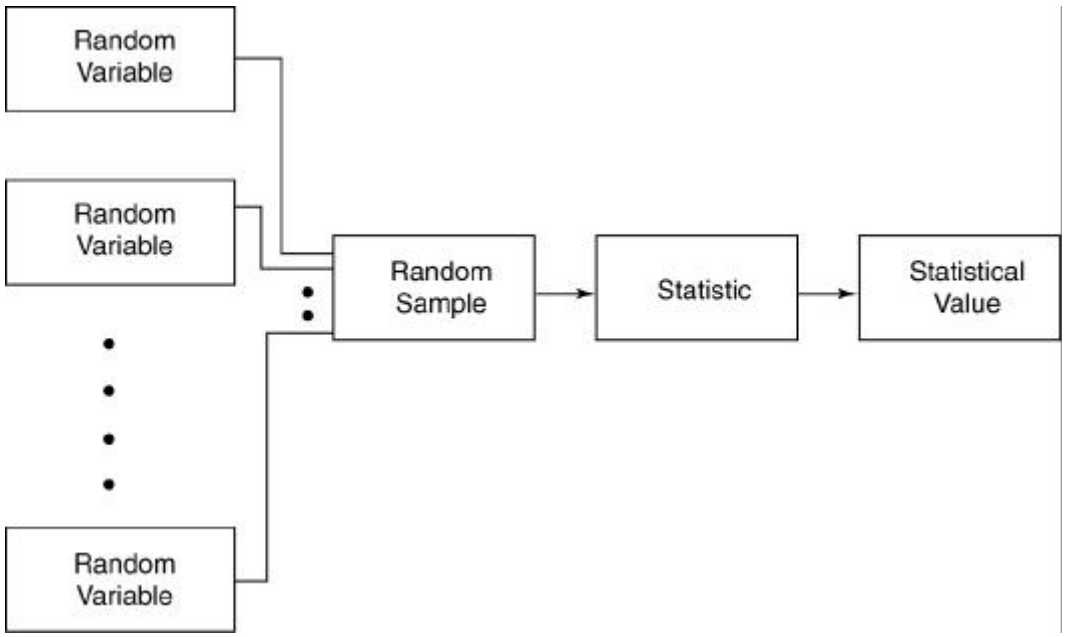

Figure A.3. Language of statistics.

Percentile amplitude statistics can be read directly from the APD. Peak and median amplitude statistics are the most widely used percentile statistics. The peak statistic is sometimes arbitrarily defined by the amplitude that is exceeded 0.0001% of the time:

$$V_p = cc^{-1}(0.000001) ,$$

where $a = cc^{-1}(P(A>a))$. The median statistic is defined by the amplitude that is exceeded 50% of the time:

$$V_{median} = cc^{-1}(0.5) .$$

The mean and RMS statistics are determined directly from the random sample values. The mean statistic is defined by:

$$V_{mean} = \frac{1}{N}\sum_{n} a_n \ ,$$

where N is the number of samples. The mean-logarithm statistic is defined by:

$$V_{mean-\log} = \frac{1}{N}\sum_{n} \log_{10}(a_n) \ ,$$

and the RMS statistic is defined by:

$$V_{RMS} = \sqrt{\frac{1}{N}\sum_{n} a_n{}^2} \ .$$

The discrete APD and its corresponding discrete PDF can be used to calculate the mean and RMS statistics if the random sample values are no longer available. The choice of histogram bin size may affect the accuracy of these statistics. In this case the mean statistic is defined by:

$$V_{mean} = \sum_{i} a_i \, p(a_i) \ ,$$

where a_i represents a discrete PDF value. The mean logarithm statistic is defined by:

$$V_{mean-\log} = \sum_{i} \log_{10}(a_i) p(a_i) \ ,$$

and the RMS statistic is defined by:

$$V_{RMS} = \sqrt{\sum_{i} a_i{}^2 \, p(a_i)} \ .$$

As a reference, statistical values for the tutorial PDF presented in section 2.1 are 4.0, 3.0, 2.8, 0.4, and 3.0 for the peak, median, mean, mean logarithm, and RMS statistics.

A.2.3 Graphing the APD

The APD of Gaussian noise is of particular interest to radio engineers because it is encountered in many practical applications. The amplitude of Gaussian noise is *Rayleigh distributed.* A Rayleigh distributed random variable is represented by a straight, negatively-sloped line on a *Rayleigh graph*. Figure A.4 shows the APDs of Gaussian and non-Gaussian noise on a Rayleigh graph.

The Rayleigh graph displays probability on the x-axis and amplitude on the y-axis. The probability is scaled by the function

$$x = 0.5\log_{10}(-\ln(P(A>a))) \ ,$$

and converted to percent to represent the "*percent (of samples or time) exceeding ordinate.*" The amplitude in volts is converted to units of power such as dBW, i.e. scaled by the function

$$y = 20log_{10}(A) ,$$

or alternatively it is displayed in dB relative to a standard noise power density or noise power.

Figure A.4 shows the statistics of Gaussian noise on a Rayleigh graph. Gaussian noise average power or RMS voltage corresponds to the power or voltage that is exceeded 37% of the time. Gaussian noise peak voltage is approximately 10 dB above RMS voltage. Gaussian noise average voltage, median voltage, and average-logarithm voltage are approximately 1dB, 2 dB, and 2.5 dB below RMS voltage respectively.

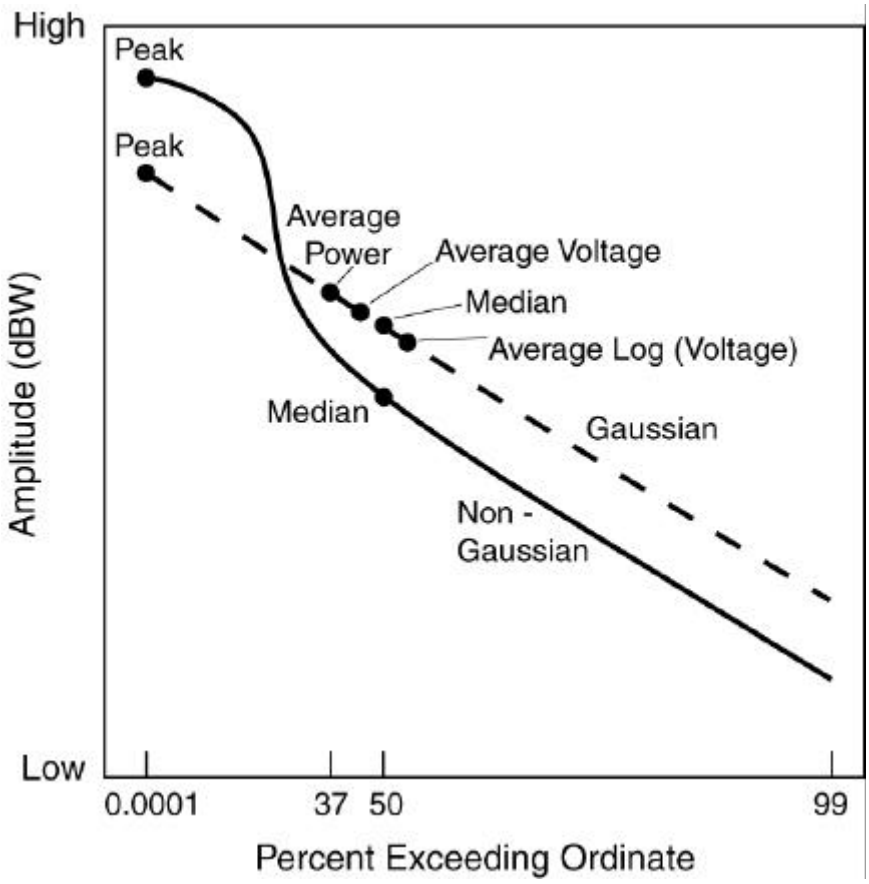

Figure A.4. Gaussian noise and non-Gaussian noise APDs plotted on a Rayleigh graph.

A.3 Tutorial APDs

A.3.1 Random Noise

Band limited random noise, i.e. the random noise present after a band limiting filter, is a random-amplitude and random-phase bandpass "signal" defined by

$$n(t) = A(t)\cos(2\pi f_c + \phi(t)) \ .$$

Band limited random noise is represented in the frequency domain by a *power spectral density* (PSD) in units of watts/Hz. The random noise "signal," amplitude, and PSD are shown in Figure A.5.

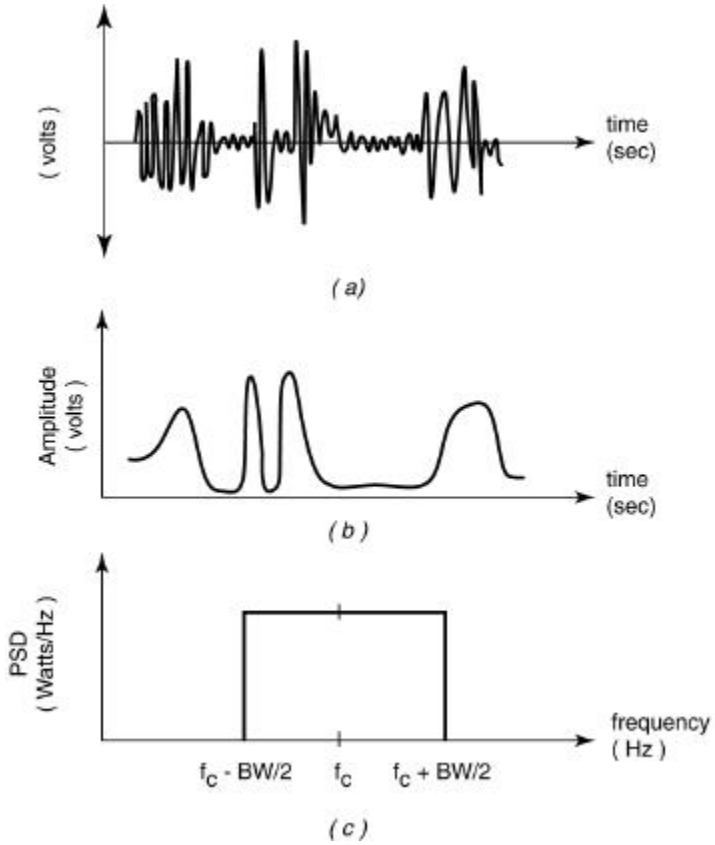

Figure A.5. Random noise (a), amplitude (b), and power spectral density (c).

Band limited noise average power is computed from the noise PSD

$$P = \int_{f_c - BW/2}^{f_c + BW/2} N(f)\,df \quad ,$$

where N(f) is the noise PSD in units of watts/Hz. Band limited *white* noise power density is constant over the band limiting filter bandwidth. As a result, the average noise power is directly proportional to the filter bandwidth and the RMS amplitude is directly proportional to the square root of bandwidth. This is sometimes referred to as the "$10\log_{10}$ bandwidth" rule. The amplitude of band limited Gaussian noise is Rayleigh distributed. Figure A.6 shows the APD of band limited white-Gaussian noise (WGN) for two different bandwidths on a Rayleigh graph.

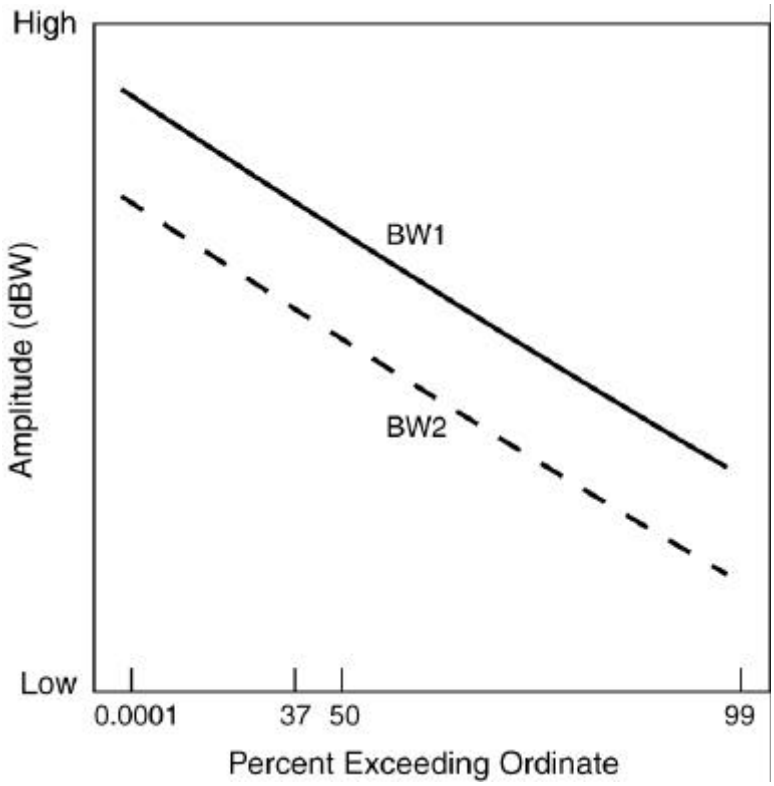

Figure A.6. Bandlimited Gaussian noise APDs with two different bandwidths. BW1 is greater than BW2.

A.3.2 Sinusoid Signal

The sinusoid (continuous wave) signal is a narrowband, constant amplitude and constant phase signal. It is defined by

$$s(t) = A\cos(2\pi f_c + \phi) .$$

The signal, signal amplitude, and amplitude spectrum are shown in Figure A.7. The APD of the sinusoid signal is a flat line from the lowest to the highest percentile on a Rayleigh graph. Changing the receiver center frequency can change the amplitude of the sinusoid signal.

Widening the bandwidth of a receiver filter in the presence of noise causes the statistics to be *Rician*. Rician statistics are dependent on the ratio of the sinusoid power to the noise power. The Rician APD corresponds to the sinusoid signal APD when noise is absent and the Rayleigh APD when the signal is absent. Sinusoid, Rician, and Rayleigh APDs are depicted in Figure A.8.

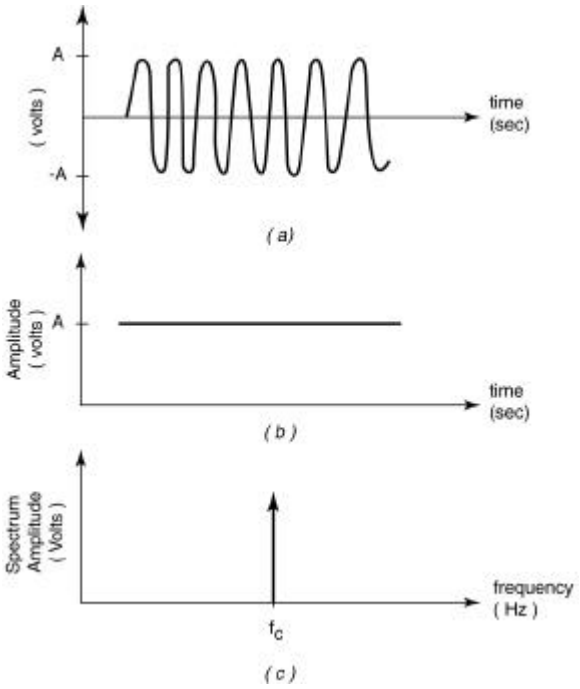

Figure A.7. Sinusoid signal (a), signal amplitude (b), and amplitude of the signal spectrum (c).

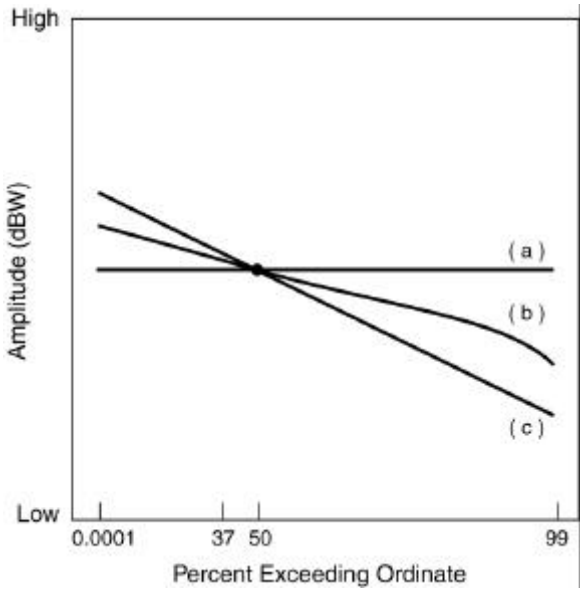

Figure A.8. Sinusoid signal APD without (a) and with (b) random noise. Sinusoid signal with random noise has Rician amplitude statistics. The Gaussian noise APD (c) is included for reference.

A.3.3 Periodically Pulsed Sinusoid

The periodically pulsed sinusoid is a deterministic, time-varying amplitude and constant phase signal defined by

$$s(t) = A(t)\cos(2\pi f_c + \theta) .$$

The amplitude varies between 'on' and 'off' pulse states. The 'on' duration is the *pulse width* (PW) and the repetition rate of pulses is the *pulse repetition rate* (PRR) or the pulse repetition frequency (PRF). Amplitude spectrum *lines* are spaced at the PRR. Amplitude spectrum *nulls* are spaced by the reciprocal of the PW. The signal, signal amplitude, and amplitude of the signal spectrum are shown in Figure A.9.

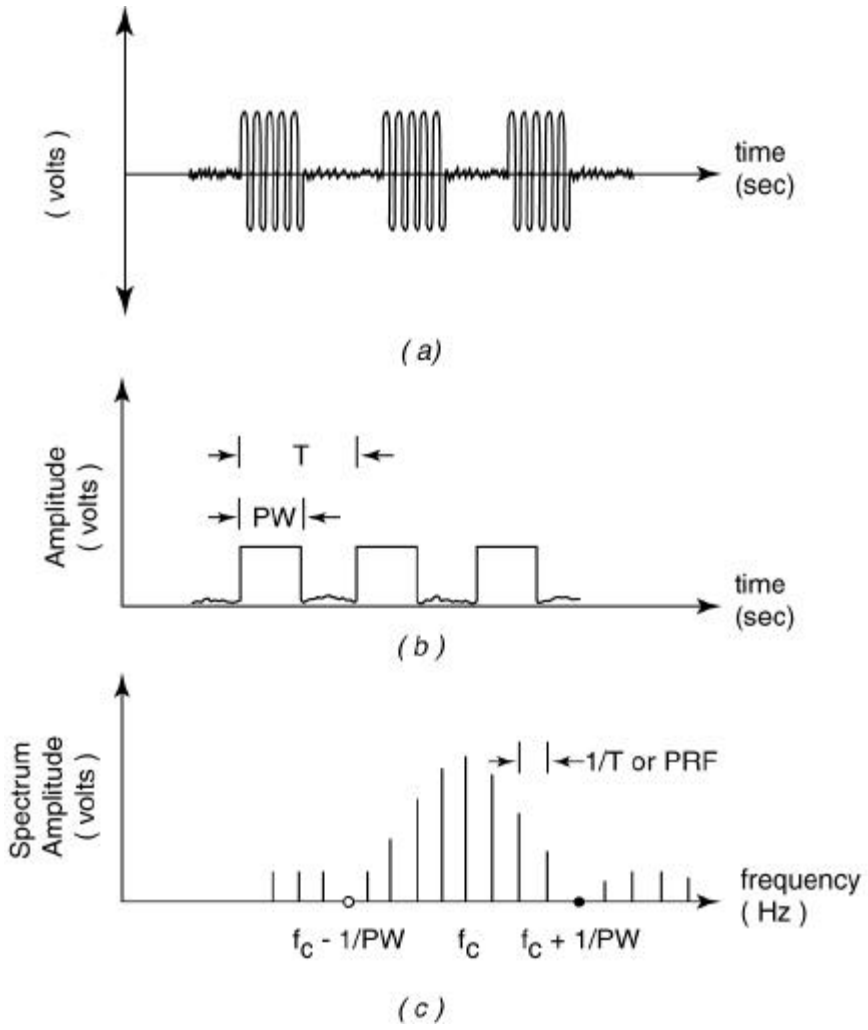

Figure A.9. Periodically pulsed sinusoid signal (a), signal amplitude (b), and amplitude of signal spectrum (c).

The APD of a periodically pulsed sinusoid is dependent on the receiver center frequency, band limiting filter parameters, and pulse parameters. *Pulse overlap distortion* is significant until the *band limited pulse* bandwidth (BW) exceeds the PRR. The band limited pulse is the pulse present at the output of the receiver filter. Analytically the band limited pulse is obtained by convolving the pulse shape with the receiver filter impulse response. Band limited pulses with minimal overlap are considered *independent* or *resolved*. The transmitted pulse shape is fairly well preserved when the filter BW is greater than 2/PW. The two graphs in Figure A.10 show a succession of APDs with the different receiver center frequency and BW combinations listed in Table A.1. The first graph has filter BWs less than the PRR while the second graph has filter BWs greater than the PRR.

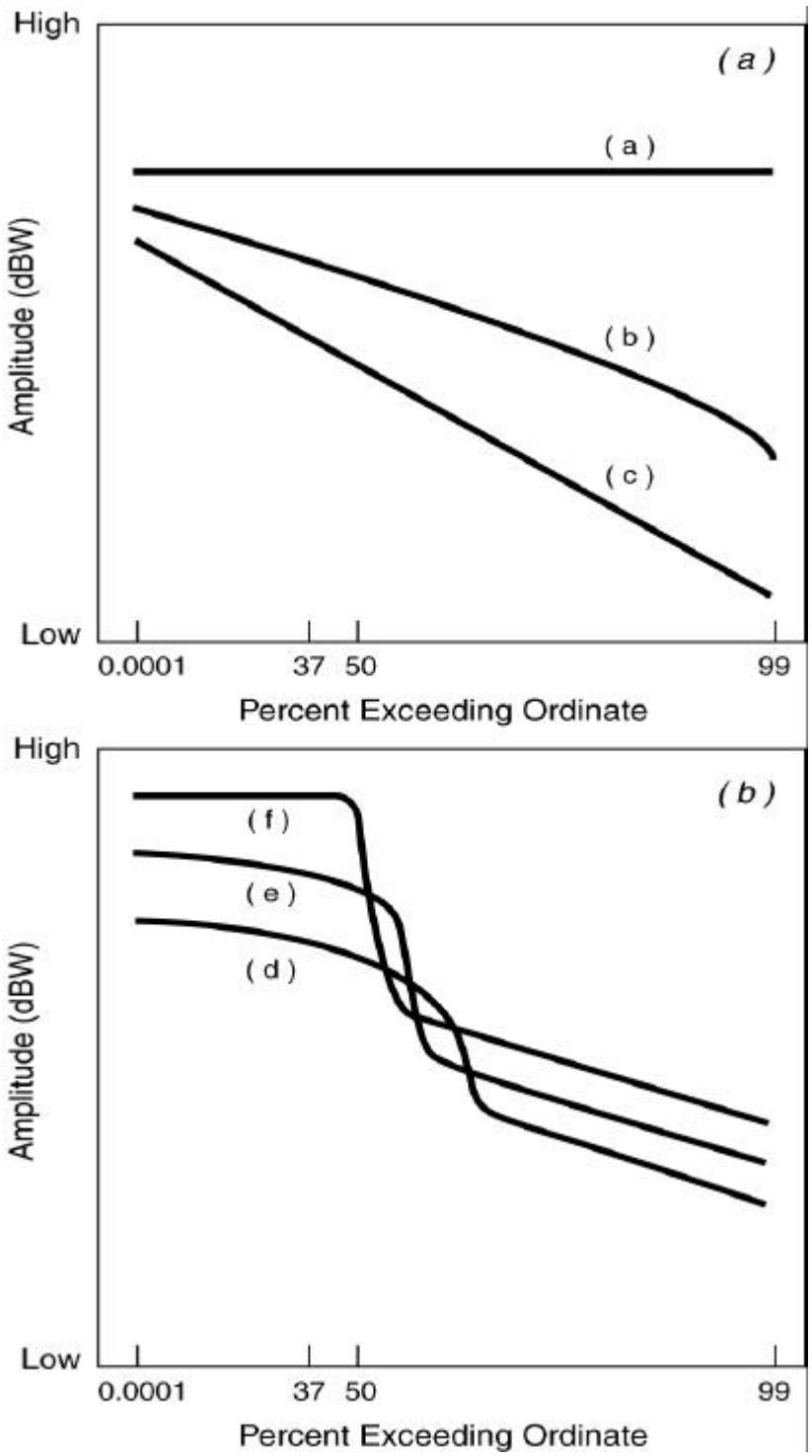

Figure A.10. Periodically pulsed sinusoid APD with pulse repetition frequencies less than (a) and greater than (b) the receiver filter bandwidth. See Table A.1 for receiver center frequency and filter bandwidth conditions for curves a-f.

Table A.1. Figure A.10 APD Conditions

Figure, Curve	**Receiver Center Frequency**	**Bandwidth**
A.10a, a	Tuned to spectral line	Filter BW<< PRR
A.10a, b	Tuned to spectral line	Filter BW< PRR
A.10a, c	Tuned off spectral line	Filter BW< PRR
A.10b, d	Tuned to pulse center frequency	Band limited pulse BW>PRR
A.10b, e	Tuned to pulse center frequency	Band limited pulse BW>>PRR
A.10b, f	Tuned to pulse center frequency	Band limited pulse BW > 2/PW

The APD takes on three characteristics when the filter bandwidth is less than the PRR, as shown in Figure A.10a. If the center frequency is tuned to a spectral line frequency and the filter bandwidth is able to *resolve* the line, it has a sinusoid APD (a). If the center frequency is tuned to a spectral line frequency, but the filter bandwidth is wider than necessary to resolve the line, it can have a Rician APD (b). If the center frequency is tuned to avoid a spectral line frequency, it has a Rayleigh APD (c).

Pulse overlap distortion decreases as the band limited pulse BW increases beyond the PRR as shown in Figure A.10b. The APDs are clearly non-Gaussian. The APD is somewhat curved at the lower probabilities for narrow filter bandwidths where there is pulse overlap (d). The APD flattens at low probabilities for wider filter bandwidths where the pulse overlap is minimal (f).

The low probability amplitudes correspond to the band limited pulse amplitudes. The high probability amplitudes correspond to the receiver noise amplitudes. The amplitudes at low probabilities are proportional to filter BW corresponding to a '$20\log_{10}$ bandwidth rule'. The amplitudes at high probabilities are proportional to the square root of filter BW corresponding to the '$10\log_{10}$ bandwidth rule'. The transition probability between these two domains is related to the band limited pulse duty cycle.

A.3.4 Summary Table

Table A.2. summarizes the APD dependencies for the three tutorial signals.

Table A.2. Tutorial Signal APD Dependencies

Signal	Receiver Center Frequency	Receiver Filter	Other Parameters
WGN	No	BW	
Sinusoid with WGN	Yes	BW	
Periodically-pulsed sinusoid with WGN	Yes	BW	PW, PRR

A.4 Band Limited UWB APDs

A.4.1 UWB Signals

The UWB signal is a train of pulses whose widths (in time) are "ultrashort" and bandwidths (in frequency) are "ultrawide". Like the periodically pulsed sinusoid, the pulses are defined by a PW and PRR. Unlike the periodically pulsed sinusoid, the impulses do not modulate a carrier frequency prior to being transmitted.

For some applications the pulse train may be pulse position modulated by a *time-dither sequence*. Time-dithering attenuates the discrete spectral line PSD component caused by periodic pulse transmission and introduces a continuous, random noise PSD component. The effectiveness of dithering is dependent on time-dither characteristics such as the distribution of dithering times, the reference time of the time-dithered pulse (absolute or relative to the last pulse), and the length of the time-dither sequence.

UWB signals are used in radar and communication devices. These devices reduce power requirements and alleviate spectral congestion by "gating" the pulse train off when continuous transmissions are not needed. They also use uncorrelated dither sequences to minimize interference to other UWB devices operating in the same room or building.

Figure A.11 shows a UWB undithered pulse train, a dithered pulse train, and a gated and dithered pulse train. Figure A.11 also shows an example UWB signal PSD with continuous and discrete components.

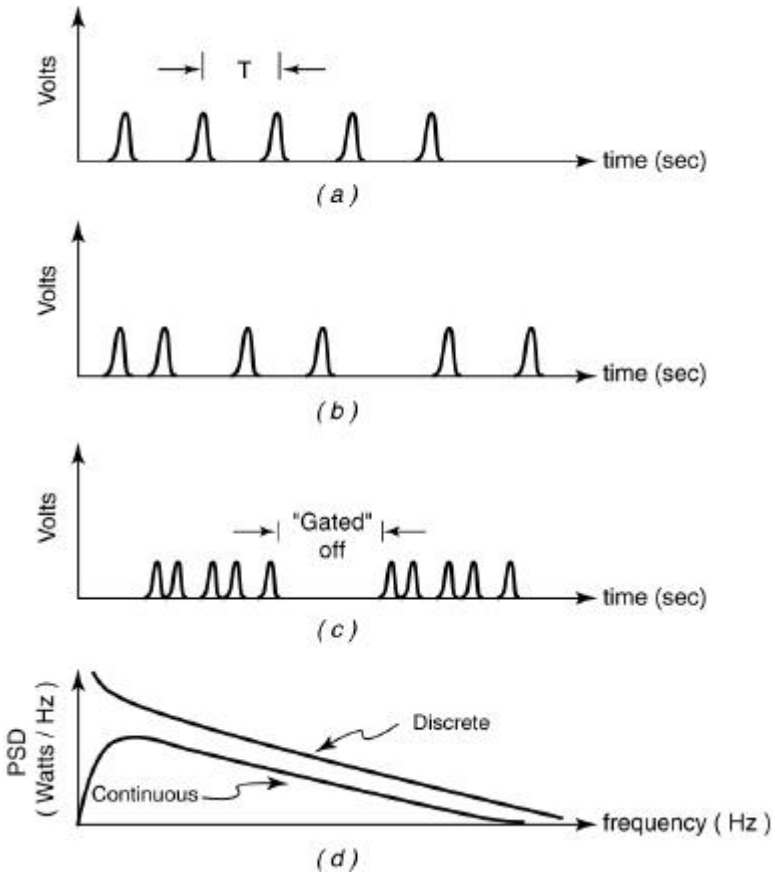

Figure A.11. Undithered (a), dithered (b), and dithered and gated (c) ultawideband signal. Dithered ultrawideband signal power spectral density (d) showing discrete and continuous components. The discrete components are represented as a curve because the lines cannot be resolved graphically.

A.4.2 Band Limited UWB Signals

The bandwidth of the interfering UWB signal is typically several orders of magnitude wider than that of the band limiting filters in the victim narrowband receiver. Thus the pulse shape and BW of the band limited pulse corresponds to the impulse response and BW of the receiver filter. Pulses are independent or resolved when the filter BW is greater than the PRR. Pulses that were independent or resolved before dithering may not be when dithering is introduced. To remain resolved, the pulse repetition period must be greater than the sum of the pulse duration and the maximum dither time.

Band limiting can occur in several of the narrowband receiver functions including demodulation, detection, and signal parameter estimation. Signal parameter estimation is necessary to provide frequency, phase, amplitude, and timing information to the demodulation and detection functions. The bandwidths associated with each of these functions may differ by several orders of magnitude. The relationships among these functions are shown in Figure A.12.

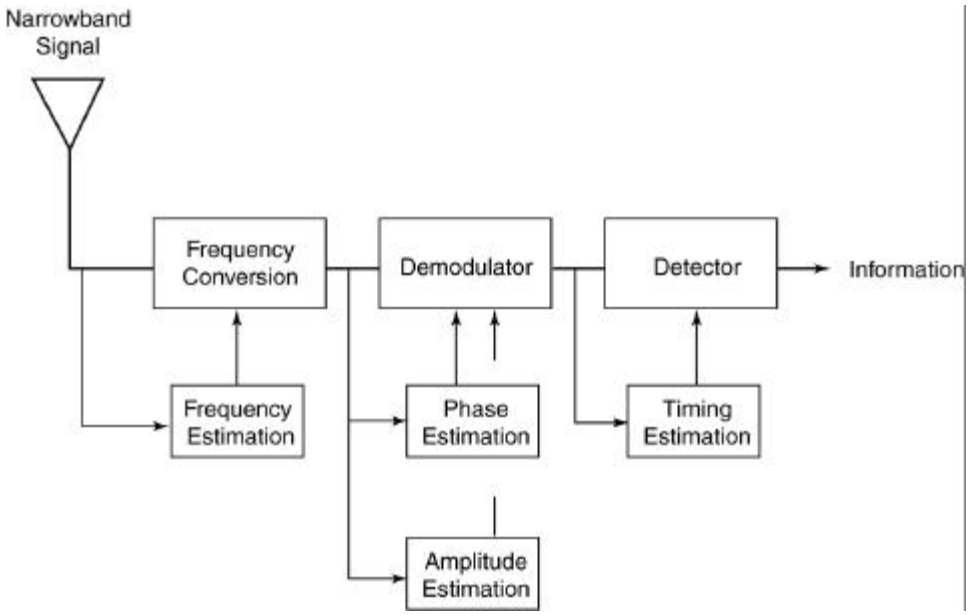

Figure A.12. Locations of band limiting filters in narrowband receivers.

A.4.3 Band Limited UWB Signal APDs

The undithered UWB signal APD will behave similarly to the periodically pulsed sinusoid APD as the filter bandwidth is varied from less than the PRR towards filter bandwidths much greater than the PRR. The dithered UWB signal APD will also behave similarly to the periodically pulsed sinusoid APD as long as the dithered pulses remain resolved. Figure A.13 shows an example of the changes that might happen to an unresolved dithered UWB signal APD when dithering is varied and BW is constant. These effects of dithering are only one possibility among many which are dependent on frequency, dithering distribution, dither reference time, length of dither sequence, gating, modulation, and filtering. In filter bandwidths less than the PRR increased dithering caused this APD to progress from the sinusoid APD to the Rician APD and finally to the Rayleigh APD. The receiver center frequency in this case was tuned to a spectral line. This progression is illustrated in Figure A.13a. In filter bandwidths comparable to the PRR, increased dithering caused this APD to progress from the non-Gaussian noise APD towards the Gaussian noise APD with Rayleigh distributed amplitudes. This progression is illustrated in Figure A.13b.

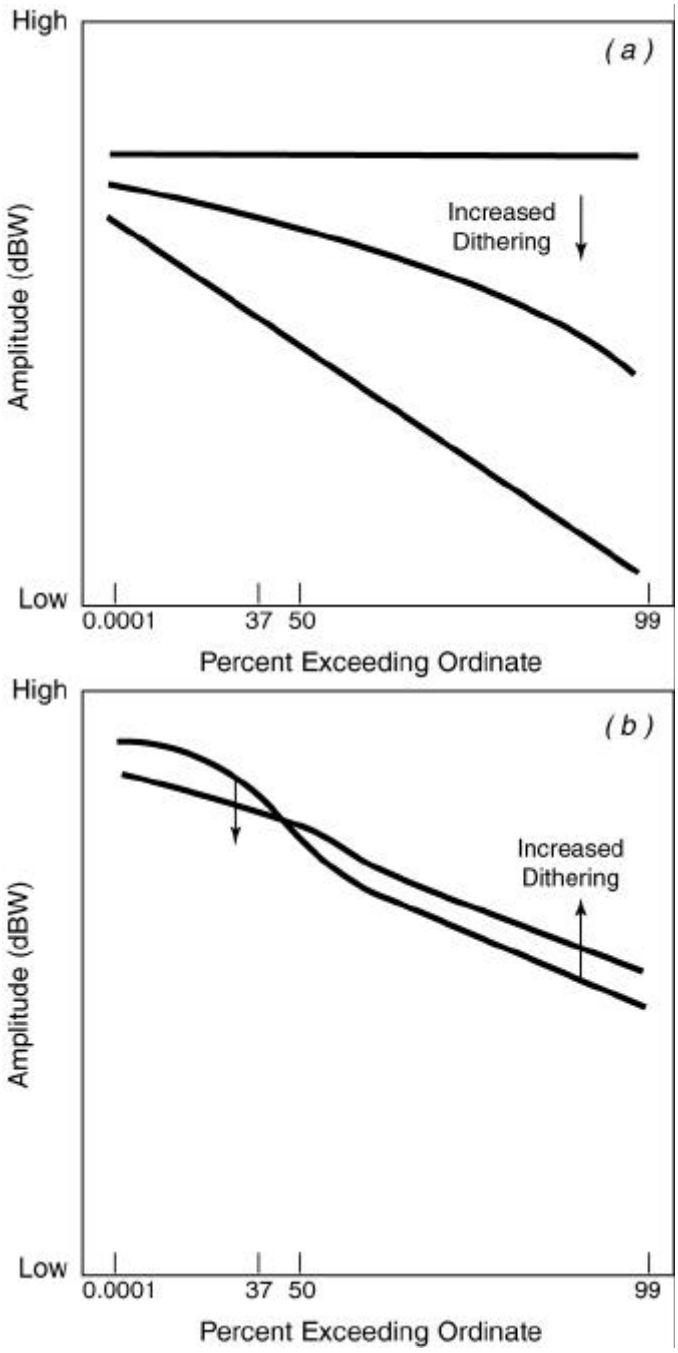

Figure A.13. Effects of increased dithering when band limiting filter bandwidth is less than (a) and comparable to (b) the pulse repetition frequency.

A.5 APD Special Topics

A.5.1 APD Measurement

Spectrum analyzer measurements can be used to estimate the APD or an amplitude statistic such as peak voltage. A block diagram of a spectrum analyzer is shown in Figure A.14. The received signal is converted to an intermediate frequency, band limited by the variable resolution bandwidth filter, and compressed by the log amplifier. Compression by the log amplifier extends the dynamic range of the measurement. The envelope detector extracts the amplitude from the band limited and compressed signal. The video bandwidth filter is used to (video) average the amplitude. The peak detector holds the highest amplitude since it was last reset.

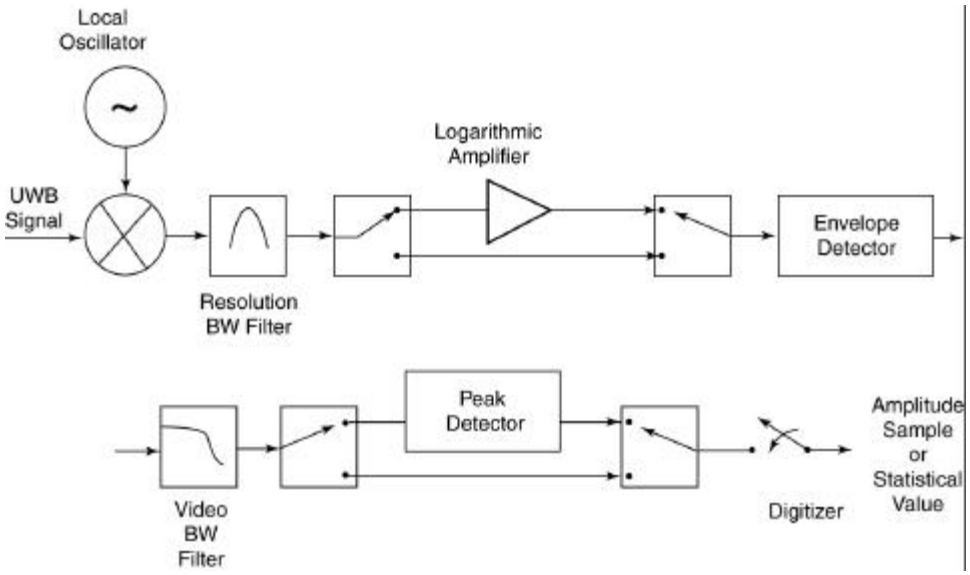

Figure A.14. Spectrum analyzer block diagram.

The statistics of the APD are derived from independent amplitude measurements. The amplitude measurements are considered independent if the sample time is 5 to 10 times the resolution bandwidth. The peak detector is bypassed and video averaging is disabled during an APD measurement. A histogram of the amplitude measurements is used to estimate the APD as shown in Section 2.1.

The peak voltage statistic is measured with the peak detector. Video averaging is disabled during peak detection. Average voltage statistics are measured with the video bandwidth filter. The log amplifier is bypassed and the peak detector is disabled for this measurement. The integration-time of the video bandwidth filter is long enough to suppress variation but surely more than the reciprocal of the resolution bandwidth. Average logarithm voltage statistics are measured in the same manner as the average voltage; however, the signal is log amplified.

A.5.2 APD of the Sum of Band Limited UWB Signals

APDs of band limited UWB signals are often collected individually in a laboratory setting. These APDs are useful for studying the interference of one UWB signal. However, in everyday life, more than one UWB device may be transmitting at a time. The statistics of the aggregate signal are conditional on the distributions of the individual band limited UWB signals and the number of signals that are to be added. Assuming the phases of the band limited UWB signals are uniformly distributed, four cases of interest emerge as shown in Table A.3.

Table A.3. Distributions of Four Aggregate APD Cases

	Distributions of band limited UWB signals	
Number of UWB signals	**Rayleigh**	**Any Distribution**
Few	(1) Rayleigh	(3) Non-Rayleigh
Many	(2) Rayleigh	(4) Rayleigh

In case 1 and 2 all the band limited UWB signals have Rayleigh distributions and the aggregate is also Rayleigh distributed. Case 4 is Rayleigh distributed by virtue of the central limit theorem of statistics. In cases 1,2, and 4 the aggregate power is simply the sum of the individual UWB signal powers. Measurement system average noise power can be removed from individual APDs before summing. In addition the average power of the individual APD may have to be reduced by attenuation due to the propagation channel to compensate for differences in location.

Case number 3 is more difficult for two reasons. First measurement system noise statistics cannot be removed from the measured statistics. Second, the computation of the aggregate APD requires using the joint statistics of a band limited UWB signal amplitude and phase distributions. For these reasons it is best to measure these statistics as an aggregate.

A.5.3 Performance Prediction

Characterizing the band limited UWB signal with an APD is not enough. Ultimately the effect that the amplitude statistics have on victim receiver performance has to be determined. The band limited UWB interference takes three guises: sinusoidal interference, Gaussian noise with Rayleigh distributed amplitudes, and non-Gaussian noise. The APD is particularly useful for predicting the performance of non-Gaussian noise.

For example, Figure A.15 shows how the non-Gaussian noise APD can be used to predict bit error rate (BER) for non-coherent binary frequency-shift keying. The straight, sloped APD is the result of band limited Gaussian noise produced in the receiver. The stepped APD is the result of band limited non-Gaussian interference. The average receiver noise power is represented by a

horizontal line on the graph. The signal-to-noise ratio (SNR) is represented as another horizontal line SNR dB above the noise power line. The BER is approximately one-half the probability where the SNR line intersects the APD curve.

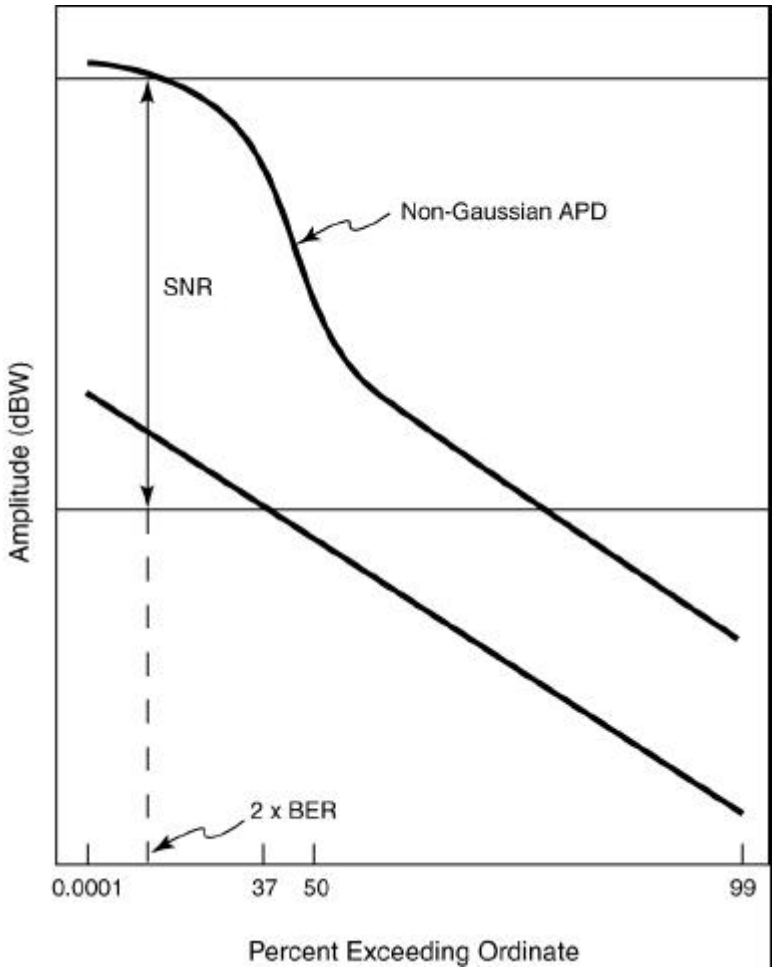

Figure A.15. Estimation of bit error rate from a non-Gaussian noise APD.

Many modern digital receivers use elaborate error correction and time-interleaving techniques to correct errors in the received bit sequence. In such receivers, the corrected BER delivered to the user will be substantially different from the received BER. Computation of BERs in these receivers will require much more detailed interference information than is contained in the APDs. For example, second-order statistics of noise amplitudes describing the time of arrival of noise amplitudes may be needed.

A.6 Concluding Remarks

This tutorial has shown that the APD is a useful tool for describing the UWB signal and analyzing UWB signal interference to victim narrowband receivers. It is useful because it 1) is measurable, 2) provides a variety of statistical values, and 3) can be used to aid in receiver performance prediction.

The APD gives insight to the potential interference from UWB signals in a wide variety of receiver bandwidths and UWB characteristics, especially when the combination of interferer and victim produces non-Gaussian interference in the victim receiver. If the interference is Gaussian, victim receiver performance degradation is correlated to the interfering signal average power alone and there is no need for further analysis using the APD. If the interference is non-Gaussian or sinusoidal, information in the APD may be critical to quantifying its effect on victim receiver performance degradation. Band limited UWB interference becomes increasingly non-Gaussian as the victim narrowband receiver bandwidth increases beyond the UWB signal PRR. Band limited UWB interference becomes increasingly sinusoidal as the victim narrowband receiver bandwidth decreases below the UWB signal PRR and a spectral line is present within the receiver bandwidth.

Spectrum regulators frequently use amplitude statistics such as peak, RMS, or average logarithm voltage to regulate transmitters. Further work is needed to determine if these statistics are strongly correlated to narrowband receiver performance. If these statistics are not correlated to receiver performance, it may be necessary to set regulatory limits in terms of the APD itself.

A.7 Bibliography

[1] A.D. Spaulding and R.T. Disney, “Man-made radio noise, part 1:Estimates for business, residential, and rural areas,” OT Report 74-38, Jun. 1974.

[2] A.D. Spaulding, “Digital system performance software utilizing noise measurement data,” NTIA Report 82-95, Feb. 1982.

[3] A.D. Spaulding,”The natural and man-made noise environment in personal communication services bands,” NTIA Report 96-330, May 1996.

[4] R.J. Achatz, Y. Lo, P.B. Papazian, R.A. Dalke, and G.A. Hufford, “Man-made noise in the 136-138-MHz VHF meteorological satellite band,” NTIA Report 98-355, Sep. 1998.

[5] R.A. Dalke, “Radio Noise,” in the *Wiley Encyclopedia of Electrical and Electronics Engineering*, Vol. 18., J.G. Webster, Ed.,John Wiley & Sons, Inc., New York: N.Y., 1998, pp. 128-140.

[6] R.J. Matheson, “Instrumentation problems encountered making man-made electromagnetic noise measurements for predicting communication system performance,” *IEEE Transactions on Electromagnetic Compatibility*, Volume EMC-12, Number 4, Nov. 1970.

[7] J.S. Bendat and A.G. Piersol, *Measurement and Analysis of Random Data*, New York, NY: John Wiley & Sons, Inc, 1966.

[8] P.L. Meyer, *Introductory Probability and Statistical Applications*, Second Edition, Reading, Mass: Addison-Wesley Publishing Company, 1970.

APPENDIX B. SIMULATIONS OF TIME AND SPECTRAL CHARACTERISTICS OF ULTRAWIDEBAND SIGNALS AND THEIR EFFECTS ON RECEIVERS

Edmund A. Quincy[1]

B.1 Introduction

In this appendix a class of time-dithered, time-hopped UWB systems is modeled and simulated from an analytic description of the system. These simulated time waveforms and Fourier spectrum results are analyzed to show the effect of a receiver's intermediate frequency (IF) bandwidth (BW) on peak and average power. These peak and average power curves provide the basis for establishing a normalized bandwidth correction factor (BWCF) curve and equation. The BWCF is used to estimate peak power over a range of bandwidths from average power measurements made in a 1 MHz BW as prescribed by the FCC for Part 15 devices. Simulation of the UWB devices complements measurements and other analytic model results for these devices.

B.2 UWB Model

The simulated time-dithered ultrawideband system block diagram is shown in Figure B.1. The system transmits a quasi-periodic, very low duty cycle, dithered pulse train *s(t)* where delta functions (narrow pulses in hardware) are pulse position modulated (PPM) and shaped with a Gaussian 2nd derivative filter *w(t)*. The analytic expression for *s(t)* and *w(t)* are provided in (1) and (1a) where d_k is the total dither in time units and N_p is the number of pulses in the pulse train. In the simulation results the number of pulses was set at 100 (10,000 ns). This was estimated to be similar to the observation window of a spectrum analyzer measurement. The model employed here is similar to that used by Win and Scholtz [1] except that their pulse trains were infinite in length, which led to smoothed spectral lines corresponding to this infinite observation window.

$$s(t) = w(t) * \sum_{k=1}^{N_p} \delta\left[t - d_k - (k-1)T\right] \qquad (1)$$

$$w(t) = \left[\ 1 - 2(\pi\ t\, f_c)^2\ \right] e^{-(\pi\ t\, f_c)^2} \qquad (1a)$$

---

[1]The author is with the Institute for Telecommunication Sciences, National Telecommunications and Information Administration, U.S. Department of Commerce, Boulder, CO 80305.

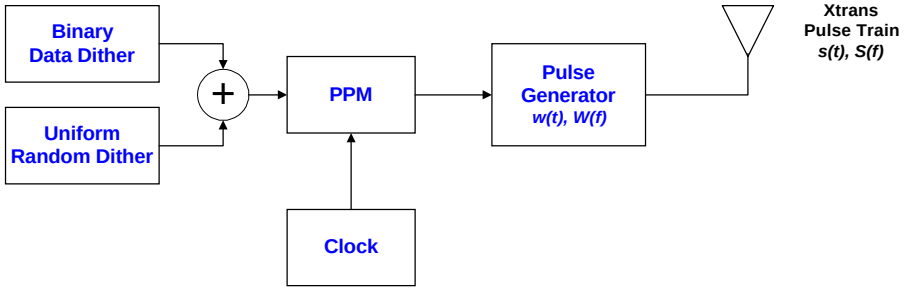

Figure B.1. Time-dithered ultrawideband system model.

The shaping filter for a specific hardware configuration depends on the transmit and receive antennas and may deviate some from this model. The specific pulse shape is probably not as important a factor in determining a receiver's narrow IF BW response as the pulse width and corresponding BW. The receiver IF filtering will remove pulse shape details if the pulse is sufficiently narrow and the corresponding BW sufficiently wide, compared to the receiver IF bandwidth. Shape details are filtered out in these simulations, as will be seen in the IF output pulses. In this system the dither consists of two components: a pseudo-random time-hopping dither and a data dither. Usually the time-hopping dither is large compared to the data dither. In our case the time-hopping dither was uniformly distributed between 0 and 0.5T (50% dither); whereas the data dither represented binary 0s and 1s with 0 or 0.045T (4.5% dither). The time-hopping dither values are commonly generated from a pseudo-noise sequence. An undithered pulse repetition rate (PRR) of 10 MHz was used, which made the nominal pulse train period T= 100 ns. Simulation results were also obtained for the 0 or the non-dithered case where the waveforms are periodic with a period T=100 ns resulting in a line spectra with a fundamental frequency equal to the PRR .

B.3 UWB Simulation

The simulation and power calculation processes are shown in the flow diagram of Figure B.2. A periodic impulse train is dithered by the combined amount of dither and then Fourier transformed using the FFT (Fast Fourier Transform). Then the spectrum is shaped using the Gaussian 2nd derivative filter transfer function *W(f)* described by the analytic expression in (2a). Alternatively, the complex Fourier spectrum, *S(f)*, can be calculated using the analytic expression in (2).

$$S(f) \quad W(f) \sum_{k\ 1}^{N_p} e^{-j2\pi f_i d_k\ (k-1)T_i} \tag{2}$$

$$W(f) \quad \left(\frac{f}{f_c}\right)^2 e^{\left[1-\left(\frac{f}{f_c}\right)^2\right]} \tag{2a}$$

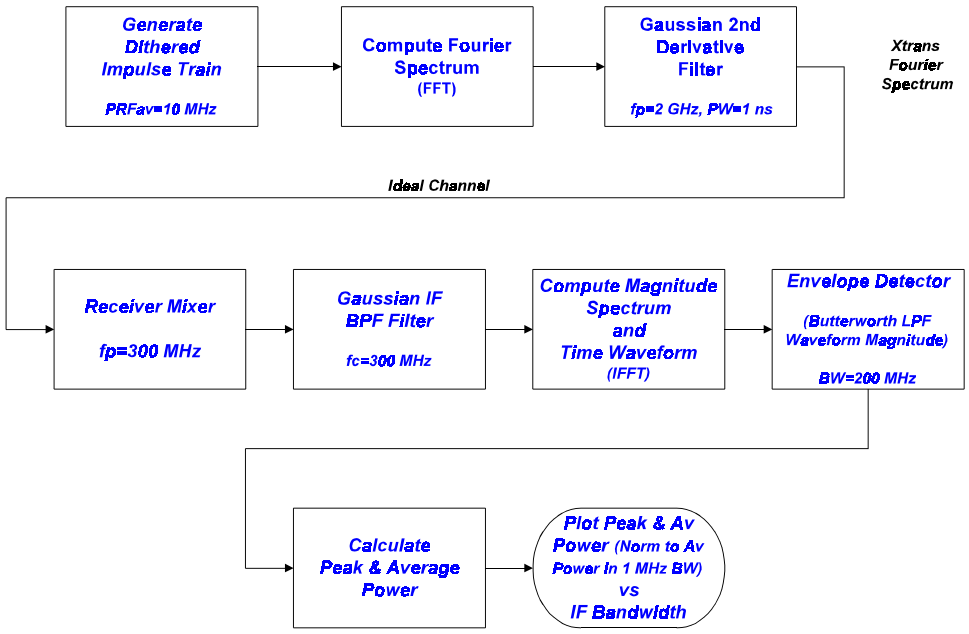

Figure B.2. Simulation and power calculation process.

The transmitted 50% dithered pulse train is shown in the top Figure B.3 plot and an individual pulse is shown in the bottom plot. The transmitted pulse width was approximately 1 ns and the corresponding wideband spectrum peaked at 2 GHz with 40 dB down from the peak occurring at frequencies of 0.25 GHz and 5 GHz. The transmitter spectra are shown in Figure B.4 with dithered pulse train spectrum (before shaping) shown in the top and the shaped transmitter output spectrum shown in the bottom. Note that the spectrum before shaping appears quite noise-like with 50% dither. This random appearance can change significantly with less dither, particularly below 25% dither. With dithers greater than 50% the random appearance does not change significantly. With BWs of 100 MHz or less centered about the peak at 2 GHz, the spectrum still appears quite flat even after shaping.

The transmitter output in Figure B.2 is fed through an ideal channel to a receiver (victim or spectrum analyzer) where the signal is mixed down to a center frequency of 300 MHz. This frequency f_c now is also the peak frequency of the spectrum. That is, the original peak frequency f_p=2 GHz was mixed down to 300 MHz. Next the mixer output is filtered by a Gaussian-shaped filter with an adjustable bandwidth. A Gaussian shape was chosen for three reasons: (1) the spectrum analyzer response, used to make measurements at an IF frequency, resembles a non-symmetric Gaussian; (2) as more stages of IF filtering are employed, their composite response usually tends towards a Gaussian; and (3) simplicity. Bandwidths were employed from 100 MHz down to 0.3 MHz. The IF filter was followed by an envelope detector implemented by computing the waveform magnitude and lowpass filtering it with a 6-pole Butterworth filter using a BW of 200 MHz. Higher bandwidths allowed some ripple through at the IF frequency.

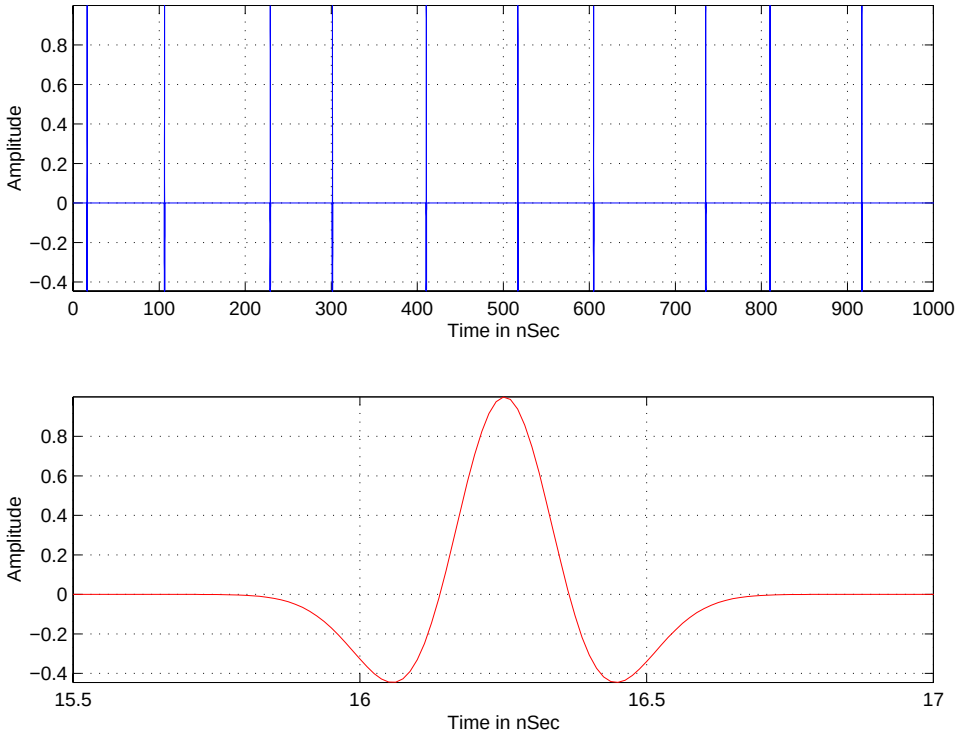

Figure B.3. Normalized 2nd derivative Gaussian dithered pulse train (50% dither); Top: full record, Bottom: exploded view.

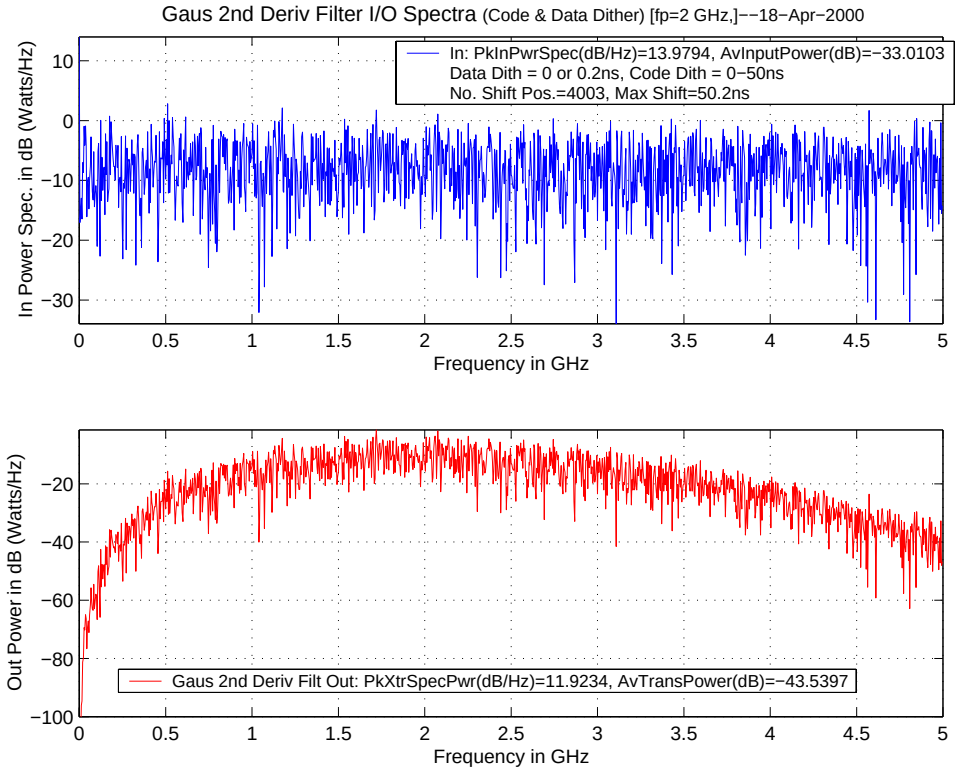

Figure B.4. Transmitter spectra (50% dither); Top: before Gaussian filter, Bottom: after Gaussian filter.

An example output is shown in Figure B.5 employing an IF BW of 30 MHz. The top plot shows the filtered received spectrum centered at 300 MHz, the center plot contains the pulse train out of the IF showing the pulsed RF oscillating at approximately the 300 MHz IF frequency. The bottom plot displays the envelope waveform out of the IF filter. Note the variable spacing of the pulses corresponding to the 50% dither. At a BW of 30 MHz the pulses out of the IF just touch each other. For wider BWs they are completely separated and for narrower BWs they are overlapped, causing peaking in the envelope as observed in Figures B.6 and B.7 for 10 MHz and 3 MHz IF bandwidths respectively. Figures B.8 compare this peaking effect of the detected envelope for these same 3 BWs over a record length of 100 pulses (10,000 ns). It is particularly interesting to compare the 50% and 0 dither cases. With the periodic (no dither) pulse train, the IF filter gets pinged by pulses at a regular interval and just provides periodic pulses out of the detector without peaking. At a BW of 3 MHz the 50% randomly dithered pulse train creates significant peaks and valleys (1 down to 0), whereas the periodic pulse train has a constant envelope coming out of the IF filter.

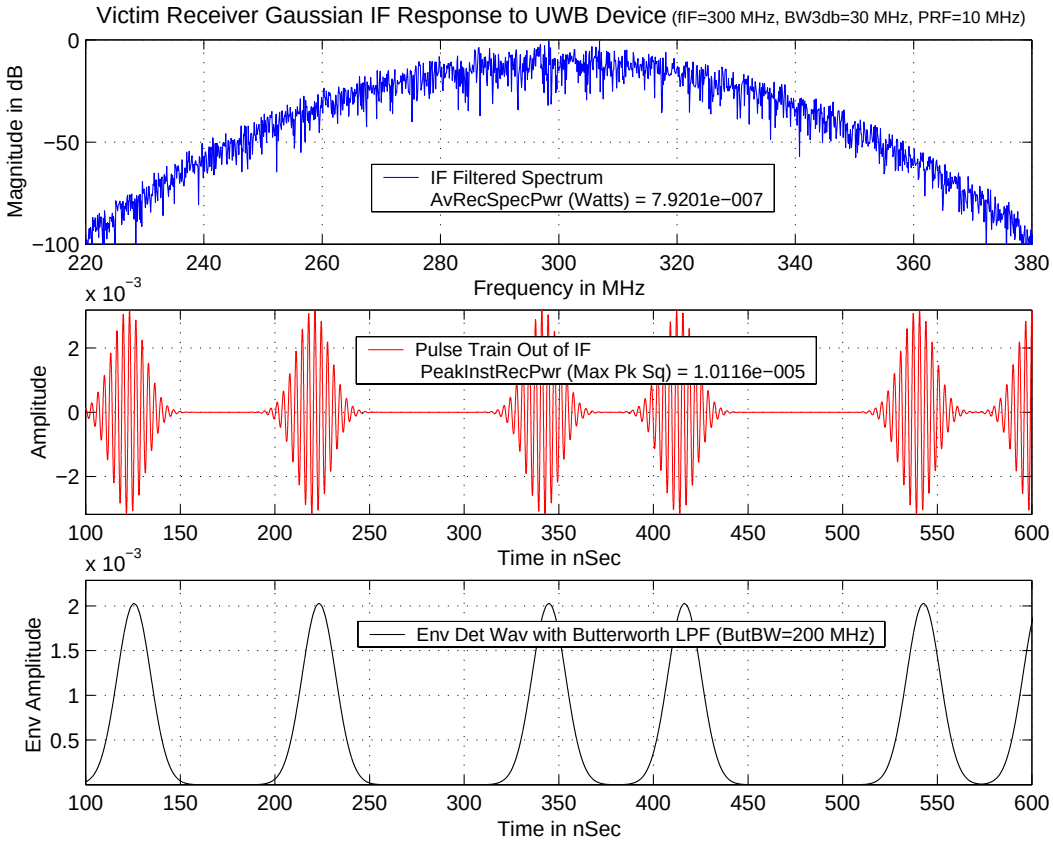

Figure B.5. Receiver 30 MHz IF bandwidth (50% dither); Top: output spectrum, Middle: pulsetrain, and Bottom: envelope detected pulse train.

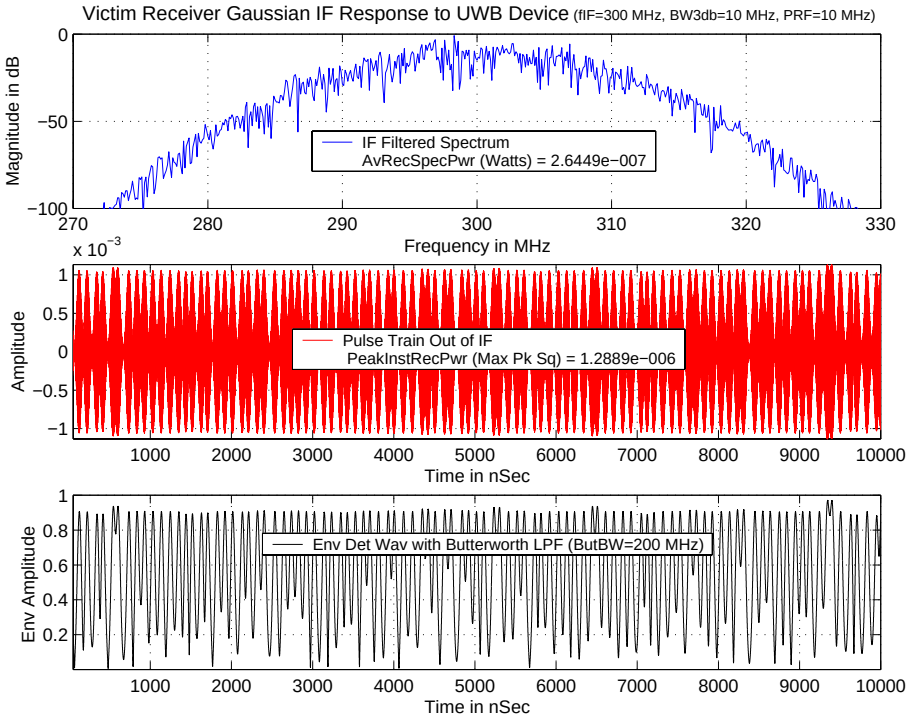

Figure B.6. Receiver 10 MHz IF bandwidth (50% dither); Top: output spectrum, Middle: pulse train, and Bottom: envelope detected pulse train.

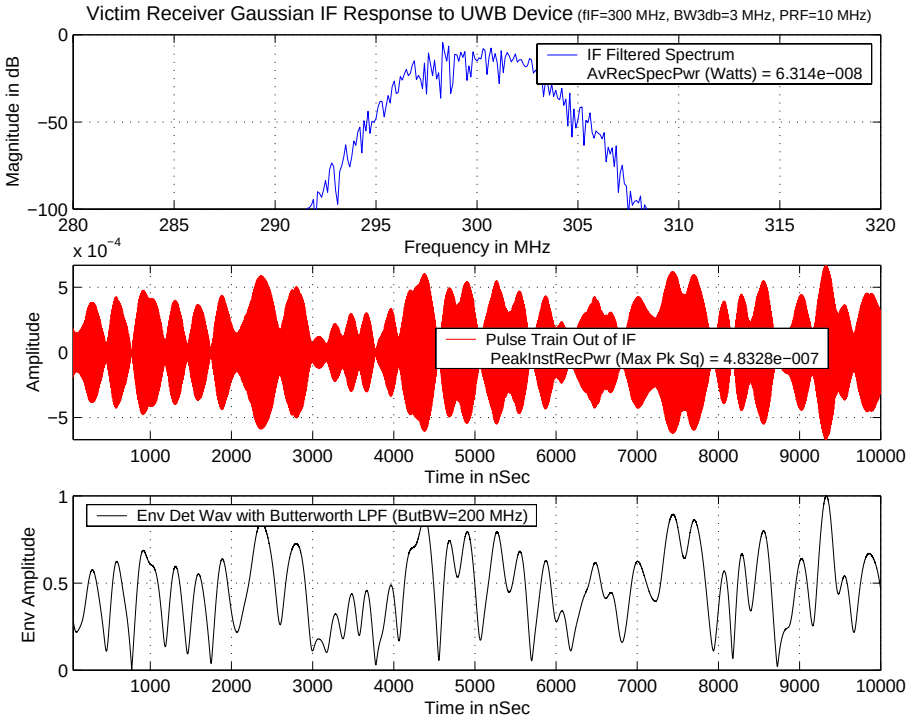

Figure B.7. Receiver 3 MHz IF bandwidth (50% dither); Top: output spectrum, Middle: pulse train, and Bottom: envelope detected pulse train.

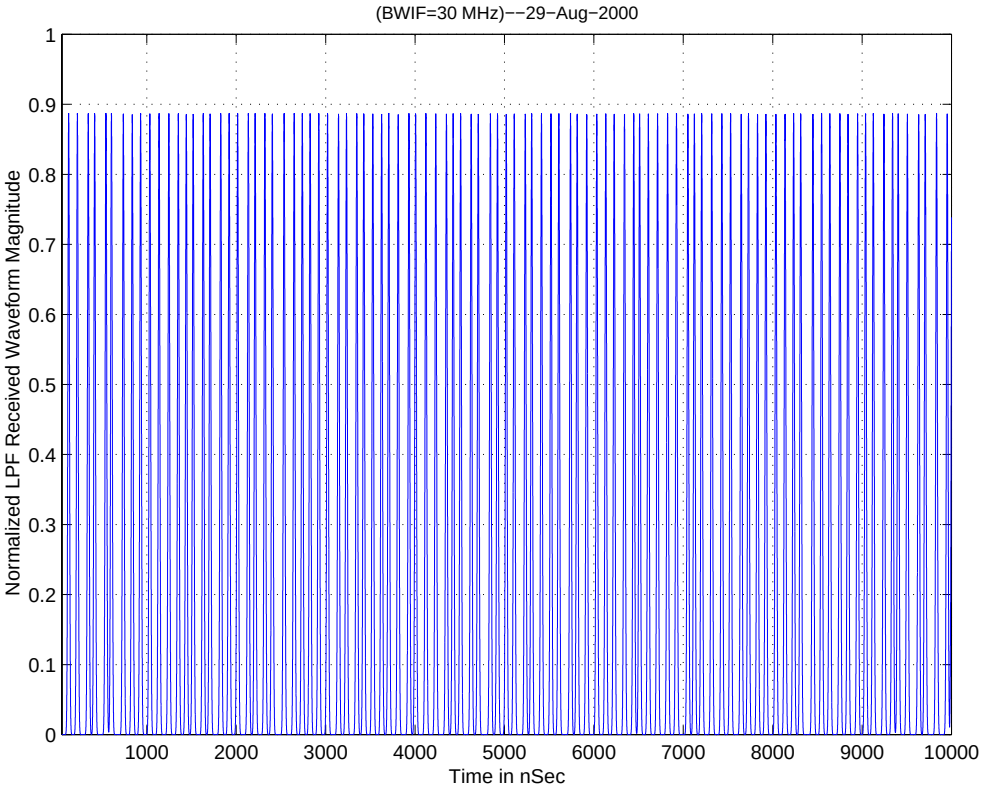

Figure B.8.A. Receiver IF envelope for 30 MHz bandwidth with 50% dither.

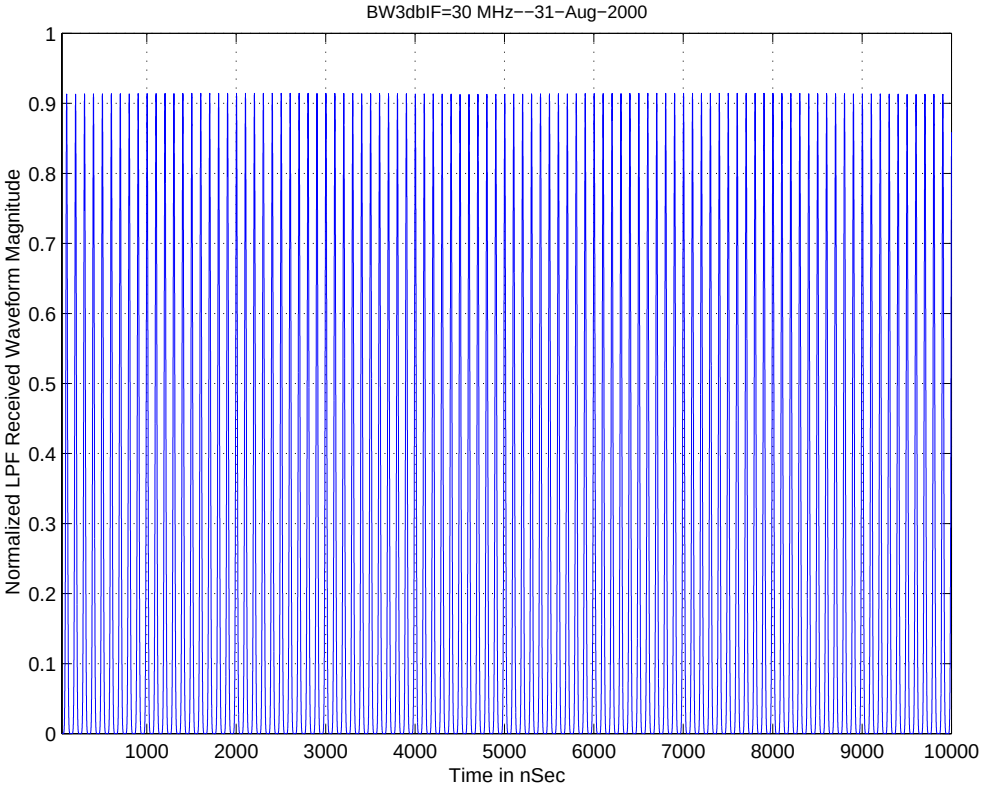

Figure B.8.B. Receiver IF envelope for 30 MHz bandwidth with 0% dither.

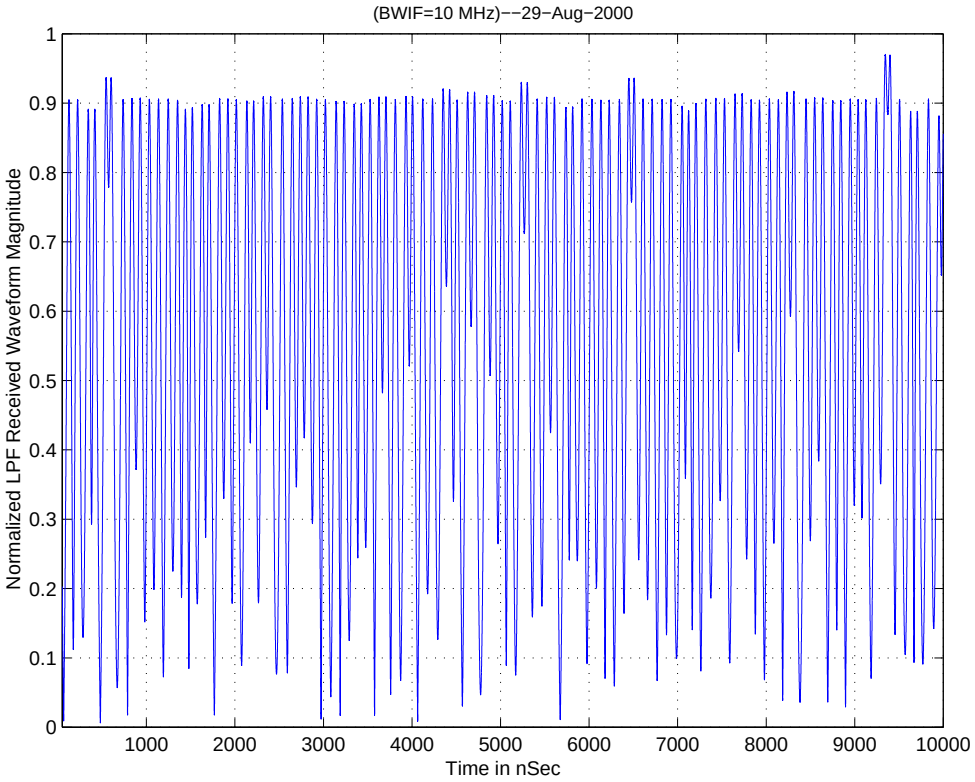

Figure B.8.C. Receiver IF envelope for 10 MHz bandwidth with 50% dither.

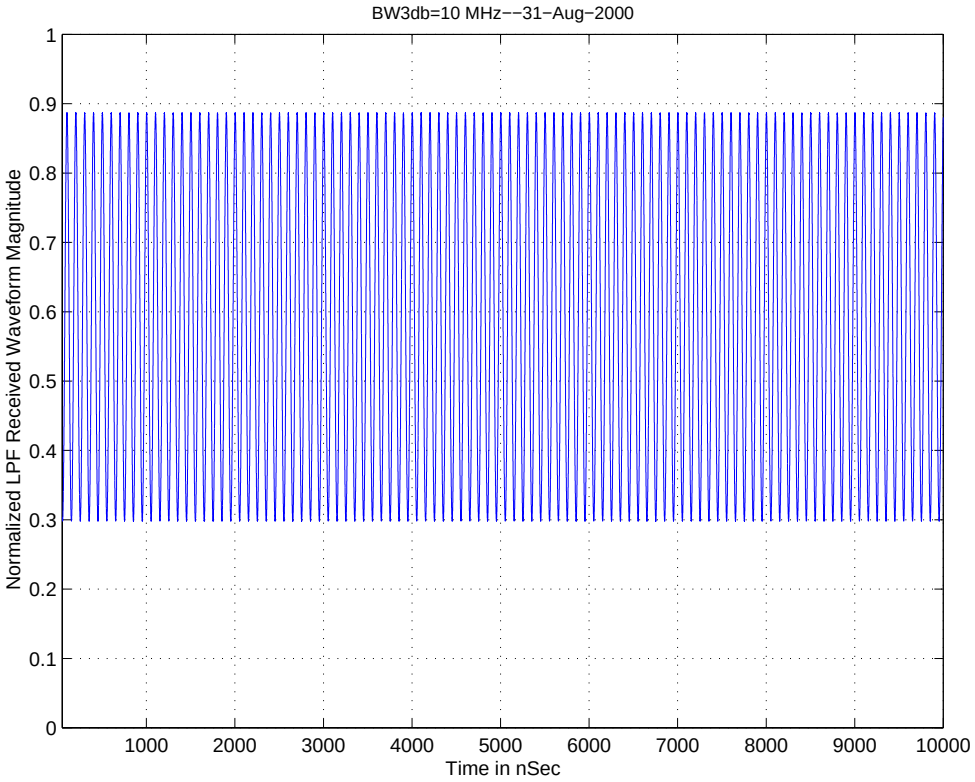

Figure B.8.D. Receiver IF envelope for 10 MHz bandwidth with 0% dither.

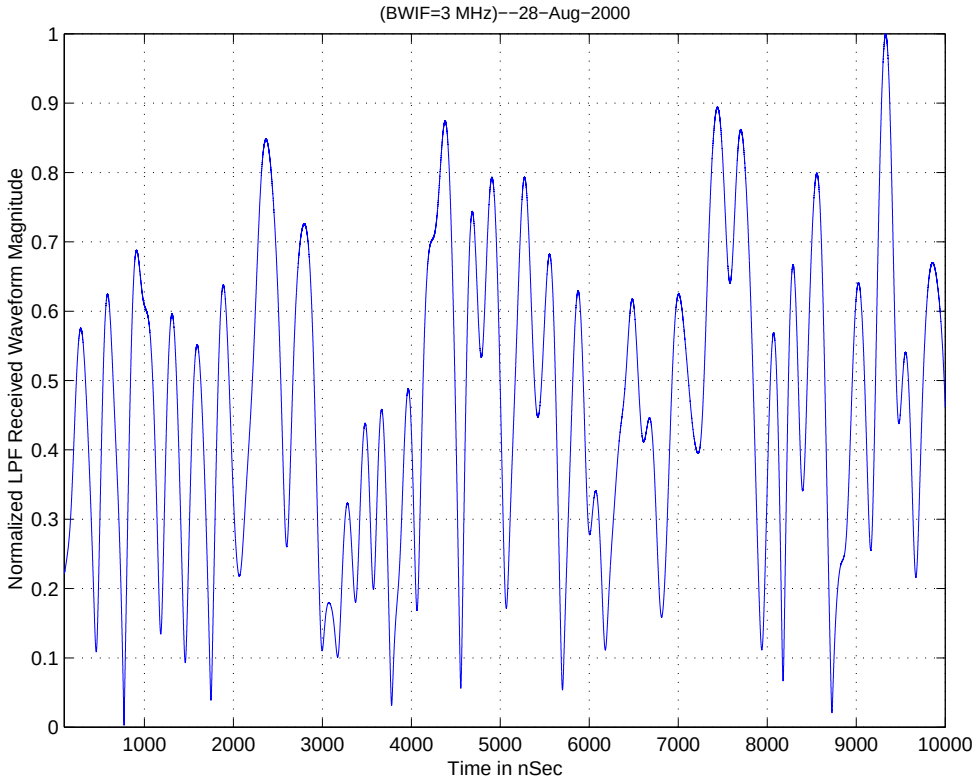

Figure B.8.E. Receiver IF envelope for 3 MHz bandwidth with 50% dither.

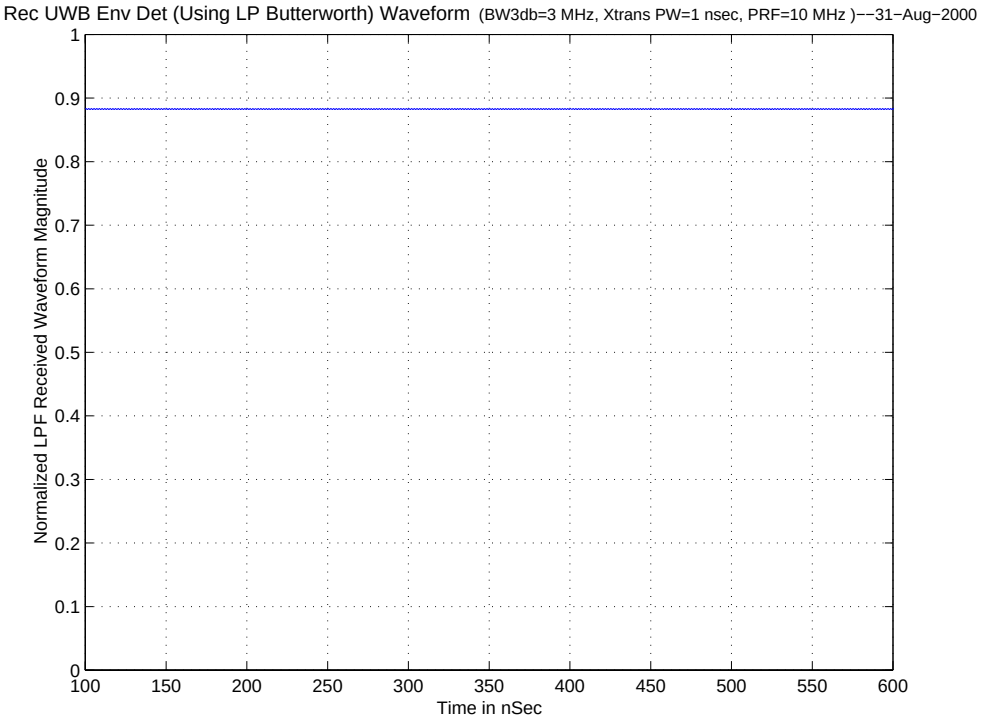

Figure B.8.F. Receiver IF envelope for 3 MHz bandwidth with 0% dither.

B.4 Power Calculations in Receiver IF Bandwidths

Figures B.9 show the received instantaneous peak and average power computed from the simulated time waveforms for receiver IF bandwidths ranging from 0.3 MHz to 100 MHz. These powers were normalized to the average power in a BW of 1 MHz (a 1-MHz BW is specified by the FCC for Part 15 average measurements). Consequently, the average power curves all go through 0 dB at 1 MHz. These curves provide the basis to develop bandwidth correction factors (BWCF). The BWCFs are used to estimate the amount of peak power at a given BW, starting with measuring the average power in this 1-MHz BW.

In addition to peak and average power curves, another guideline is provided. This straight line on a log-log plot is the 10 $\log_{10}$(BW) average power trend line. It follows the average power quite well for 50% dither (both pre-detection and post-detection); however, for the non-dithered case it follows the average power only for BWs greater than or equal to 10 MHz where the pulses are separated. As pulses overlap for narrower BWs of this non-dithered case, the envelope is constant and the peak and average power are constant as expected. Consequently the power does not change as a function of BW. Another way to look at this is in the frequency domain. An undithered PRR of 10 MHz results in a spectral line at 10 MHz and its harmonics. There is therefore a line at 2 GHz which is down converted to 300 MHz, the center frequency of the IF filter. As the BW increases above 10 MHz, more lines are included in the passband and the power increases linearly with BW. At 10 MHz and below there is a single line in the passband so that the power remains constant. This is in contrast to the 50% dithered case for narrow BWs where the peak and average powers change according to a 10 $\log_{10}$BW rule.

For both the 50% dithered and non-dithered cases, the peak power for BWs greater than or equal to 10 MHz (also the PRR) increases as 20 $\log_{10}$(BW). This is the BW where pulses become distinct in the pulsetrain at the output of the IF, as can be seen in the envelopes shown in Figure B.8.C through Figure B.8.F.

B.5 Reference

[1] M.Z. Win and R.B. Scholtz, “Impulse radio: How it works,” *IEEE Communications Letters,* pp. 10-12, Jan. 1998.

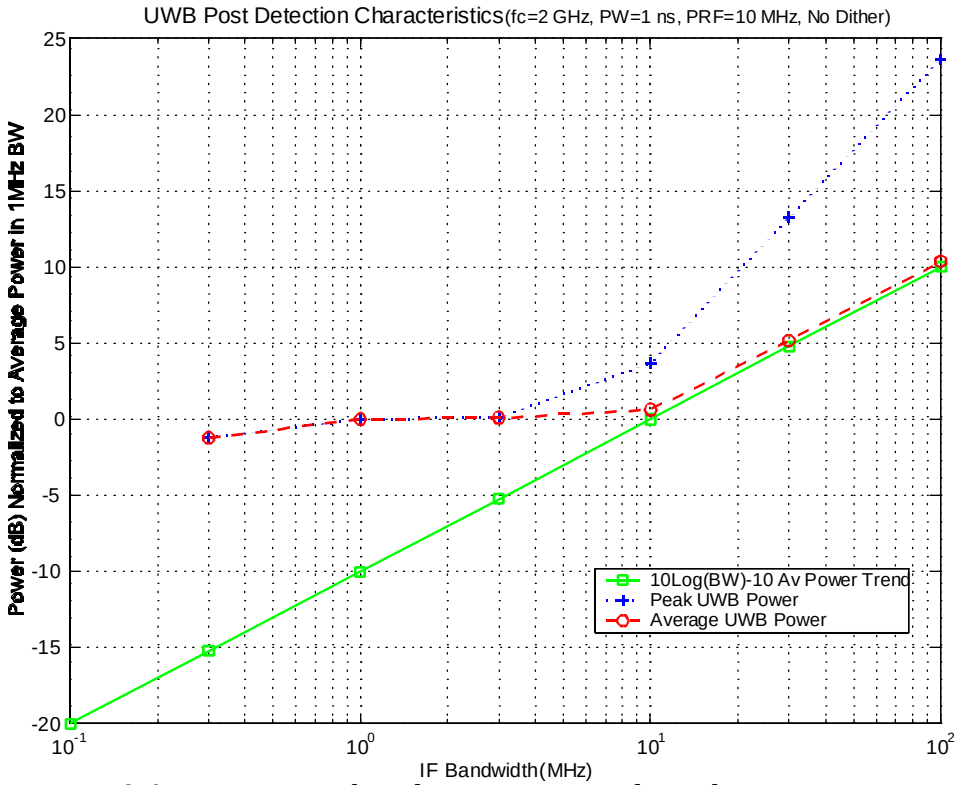

Figure B.9.A. Receiver peak and average power dependence on IF bandwidth (post detection, no dither).

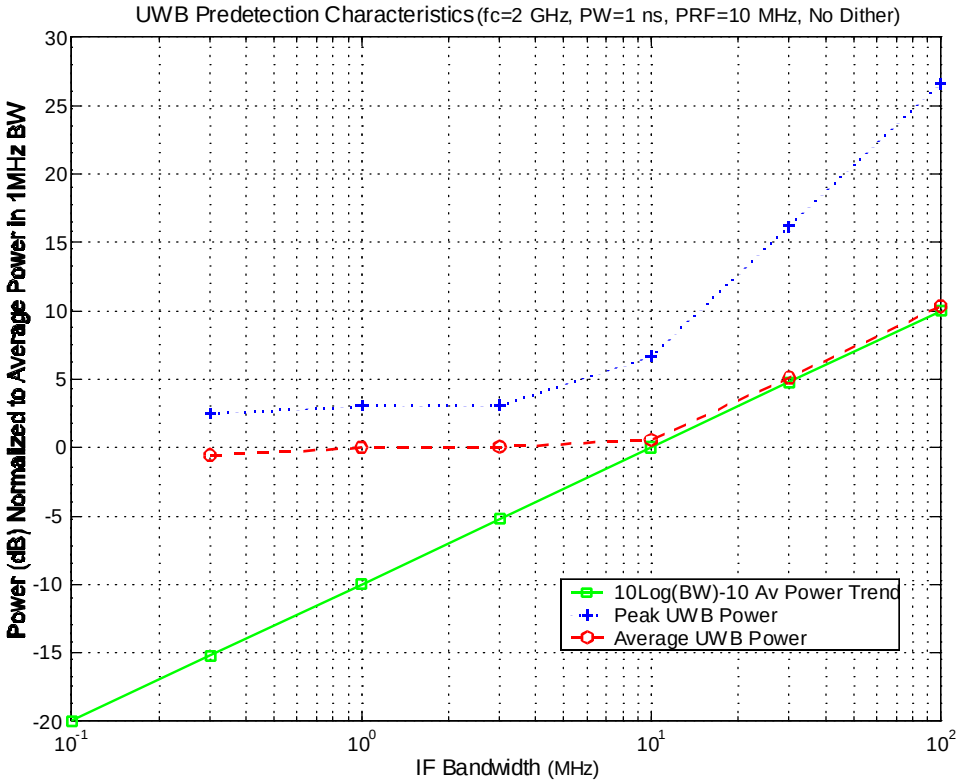

Figure B.9.B. Receiver peak and average power dependence on IF bandwidth (predetection, no dither).

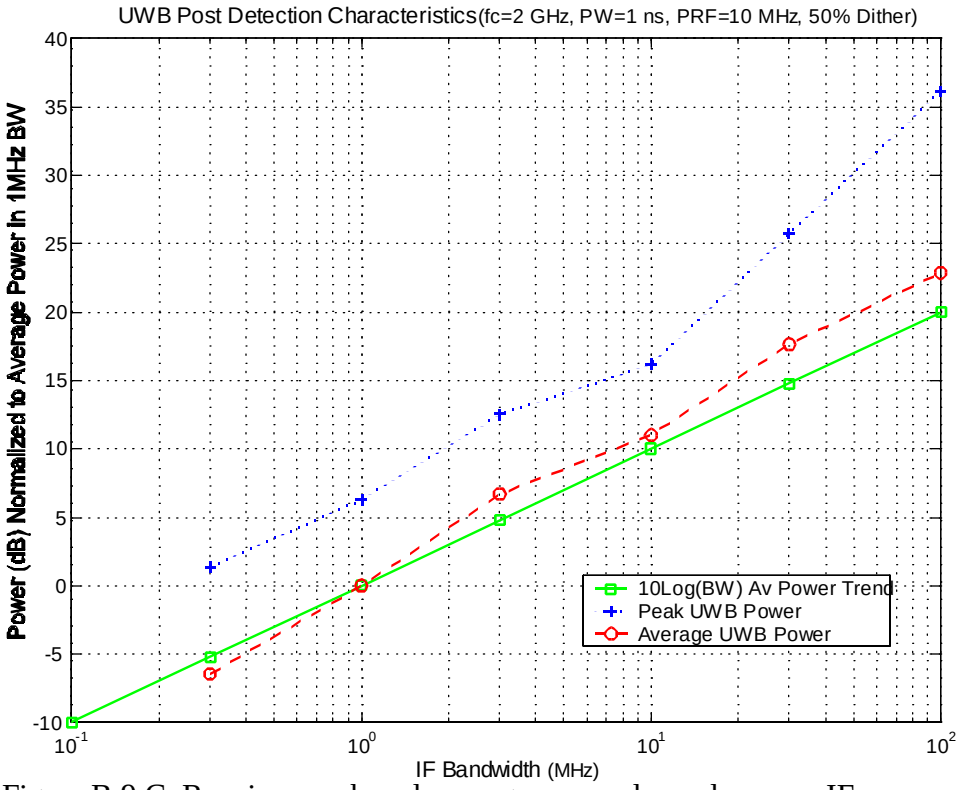

Figure B.9.C. Receiver peak and average power dependence on IF bandwidth (post-detection, 50% dither).

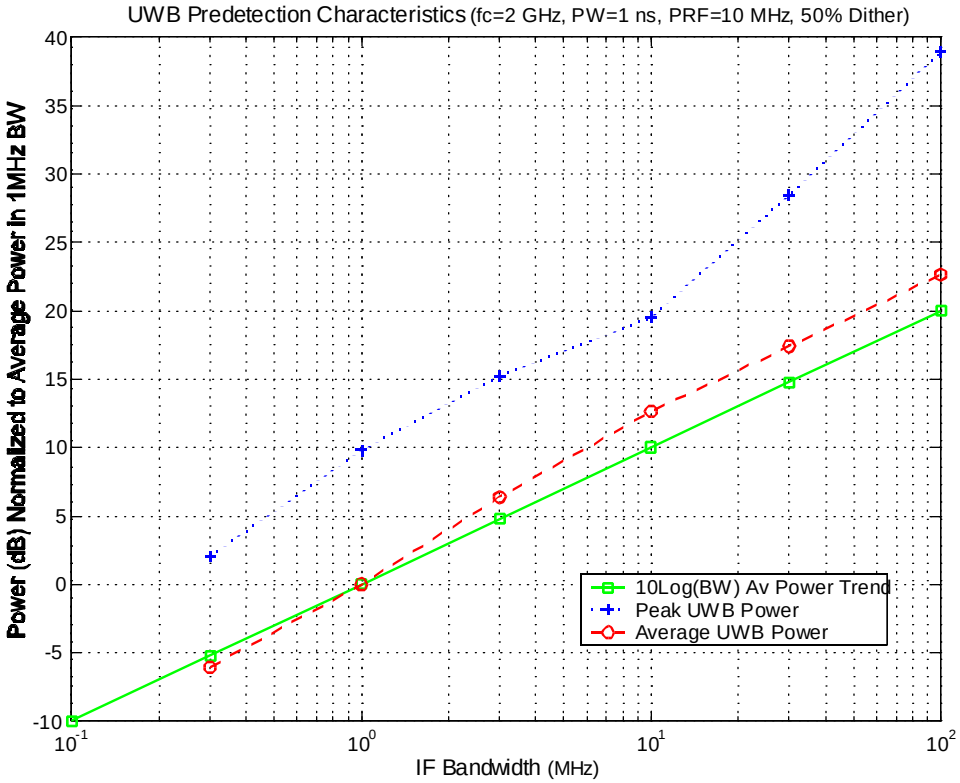

Figure B.9.D. Receiver peak and average power dependence on IF bandwidth (pre-detection, 50% dither).

APPENDIX C. CONVERSION OF POWER MEASURED IN A CIRCUIT TO INCIDENT FIELD STRENGTH AND INCIDENT POWER DENSITY, AND CORRECTIONS TO MEASURED EMISSION SPECTRA FOR NON-CONSTANT EFFECTIVE APERTURE MEASUREMENT ANTENNAS

Frank Sanders[1]

This appendix derives conversions between power measured in a circuit and incident field strength and effective radiated power from a transmitter.[2] Necessary corrections to measured emission spectra for non-constant effective aperture measurement antennas are also derived and explained.

C.1 Directivity, Gain, Effective Antenna Aperture, and Antenna Correction Factor

The starting point is *directivity* and *gain*, which are both measures of how well energy is concentrated in a given direction. *Directivity*, *d*, is the ratio of power density, p_{den} in that direction, to the power density that would be produced if the power were radiated isotropically, $p_{den\text{-}iso}$:

$$d = \frac{p_{den}}{p_{den-iso}} \quad . \tag{C.1}$$

The reference can be linearly or circularly polarized. By geometry, directivity is:

$$d = \frac{4\pi p_{den}}{\frac{\sqrt{E}}{m}\int\int E^2 d\Omega} \tag{C.2}$$

where E is the field strength [1]. Directivity makes reference only to power in space around the antenna; it is unrelated to power at the antenna terminals. There is loss between the terminals and free space. *Gain*, *g*, includes these antenna losses; gain is the field intensity produced in the given direction by a fixed input power, p_{in}, to the antenna. Gain and directivity are related by efficiency, , :

---

[1]The author is with the Institute for Telecommunication Sciences, National Telecommunications and Information Administration, U.S. Department of Commerce, Boulder, Colorado 80305.

[2] In this appendix, quantities in linear units (e.g., milliwatts) are written in lower case; decibel quantities [10 log (linear power ratio)] are written in upper case.

$$g = d\epsilon \tag{C.3}$$

or,

$$g = \frac{(4\pi\ p_{den})}{p_{in}} \quad . \tag{C.4}$$

Through reciprocity, directivity is independent of transmission or reception, as is gain. *Effective antenna aperture*, a_e is unrelated to the physical aperture of an antenna. a_e is defined as:

$$a_e = \frac{\lambda^2 g}{4\pi} \tag{C.5}$$

where λ is the free-space wavelength. Note that a_e has the units of area. For an antenna matched to a load, the power in the load, p_{load}, is related to the free-space power density by a_e:

$$p_{load} = p_{den} \cdot a_e \quad . \tag{C.6}$$

If p_{load} is in a 50-ohm circuit and p_{den} is in a free-space impedance of 377 ohms, then the following relations apply:

$$p_{load} = \frac{V_{load}^2}{50} \tag{C.7a}$$

and

$$p_{den} = \frac{V_{space}^2}{377} \quad . \tag{C.7b}$$

Rewriting Eq. C.6 gives:

$$\frac{V_{load}^2}{50} = a_e \cdot \left(\frac{V_{space}^2}{377} \right) \tag{C.8}$$

Note that the voltage in the circuit, V^2_{load}, is in units of volts, but that the free-space field strength, V^2_{space} is in units of volts/m. The effective aperture, in units of m^2, converts the free-space power density on the right to the power in a circuit on the left.

At this point, we introduce the *antenna correction factor*, *acf*, which is defined as follows:

$$acf = \frac{V_{space}^2}{V_{load}^2} \quad . \tag{C.9}$$

Note that acf has the units of m^{-2}. Rewriting Eq. C.8 with this substitution for acf gives:

$$acf = \frac{377}{50} \cdot \left(\frac{1}{a_e} \right) \quad . \tag{C.10}$$

Because a_e is dependent upon both gain and frequency, so is acf. Substituting Eq. C.5 into Eq. C.6 gives:

$$acf = \left(\frac{377}{50} \right) \left(\frac{4\pi}{\lambda^2 g} \right) \quad . \tag{C.11}$$

If the frequency, f, is in megahertz, then the substitution [$\lambda = c/(f \times 10^6) = 3 \times 10^8/(f \times 10^6)$] gives:

$$acf = \left(\frac{377}{50} \right) (4\pi) \left[\left(\frac{10^{12}}{(3 \cdot 10^8)^2} \right) \cdot (f, MHz)^2 \cdot \left(\frac{1}{g} \right) \right] \tag{C.12}$$

which, calculating the constant term values, gives:

$$acf = (1.03 \cdot 10^{-3}) \cdot (f, MHz)^2 \cdot \left(\frac{1}{g} \right) \quad . \tag{C.13}$$

Taking 10log(*acf*) gives *ACF* in dB:

$$(ACF, dB) = (-29.78\ dB) + 20\log(f, MHz) - 10\log(g) \quad . \tag{C.14}$$

C.2 Free Space Field Strength Conversion

Signals are commonly measured in circuits as either voltages or log-detected voltages proportional to power. In either case, the signal measurement within a circuit is usually converted to equivalent power in the circuit impedance. This conversion is usually accomplished automatically within the measurement device (e.g., a spectrum analyzer). This measured power within a circuit, p_{load}, is converted to incident field strength using either the antenna correction

factor or antenna gain relative to isotropic, as follows. Writing Eq. C.6 with a substitution for a_e from Eq. C.5 gives:

$$p_{load} = \left(\frac{\lambda^2 \cdot g \cdot (V_{space})^2}{4\pi \cdot 377} \right) \quad , \tag{C.15}$$

and substituting for (λ= c/f), $f = 10^6 \cdot f$(MHz), and c = $3 \cdot 10^8$ m/s gives:

$$p_{load} = \left[\frac{(3 \cdot 10^8)^2 \cdot g \cdot (V_{space})^2}{(f, MHz)^2 \cdot (10^6)^2 \cdot 4\pi \cdot 377} \right] \quad . \tag{C.16}$$

For power in milliwatts and field strength in microvolts/meter, the conversions (power, mW) = 1000$\cdot$(power, W) and (field strength, v/m) = $10^{-6} \cdot$(field strength, µV/m) are used:

$$(p_{load}, mW) = \left[\frac{1000 \cdot (3 \cdot 10^8)^2 \cdot g \cdot (10^{-6})^2 \cdot (V_{space}, \mu V/m)^2}{(f, MHz)^2 \cdot (10^6)^2 \cdot 4\pi \cdot 377} \right] \tag{C.17}$$

which, upon computing the constant terms, becomes:

$$(p_{load}, mW) = \left[\frac{1.90 \cdot 10^{-8} \cdot g \cdot (V_{space}, \mu V/m)^2}{(f, MHz)^2} \right] \quad . \tag{C.18}$$

Taking 10log of both sides gives:

$$10\log(p_{load}, mW) = (-77.2\ dB) + 10\log(g) + 20\log(V_{space}, \mu V/m) - 20\log(f, MHz) \quad . \tag{C.19}$$

Rearrangement of terms yields:

$$(field\ strength, dB\mu V/m) = (P_{load}, dBm) + (77.2\ dB) + 20\log(f, MHz) - G \quad . \tag{C.20}$$

Note that P_{load} is related to the power measured within a circuit (e.g., a spectrum analyzer) by the correction for path gain between the antenna and the analyzer: $P_{load} = P_{meas}$ - (path gain to antenna). This changes Eq. C.20 to:

$$(fieldstrength, dB\mu V/m) = (P_{meas}, dBm) - (path\ gain) + (77.2\ dB) + 20\log(f, MHz) - G. \tag{C.21}$$

Eq. C.21 is key for the conversion of measured power in a circuit into incident field strength in dBµV/m. For example, suppose that an antenna has gain G = 17 dB, at a frequency of 2300

MHz, with 28 dB path gain between the antenna and the spectrum analyzer. The measured power is -12 dBm on the spectrum analyzer display. Then field strength is +87 dBµV/m.

If an equation is required to relate field strength in dBµV/m to the *ACF*, then Eq. C.8 is used to relate acf to voltage in a circuit and free-space field strength:

$$\frac{V_{load}^2}{50} = (p_{load}) = \frac{V_{space}^2}{(50 \cdot acf)} \quad . \tag{C.22}$$

Converting power in watts into power in milliwatts, and converting voltage in volts/meter into microvolts/meter, gives

$$(p_{load,\ mW}) = \left[\frac{1000 \cdot (10^{-6})^2 \cdot (V_{space,\ \mu V/m})^2}{50 acf}\right] \tag{C.23}$$

which, upon computing the group of constant terms, gives:

$$(p_{load,\ mW}) = \frac{(2 \cdot 10^{-11}) \cdot (V_{space,\ \mu V/m})^2}{acf} \tag{C.24}$$

and which, taking 10log of both sides, means that

$$(P_{load,\ dBm}) = (-107\ dB) + (V_{space,\ dB\mu V/m}) - ACF \quad . \tag{C.25}$$

Rearranging terms and substituting [P_{meas} - (path gain)] for P_{load}:

$$V(dB\mu V/m) = P_{meas} - (path\ gain) + (107\ dB) + ACF \quad . \tag{C.26}$$

For example, suppose a measurement of -12 dBm is taken on a spectrum analyzer, with 28 dB net gain in the path between the antenna and the analyzer, and measurement antenna acf of 111 (corresponding to G = 17 dBi at 2300 MHz, as in the example above). Then *ACF* = 20.5 dB, and the corresponding free-space field strength is computed using Eq. C.26 to be +87 dBµV/m.

C.3 Effective Isotropic Radiated Power Conversion

It may be necessary to know the effective isotropic radiated power (EIRP) that a device transmits. The conversion from measured power in a circuit to EIRP is described in this section.

Free space loss must be determined: For transmit power (watts) p_t; transmit antenna gain relative to isotropic g_t; receive antenna gain relative to isotropic g_r; receive power (watts) p_r; and receive antenna effective aperture a_e; the effective isotropic radiated power is

$$(eirp) = (p_t \cdot g_t) \tag{C.27}$$

and

$$p_r = a_e \cdot \left(\frac{eirp}{4\pi r^2} \right) \tag{C.28}$$

with r being the distance between the transmit and receive antennas.

The effective aperture of the antenna is the effective aperture of an isotropic antenna multiplied by the antenna's gain over isotropic, or

$$a_e = \left(\frac{\lambda^2}{4\pi} \right) \cdot g_r \quad . \tag{C.29}$$

A change to decibel units makes Eq. C.28:

$$P_r = EIRP + G_r + 20\log(\lambda) - 20\log(4\pi) - 20\log(r) \quad . \tag{C.30}$$

Substituting c/f for 8,

$$P_r = EIRP + G_r + 20\log(c) - 20\log(f) - 20\log(4\pi) - 20\log(r) \quad . \tag{C.31}$$

If frequency is in megahertz and distance is in meters, then Eq. C.31 becomes

$$P_r = EIRP + G_r + 20\log(c) - 20\log(f, MHz \cdot 10^6) - 20\log(4\pi) - 20\log(r) \quad , \tag{C.32}$$

which yields

$$P_r = EIRP + G_r + 169.5 - 20\log(f, MHz) - 120 - 22 - 20\log(r, meters) \tag{C.33}$$

or

$$P_r = EIRP + G_r + 27.5 - 20\log(f,MHz) - 20\log(r, meters) \quad , \tag{C.34}$$

Similarly, for r in kilometers, Eq. C.31 becomes

$$P_r = EIRP + G_r - 32.5 - 20\log(f, MHz) - 20\log(r, km) \quad \text{(C.35)}$$

and Eq. C.31 for r in miles is

$$P_r = EIRP + G_r - 36.5 - 20\log(f, MHz) - 20\log(r, miles) \quad . \quad \text{(C.36)}$$

For measurements of Part 15, Part 18, and ultrawideband transmitters, Eq. C.34 is convenient. If the gain of the receive antenna is known and the received power has been measured at a known distance from the emitter, then Eq. C.34 can be rearranged to yield *EIRP:*

$$(EIRP, dBW) = (P_r, dBW) - G_r - 27.5 + 20\log(f, MHz) + 20\log(r, meters) \quad . \quad \text{(C.37)}$$

If the received power is measured in dBm rather than dBW, Eq. C.37 becomes

$$(EIRP, dBW) = (P_r, dBm) - G_r - 57.5 + 20\log(f, MHz) + 20\log(r, meters) \quad . \quad \text{(C.38)}$$

If EIRP in decibels relative to a picowatt (dBpW) is required, then Eq. C.38 becomes:

$$(EIRP, dBpW) = (P_r, dBm) - G_r + 62.5 + 20\log(f, MHz) + 20\log(r, meters) \quad . \quad \text{(C.39)}$$

For example, if a value of -10 dBm is measured at a frequency of 2450 MHz, with an antenna gain +16.9 dBi, at a distance of 3 meters, then the EIRP value is +113 dBpW.

Effective radiated power relative to a dipole (ERP_{dipole}) is sometimes required. EIRP is 2.1 dB higher than ERP_{dipole}.

Finally, the conversion to incident power density is considered. The incident power density, P_{den}, in W/m^2, is equal to the incident field strength squared (units of $(V/m)^2$), divided by the ohmic impedance of free space:

$$(P_{den}, W/m^2) = \left(\frac{(field\ strength, V/m)^2}{377} \right) \quad . \quad \text{(C.40)}$$

Using more common units for field strength of (dBµ*V/m*), and more common units for incident power of ($\mu W/cm^2$):

$$(1\ W/m^2) = \frac{100\ \mu W}{cm^2} = \frac{10^{12}}{377}(\mu V/m)^2 \quad \text{(C.41)}$$

gives

$$1\ (\mu W/cm^2) = \frac{10^{10}\ (\mu V/m)^2}{377} \quad . \tag{C.42}$$

The incident power density is thus

$$(P_\rho,\ \mu W/cm^2) = \frac{377}{10^{10}} \cdot (field\ strength,\ \mu V/m)^2 \tag{C.43}$$

or

$$(P_\rho,\ \mu W/cm^2) = 3.77 \cdot 10^{-8} \cdot (field\ strength,\ \mu V/m)^2 \quad . \tag{C.44}$$

C.4 Correction of Measured Emission Spectra for Non-Constant Effective Aperture Measurement Antennas

With reference to Eq. C.5, the effective aperture of an isotropic antenna as a function of frequency, f, is:

$$a_e = \frac{g}{4\pi f^2} \tag{C.45}$$

or

$$A_e = G - 10\log(4\pi) - 20\log(f) \quad . \tag{C.46}$$

If gain relative to isotropic, g, is arbitrarily normalized to 4B, then the functional dependence of effective aperture on frequency is clear:

$$A_e \propto -20\log(f) \quad . \tag{C.47}$$

The effective aperture of a constant-gain isotropic antenna decreases as the square (i.e., 20 log) of the frequency. If an isotropic antenna were realized physically, and were then used to measure an emission spectrum, it would be necessary to correct the measured spectrum for this drop in aperture with increasing frequency.

For an isotropic antenna, the measured spectrum amplitudes would have to be increased as (20log(frequency)) to represent the energy that would be coupled into a constant effective aperture. Parabolic reflector antennas in principle have constant apertures; their gain nominally

increases at the rate of (20 log(frequency)). Consequently emission spectra measured with high-performance parabolic antennas do not require antenna aperture corrections.

Wideband horn antennas represent an intermediate case between the (-20 log) decrease in effective aperture of theoretical isotropic antennas and the constant-aperture condition of nominal parabolic reflector antennas. For example, the gain curve of a widely used double-ridged waveguide horn (Figure C.1) increases with frequency, but at the rate of approximately (6.7 log(frequency)). Since this is [(20-6.7)log] = 13.3 log below a constant-aperture condition, the spectra measured with such an antenna must be corrected at the rate of (13.3 log(frequency)).

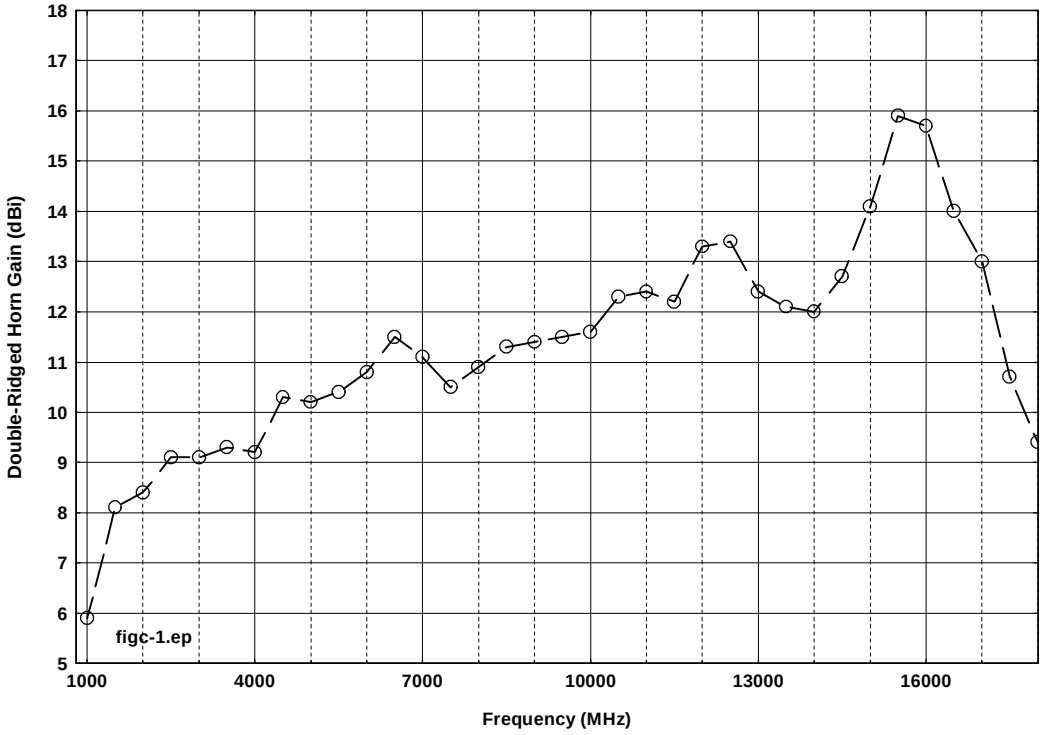

Figure C.1. Broadband double-ridged waveguide antenna gain as a function of frequency. The effective aperture would be constant if the gain curve varied as 20log frequency).

Operationally, this correction is performed by ITS engineers as follows: The spectrum is measured across a given frequency range and the uncorrected curve is stored. During the data analysis phase, the original spectrum is corrected relative to an arbitrarily chosen frequency, according to the following equation:

$$\left(P_{corrected}\right) = \left(P_{measured}\right) + 13.3\left[\log\left(\frac{f_{measured}}{f_{reference}}\right)\right] \quad . \qquad \text{(C.48)}$$

For example, if a spectrum is measured between 1 GHz and 5 GHz, a convenient reference frequency might be 1 GHz, since the corrected spectrum will then have a zero correction at the left-hand side of the graph. The correction will increase from zero at 1 GHz to a maximum of 9.3 dB at 5 GHz on the right-hand side of the graph, as in Figure C.2.

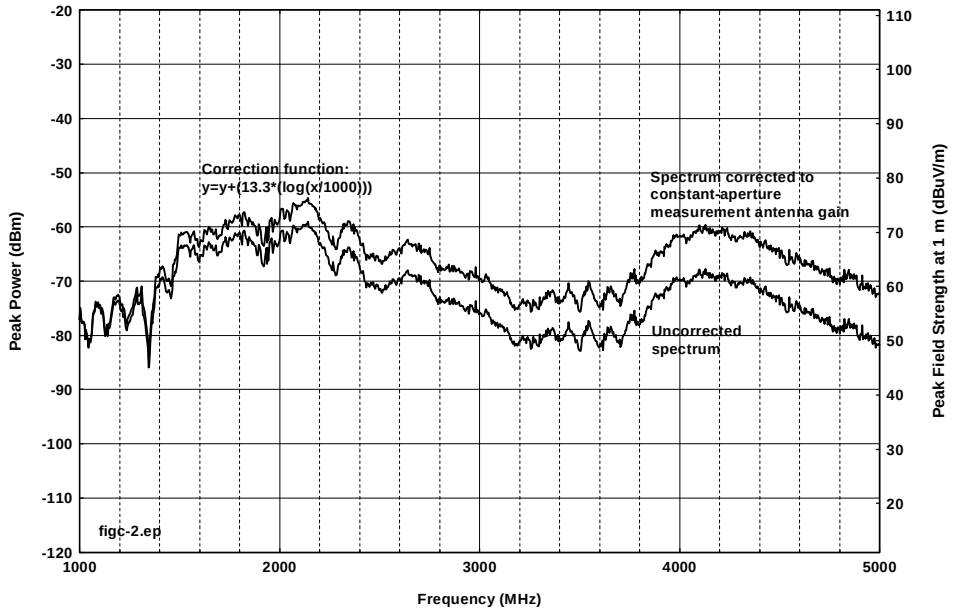

Figure C.2. Demonstration of emission spectrum measurement corrected to a constant effective aperture measurement antenna. With this correction it becomes possible to add a second axis for incident field strength.

The graph's power-axis label needs to reflect the fact that the spectrum has been rendered as measured with a constant-effective-aperture antenna. This can be done in two ways. The first is to reference the antenna's gain relative to isotropic at the reference frequency. If the antenna in question had 5.9 dBi gain at the reference frequency of 1 GHz, then the axis label could read: "Power measured with constant-aperture antenna, 5.9 dBi gain at 1 GHz (dBm)."

The label above might as easily refer to the antenna correction factor (acf) of the antenna at the reference frequency. The second method is to compute the effective aperture of the antenna and quote that in the label. In this example, the gain of 5.9 dBi at 1 GHz yields an effective aperture in Eq. C.45 of 3.1×10^{-7} m^2. The corresponding axis label could read:

"Power measured with antenna of constant effective aperture 3.1×10^{-7} m^2 (dBm)"

While accurate, this expression's reference to an effective aperture is unconventional.

An advantage of correcting a measured emission spectrum to constant measurement antenna effective aperture is that a second axis can be added to the right-hand side of the graph showing

field strength. With the effective aperture correction having been made, the field strength becomes an additive factor to the power measured in a circuit. In this example (5.9 dBi gain at 1 GHz, constant aperture correction made to the rest of the spectrum), Eq. C.21 is used to arrive at the following conversion to field strength:

$$(Field\ strength,\ dB\mu V/m) = P_{meas} - (path\ gain) + 77.2 + (60 - 5.9) \qquad \text{(C.49)}$$

or

$$(Field\ strength,\ dB\mu V/m) = P_{meas} - (path\ gain) + (131\ dB) \quad . \qquad \text{(C.50)}$$

Figure C.2 shows an example of a corrected spectrum with the field strength axis added in accordance with Eq. C.48 and Eq. C.50.

C.5 References

[1] E. C. Jordan, Ed., *Reference Data for Engineers: Radio, Electronics, Computer, and Communications,* Seventh ed., Macmillan, 1989, pg. 32-33.

This Page Intentionally Left Blank

This Page Intentionally Left Blank

APPENDIX D. EMISSION DATA FOR ULTRAWIDEBAND TRANSMITTERS

Frank Sanders,[1] Brent Bedford,[1] Robert T. Johnk,[2] and Robert Matheson[1], David R. Novotny[2]

This appendix contains measured emission spectra and time waveforms for five ultrawideband transmitters, and also for a Part 15 device (specifically, an electric drill). Measurement techniques are described in Sections 5 and 6. Analysis and commentary are provided in Section 8.

[1]The authors are with the Institute for Telecommunication Sciences, National Telecommunications and Information Administration, U.S. Department of Commerce, Boulder, CO 80305.

[2]The authors are with the Radio-Frequency Technology Division, National Institute for Standards and Technology, U. S. Department of Commerce, Boulder, CO 80305.

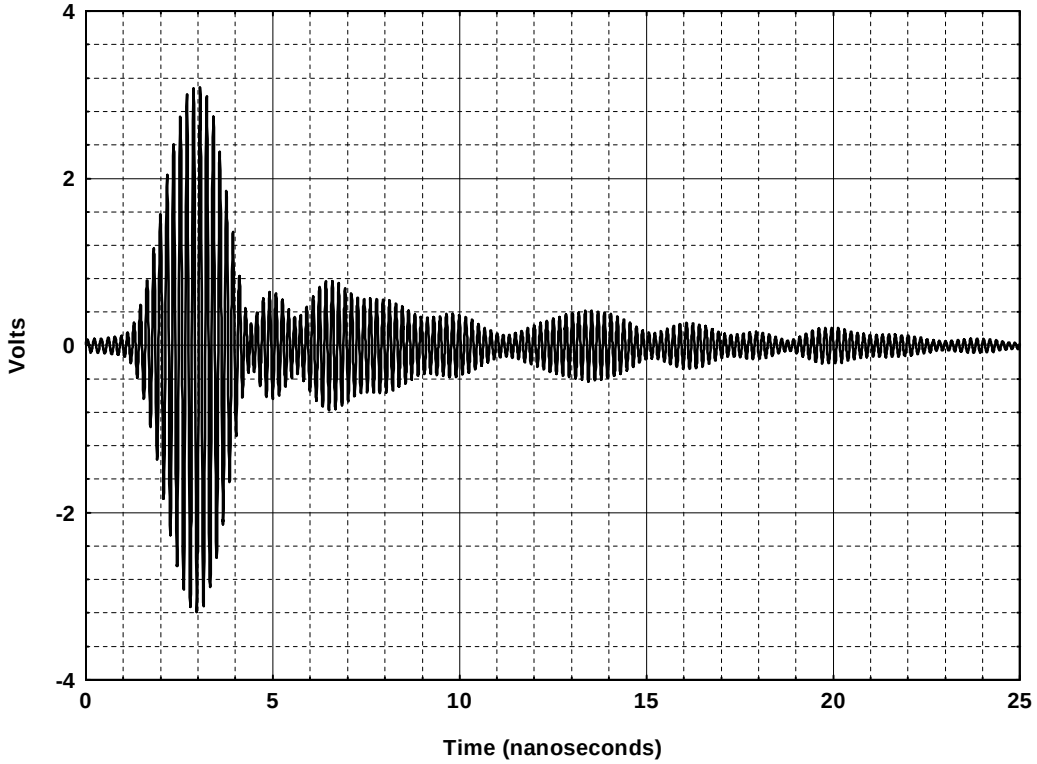

Figure D.A.1. Device A, conducted time-domain waveform.

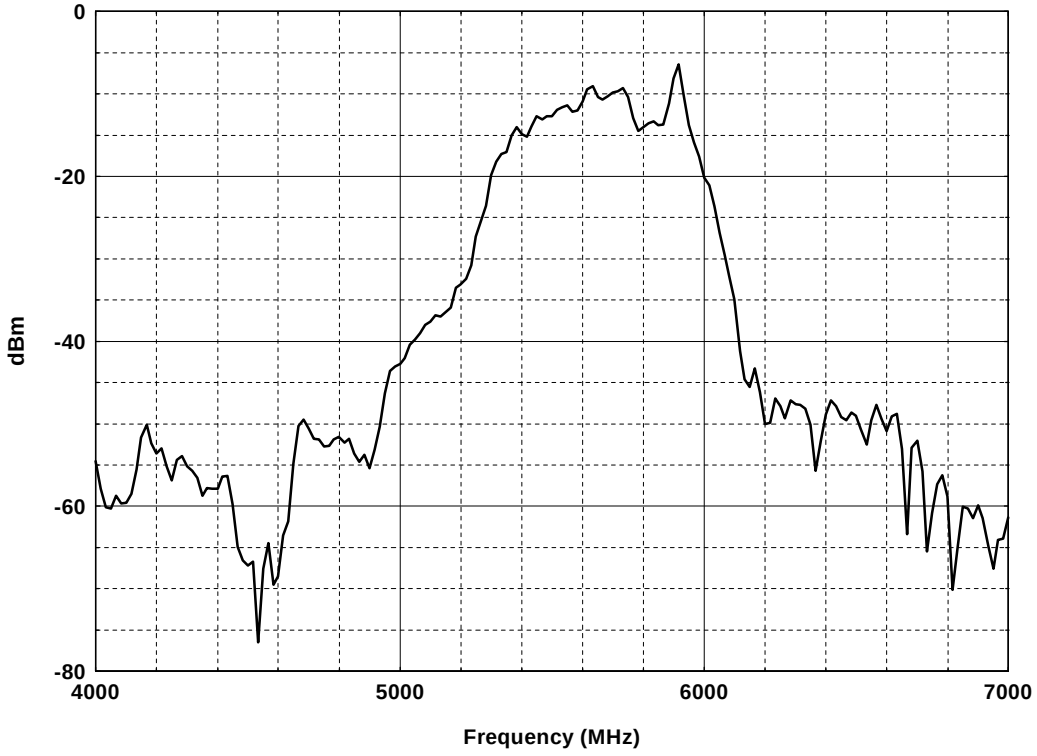

Figure D.A.2. Device A, conducted power spectrum,) f = 16.67 MHz.

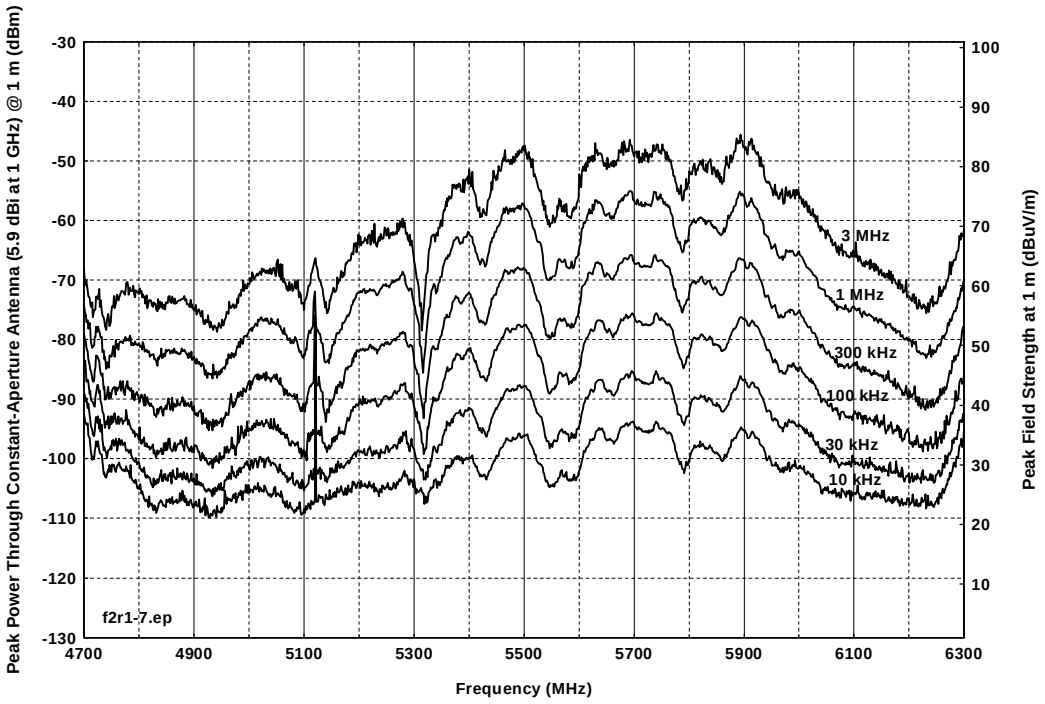

Figure D.A.3. Device A, spectra as a function of measurement bandwidth.

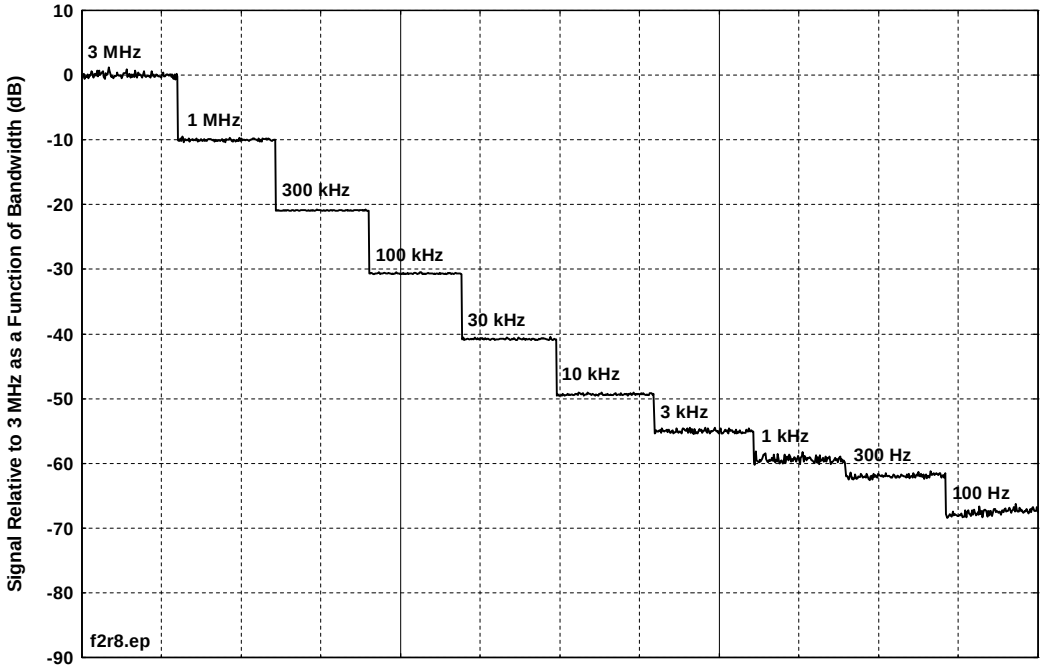

Figure D.A.4. Device A, peak signal level as a function of bandwidth.

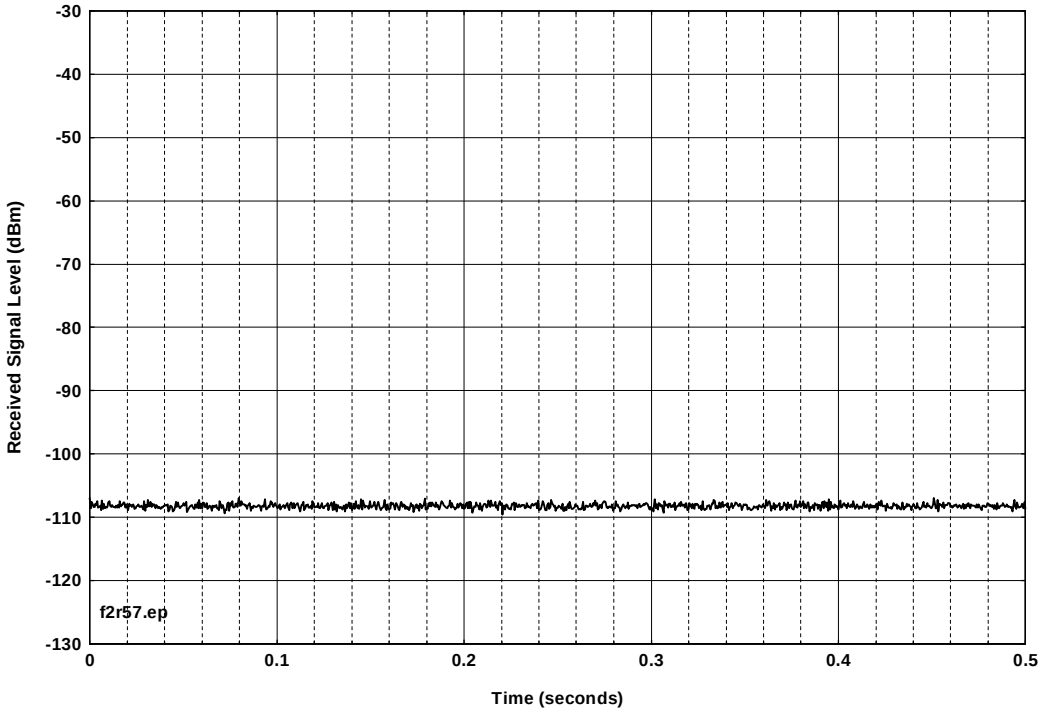

Figure D.A.5. Device A, emission in 10-kHz video bandwidth.

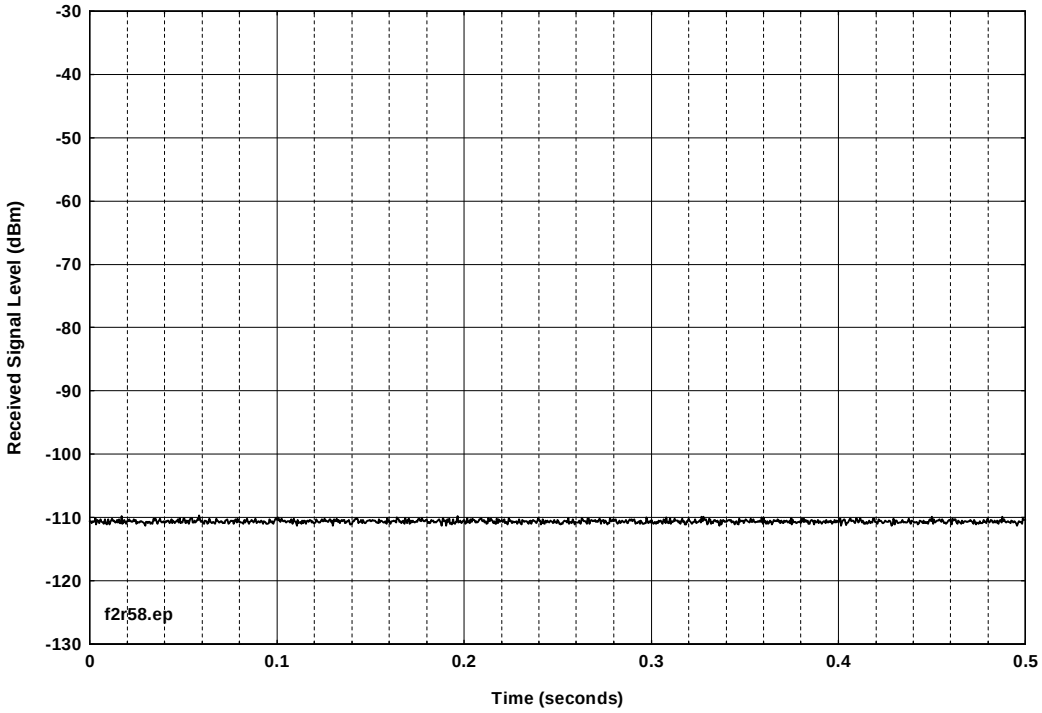

Figure D.A.6. Device A, emission in 3-kHz video bandwidth.

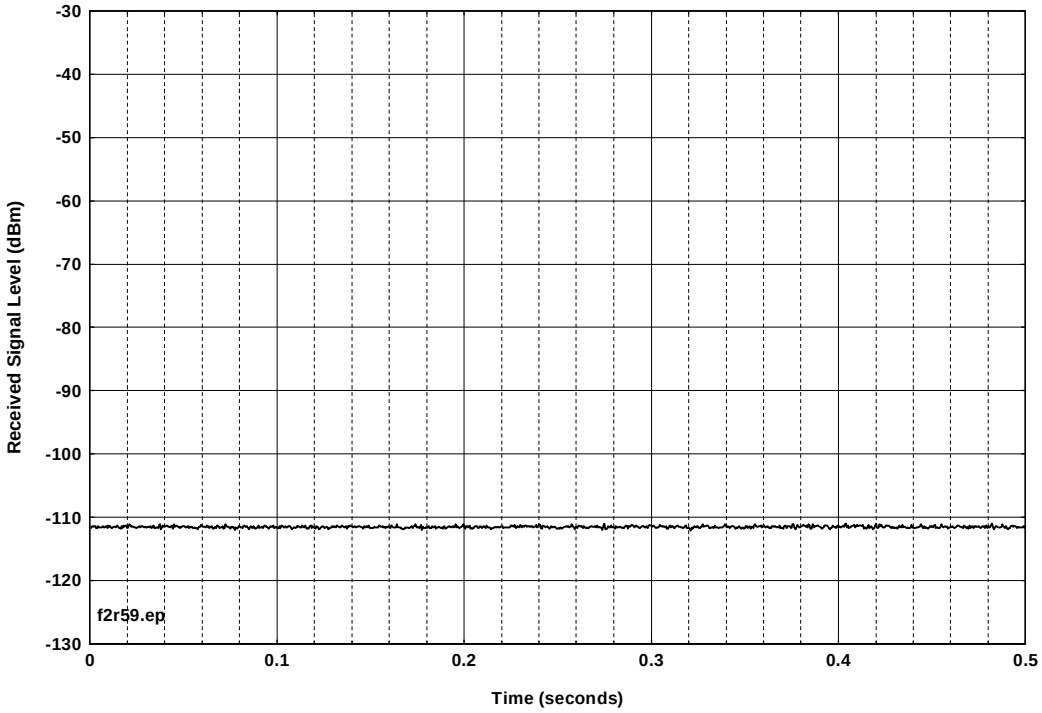

Figure D.A.7. Device A, emission in 1-kHz video bandwidth.

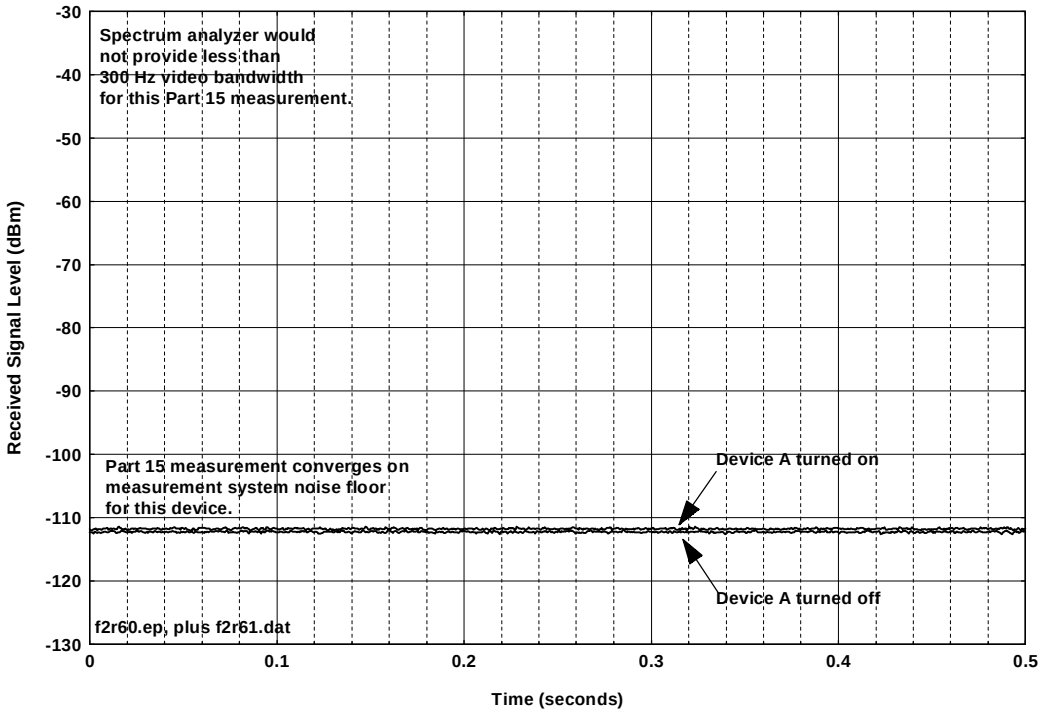

Figure D.A.8. Device A, emission in 300-Hz video bandwidth: converges on measurement system noise floor.

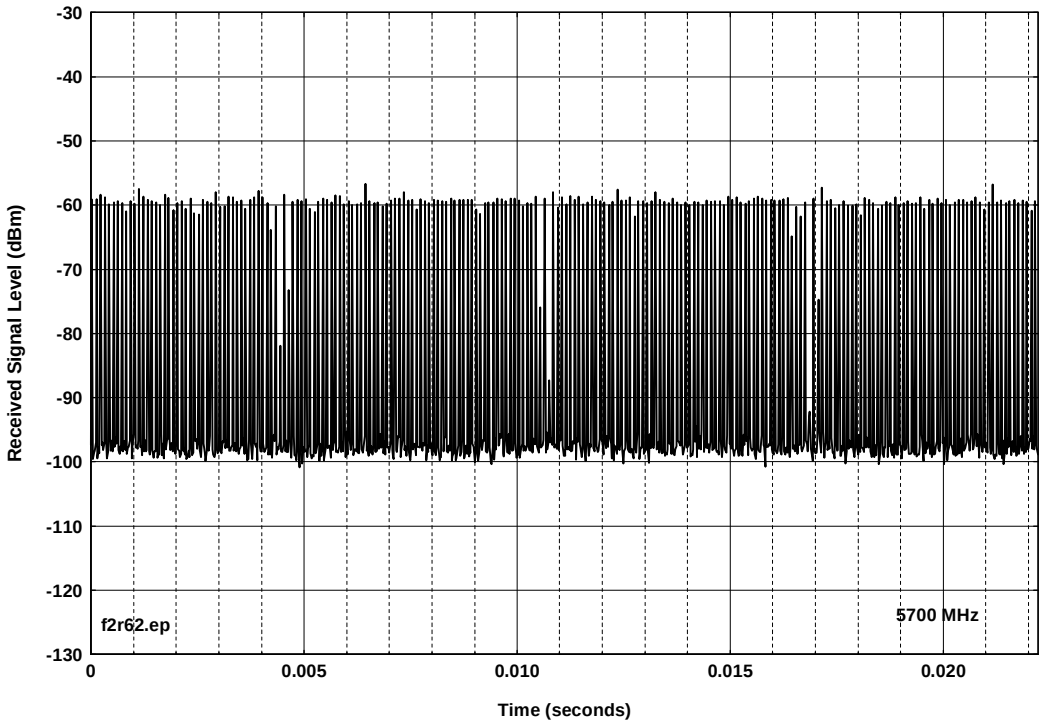

Figure D.A.9. Device A, peak emission in 3-MHz IF bandwidth.

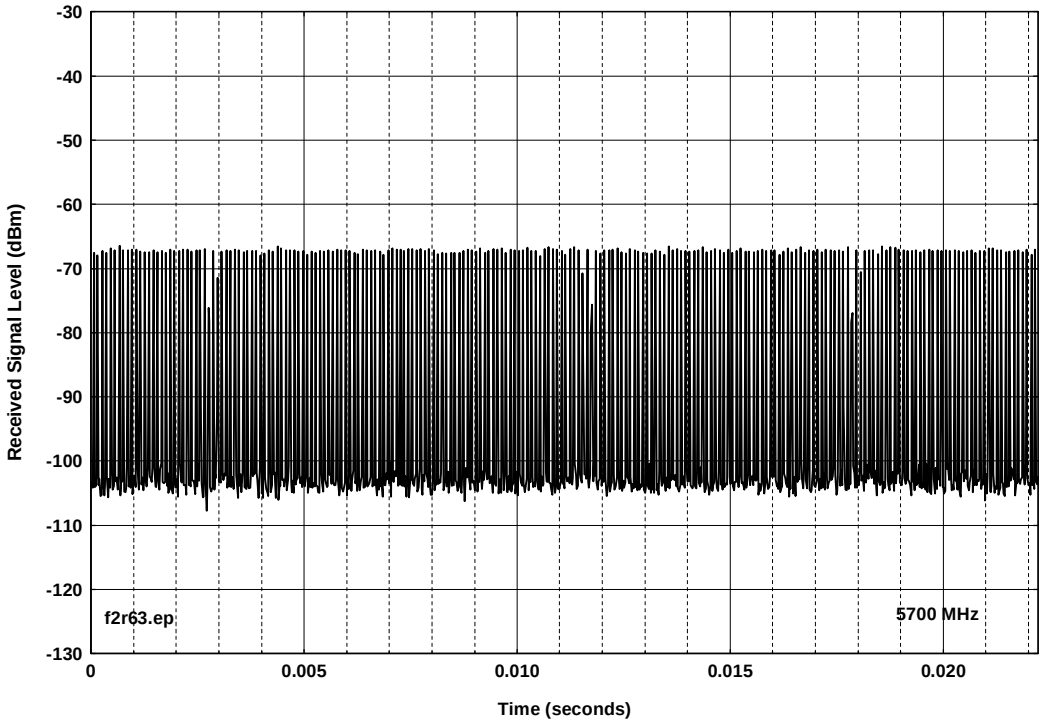

Figure D.A.10 Device A, peak emission in 1-MHz IF bandwidth.

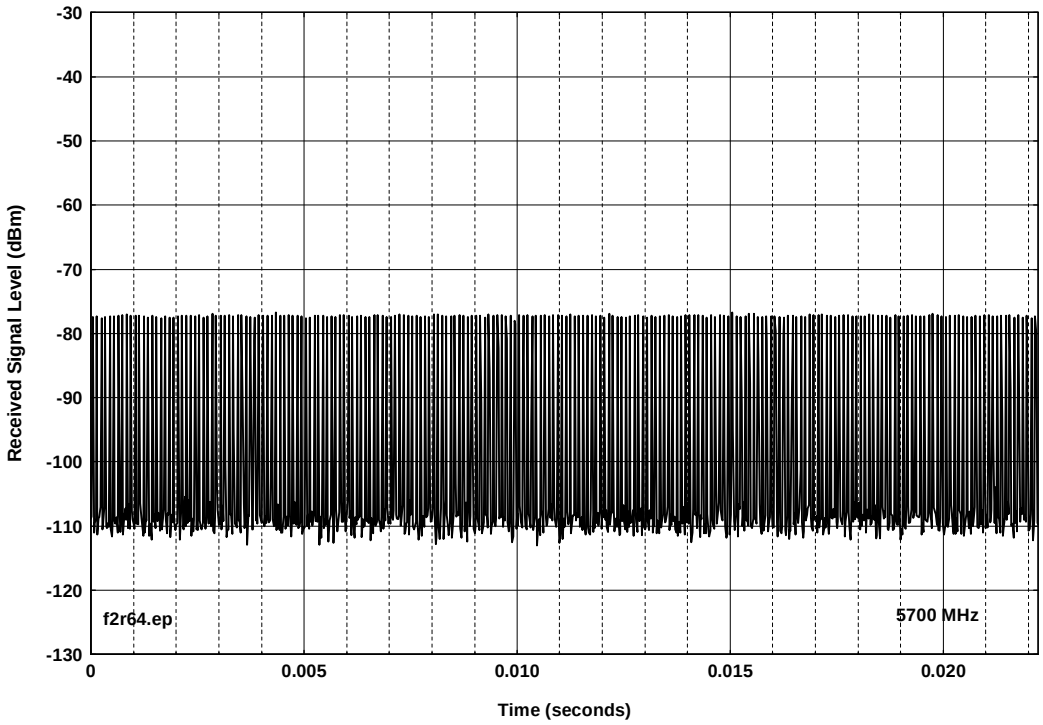

Figure D.A.11. Device A, peak emission in 300-kHz IF bandwidth.

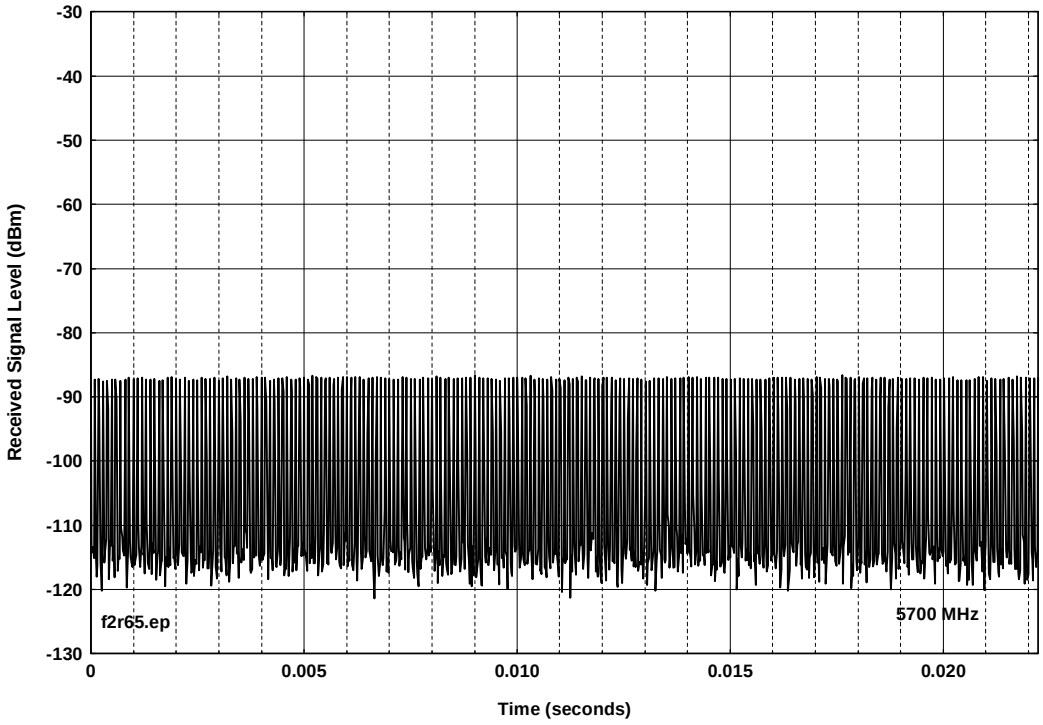

Figure D.A.12. Device A, peak emission in 100-kHz IF bandwidth.

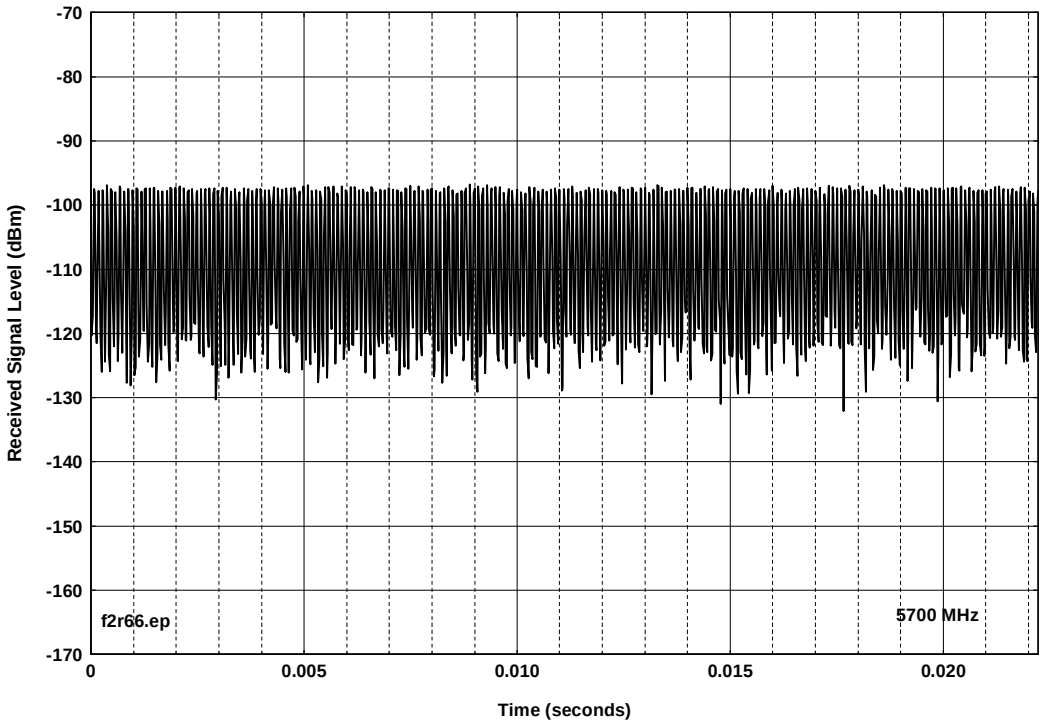

Figure D.A.13. Device A, peak emission in 30-kHz IF bandwidth.

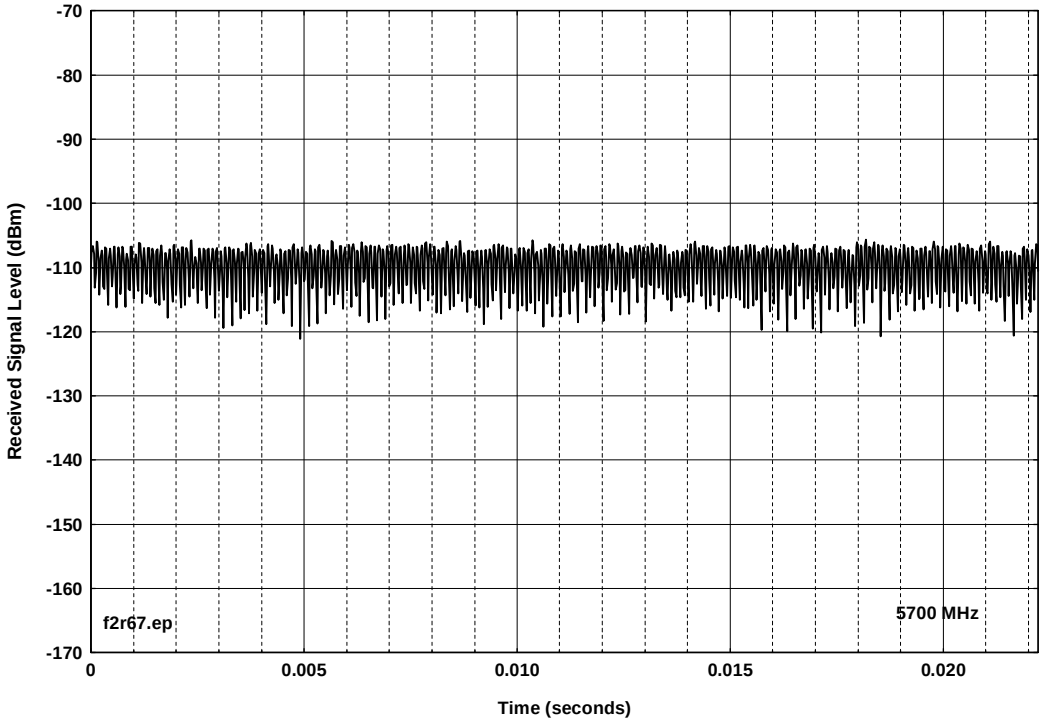

Figure D.A.14. Device A, peak emission in 10-kHz IF bandwidth.

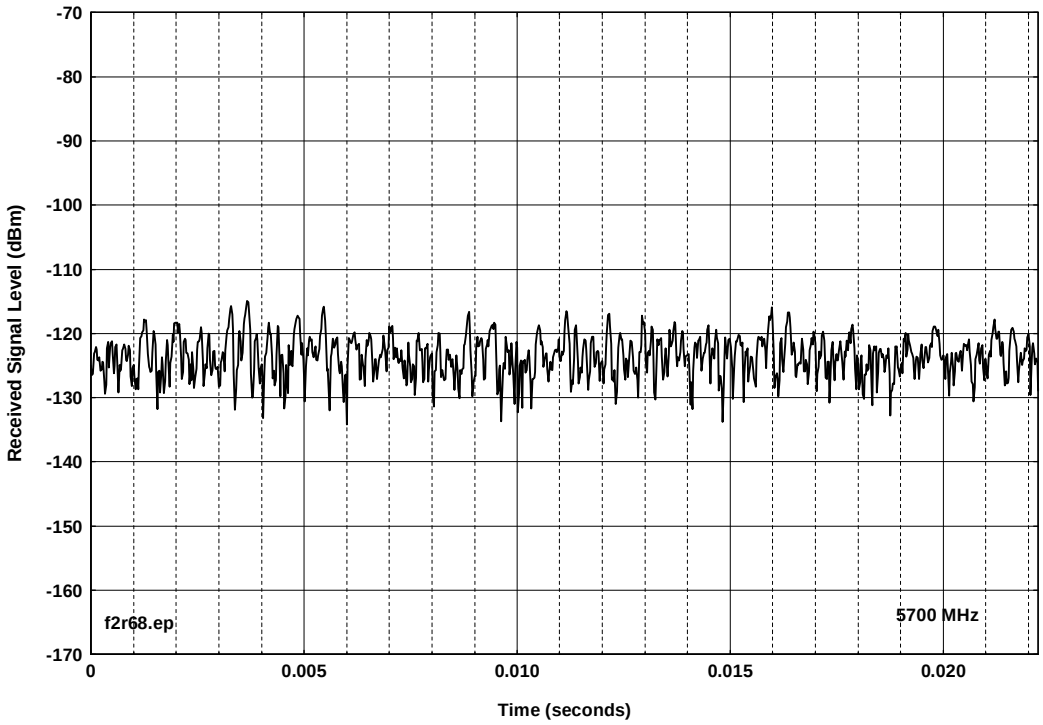

Figure D.A.15. Device A, peak emission in 3-kHz IF bandwidth.

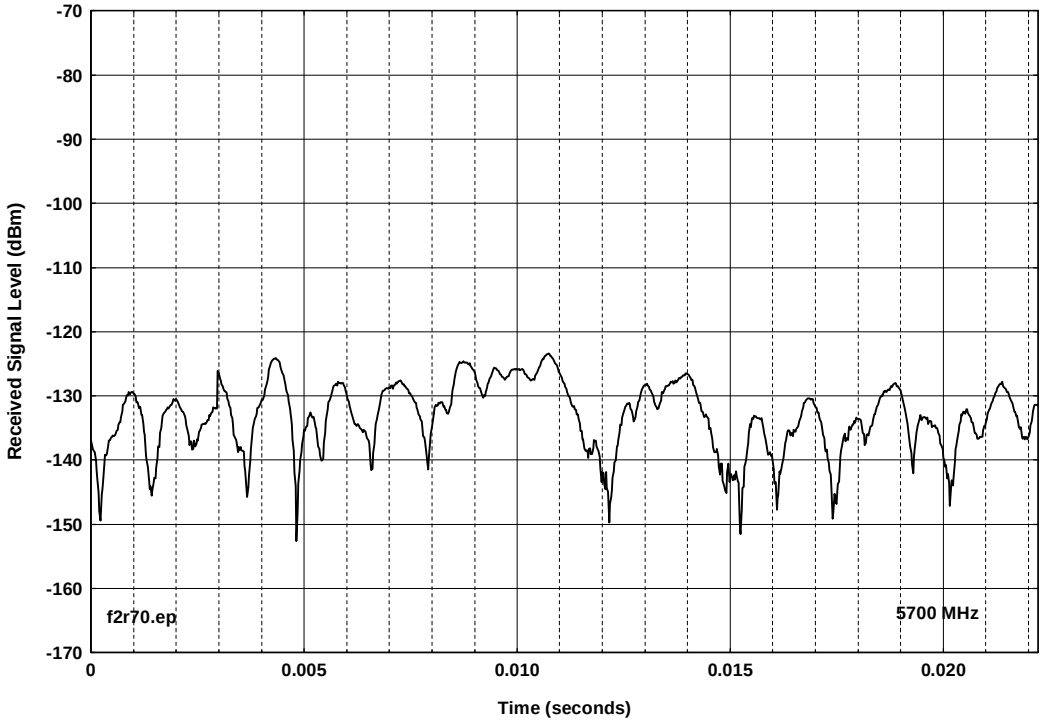

Figure D.A.16. Device A, peak emission in 1-kHz IF bandwidth.

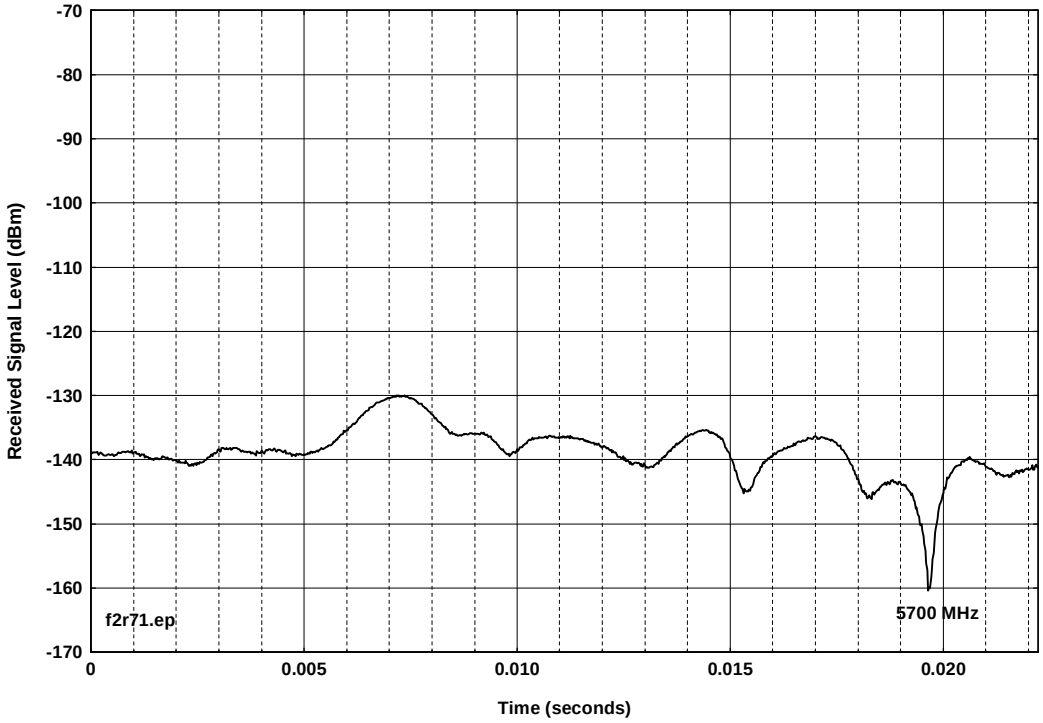

Figure D.A.17. Device A, peak emission in 300-Hz IF bandwidth.

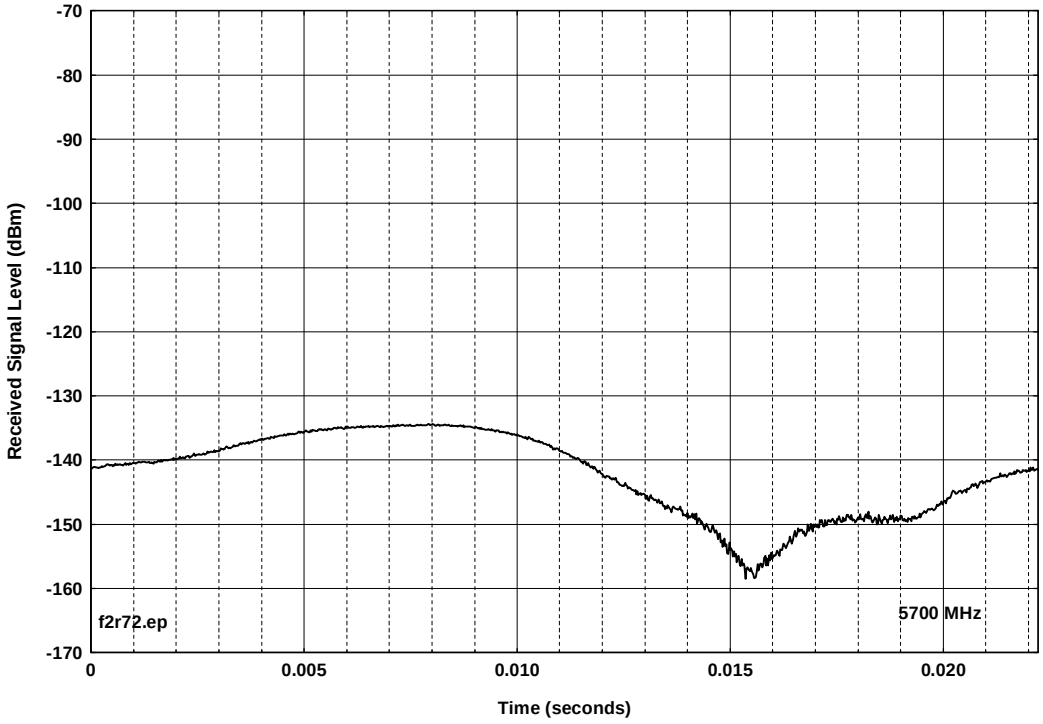

Figure D.A.18. Device A, peak emission in 100-Hz IF bandwidth.

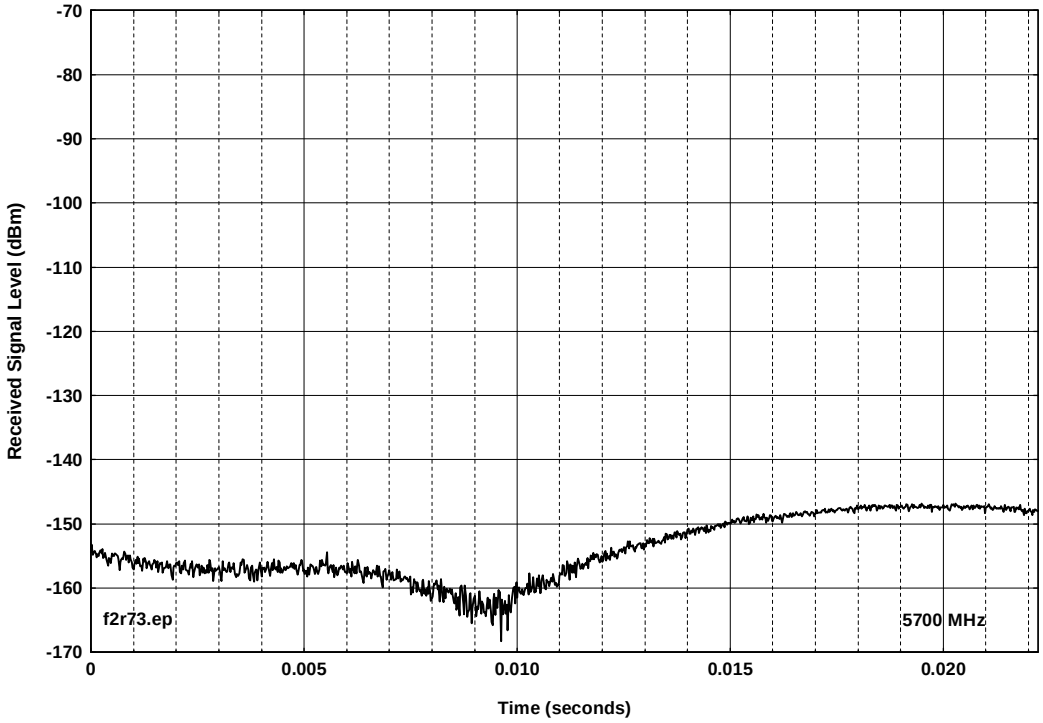

Figure D.A.19. Device A, peak emission in 30-Hz IF bandwidth.

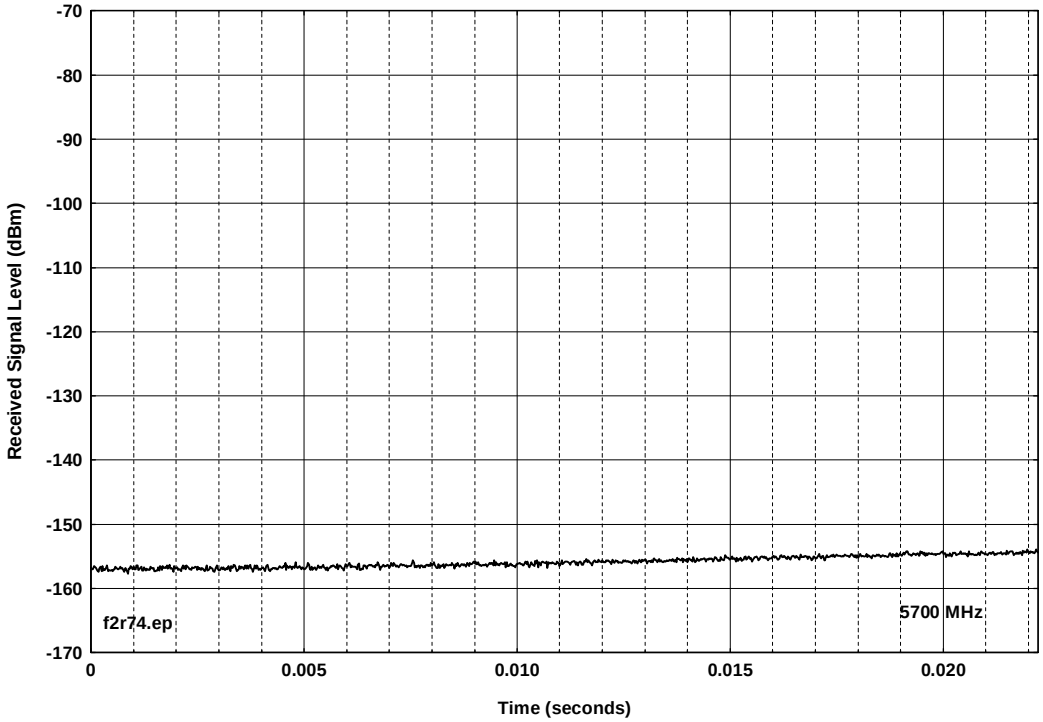

Figure D.A.20. Device A, peak emission in 10-Hz IF bandwidth.

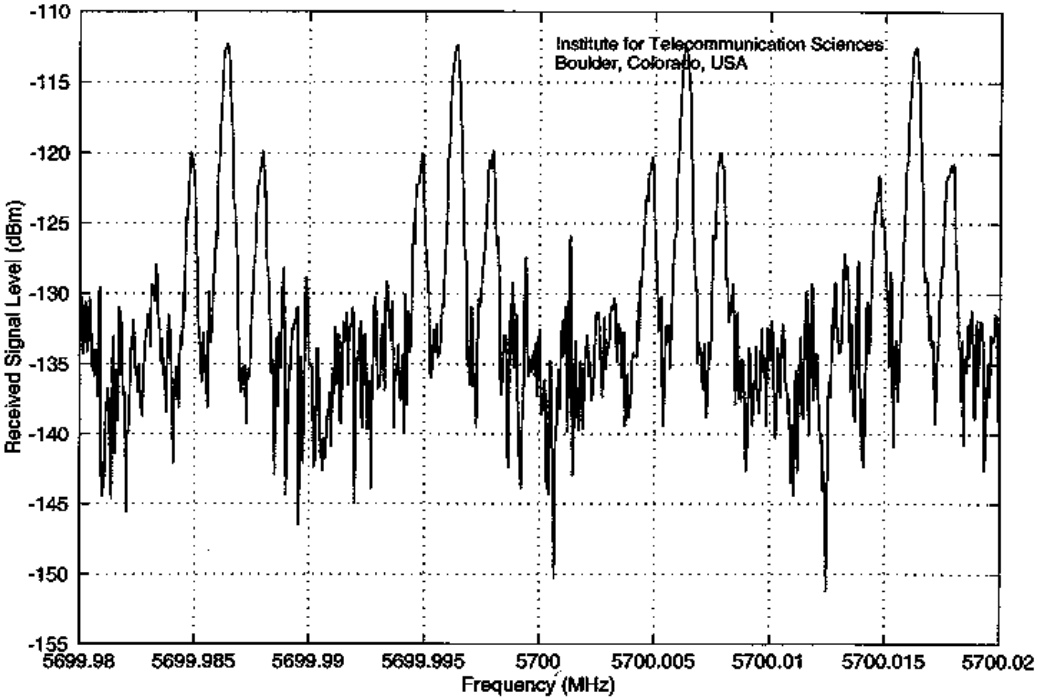

Figure D.A.21. Device A, spectrum fine structure.

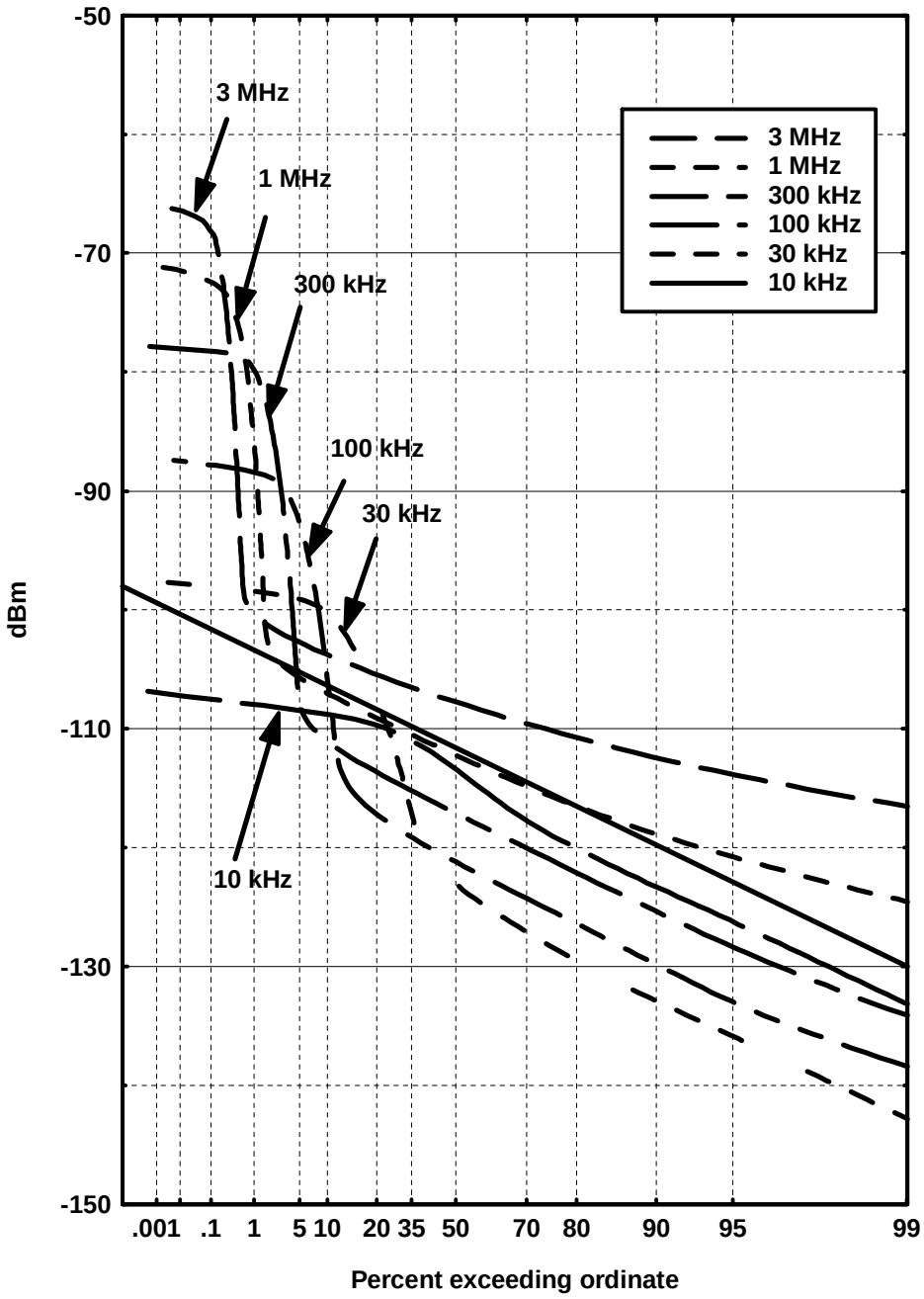

Figure D.A.22. Device A, APDs.

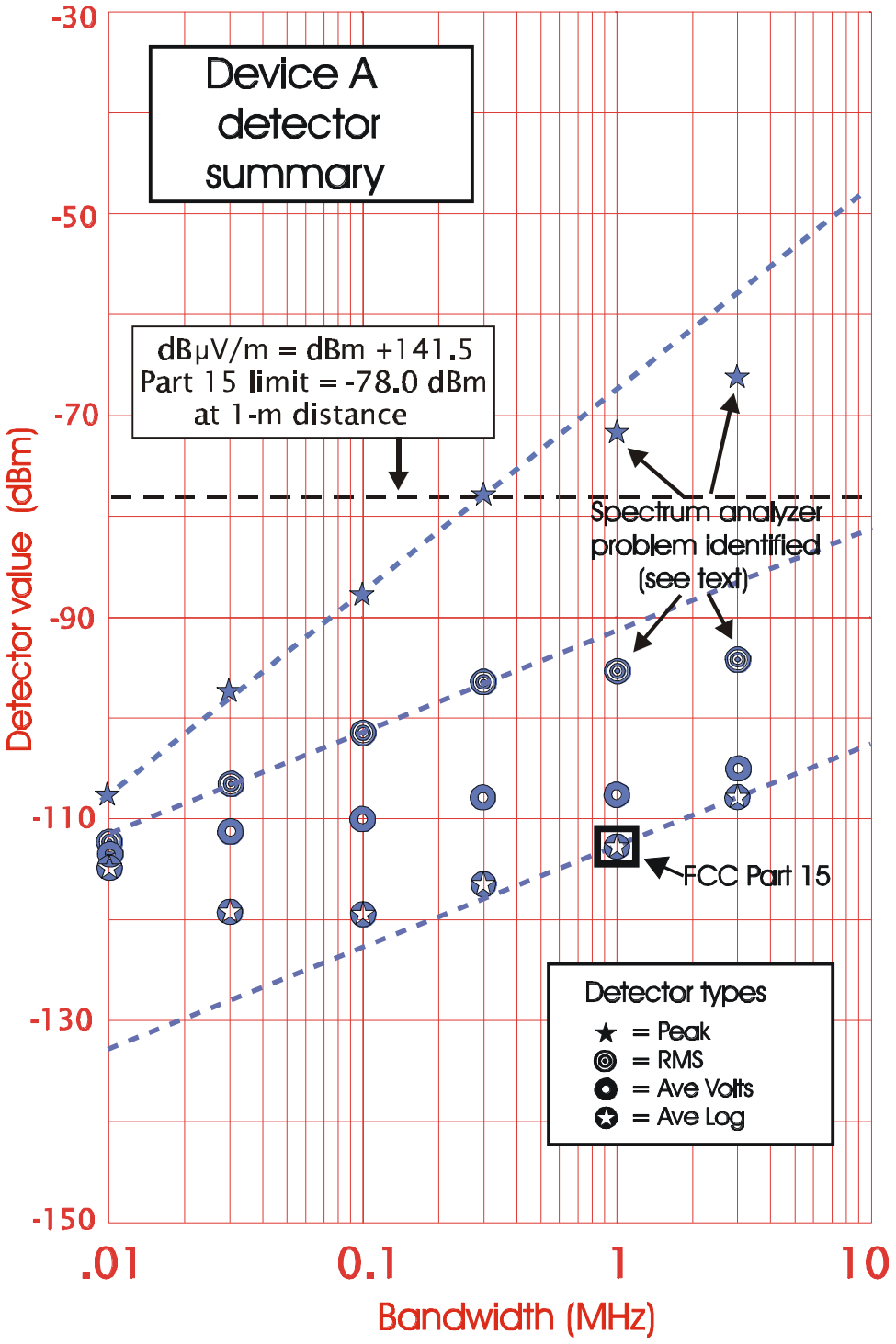

Figure D.A.23. Device A, detector summary.

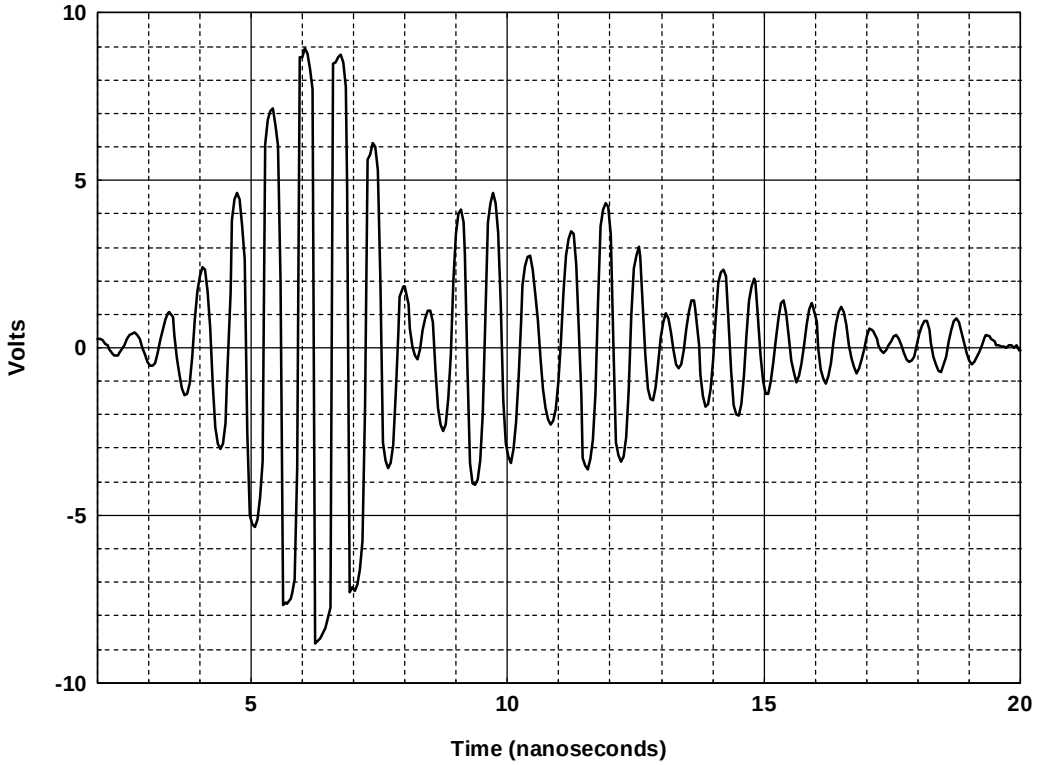

Figure D.B.1. Device B, conducted time-domain waveform.

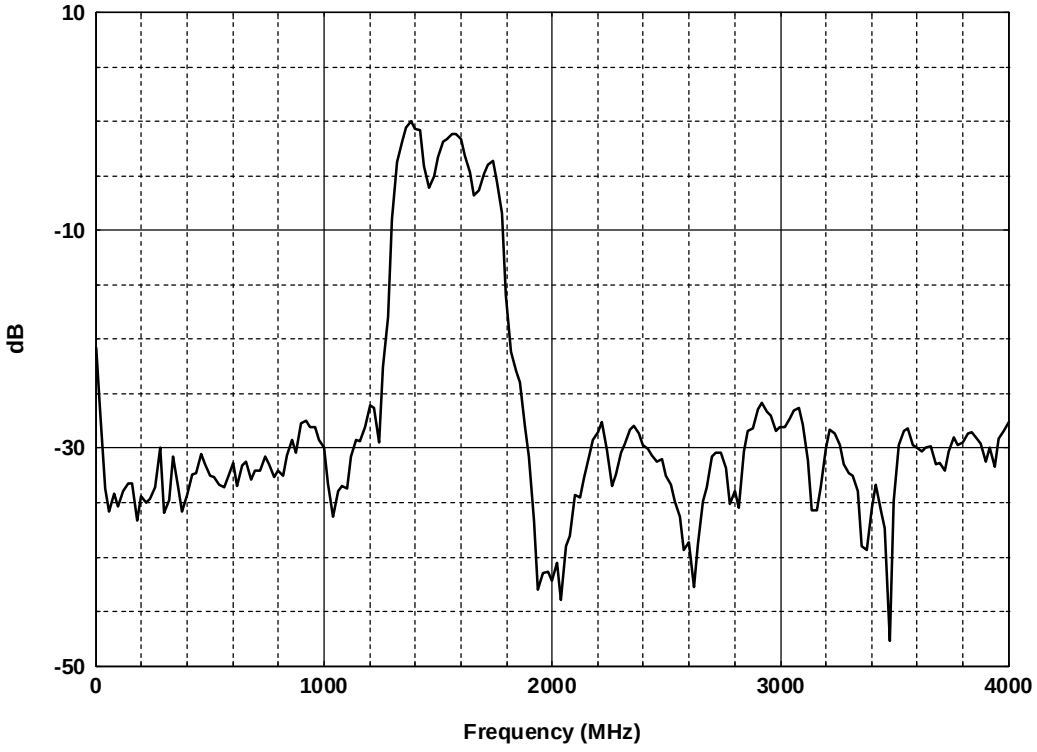

Figure D.B.2. Device B, conducted power spectrum,) f = 20 MHz.

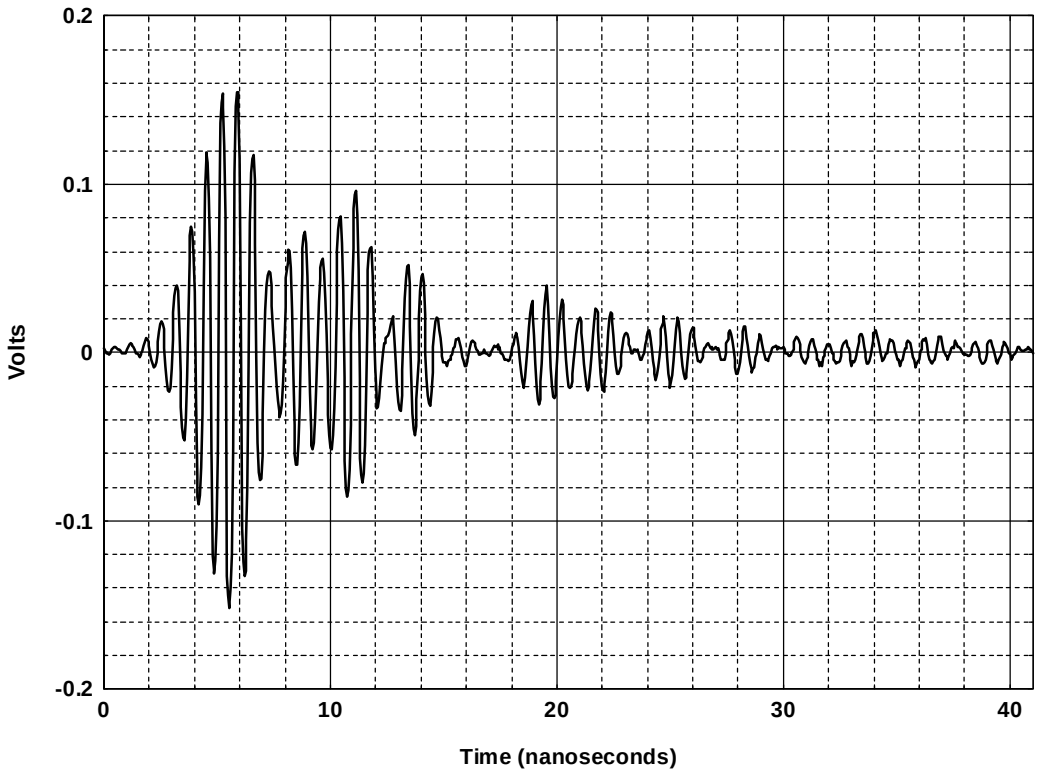

Figure D.B.3. Device B, radiated time-domain waveform.

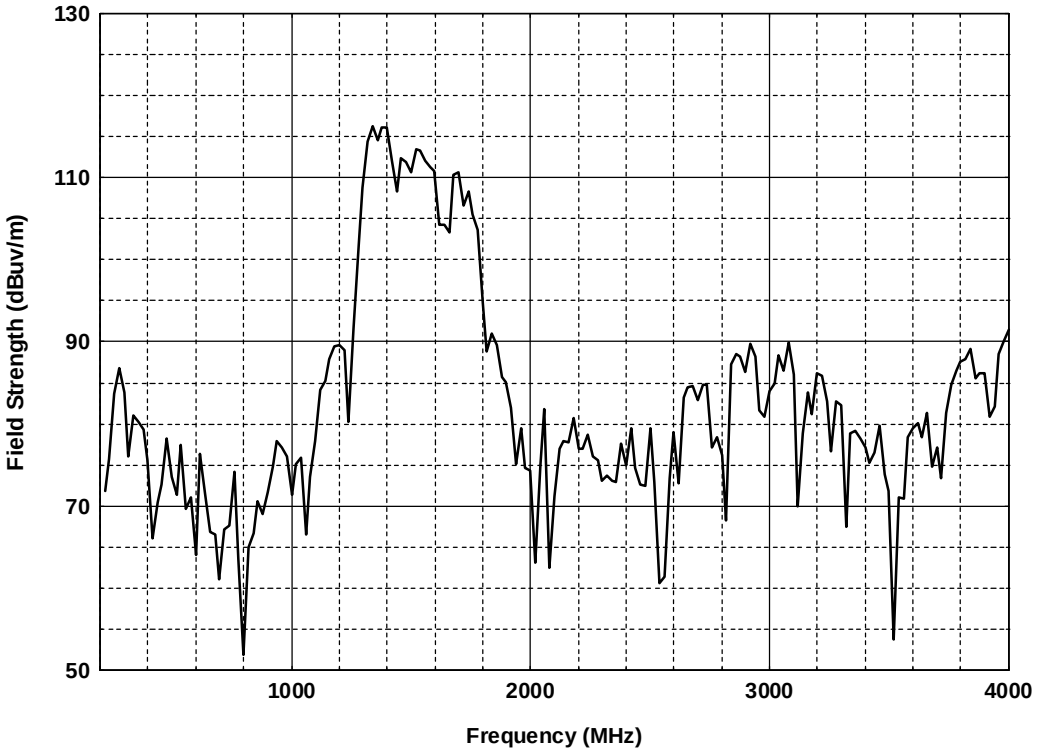

Figure D.B.4. Device B, radiated peak field strength at 1 m,) f = 20 MHz.

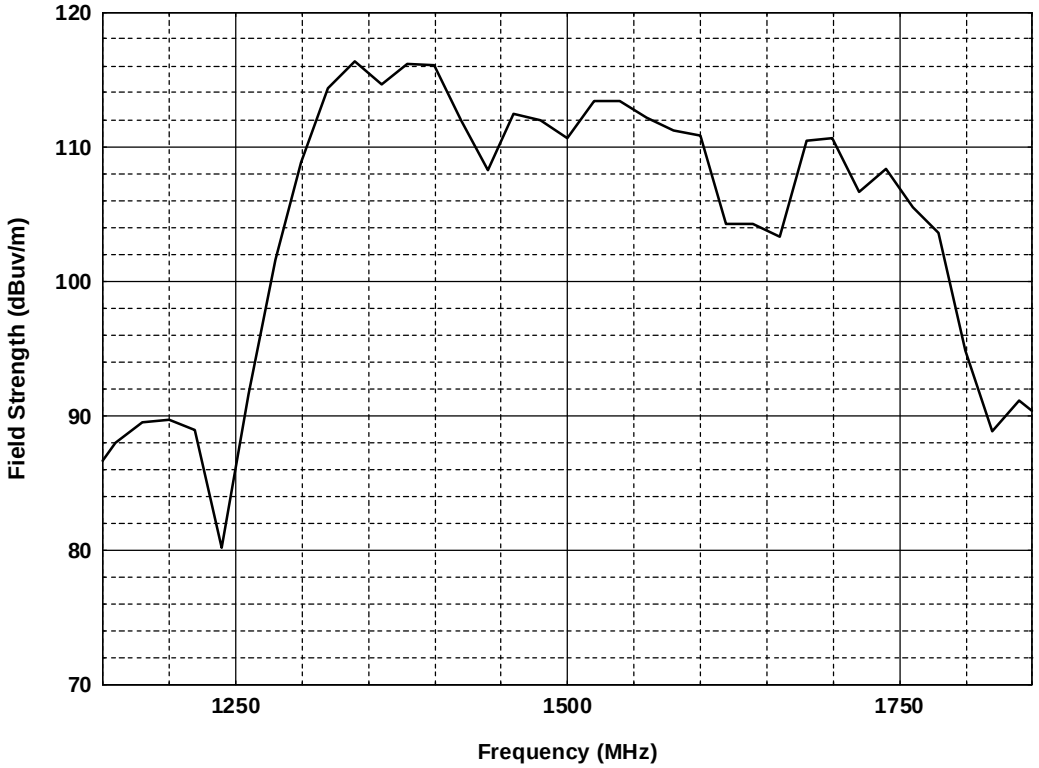

Figure D.B.5. Device B, radiated peak field strength at 1 m,) f = 20 MHz.

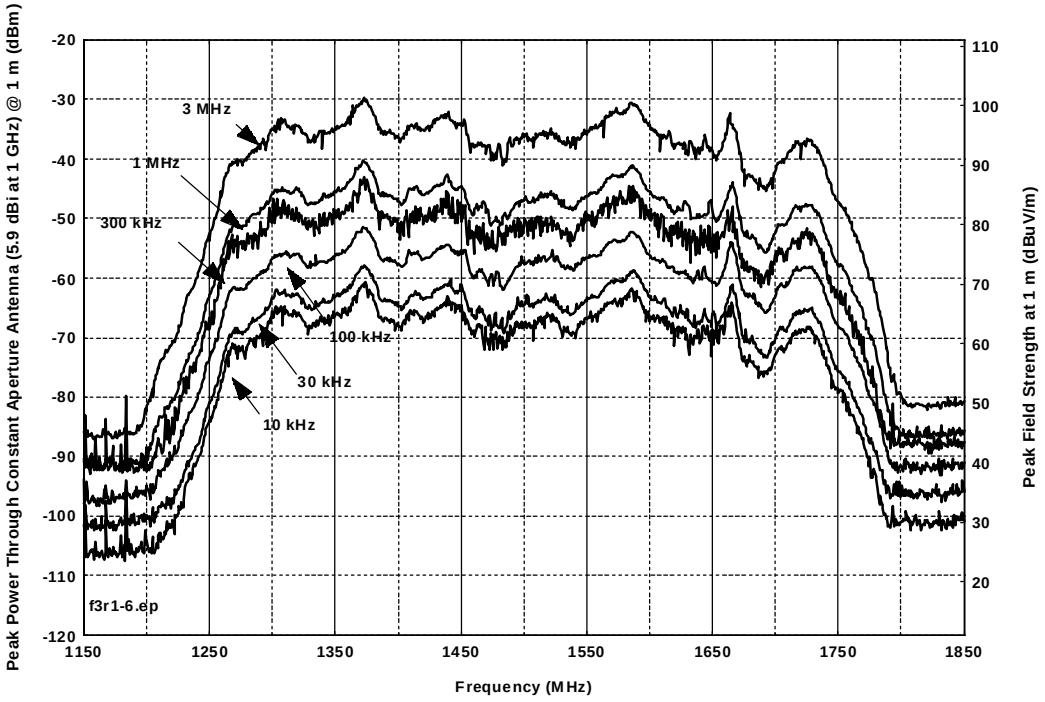

Figure D.B.6. Device B, spectra as a function of bandwidth, 16-kB/s voice mode.

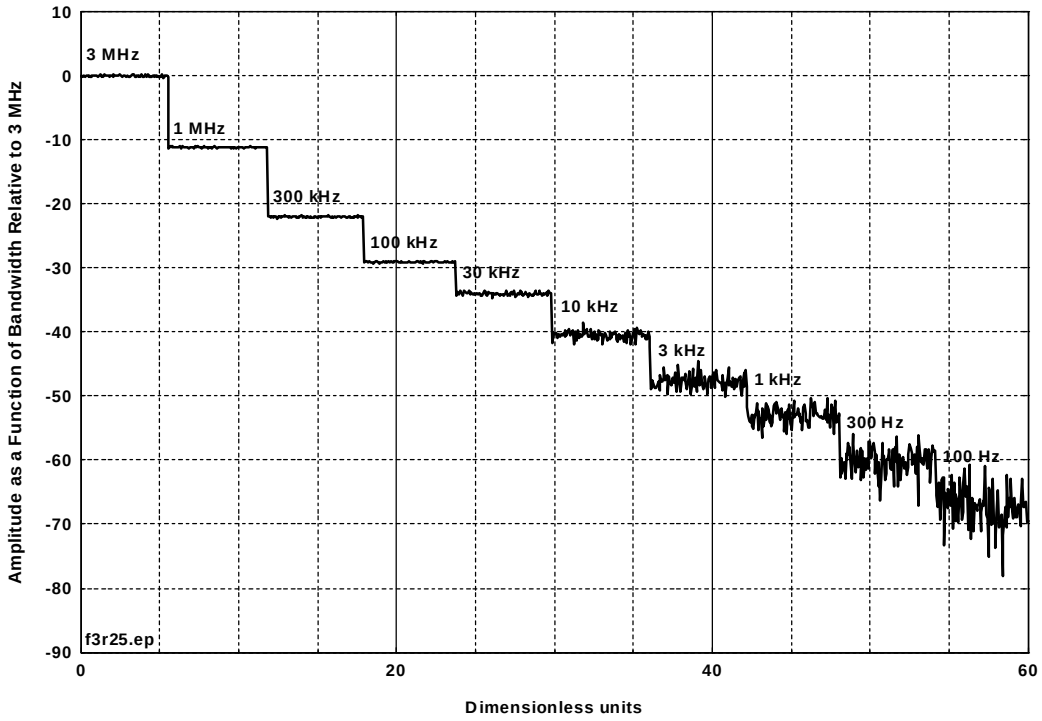

Figure D.B.7. Device B, in 16-kB/sec voice mode, bandwidth progression stairstep.

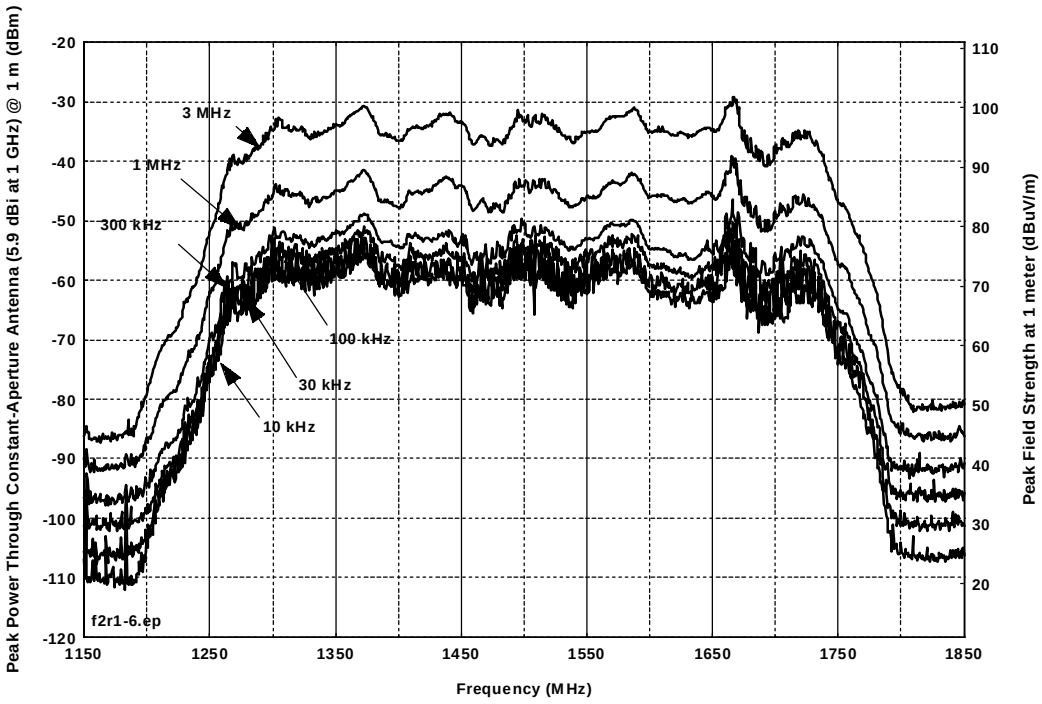

Figure D.B.8. Device B, spectra as a function of bandwidth, 128-kB/sec voice mode.

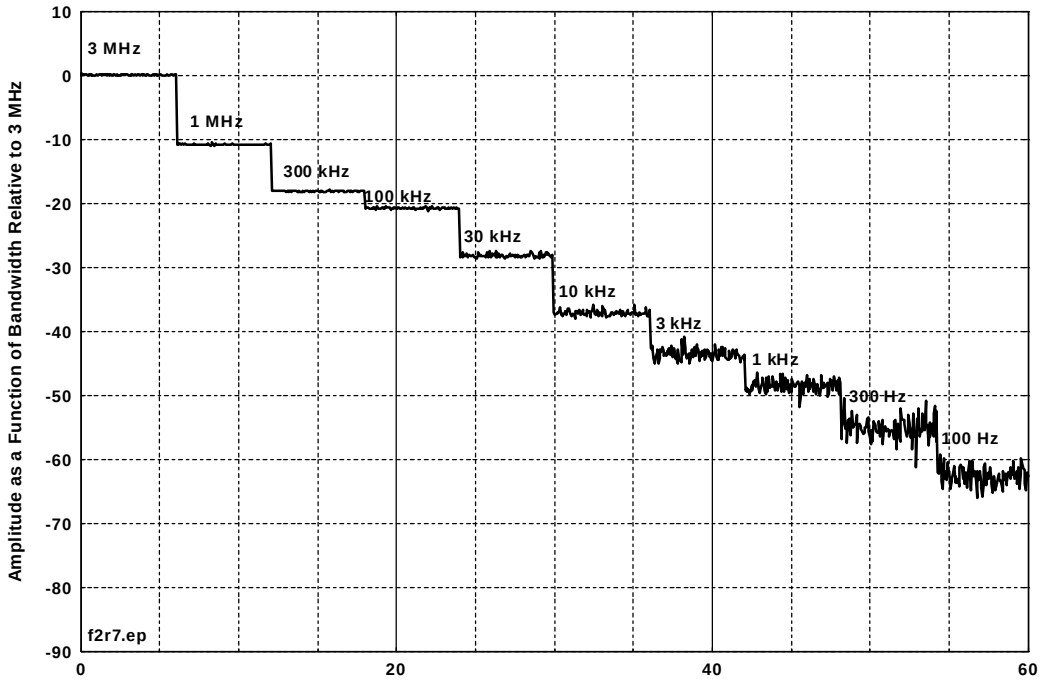

Figure D.B.9. Device B, in 128-kB/sec voice mode, bandwidth progression stairstep.

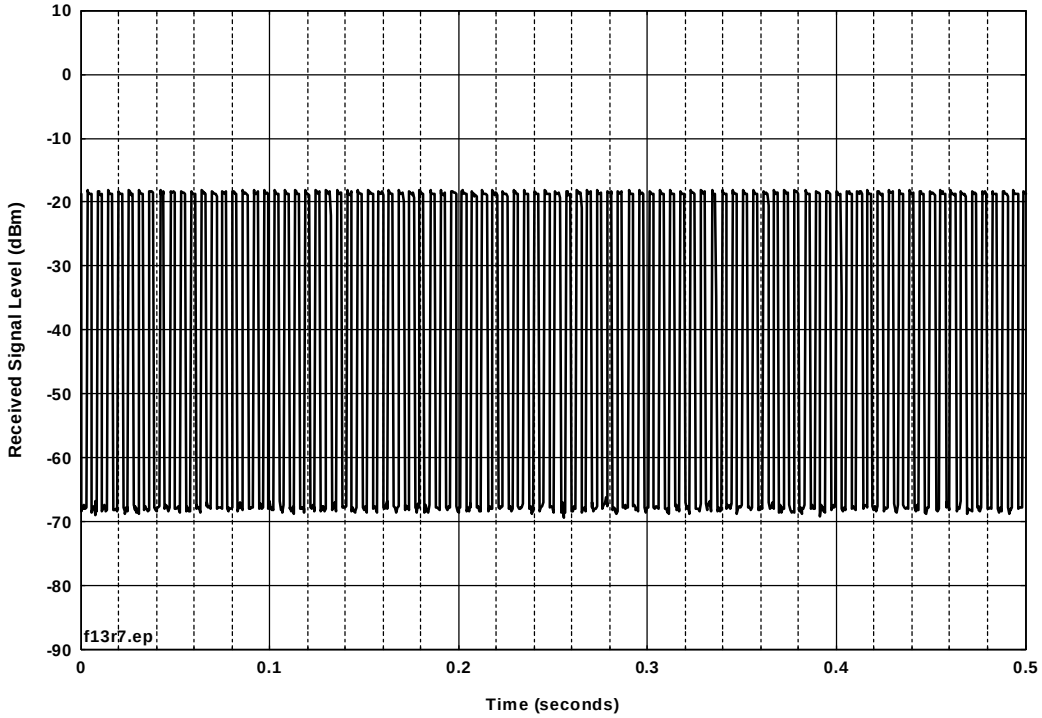

Figure D.B.10. Device B, 0.5 seconds, 128-kBit/sec mode.

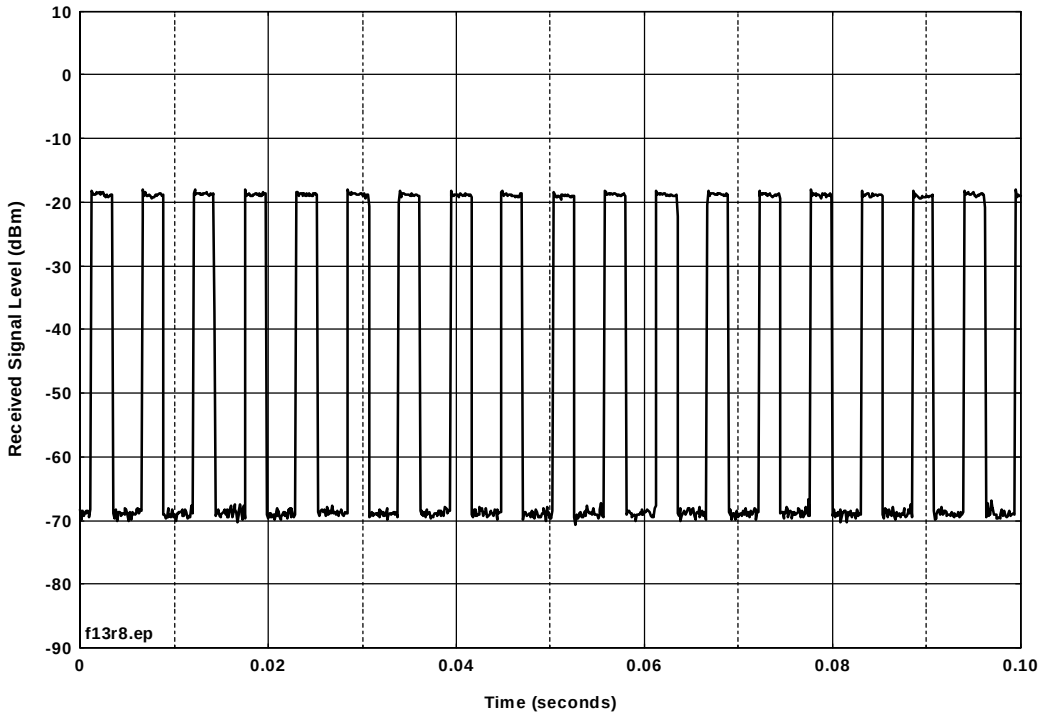

Figure D.B.11. Device B, 128-kBit/sec mode, 0.1 seconds.

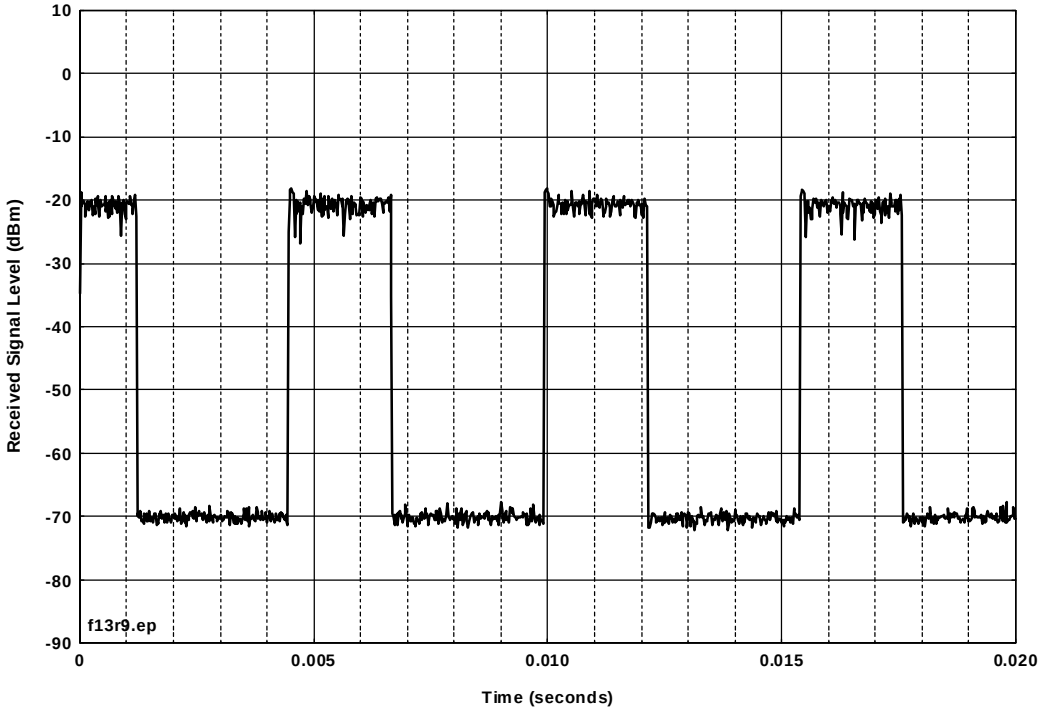

Figure D.B.12. Device B, 128-kBit/second mode, 0.02 seconds.

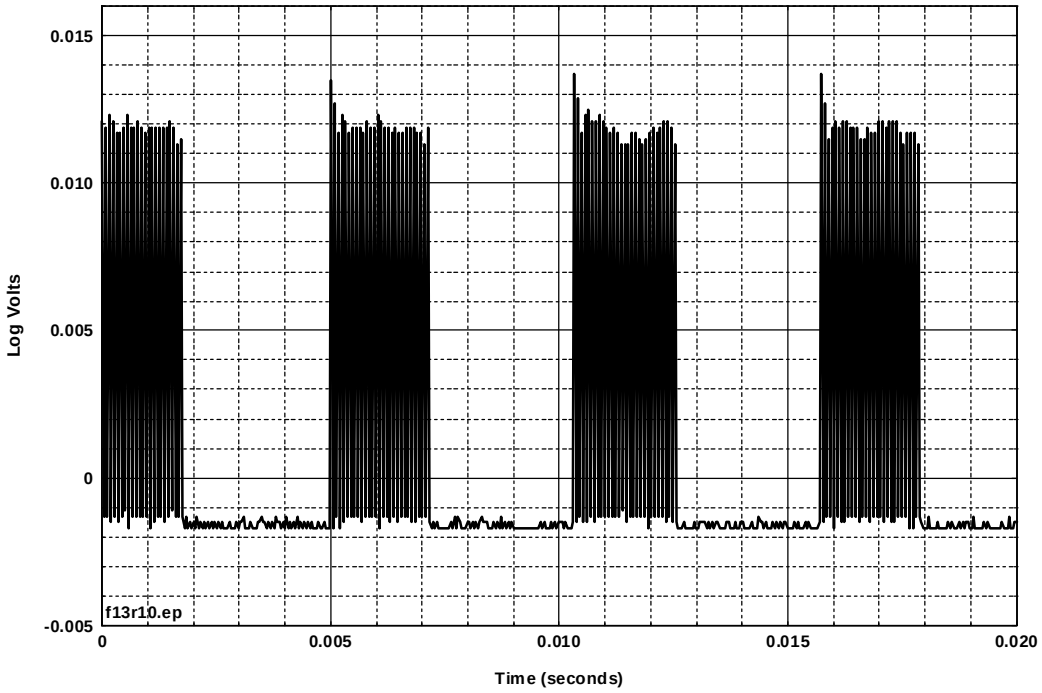

Figure D.B.13. Device B, 128-kBit/second mode, 0.02 seconds, external log detector.

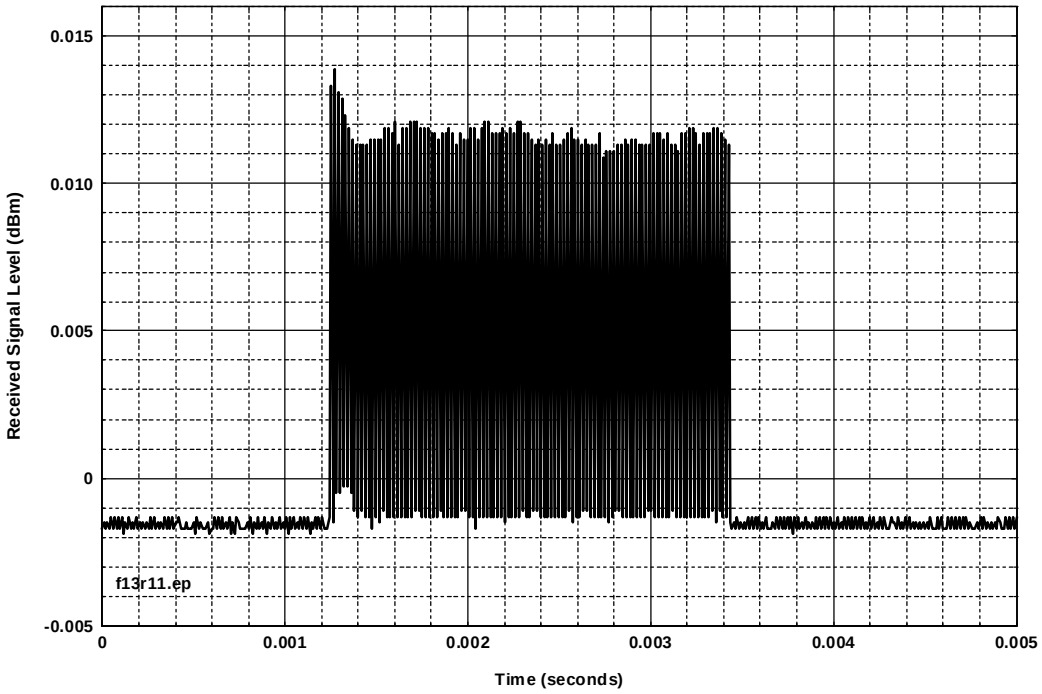

Figure D.B.14. Device B, 128-kBit/second mode, 0.005 seconds, external detector.

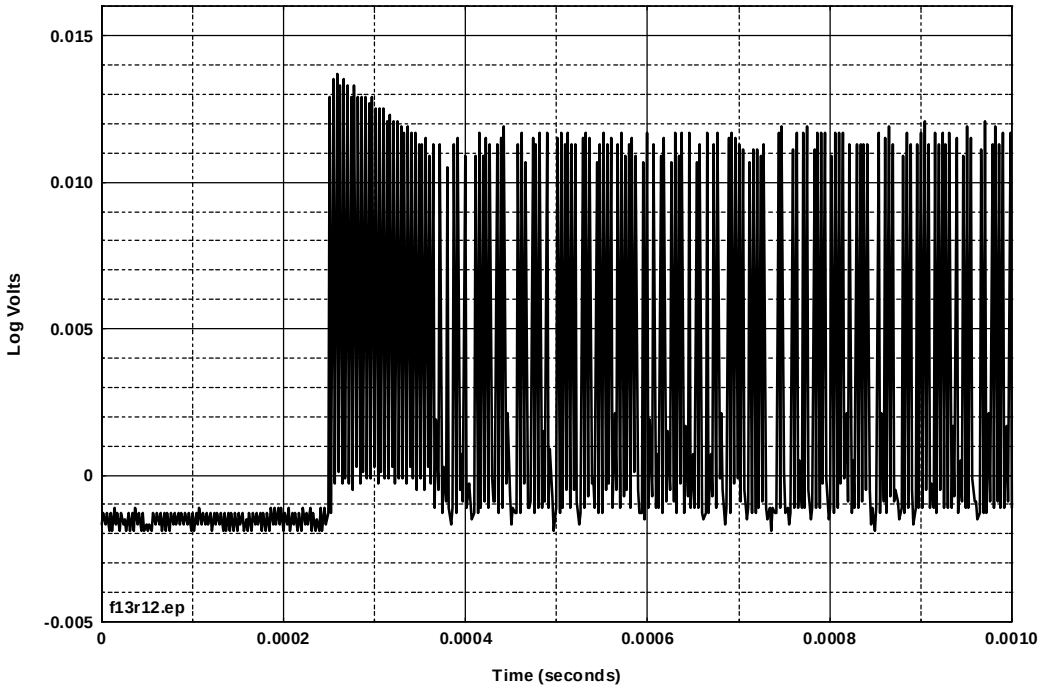

Figure D.B.15. Device B, 128-kBit/second mode, 0.001 seconds, external log detector.

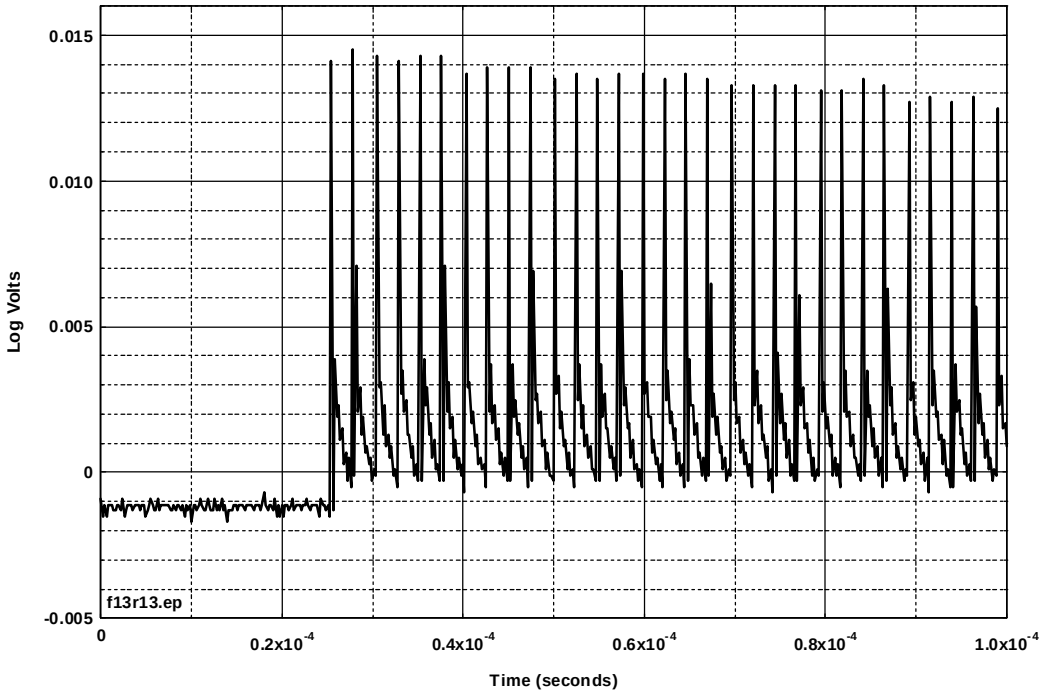

Figure D.B.16. Device B, 128-kBit/second mode, 0.1 msec, external log detector.

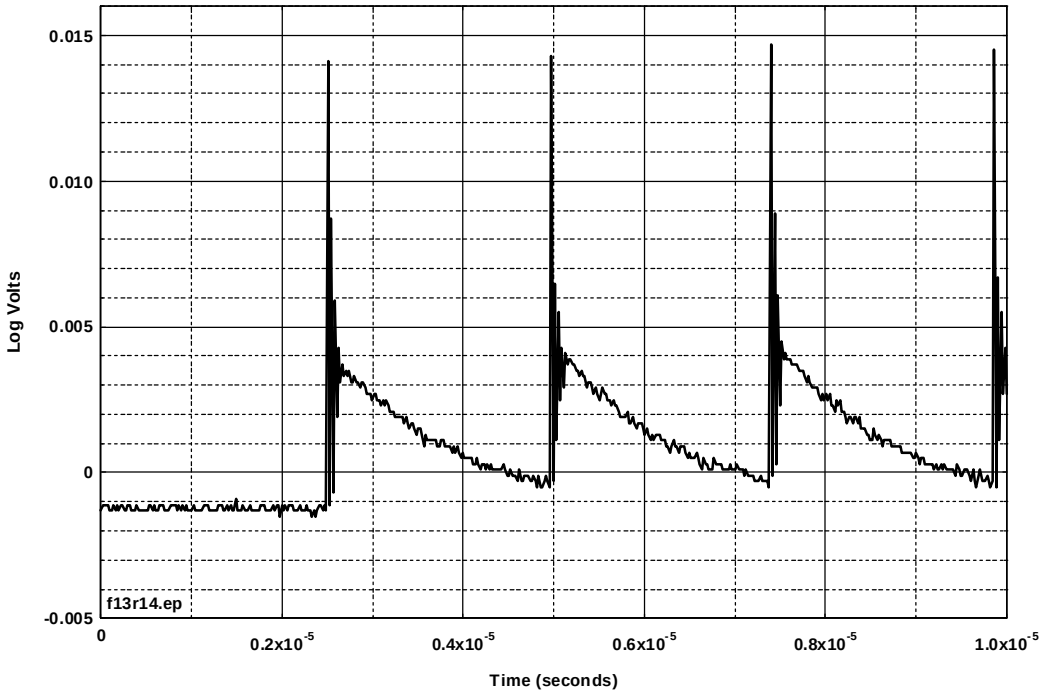

Figure D.B.17. Device B, 128-kBit/second mode, 10 us, external log detector.

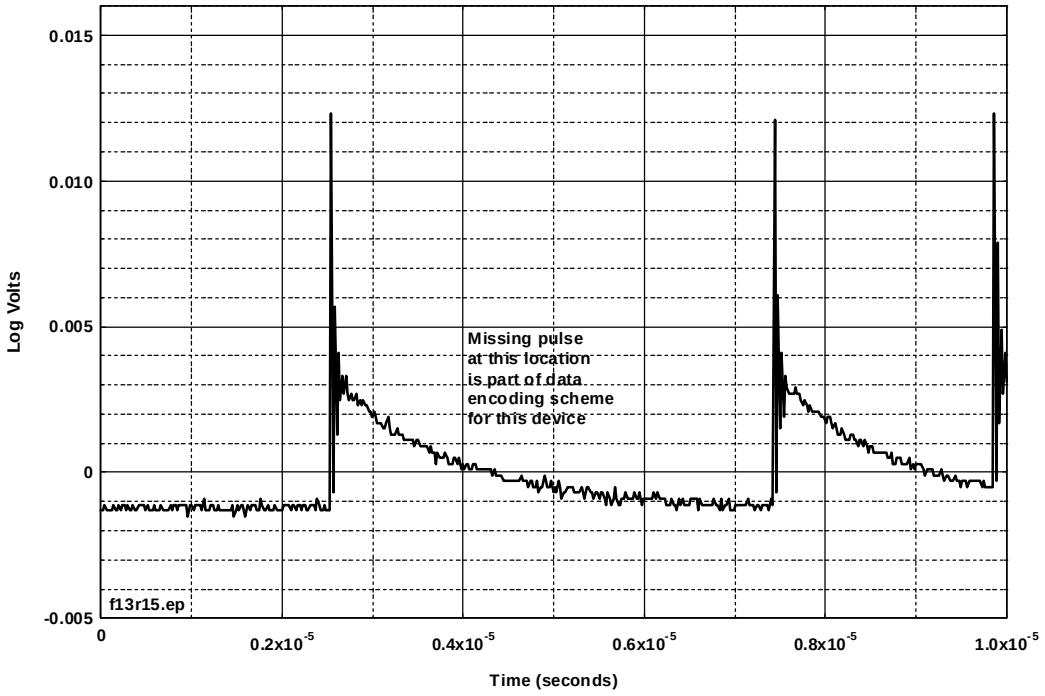

Figure D.B.18. Device B, 128-kBit/second mode, 10 us, external log detector.

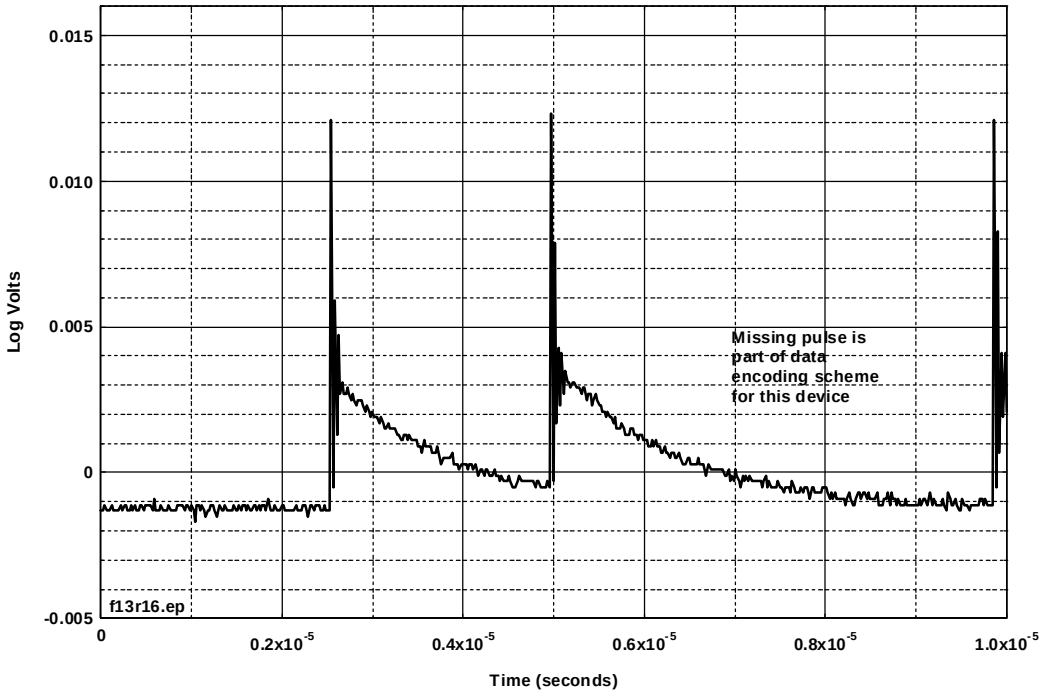

Figure D.B.19. Device B, 128-kBit/second mode, 10 us, external log detector.

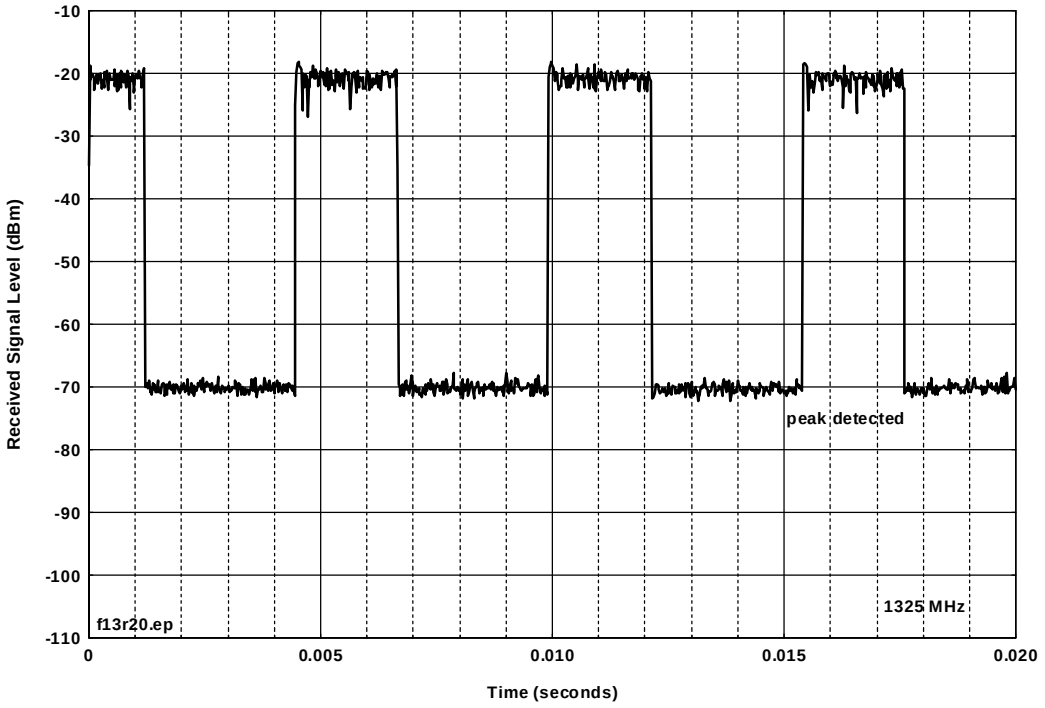

Figure D.B.20. Device B, 128-kBit/second mode, 3-MHz IF bandwidth.

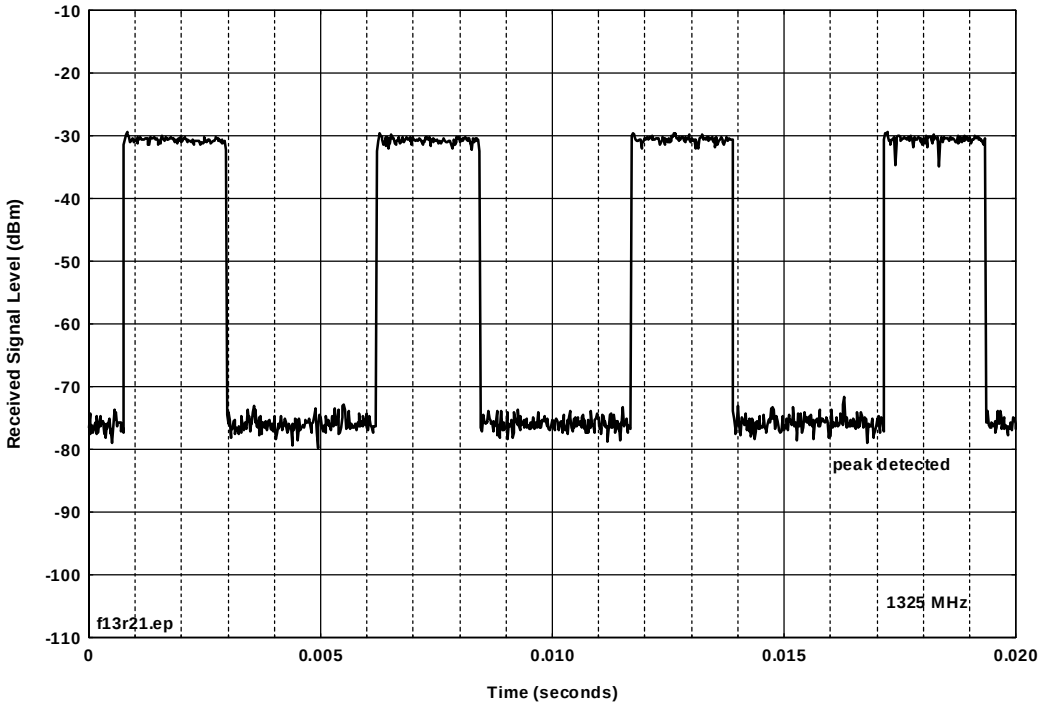

Figure D.B.21. Device B, 128-kBit/second mode, 1-MHz IF bandwidth.

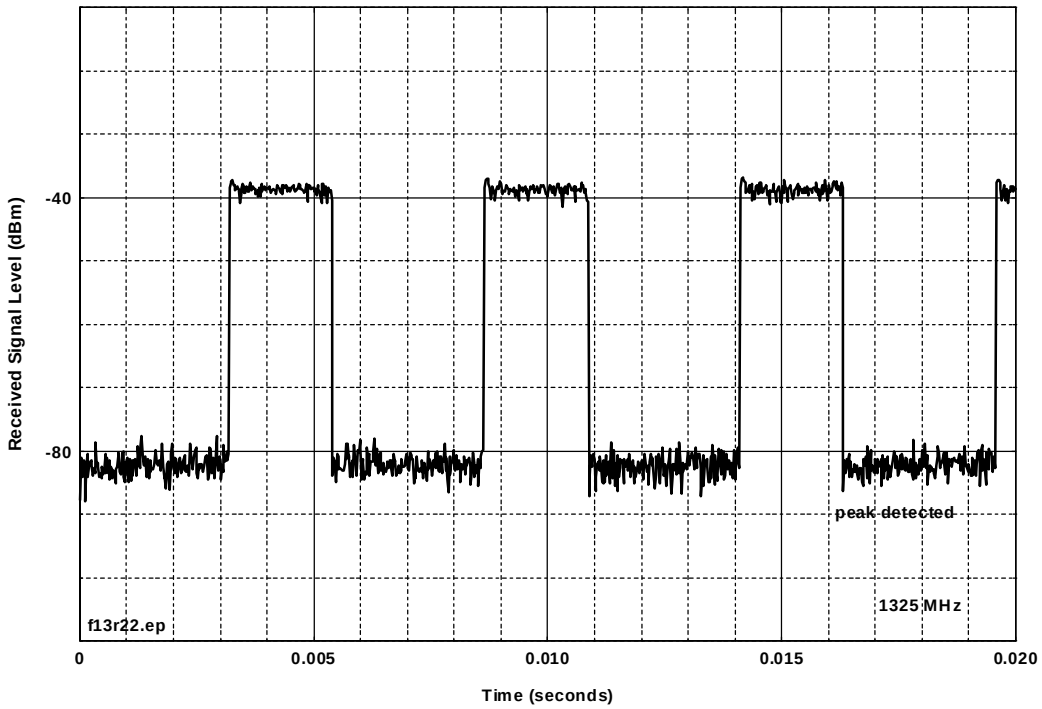

Figure D.B.22. Device B, 128-kBit/second mode, 300-kHz IF bandwidth.

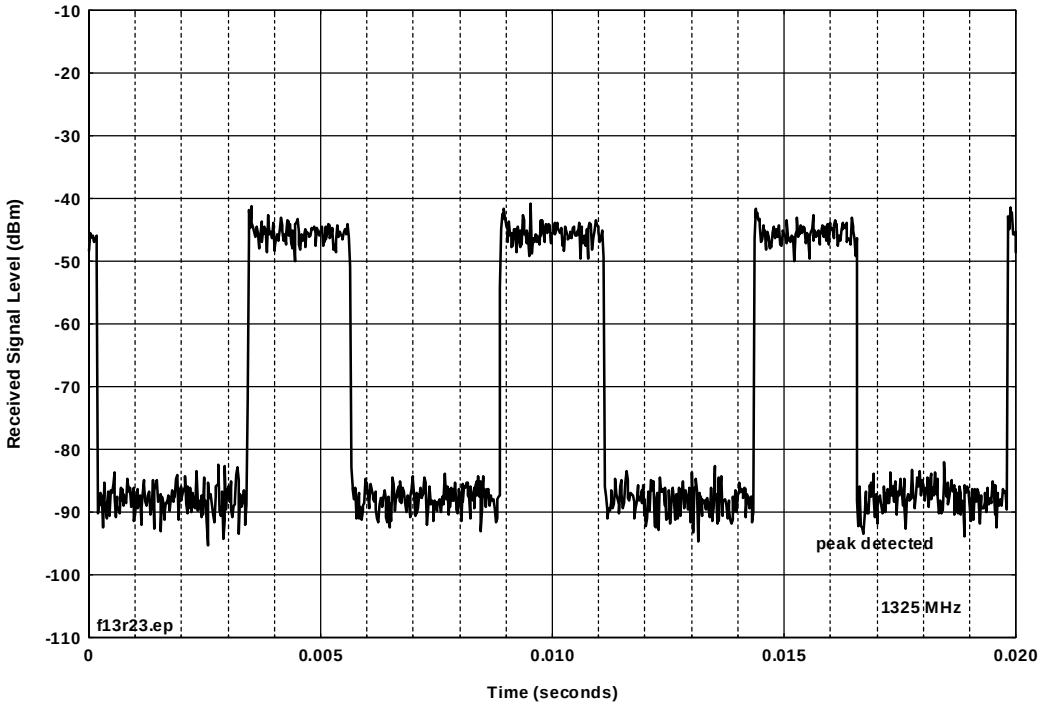

Figure D.B.23. Device B, 128-kBit/second mode, 100-kHz IF bandwidth.

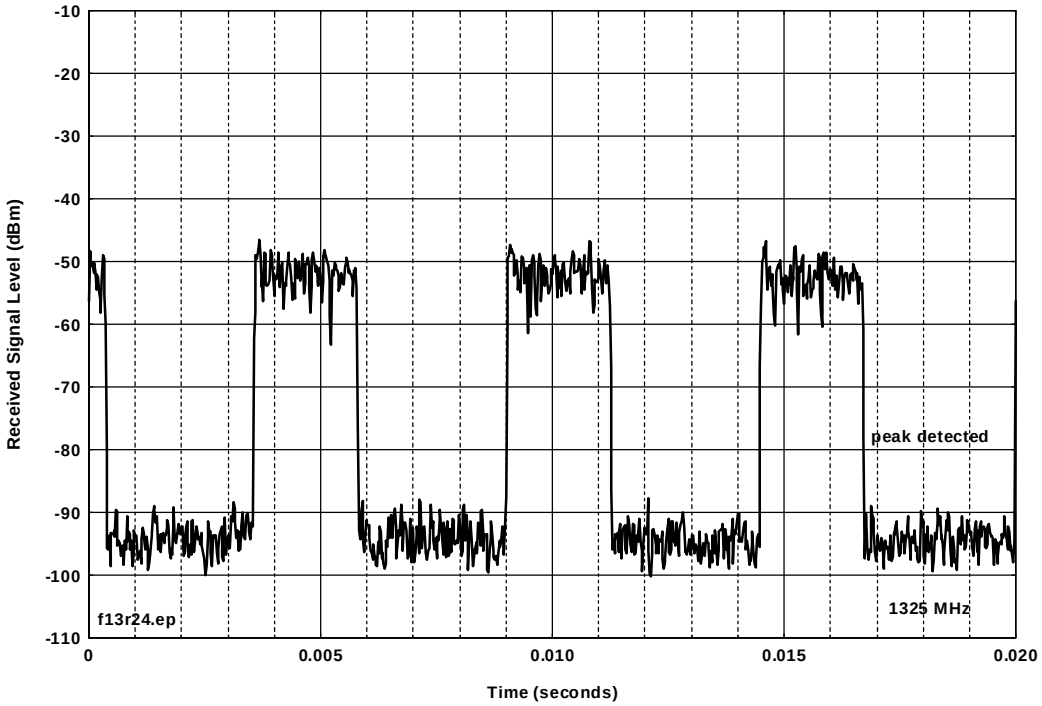

Figure D.B.24. Device B, 128-kBit/second mode, 30-kHz IF bandwidth.

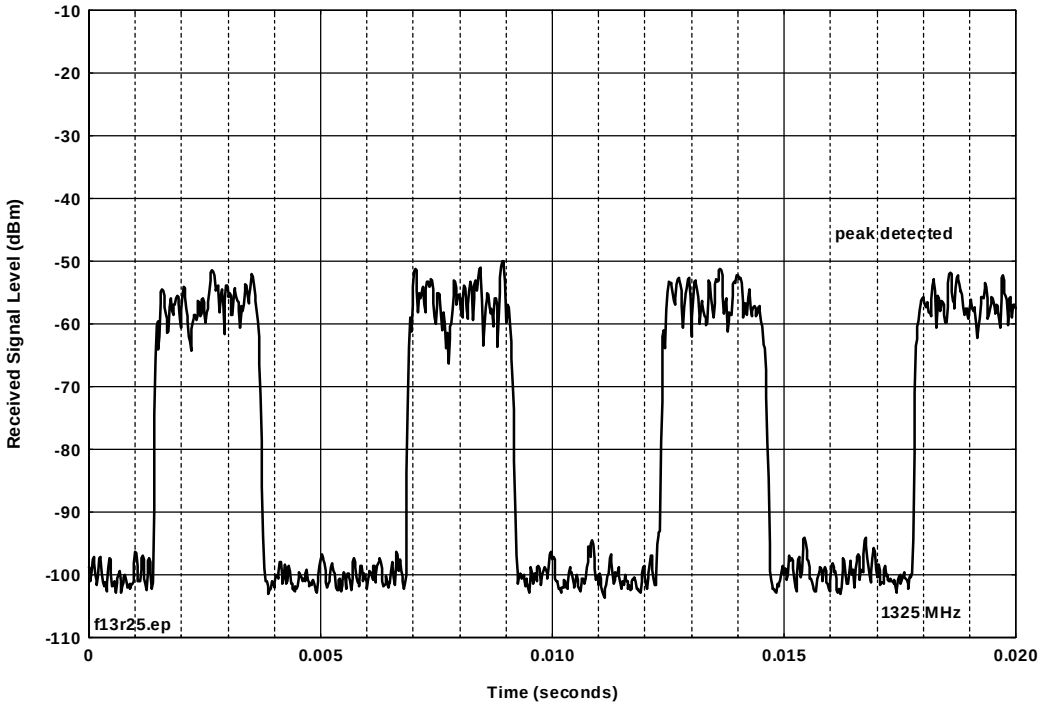

Figure D.B.25. Device B, 128-kBit/second mode, 10-kHz IF bandwidth.

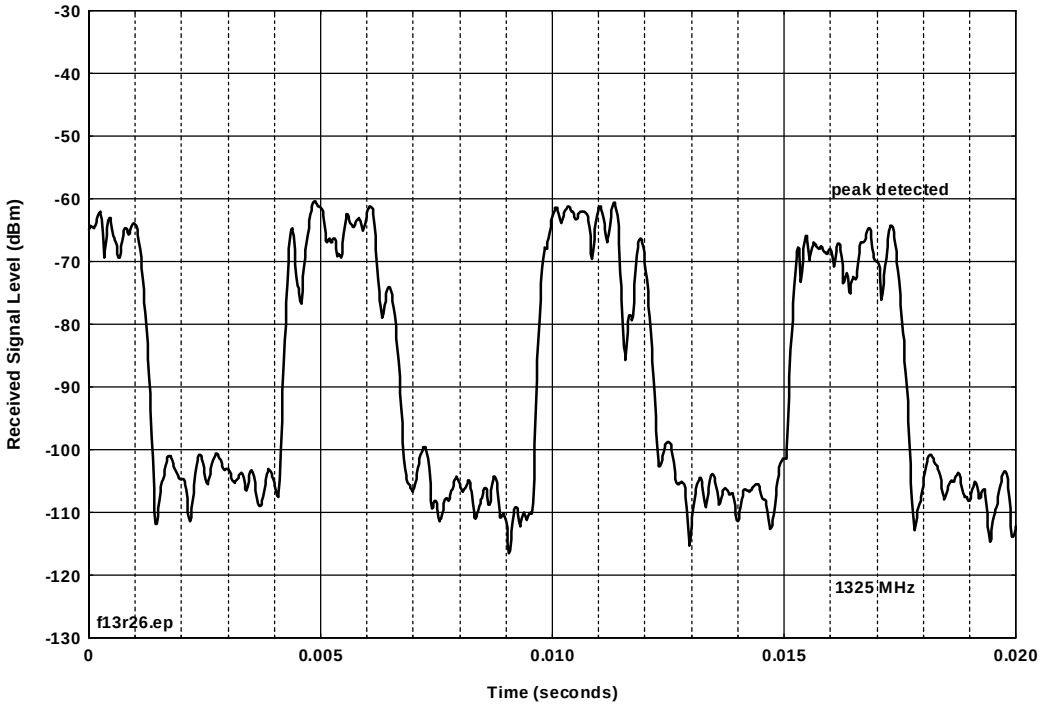

Figure D.B.26. Device B, 128-kBit/second mode, 3-kHz IF bandwidth.

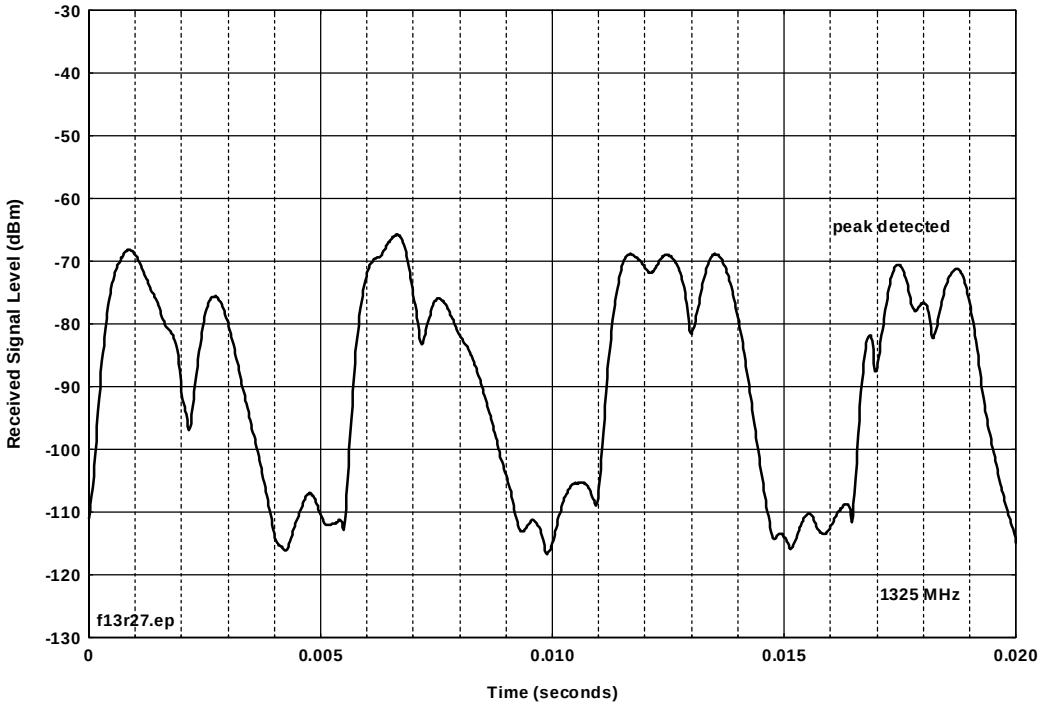

Figure D.B.27. Device B, 128-kBit/second mode, 1-kHz IF bandwidth.

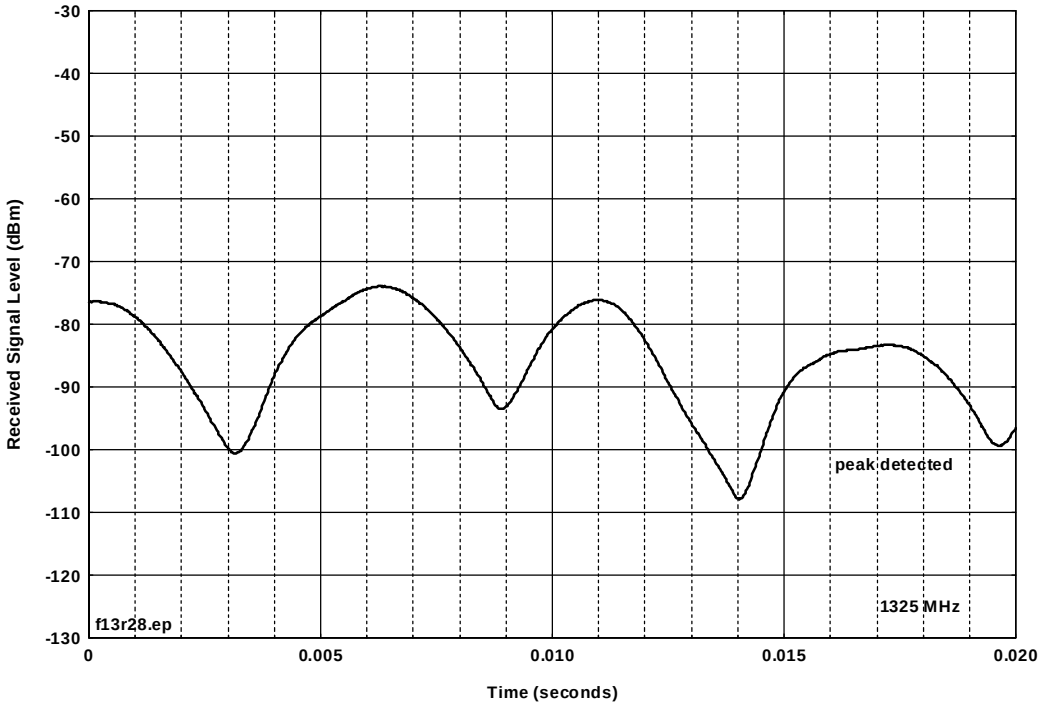

Figure D.B.28. Device B, 128-kBit/second mode, 300-Hz IF bandwidth.

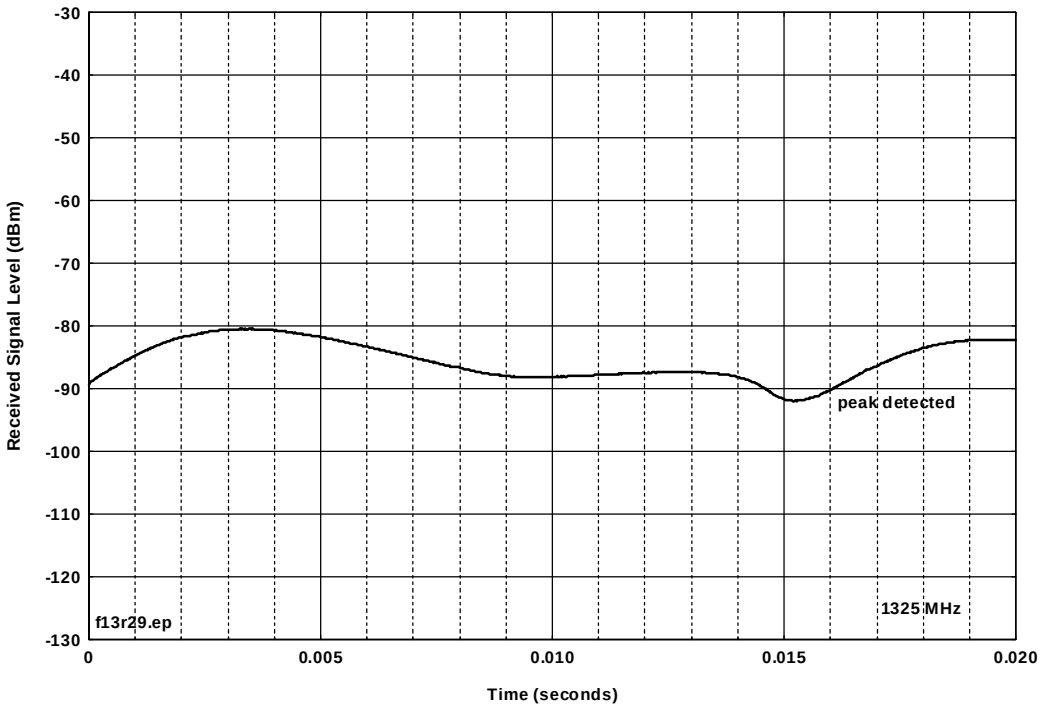

Figure D.B.29. Device B, 128-kBit/second mode, 100-Hz IF bandwidth.

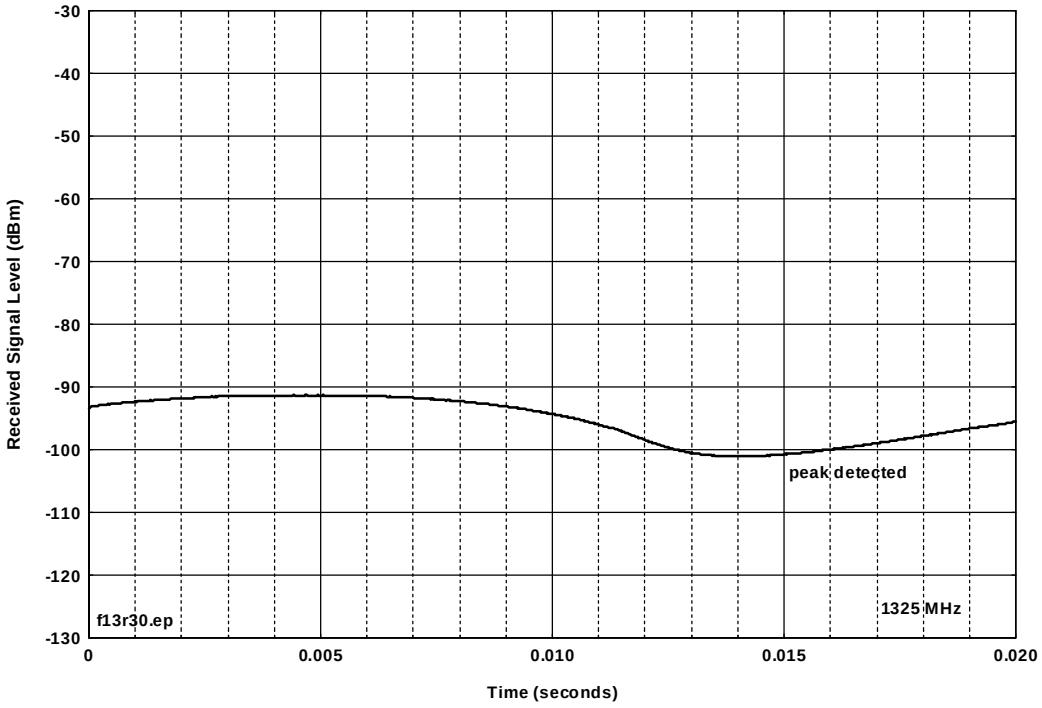

Figure D.B.30. Device B, 128-kBit/second mode, 30-Hz IF bandwidth.

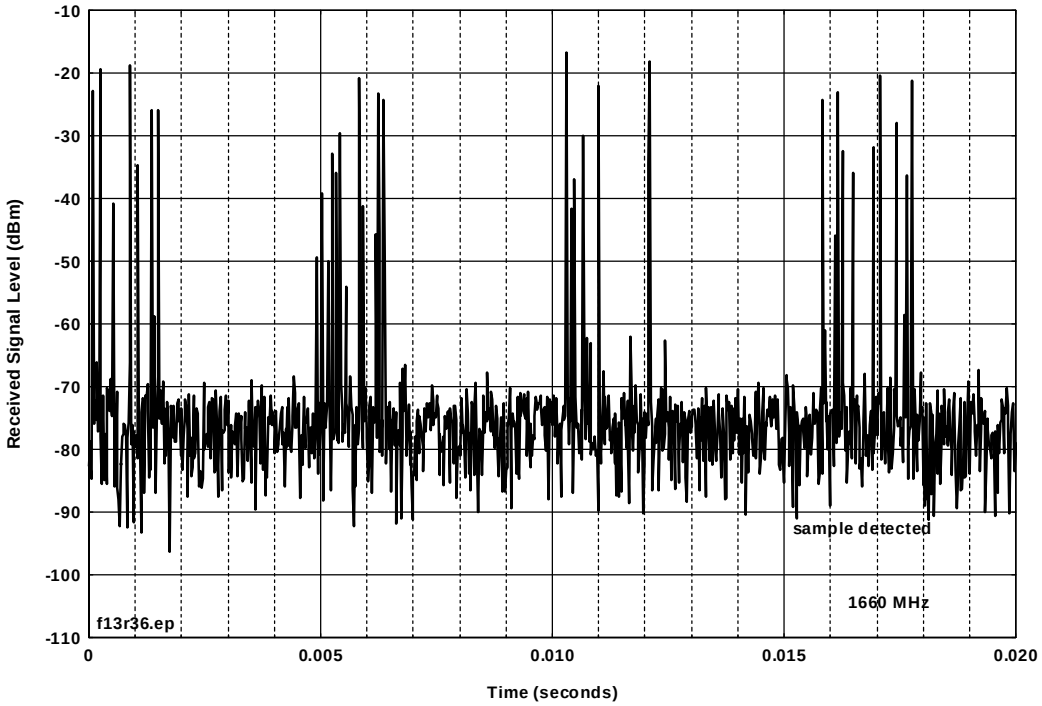

Figure D.B.31. Device B, 128-kBit/second mode, 3-MHz video bandwidth.

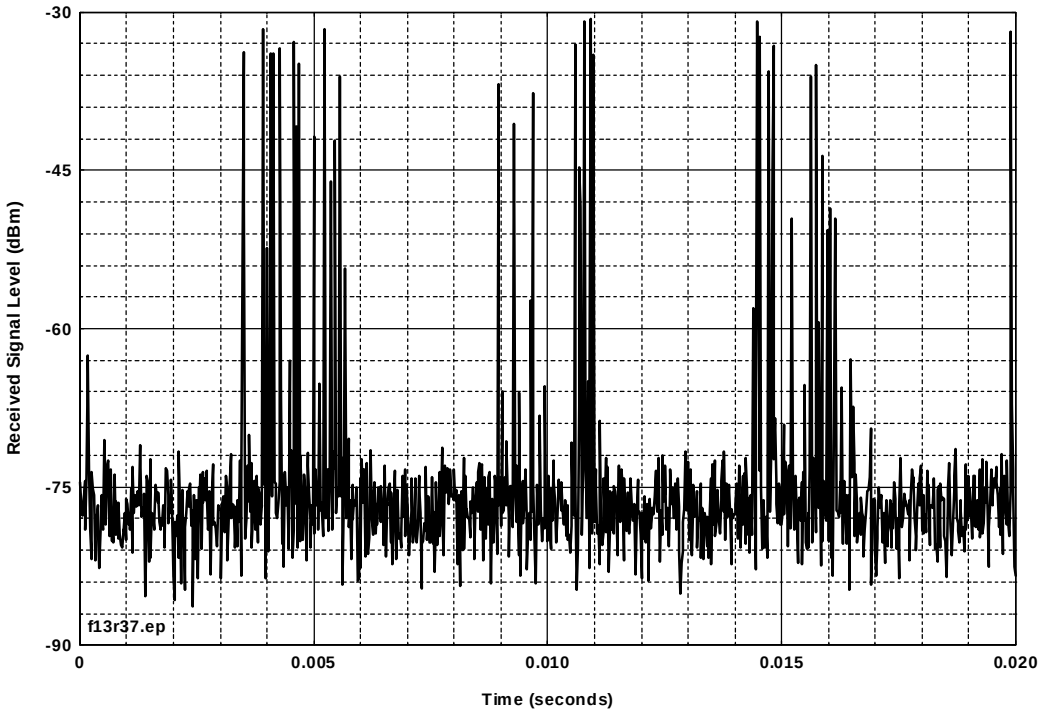

Figure D.B.32. Device B, 128-kBit/second mode, 1-MHz video bandwidth.

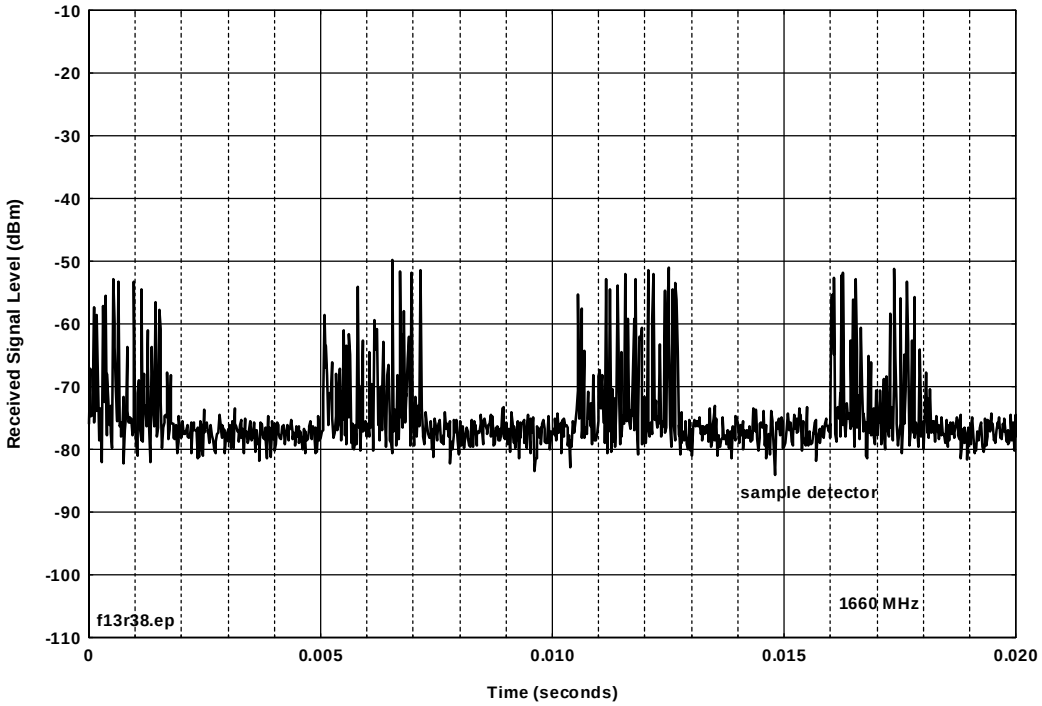

Figure D.B.33. Device B, 128-kBit/second mode, 300-kHz video bandwidth.

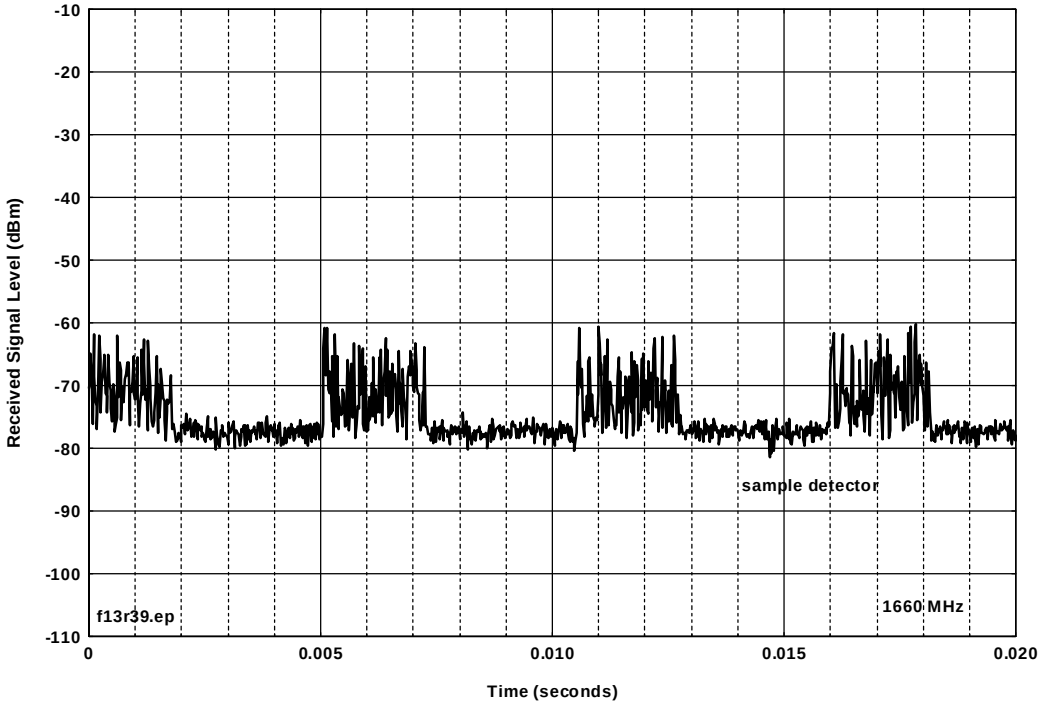

Figure D.B.34. Device B, 128-kBit/second mode, 100-kHz video bandwidth.

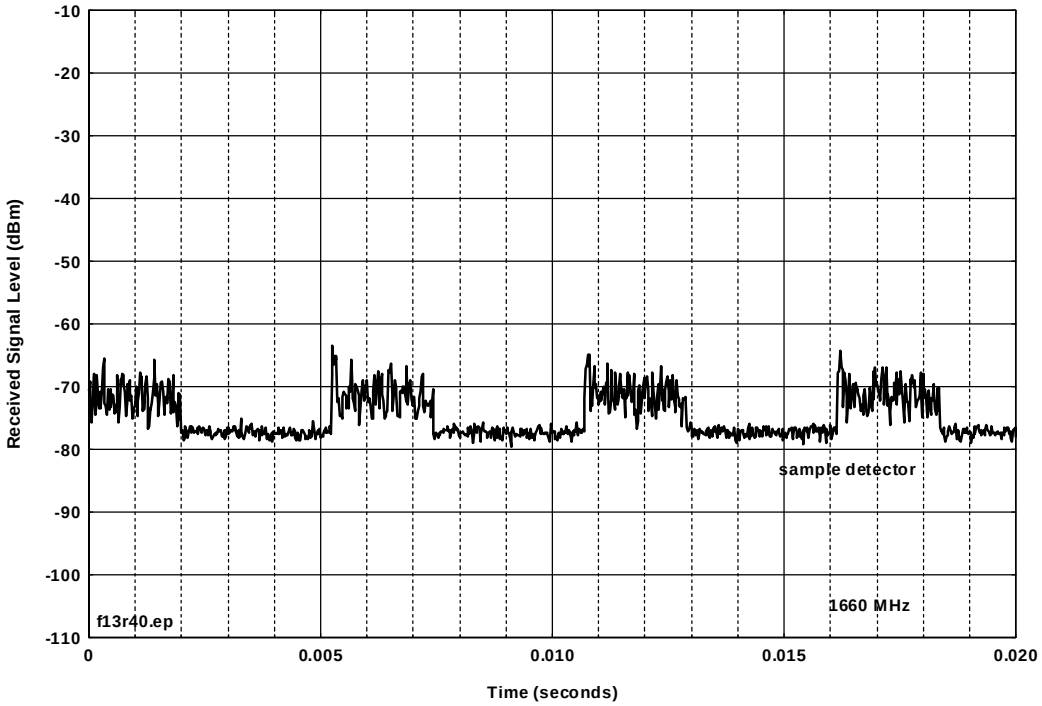

Figure D.B.35. Device B, 128-kBit/second mode, 30-kHz video bandwidth.

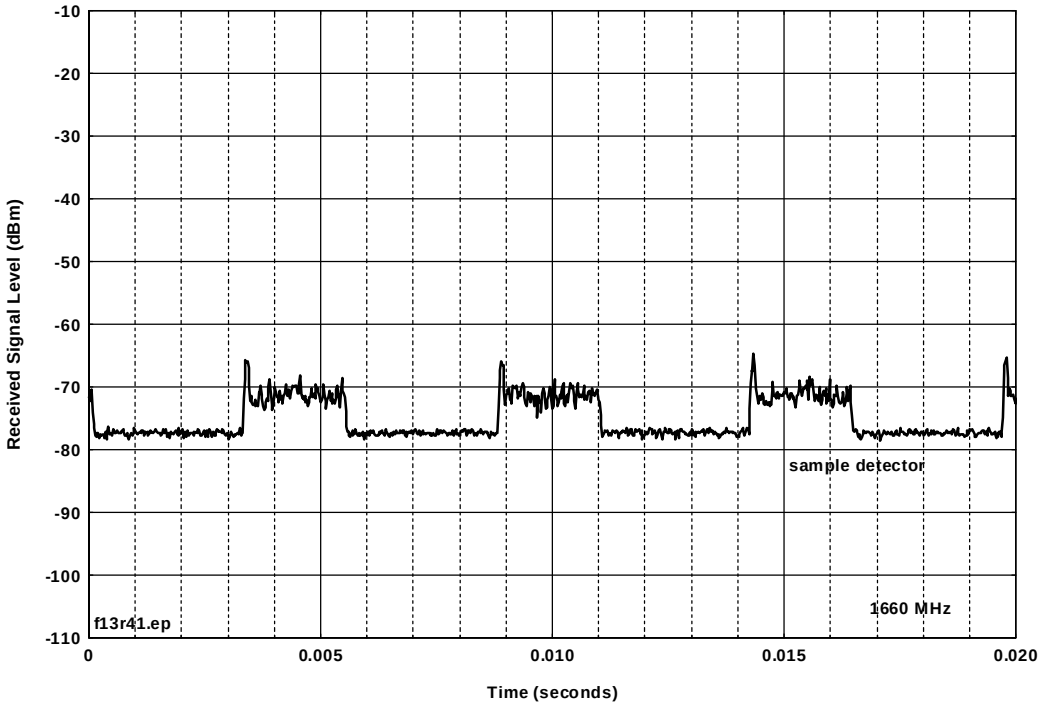

Figure D.B.36. Device B, 128-kBit/second mode, 10-kHz video bandwidth.

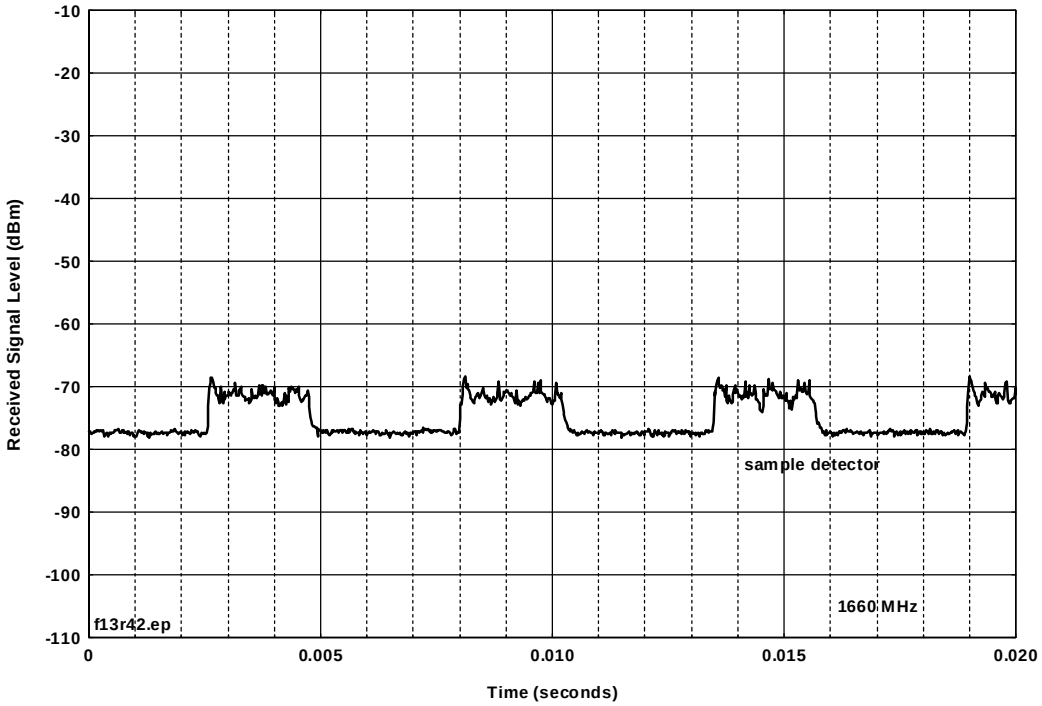

Figure D.B.37. Device B, 128-kBit/second mode, 3-kHz video bandwidth.

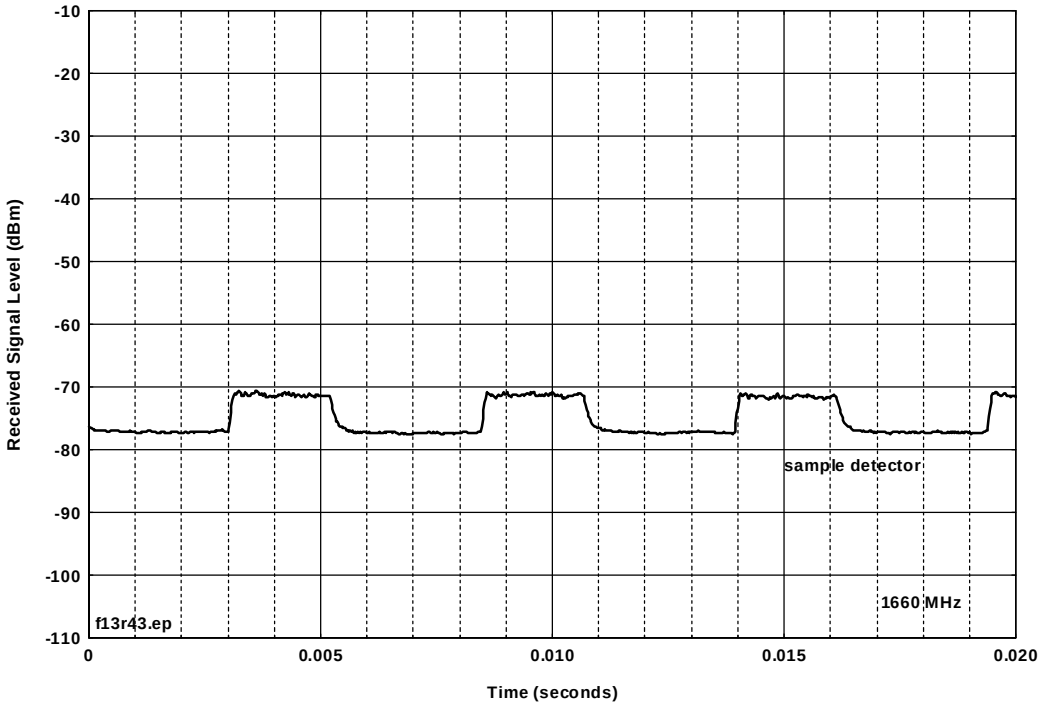

Figure D.B.38. Device B, 128-kBit/sec mode, 1-kHz video bandwidth.

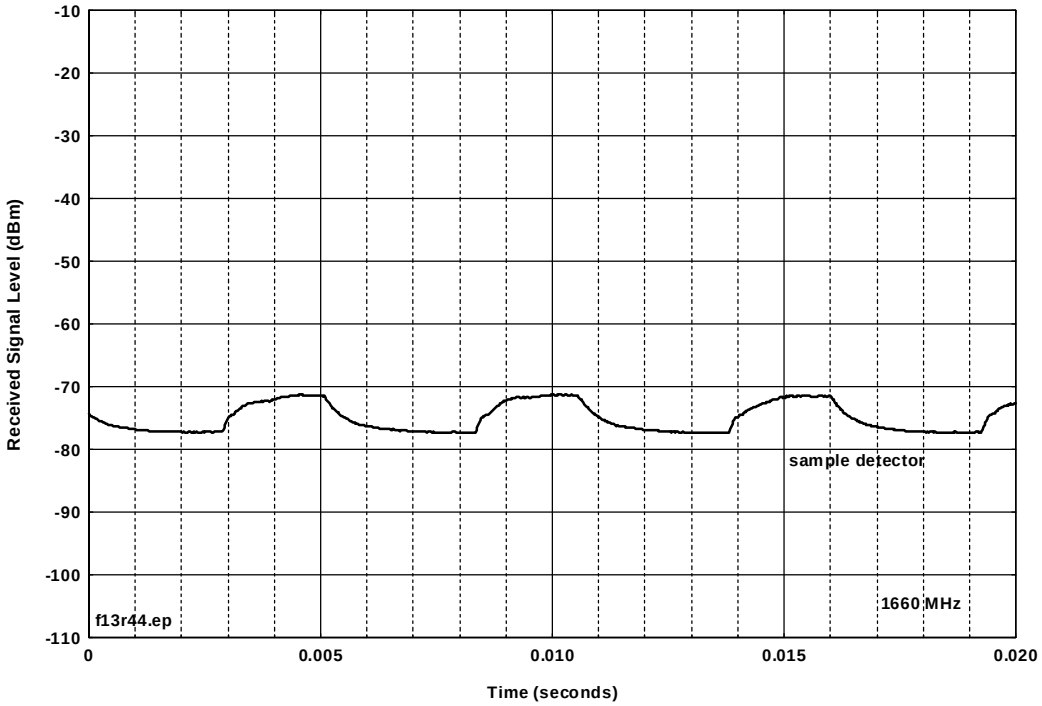

Figure D.B.39. Device B, 128-kBit/second mode, 300-Hz video bandwidth.

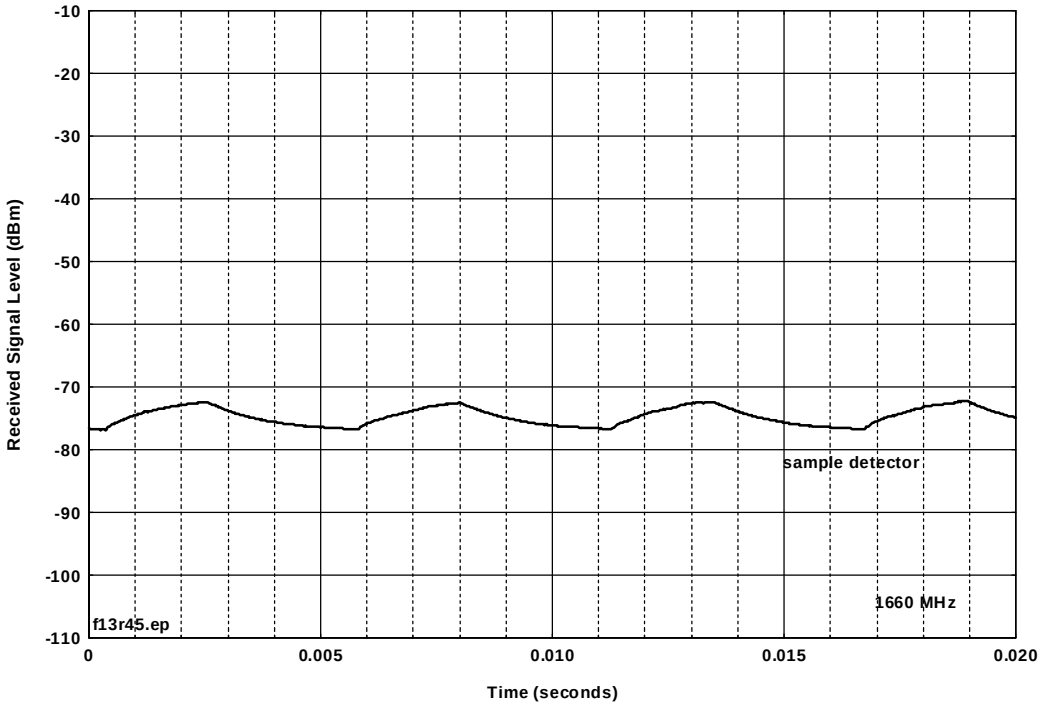

Figure D.B.40. Device B, 128-kBit/second mode, 100-Hz video bandwidth.

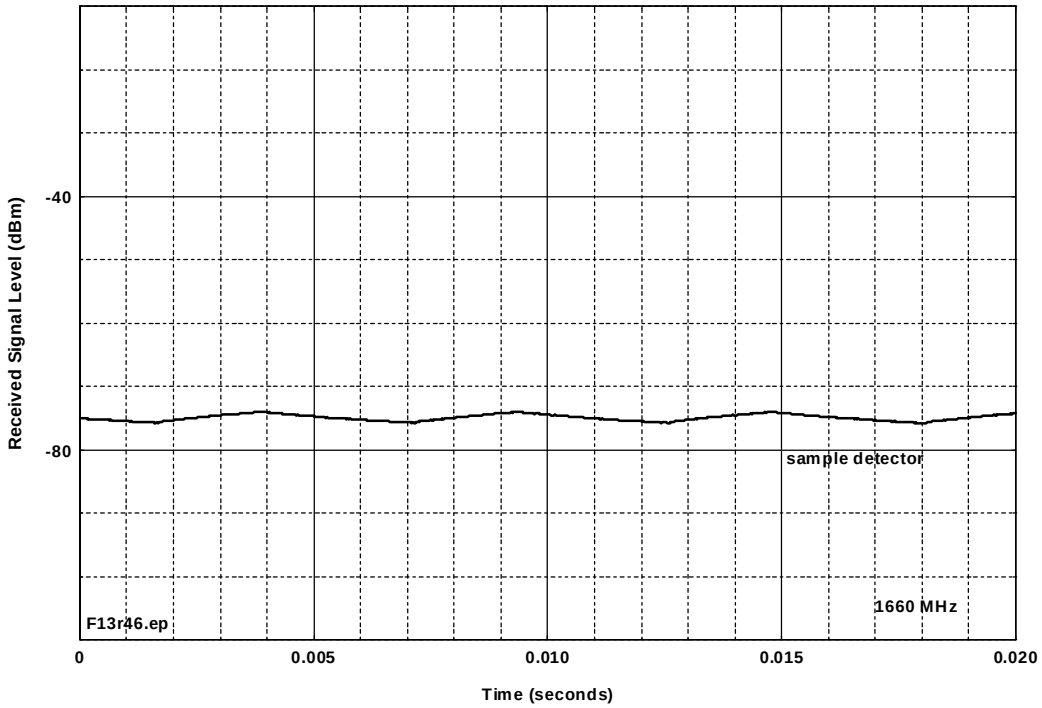

Figure D.B.41. Device B, 128-kBit/second mode, 30-Hz video bandwidth.

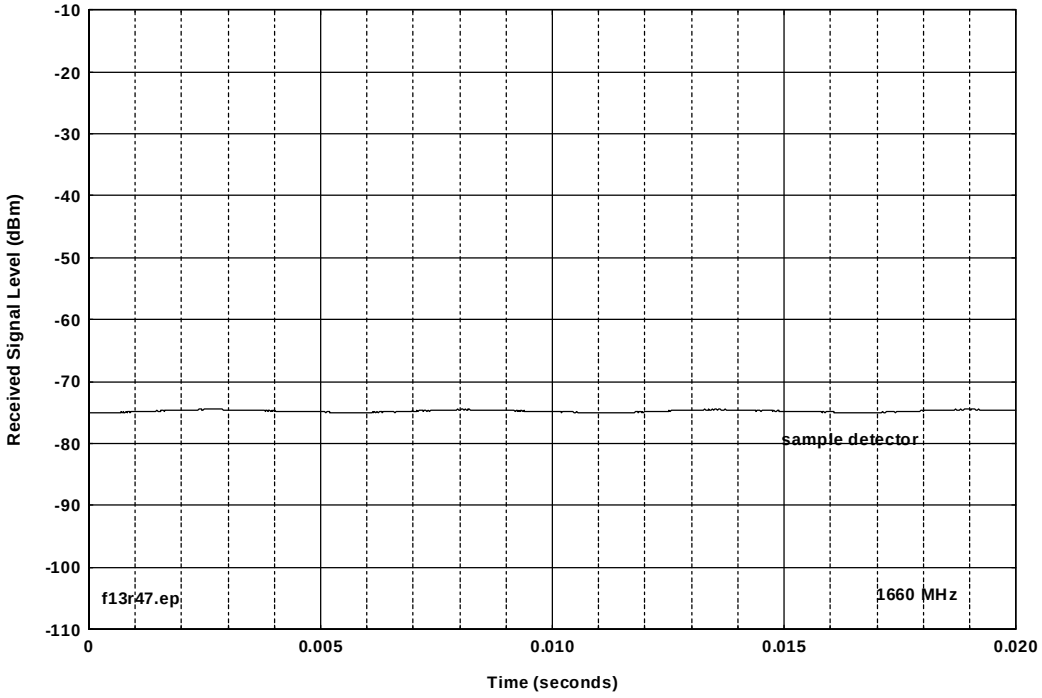

Figure D.B.42. Device B, 128-kBit/second mode, 10-Hz video bandwidth.

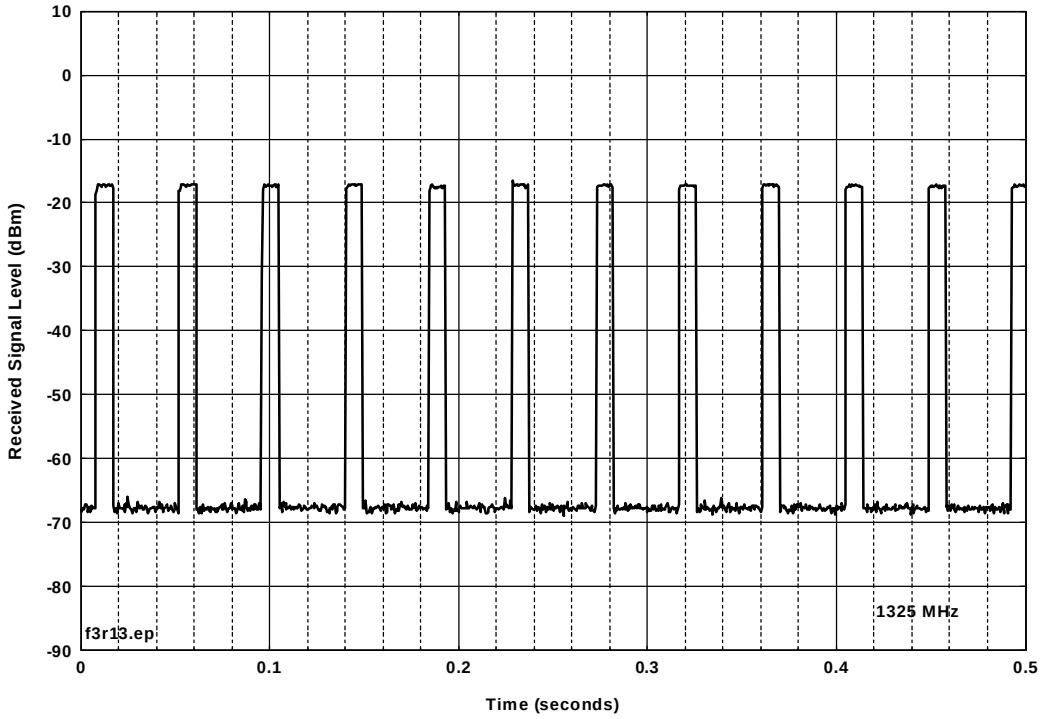

Figure D.B.43. Device B, 16-kBit/second mode, 3-MHz IF bandwidth, positive peak detector.

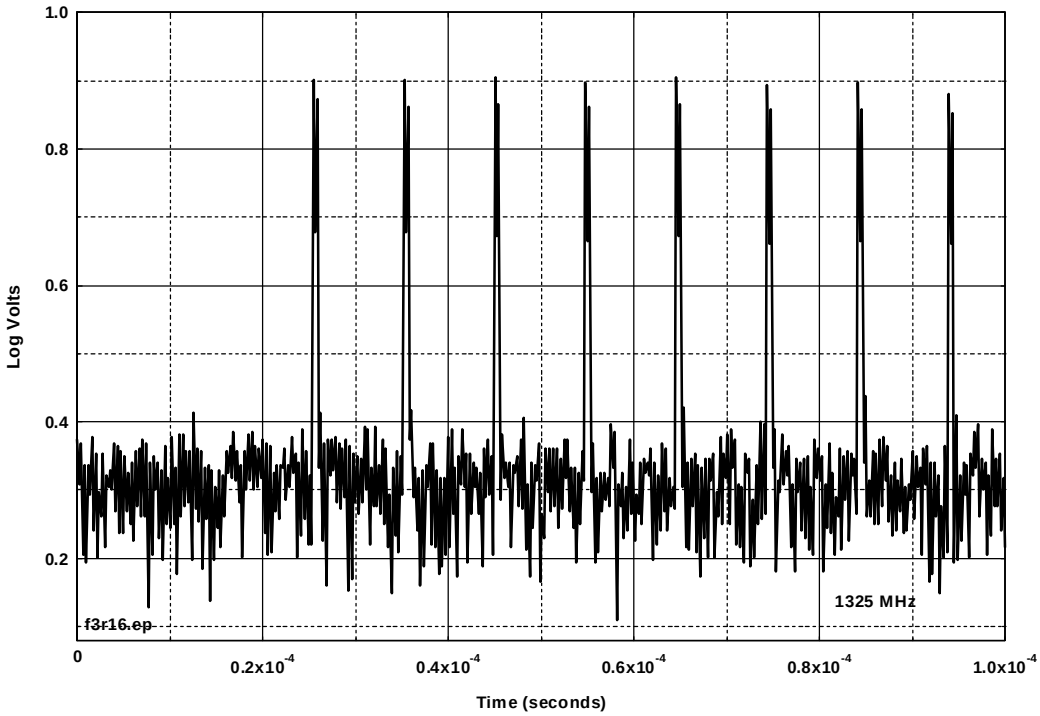

Figure D.B.44. Device B, 16-kBit/second mode, external log detector.

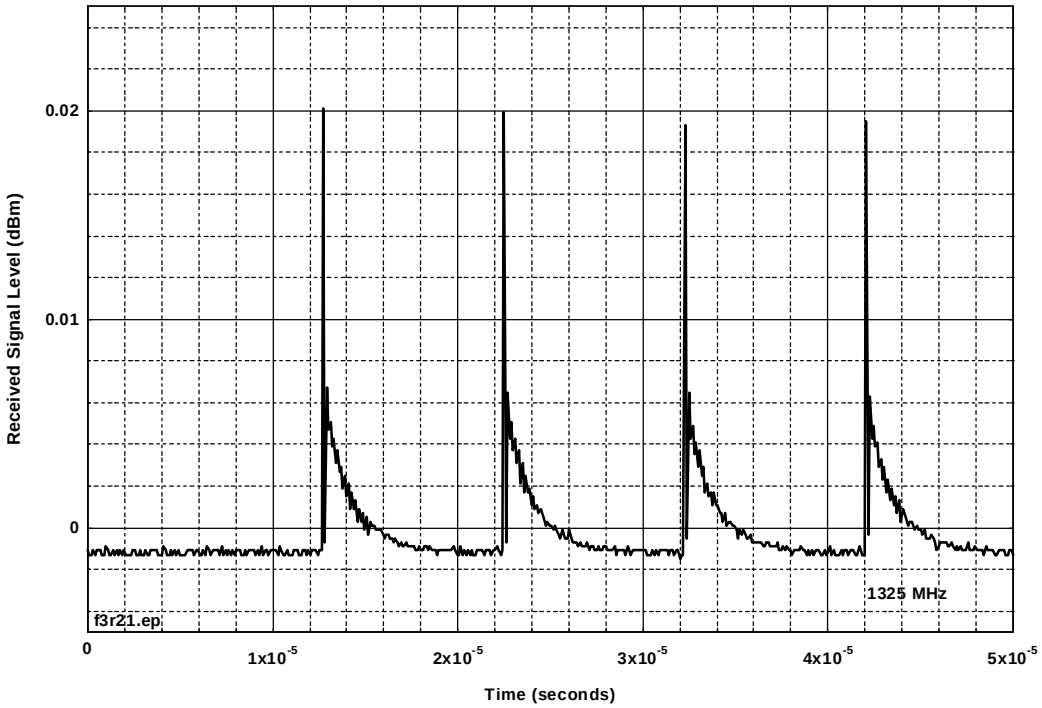

Figure D.B.45. Device B, 16-kBit/second mode, external detector.

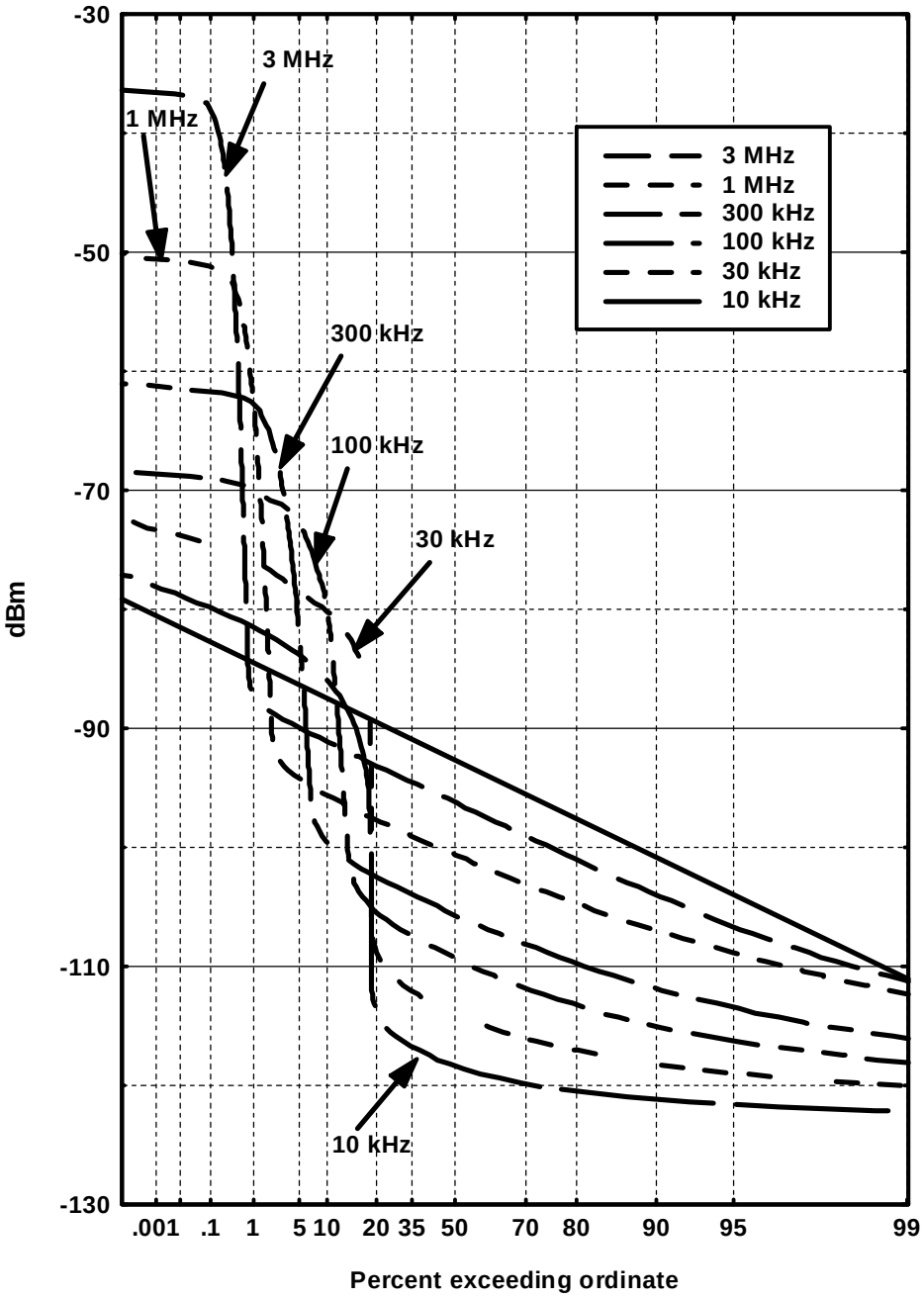

Figure D.B.46. Device B, 16 kb/s APDs.

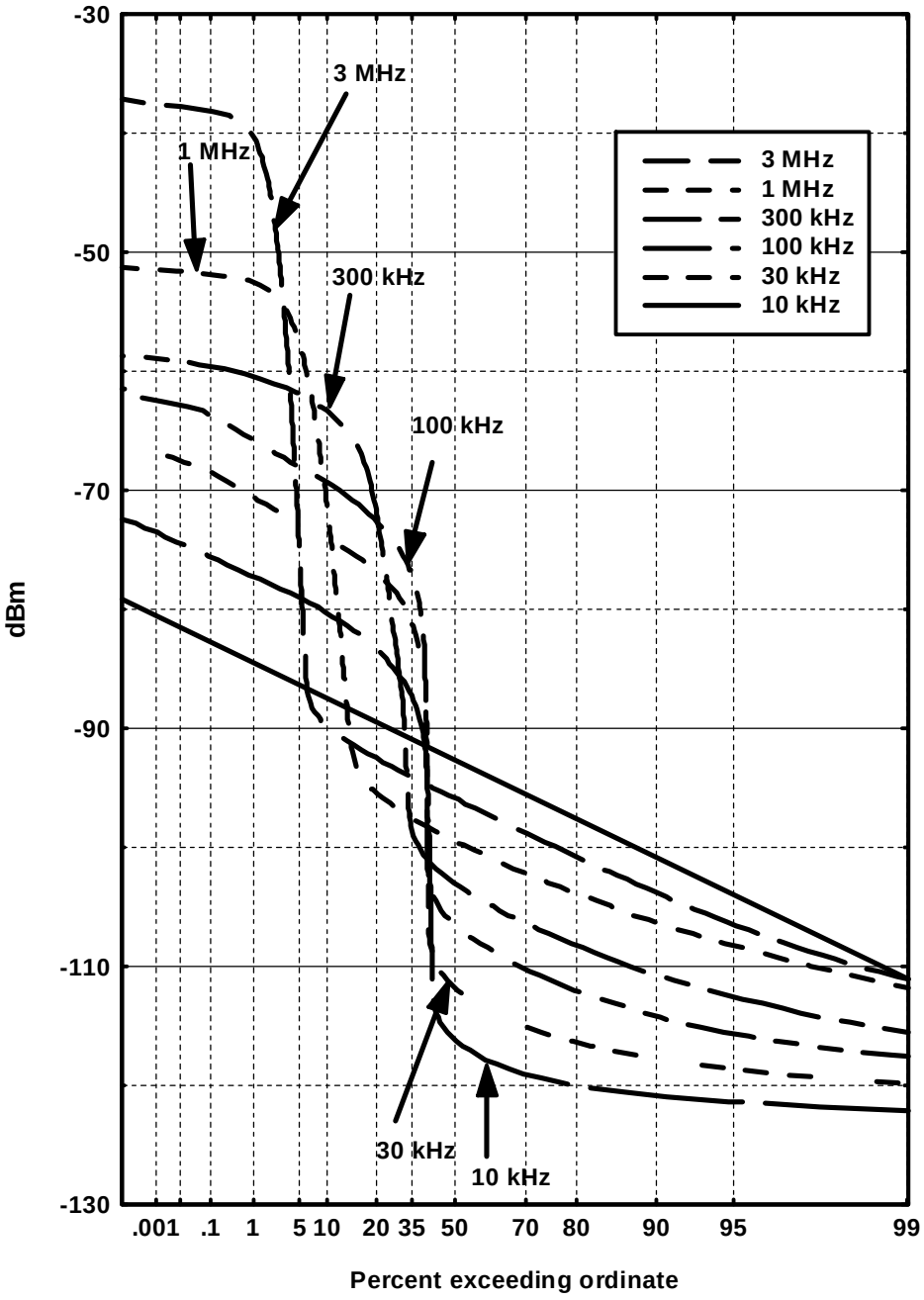

Figure D.B.47. Device B, 128 kb/s APDs.

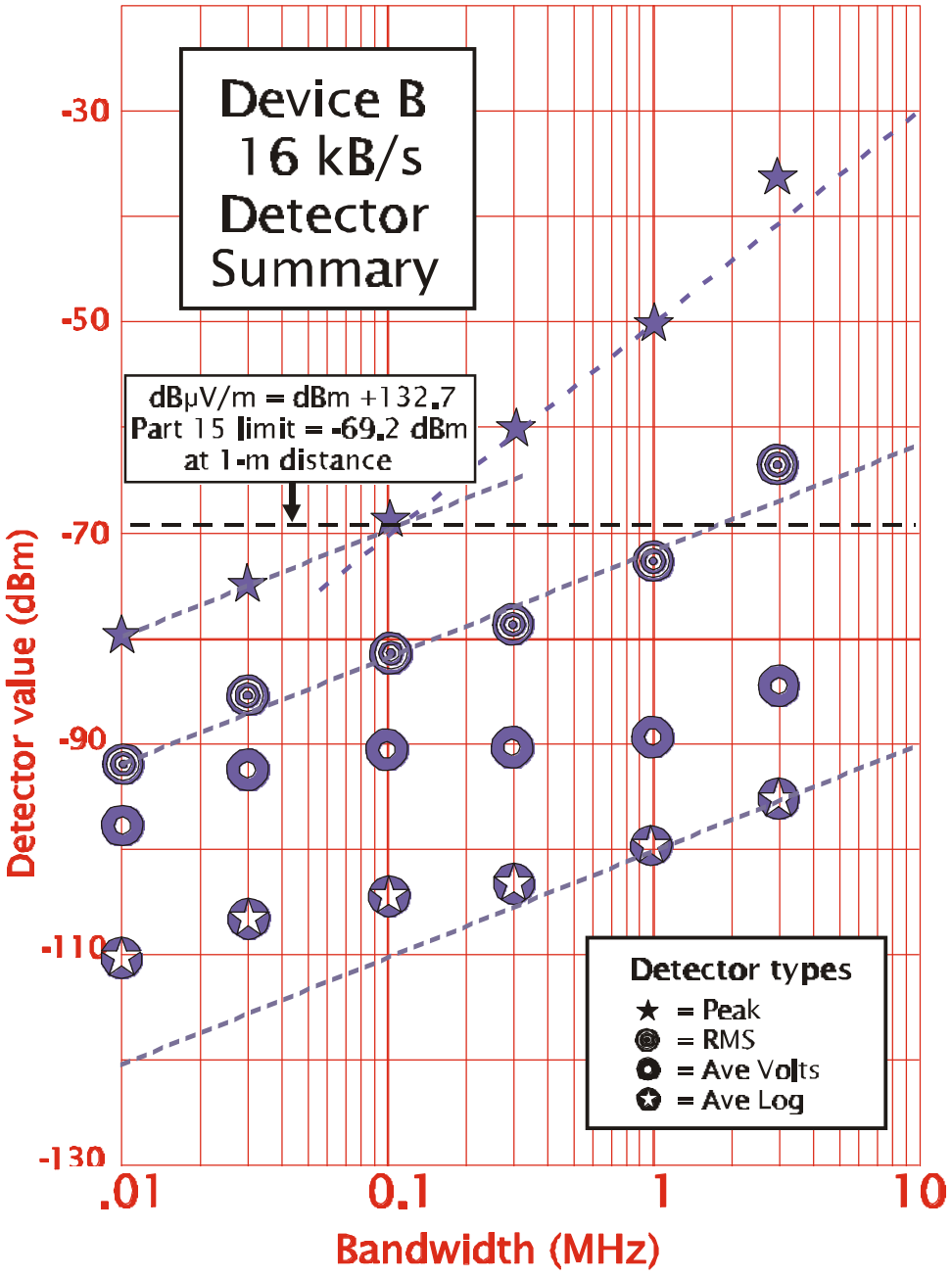

Figure D.B.48. Device B, detector summary.

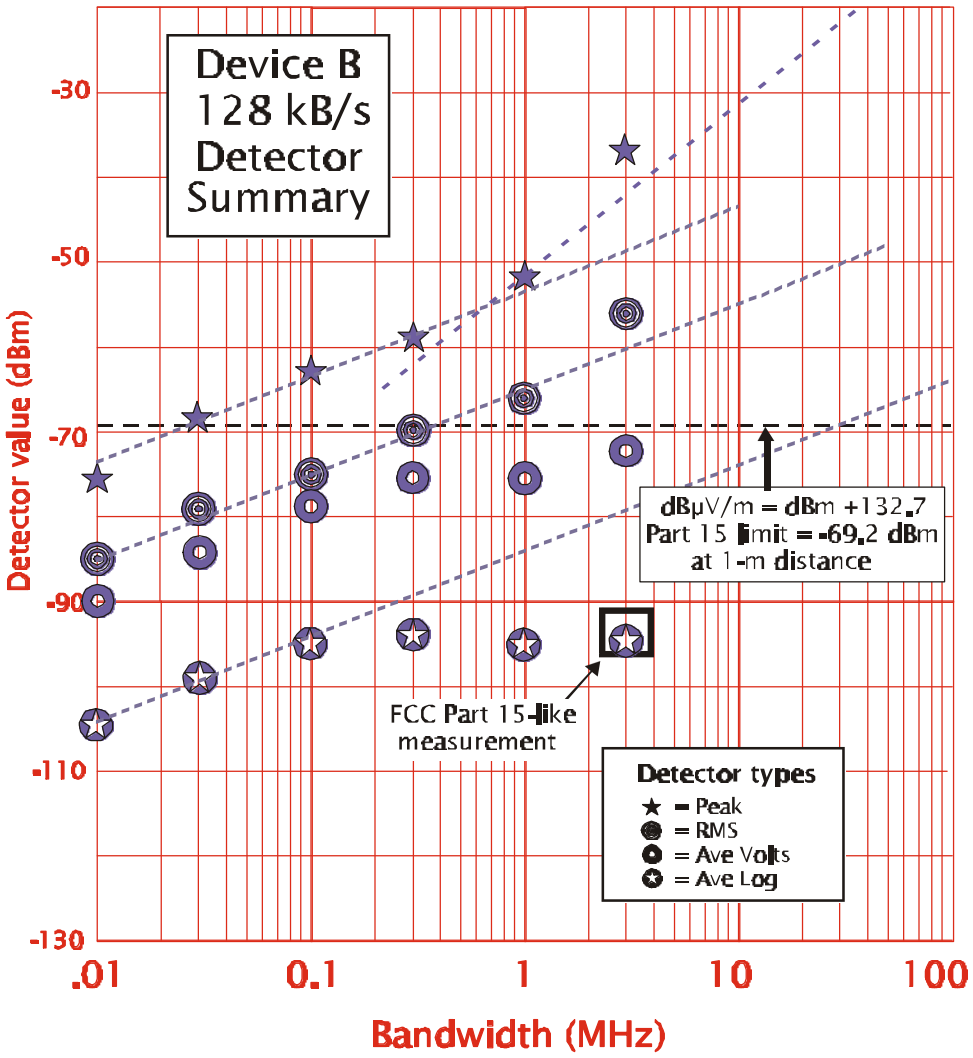

Figure D.B.49. Device B, detector summary

This Page Intentionally Left Blank

This Page Intentionally Left Blank

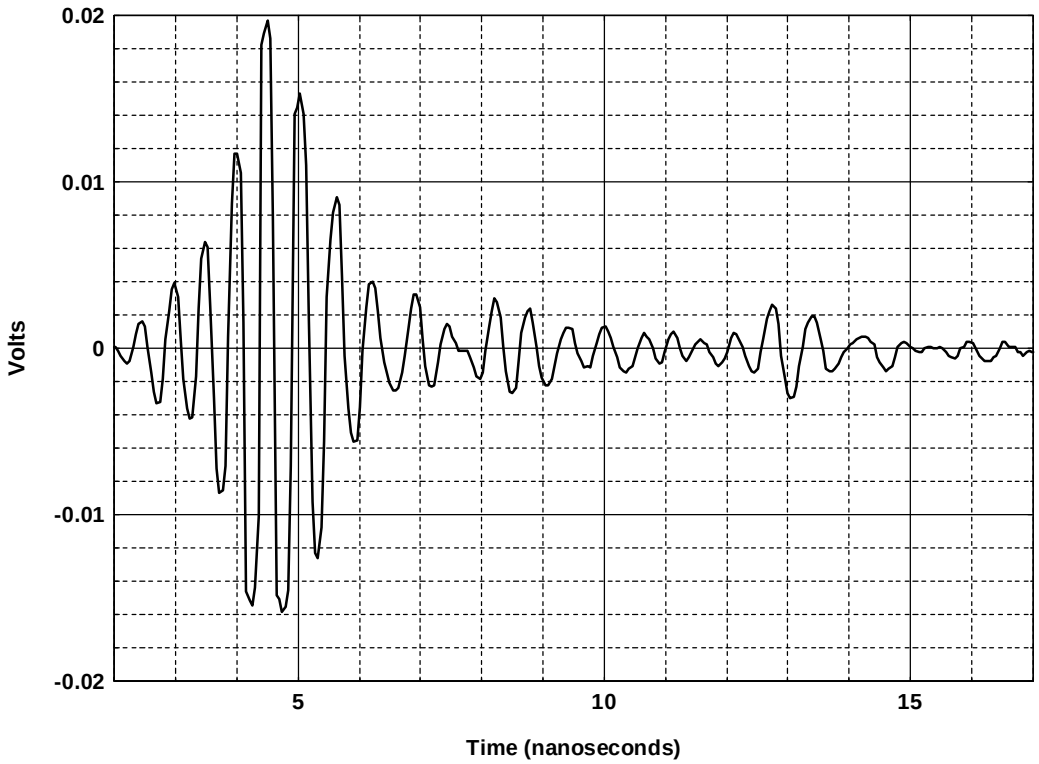

Figure D.C.1. Device C, radiated time-domain waveform.

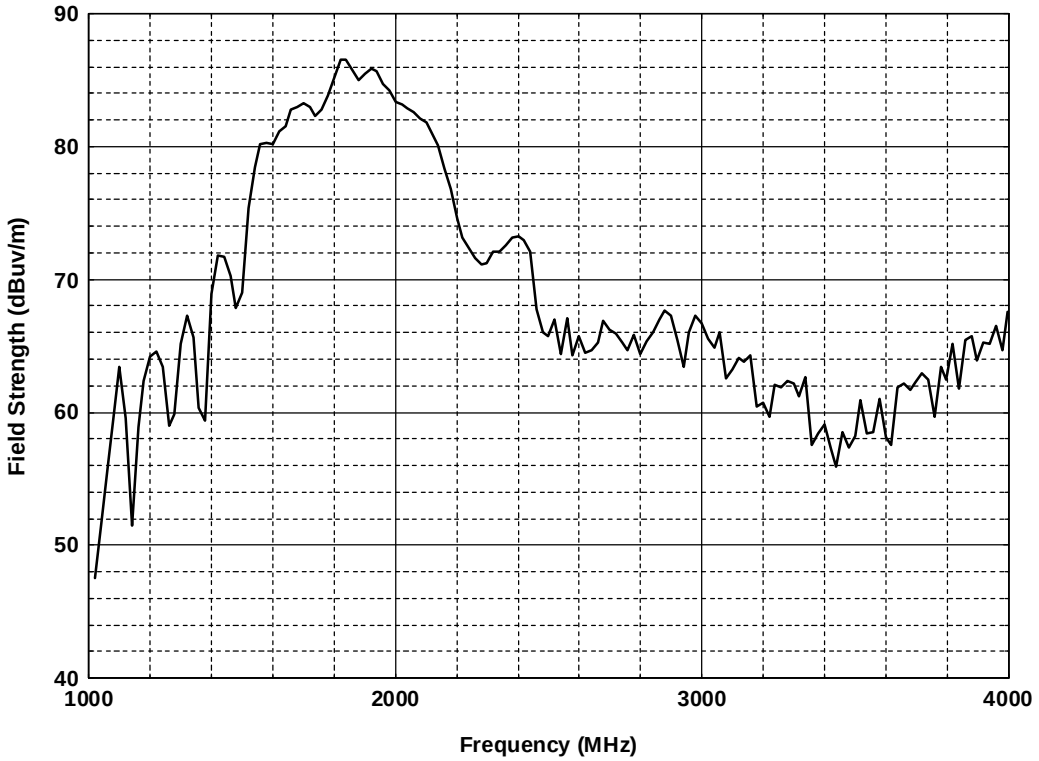

Figure D.C.2. Device C, radiated peak field strength at 1 m,) f = 20 MHz.

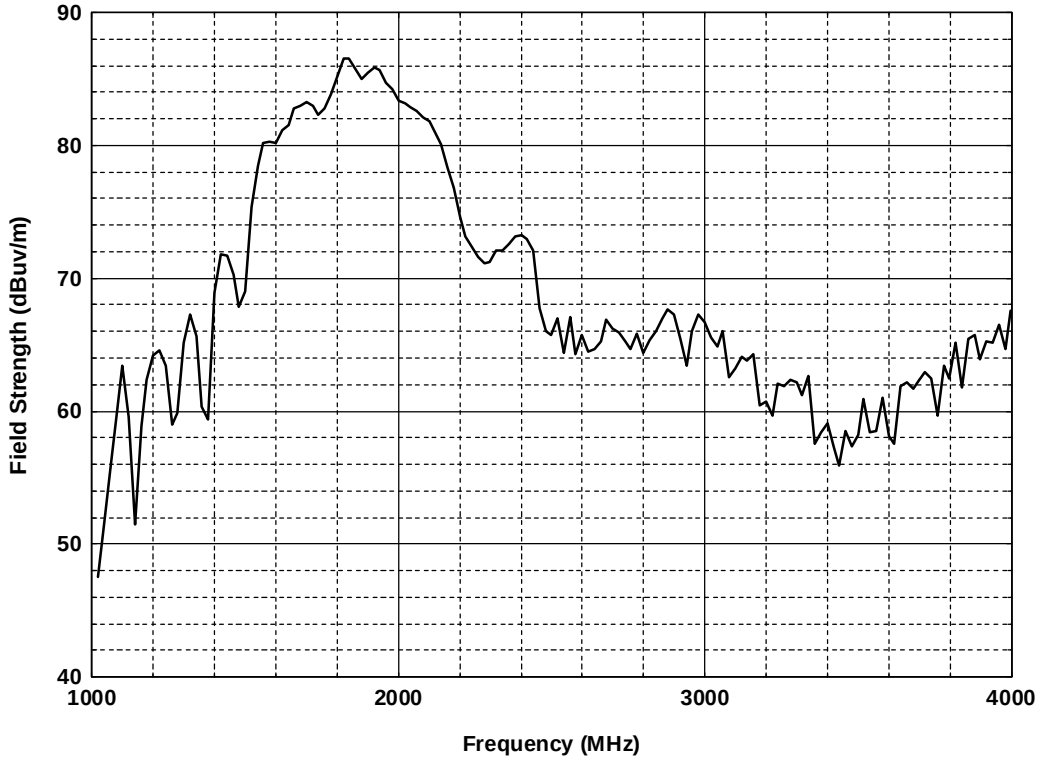

Figure D.C.3. Device C, radiated peak field strength at 1 m,) f = 20 MHz.

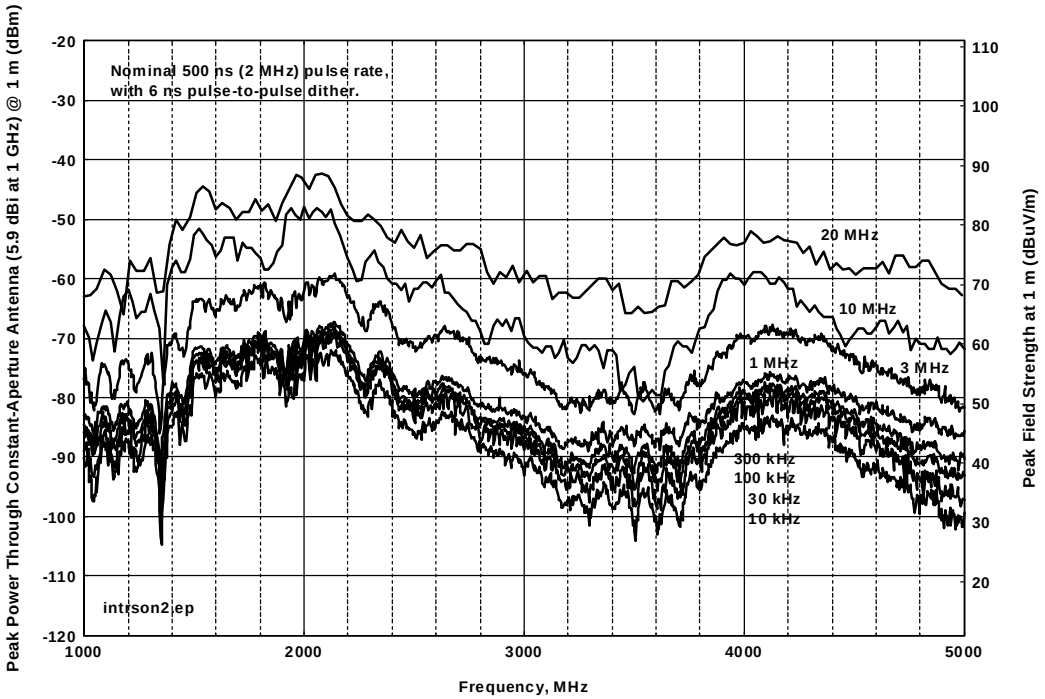

Figure D.C.4. Device C, 1.25% pulse-to-pulse dithered.

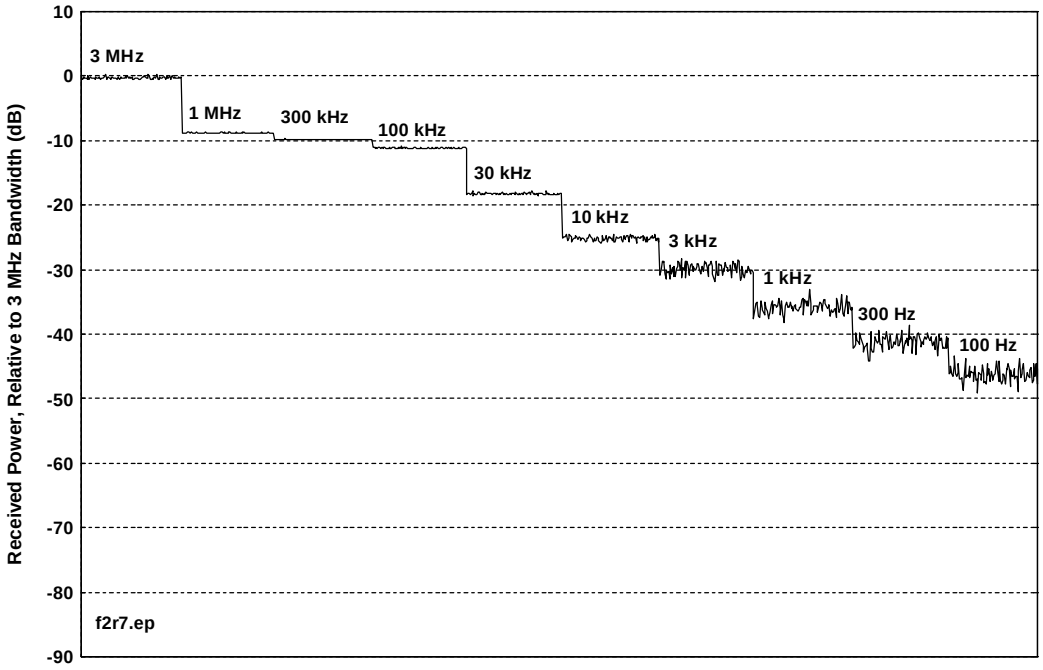

Figure D.C.5. Device C, bandwidth progression stairstep.

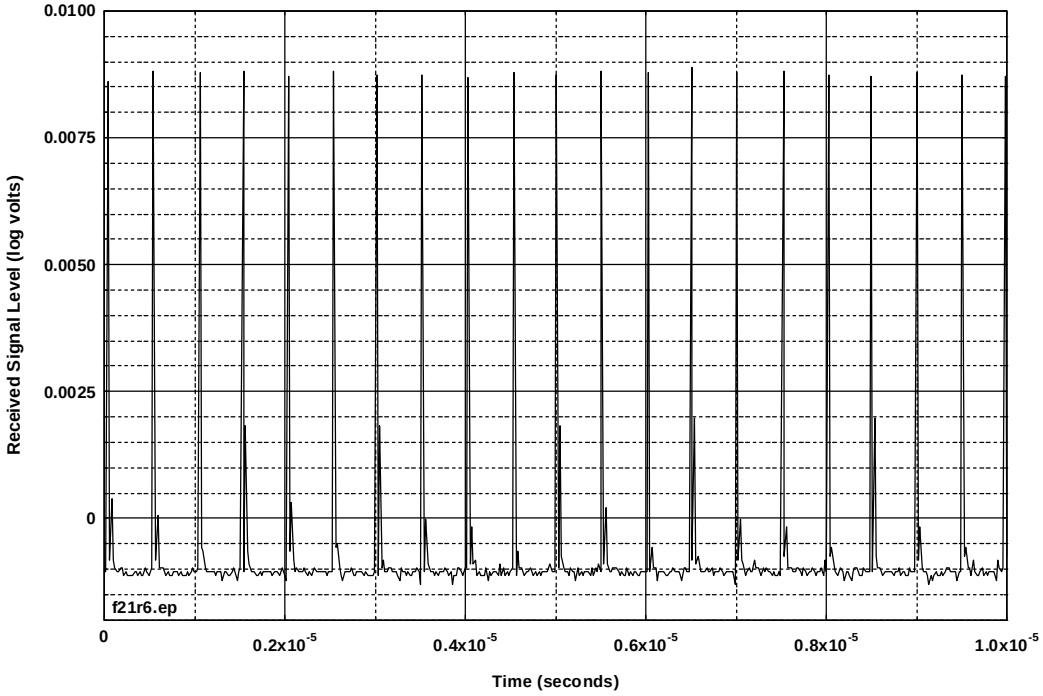

Figure D.C.6. Device C, time waveform for 10 microseconds, 18-Ghz envelope detector.

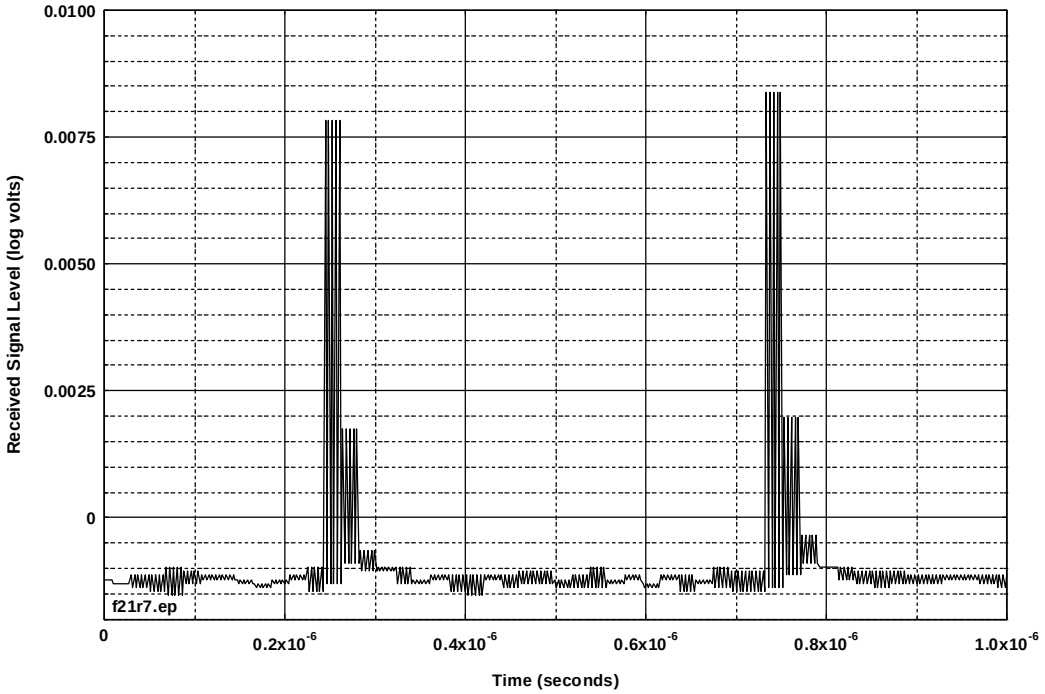

Figure D.C.7. Device C, time waveform, 1 microsecond, 18-GHz envelope detector.

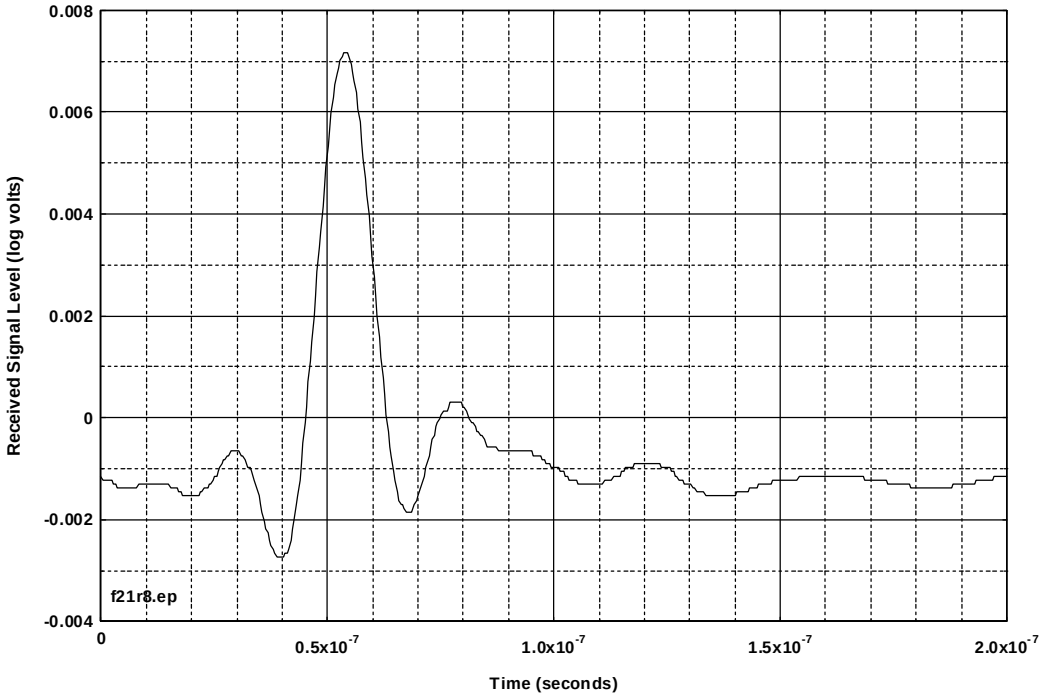

Figure D.C.8. Device C, time waveform, 200 nsec, bandwidth-limited by oscilloscope.

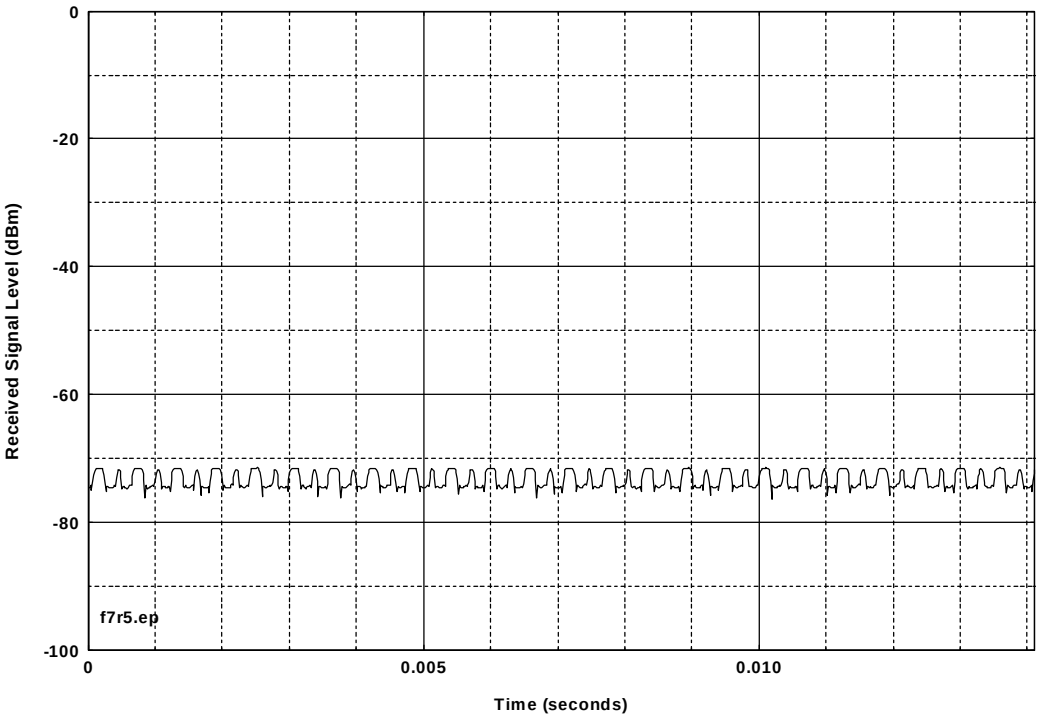

Figure D.C.9. Device C, Part 15 measurement in 10-kHz video bandwidth.

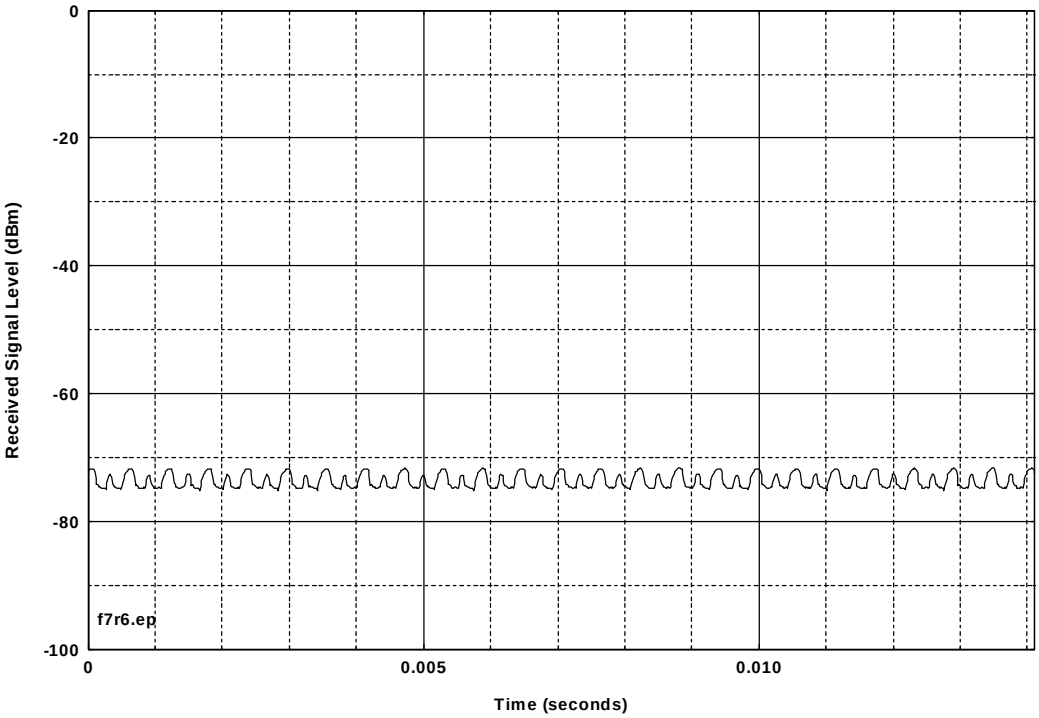

Figure D.C.10. Device C, Part 15 measurement in 3-kHz video bandwidth.

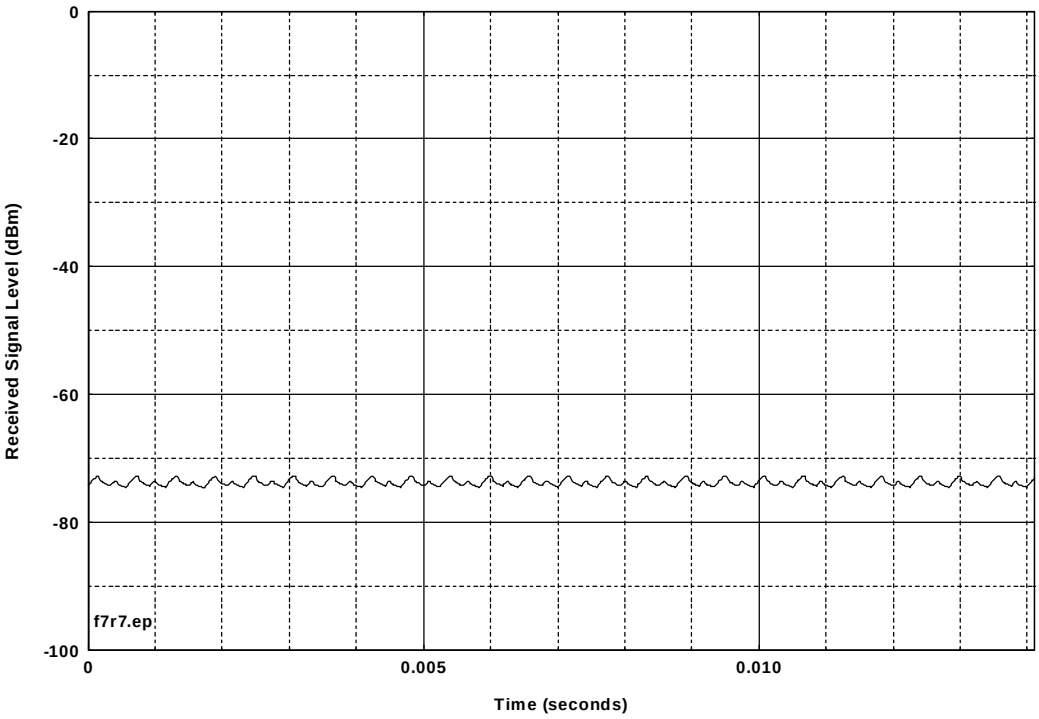

Figure D.C.11. Device C, Part 15 measurement in 1-kHz video bandwidth.

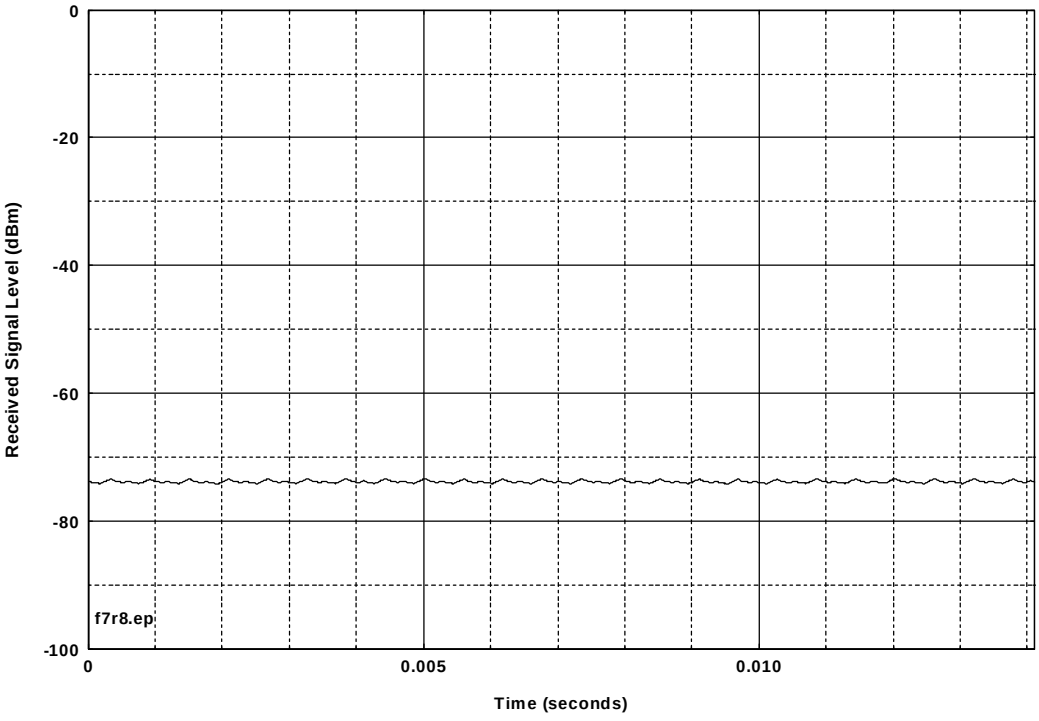

Figure D.C.12. Device C, Part 15 measurement in 300-Hz video bandwidth.

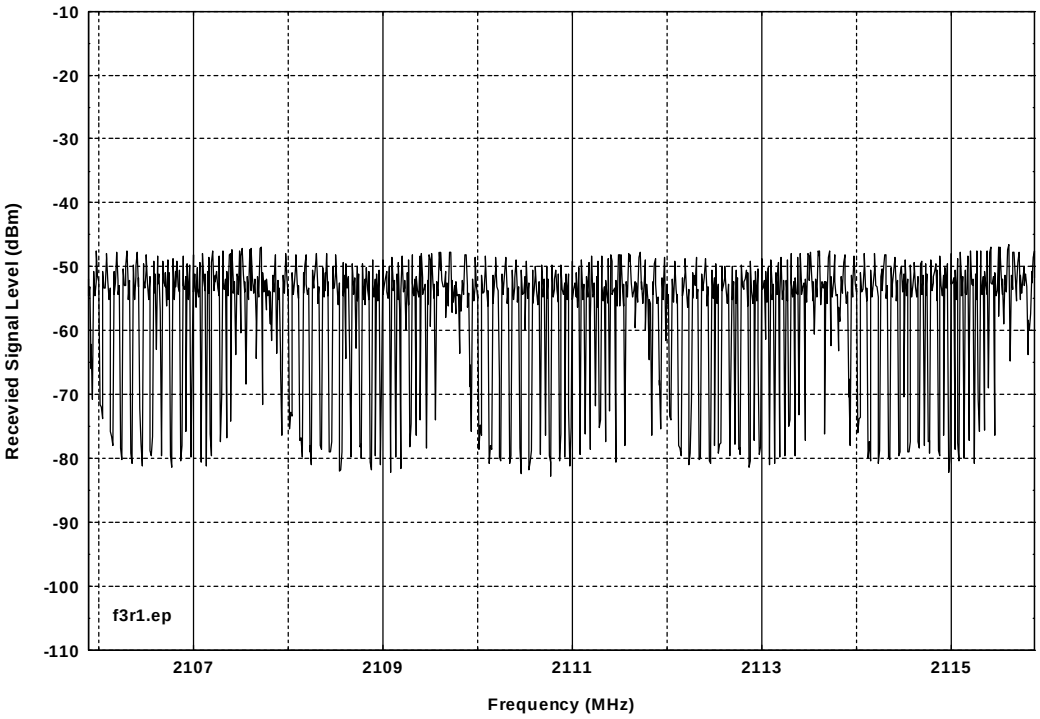

Figure D.C.13. Device C, peak-detected to show lines in noise.

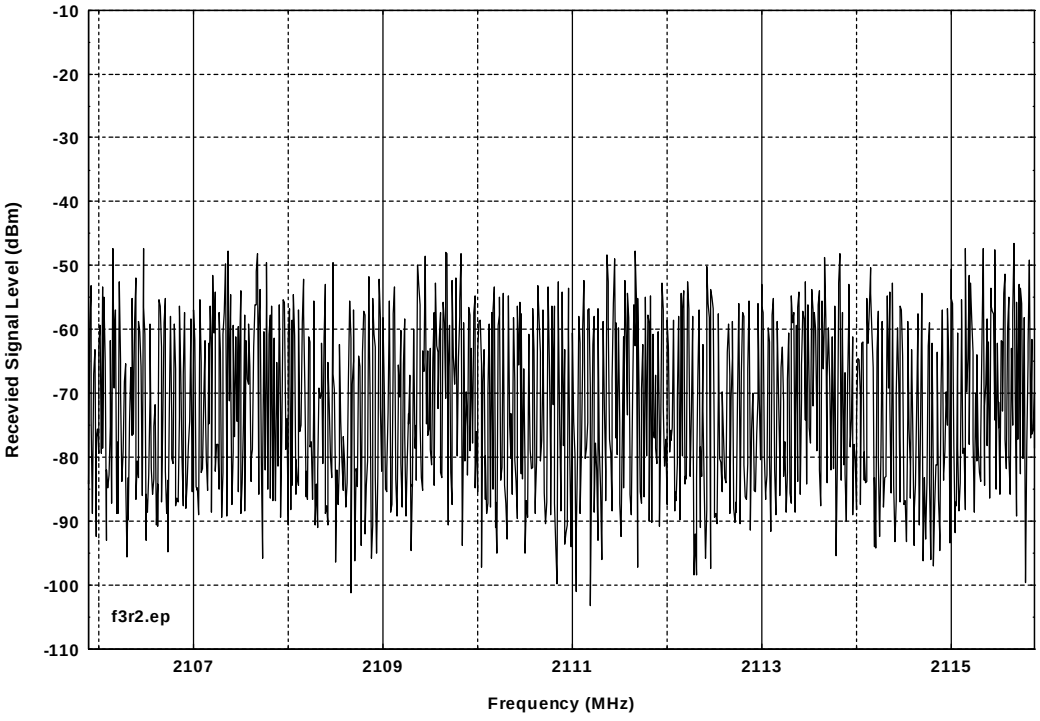

Figure D.C.14. Device C, sample-detected to show how lines are not normally visible.

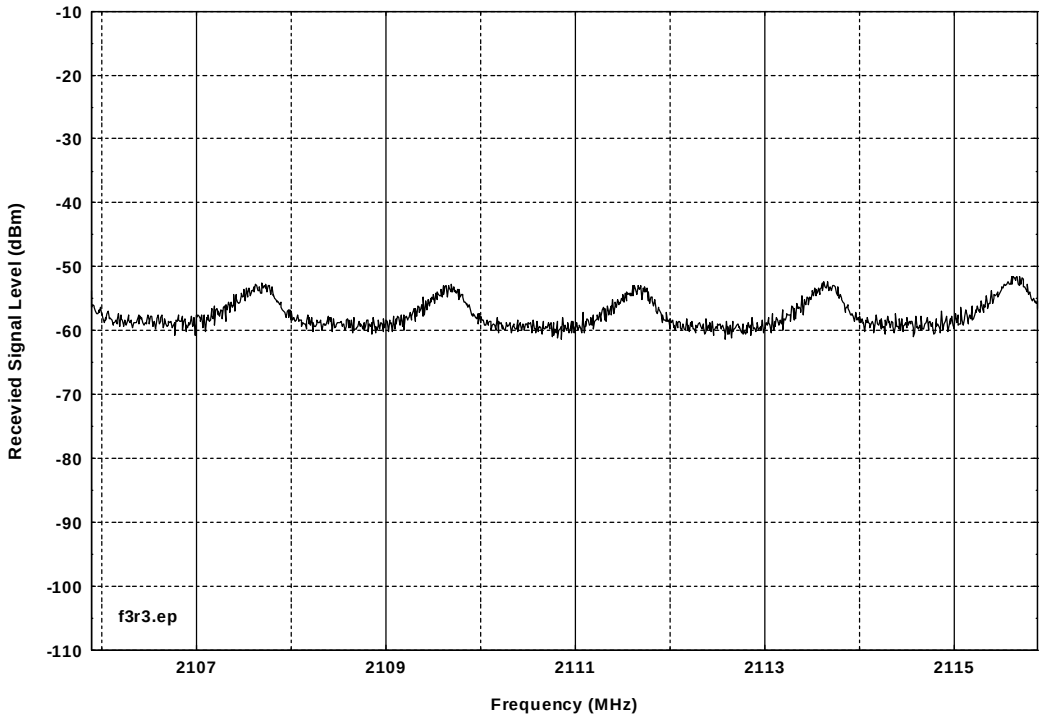

Figure D.C.15. Device C, video-averaged with peak detector to force lines to show.

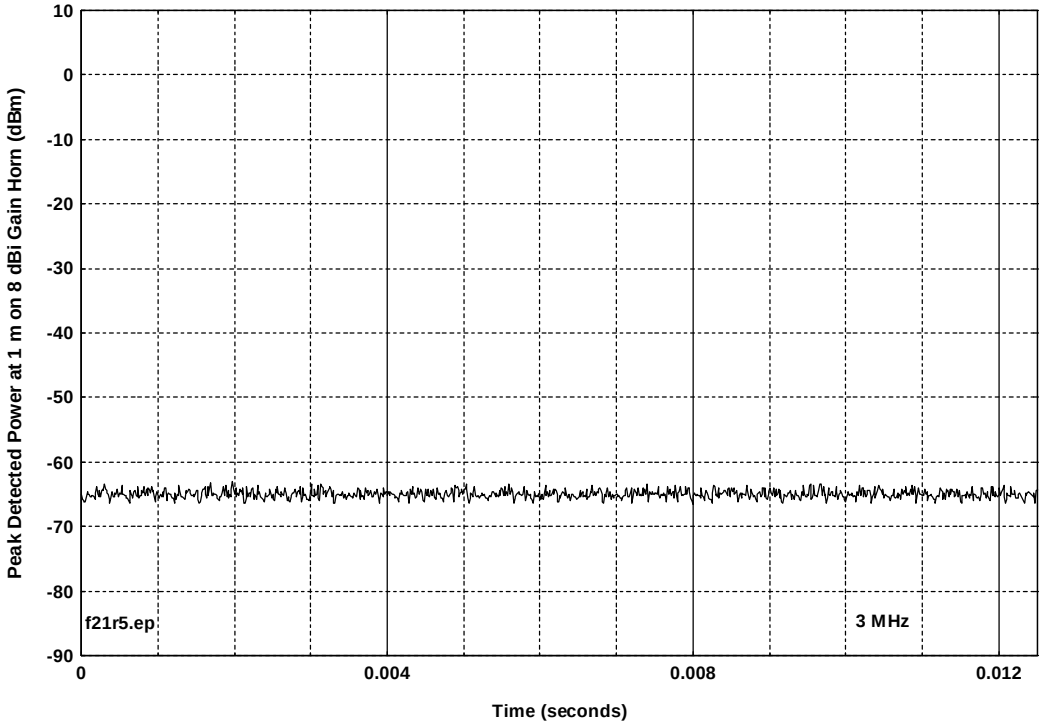

Figure D.C.16. Device C, output in 12 milliseconds.

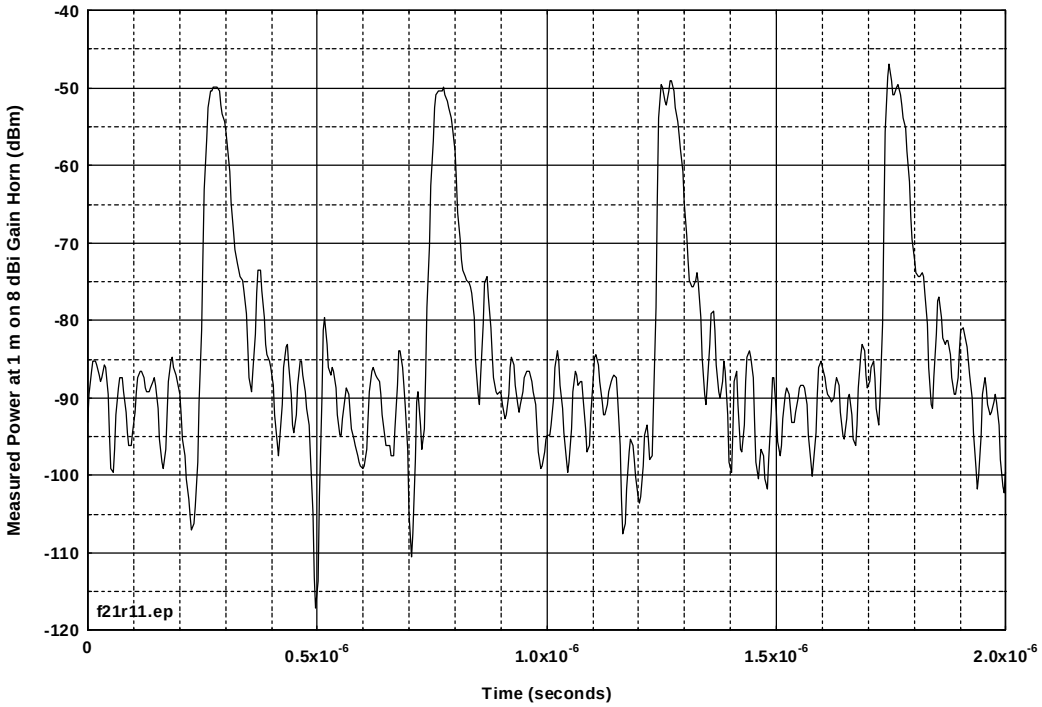

Figure D.C.17. Device C, time waveform in 20-MHz bandwidth.

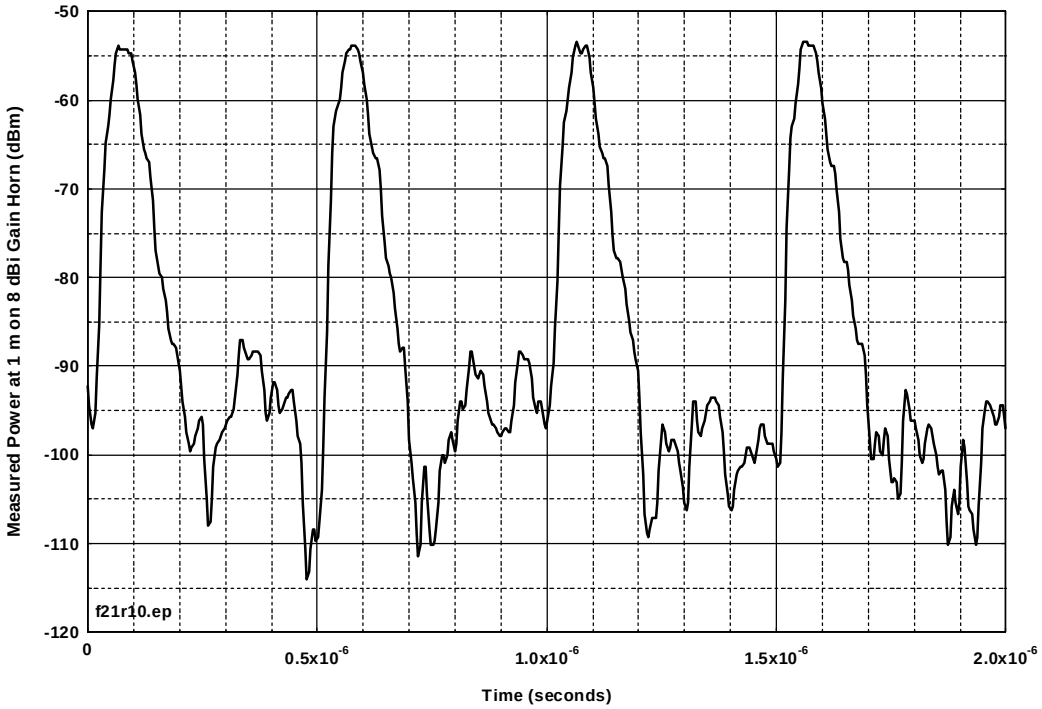

Figure D.C.18. Device C, time waveform in 10-MHz bandwidth.

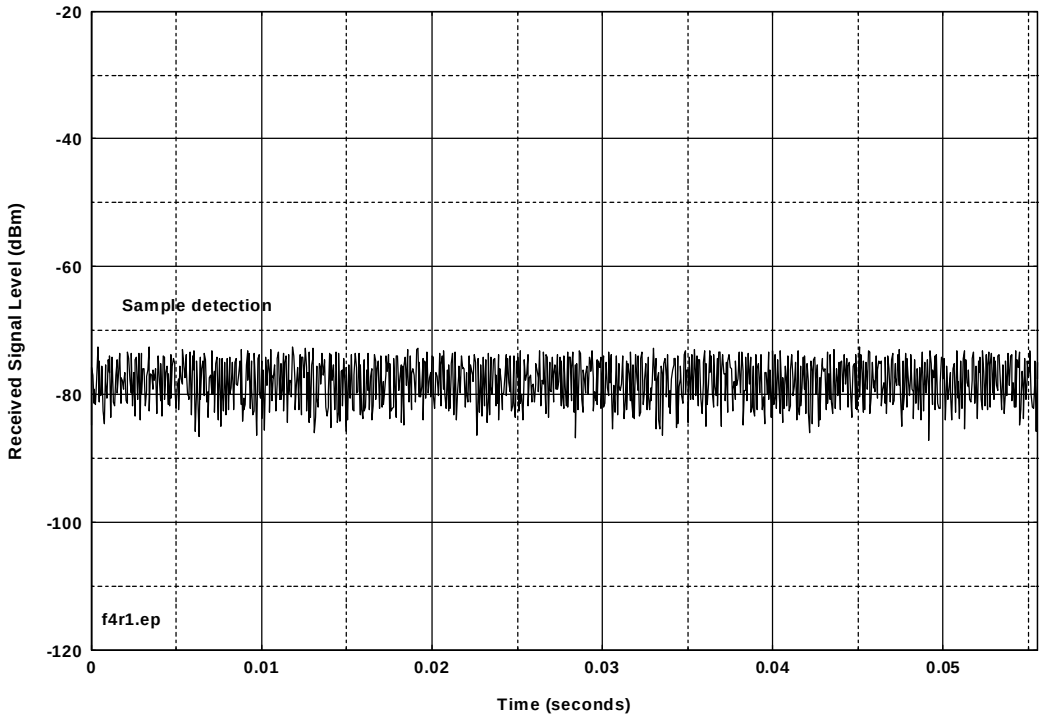

Figure D.C.19. Device C, time waveform in 55 ms, 3-MHz IF bandwidth.

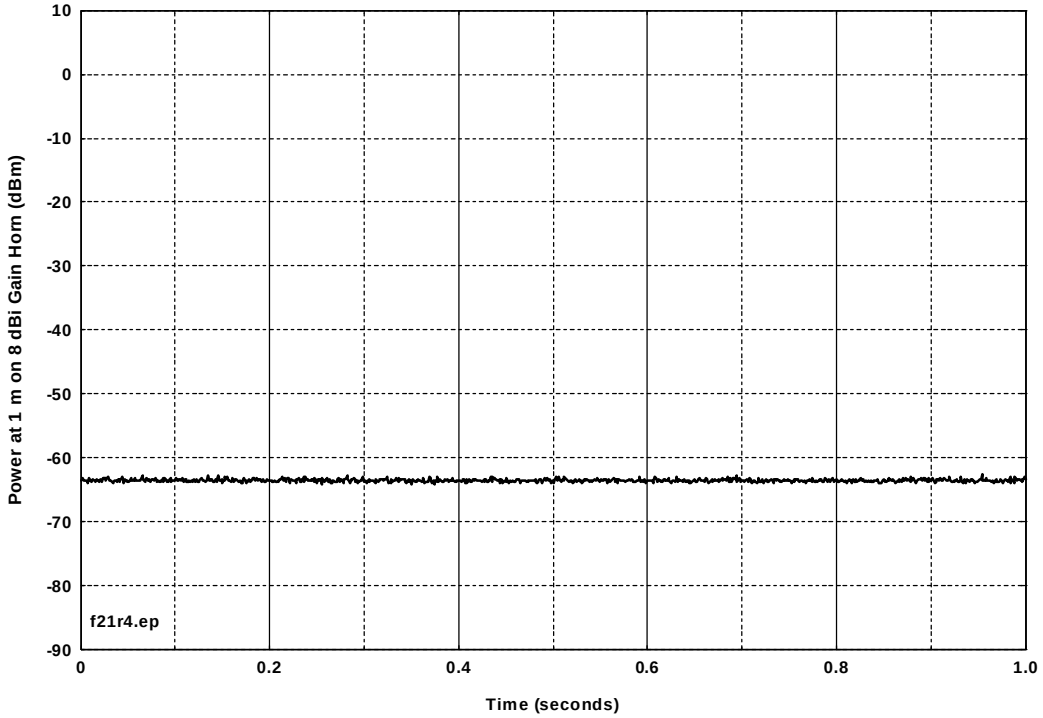

Figure D.C.20. Device C, output in one second.

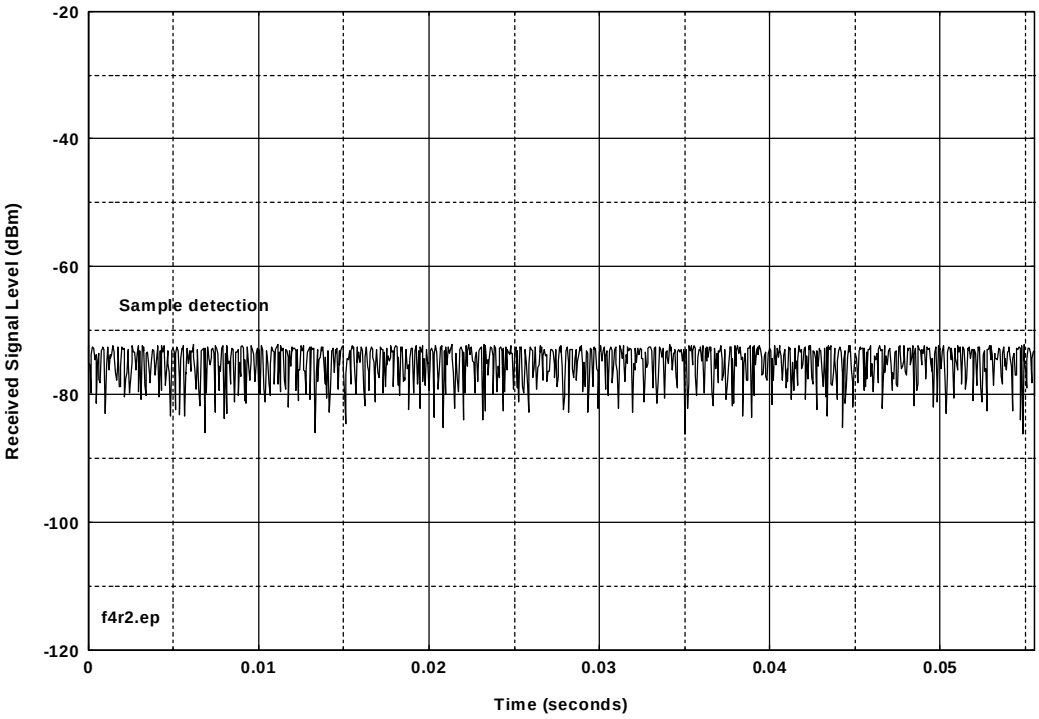

Figure D.C.21. Device C, time waveform, 55 ms, 1-MHz IF bandwidth.

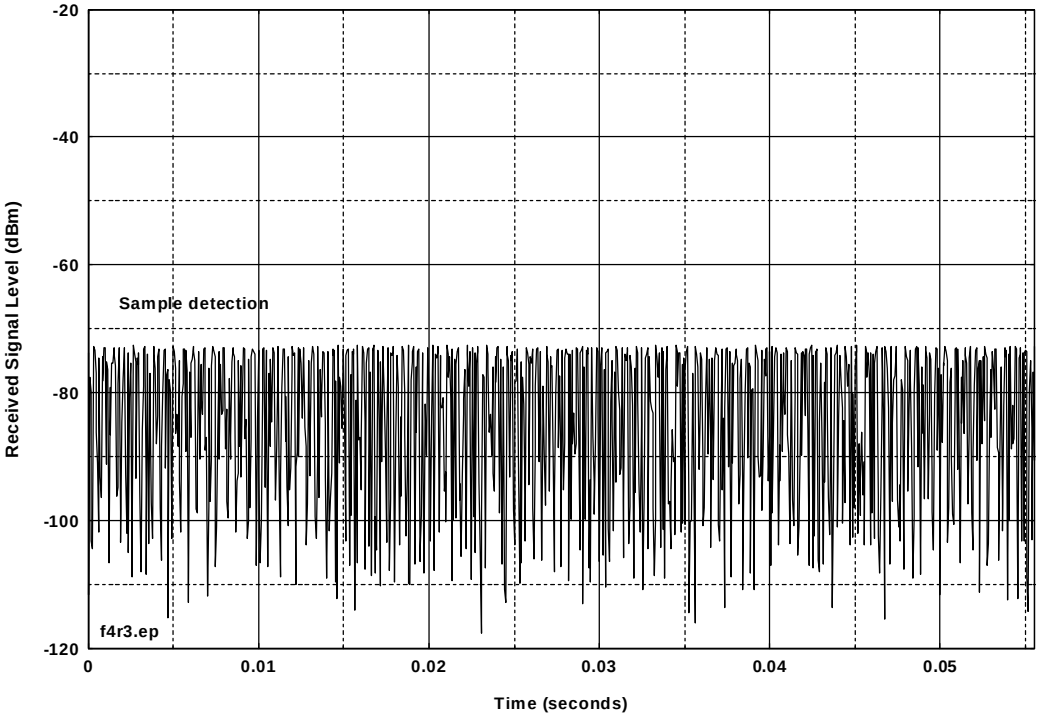

Figure D.C.22. Device C, time waveform, 55 ms, 300-kHz IF bandwidth.

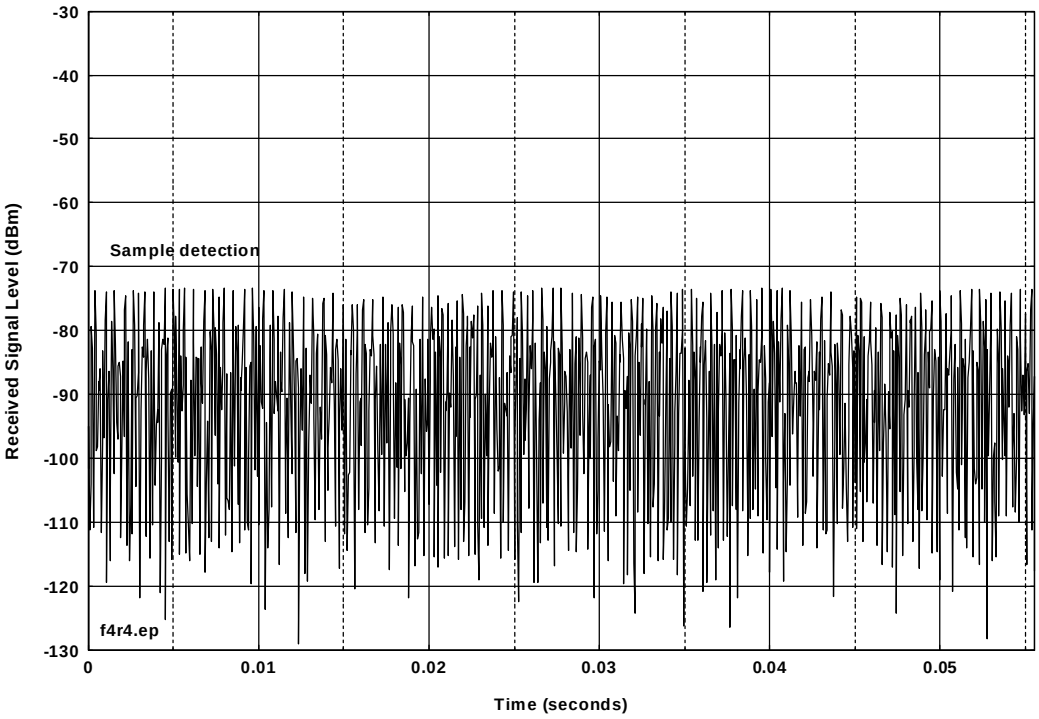

Figure D.C.23. Device C, time waveform, 55 ms, 100-kHz IF bandwidth.

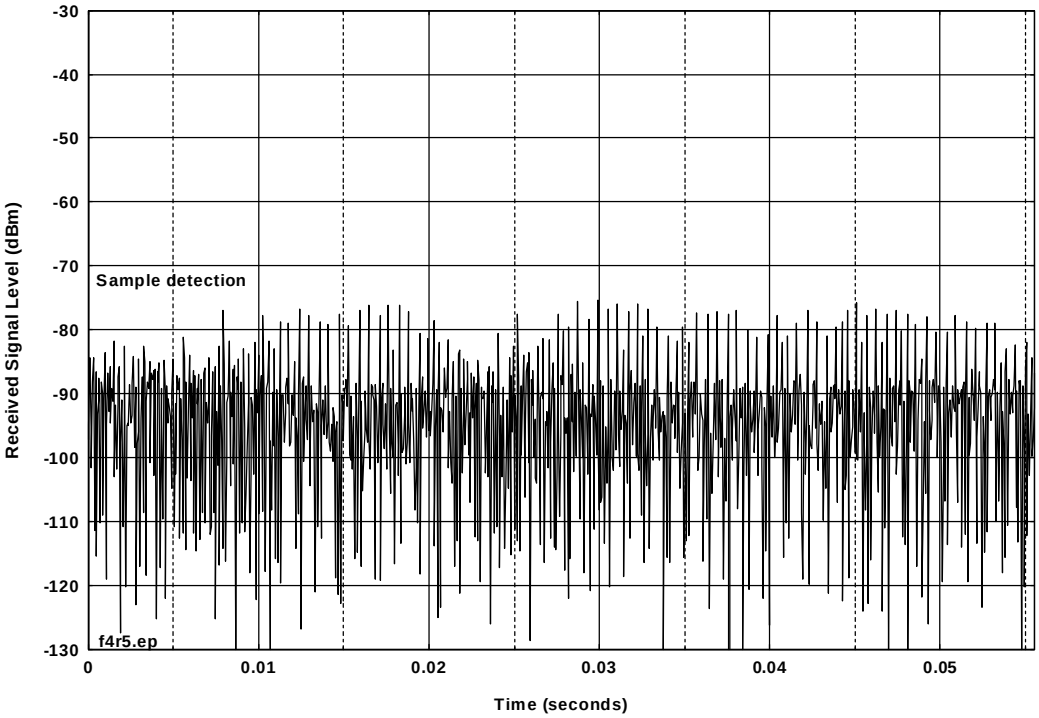

Figure D.C.24. Device C, time waveform, 55 ms, 30-kHz IF bandwidth.

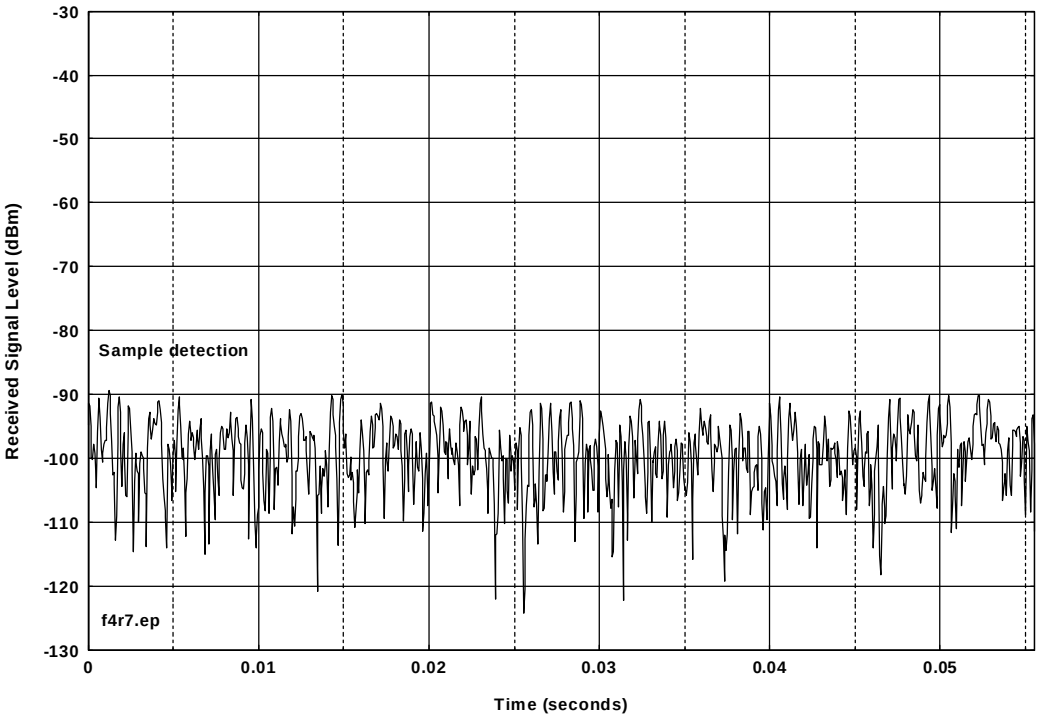

Figure D.C.25. Device C, time waveform, 55 ms, 3-kHz IF bandwidth.

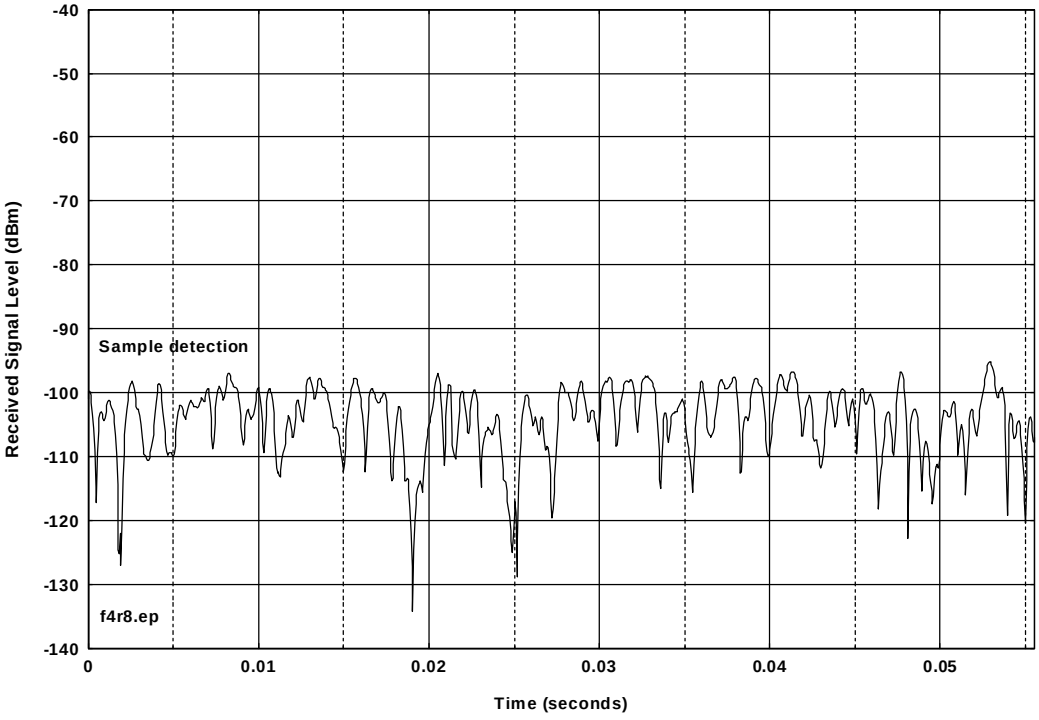

Figure D.C.26. Device C, time waveform, 55 ms, 1-kHz IF bandwidth.

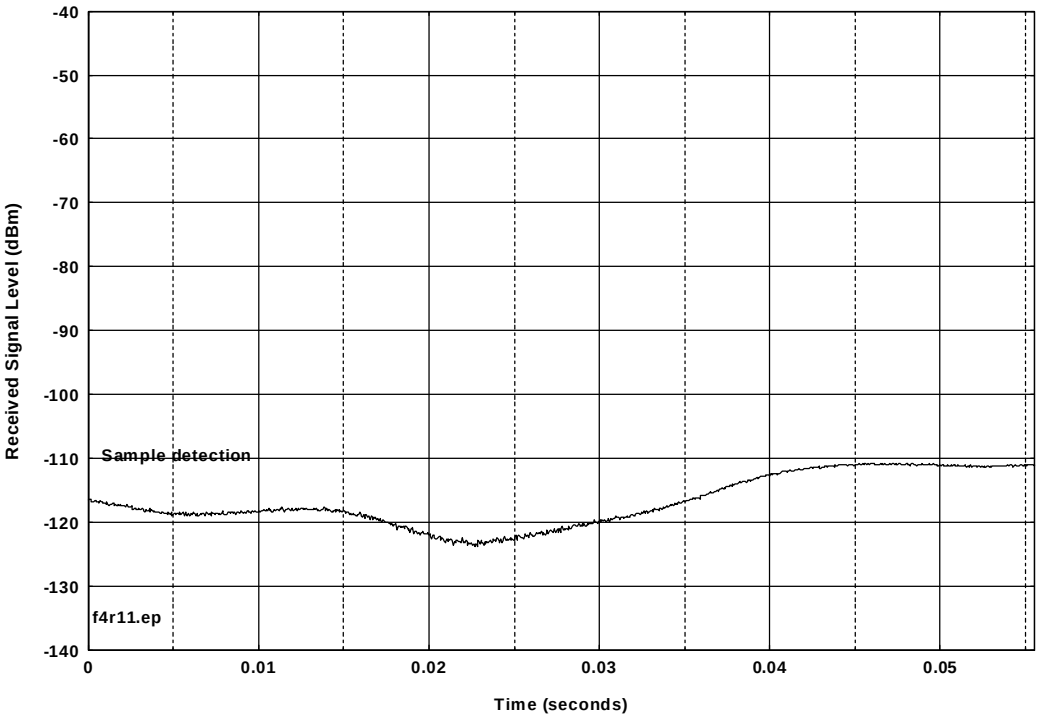

Figure D.C.27. Device C, time waveform, 55 ms, 30-Hz IF bandwidth.

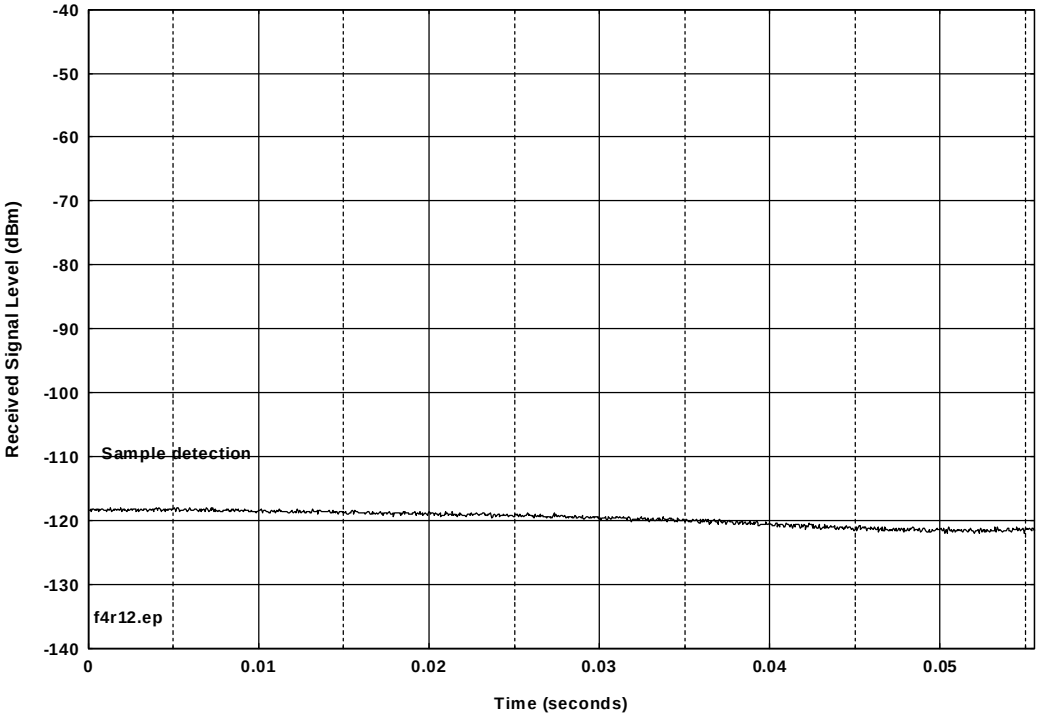

Figure D.C.28. Device C, time waveform, 55 ms, 10-Hz IF bandwidth.

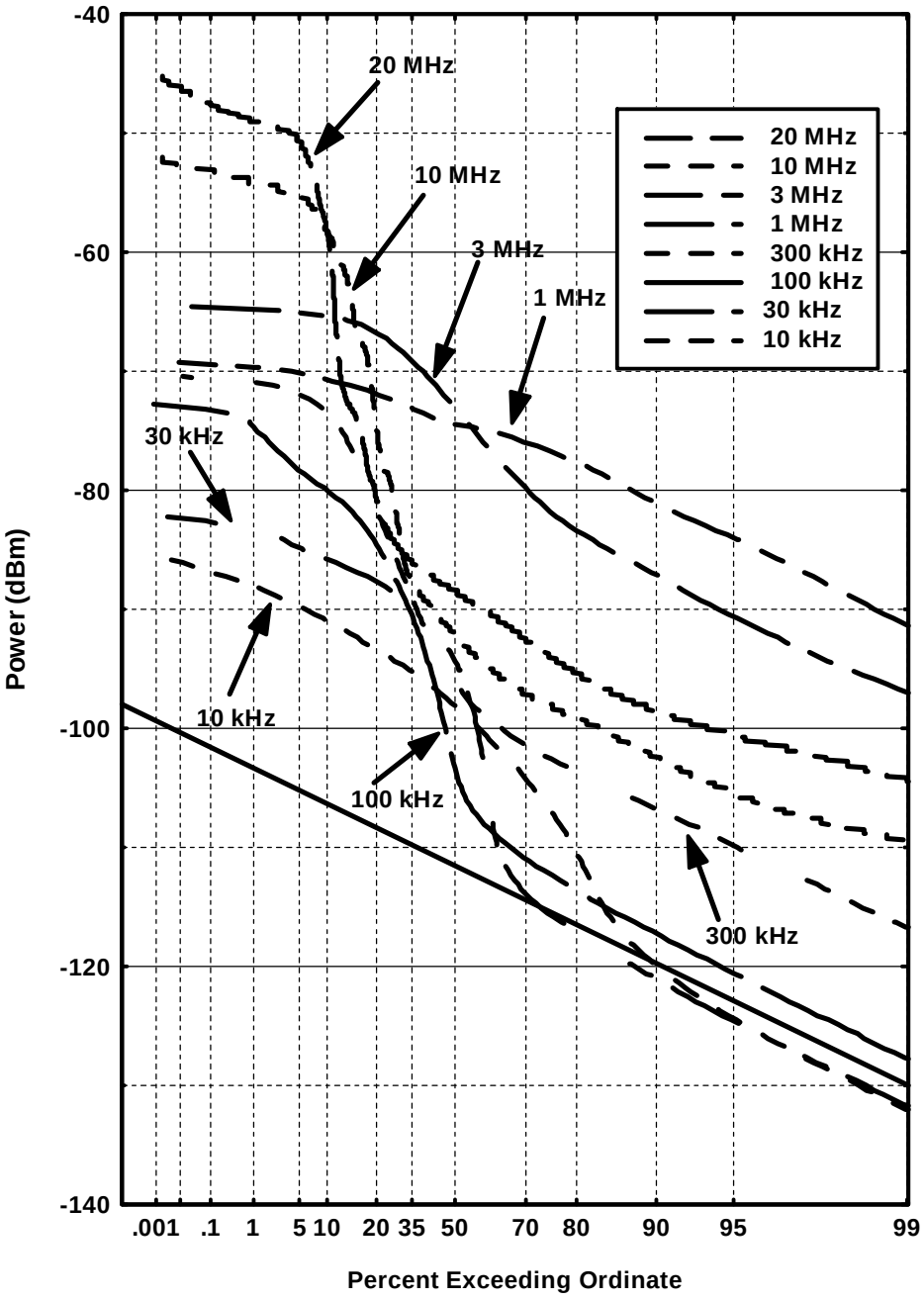

Figure D.C.29. Device C, APDs, between lines.

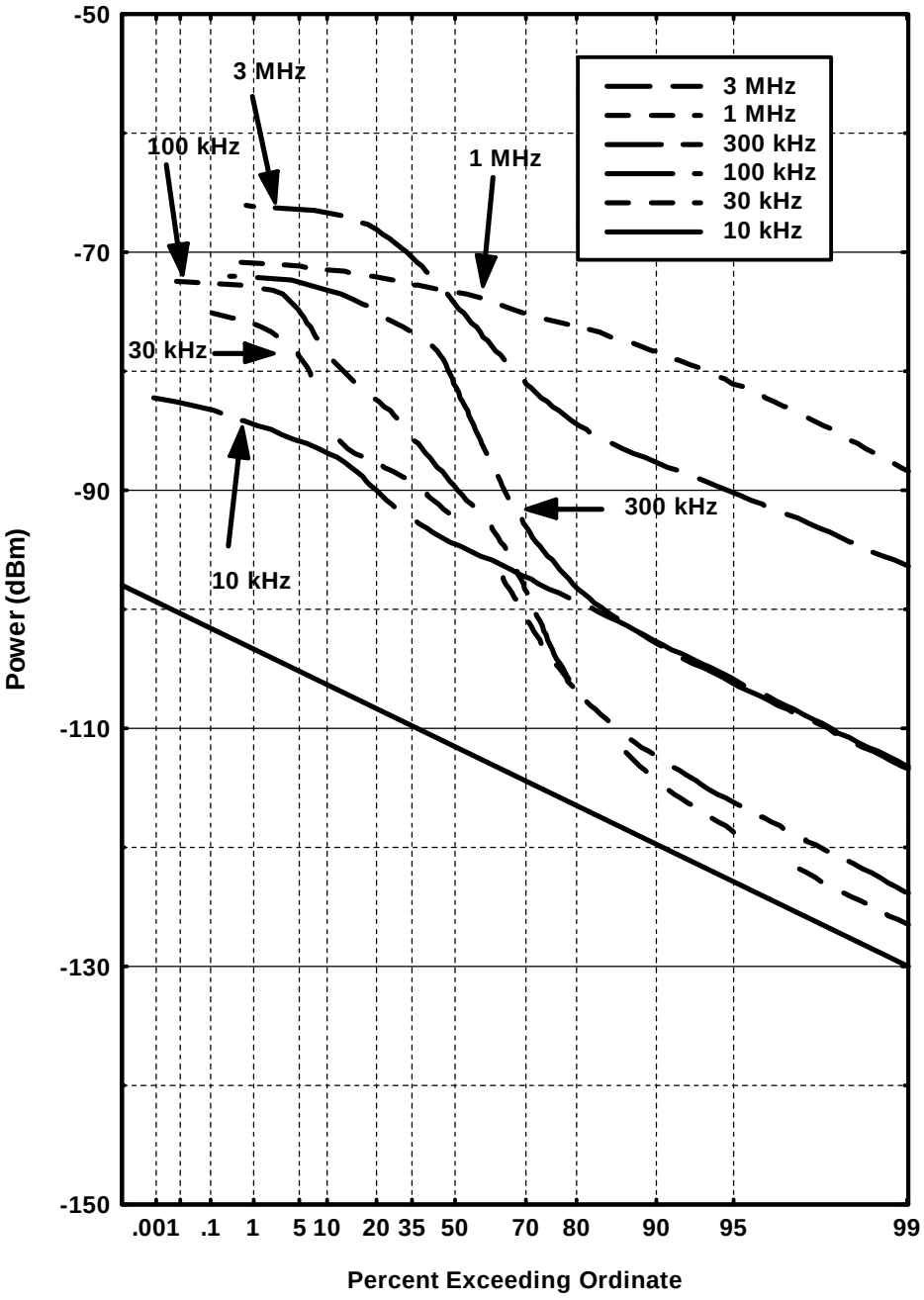

Figure D.C.30. Device C, APDs, on lines.

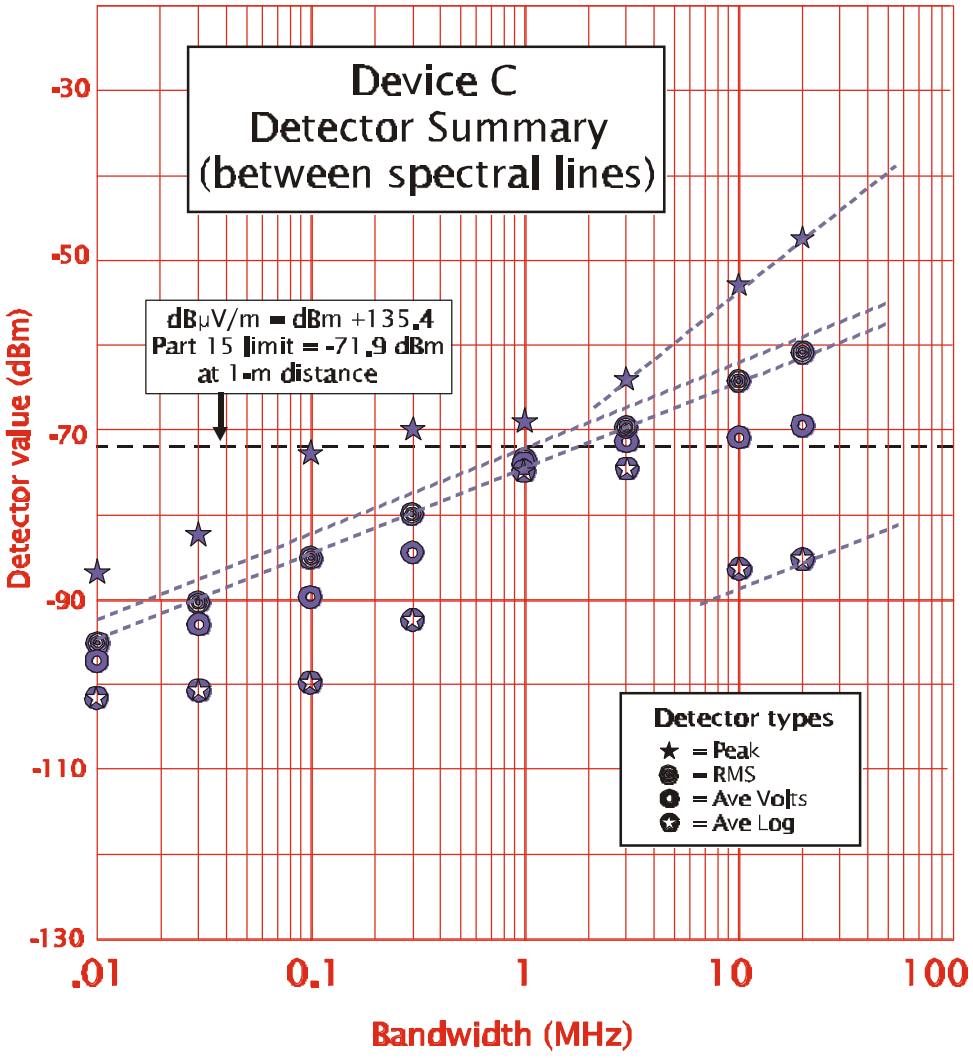

Figure D.C.31. Device C, detector summary (between spectral lines).

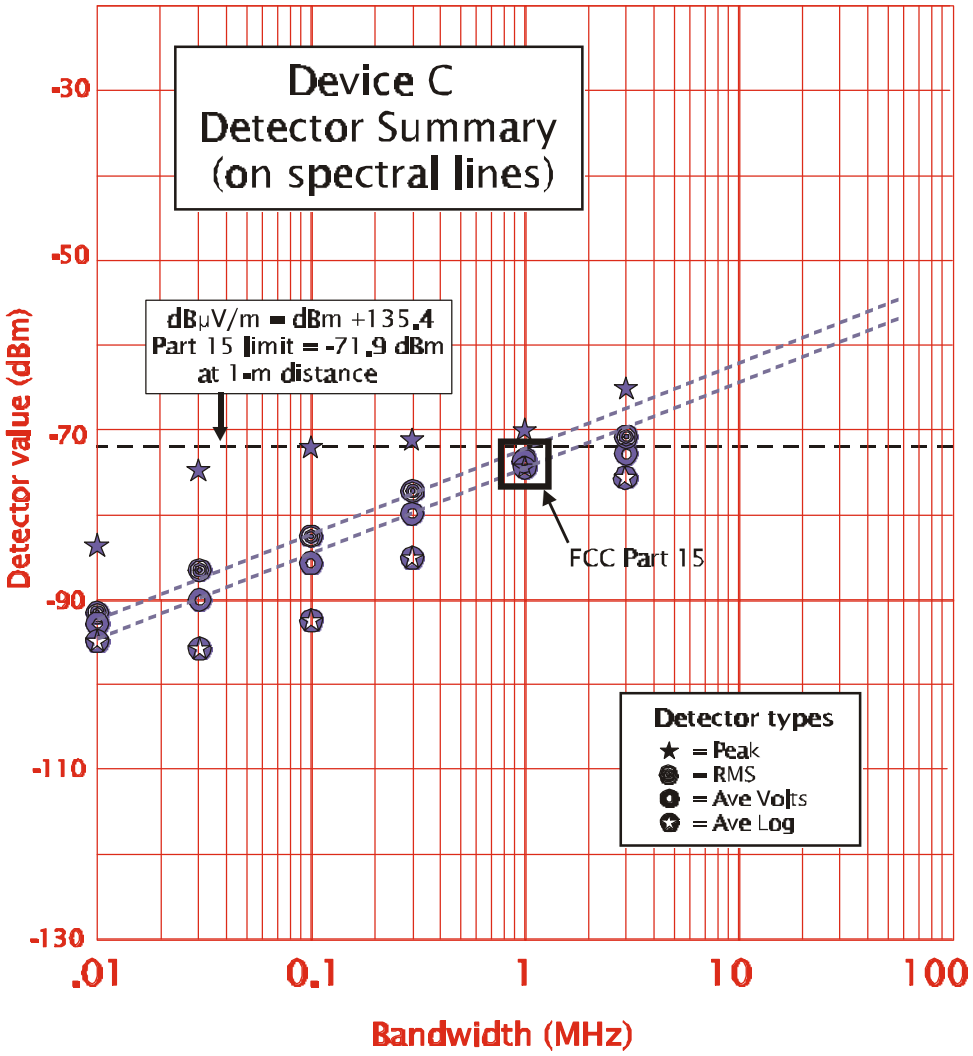

Figure D.C.32. Device C, detector summary (on spectral lines).

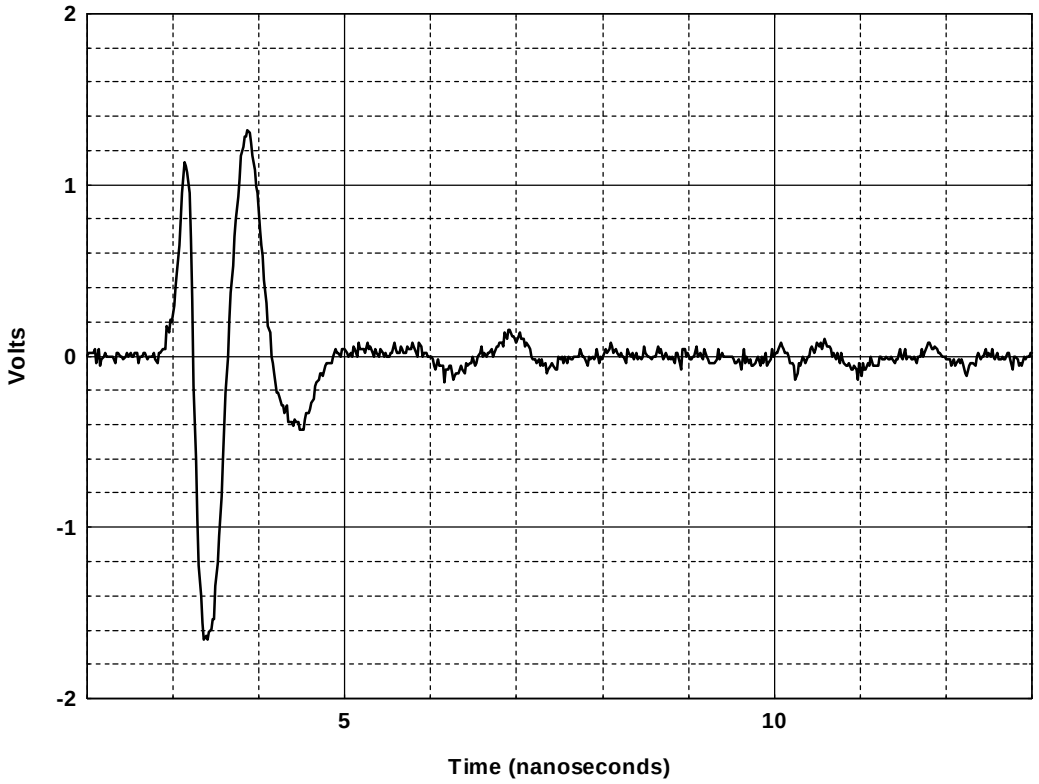

Figure D.D.1. Device D, conducted time-domain waveform.

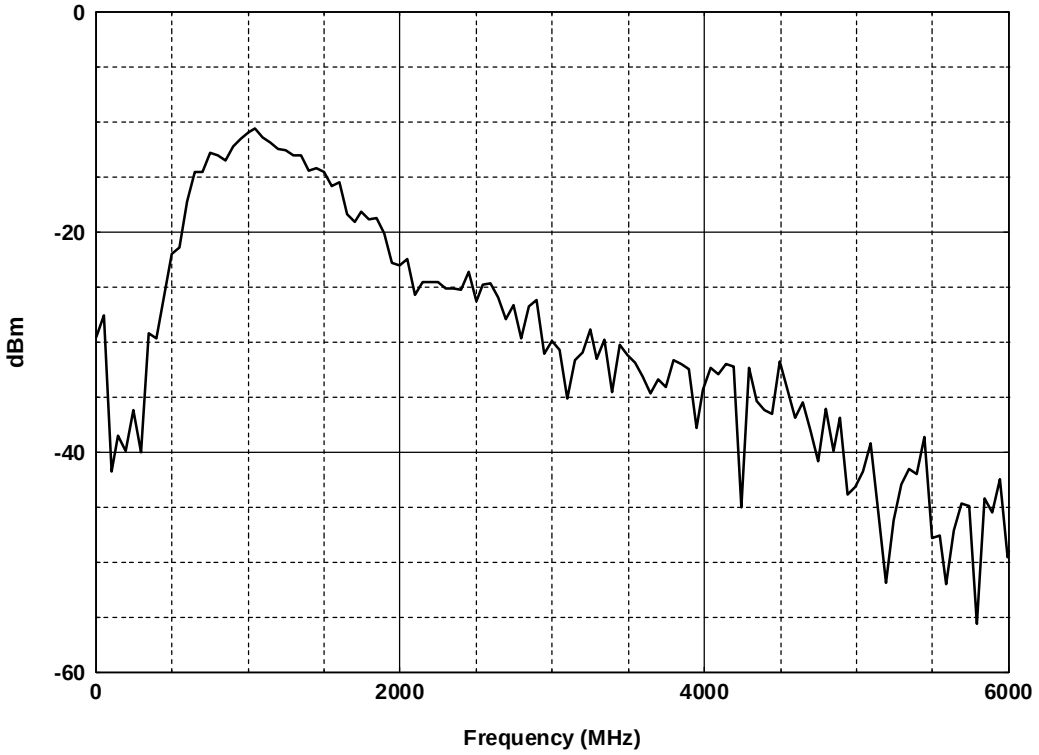

Figure D.D.2. Device D, conducted power spectrum,) f = 49.95 MHz.

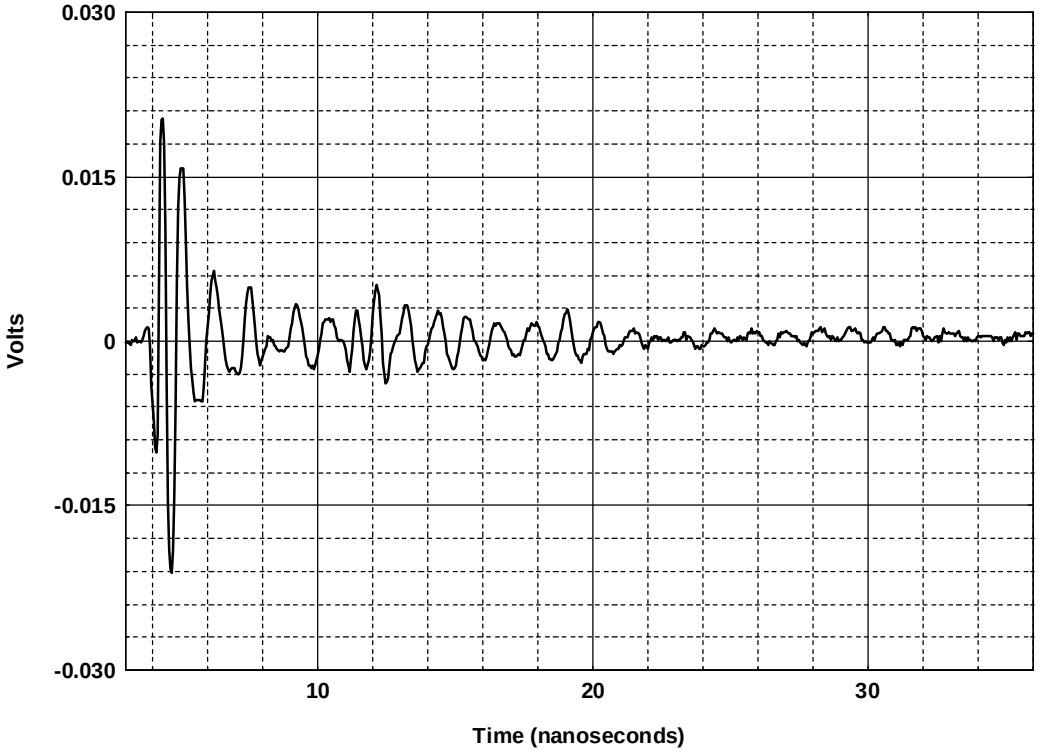

Figure D.D.3. Device D, radiated time-domain waveform.

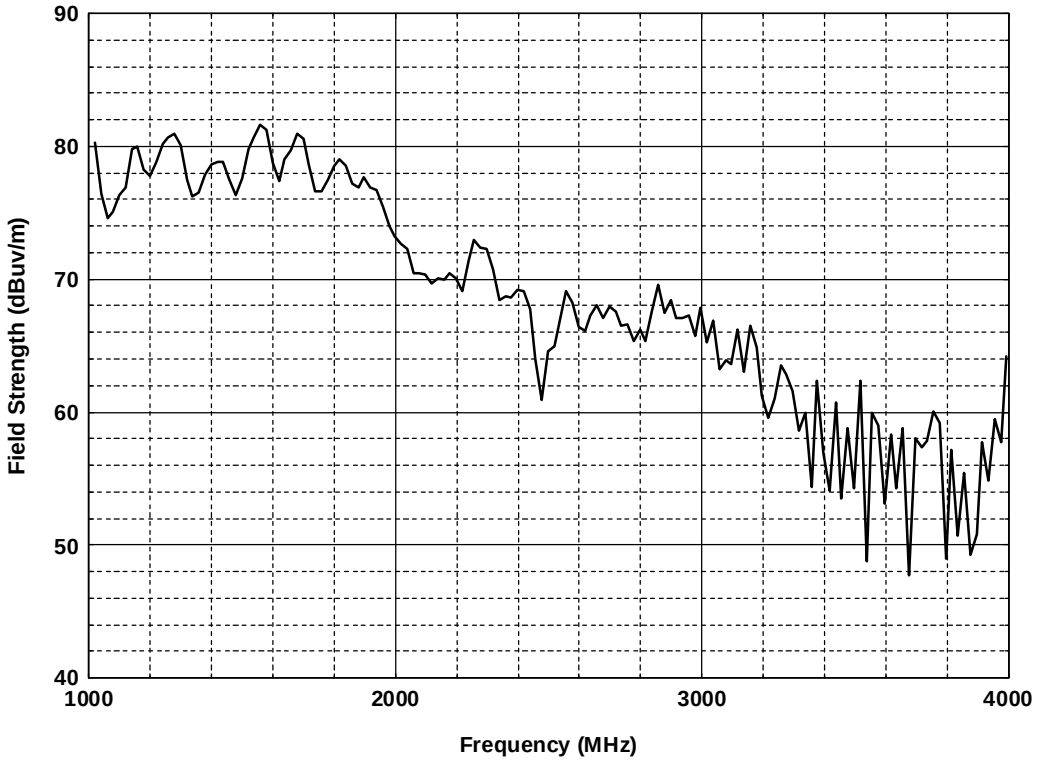

Figure D.D.4. Device D, radiated peak field strength at 1 m,
) f = 19.98 MHz.

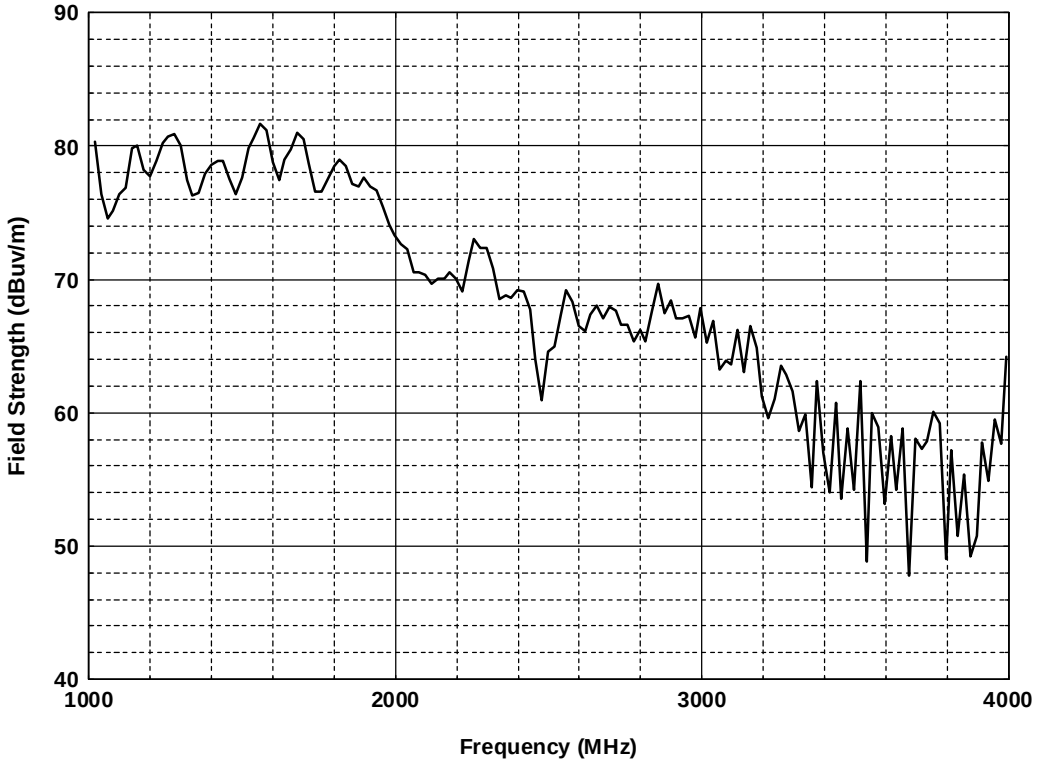

Figure D.D.5. Device D, radiated peak field strength at 1 m,
) f = 19.98 MHz.

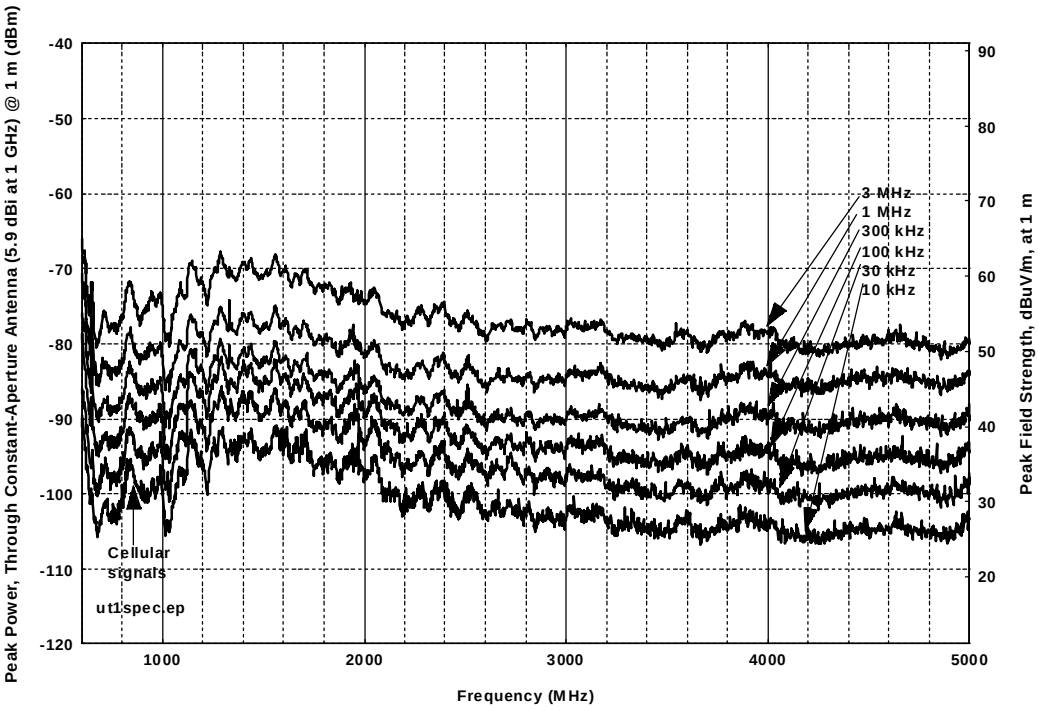

Figure D.D.6. Device D, absolute dither, 1-MHz nominal PRR, no gating.

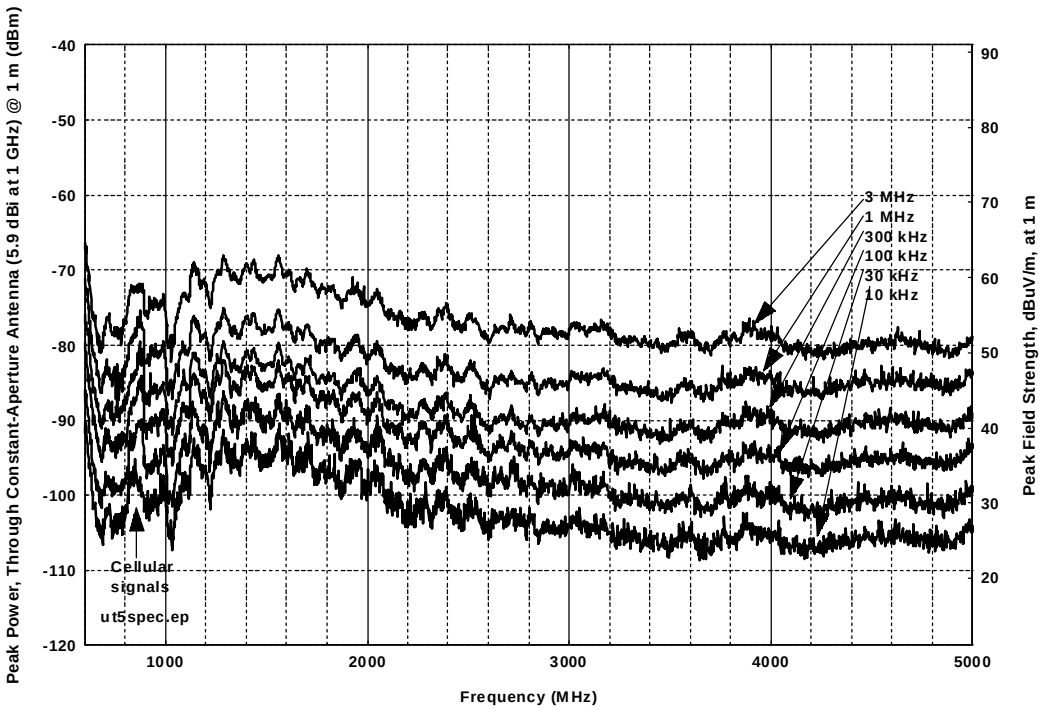

Figure D.D.7. Device D, absolute dither, 1-MHz nominal PRR, 25% gating.

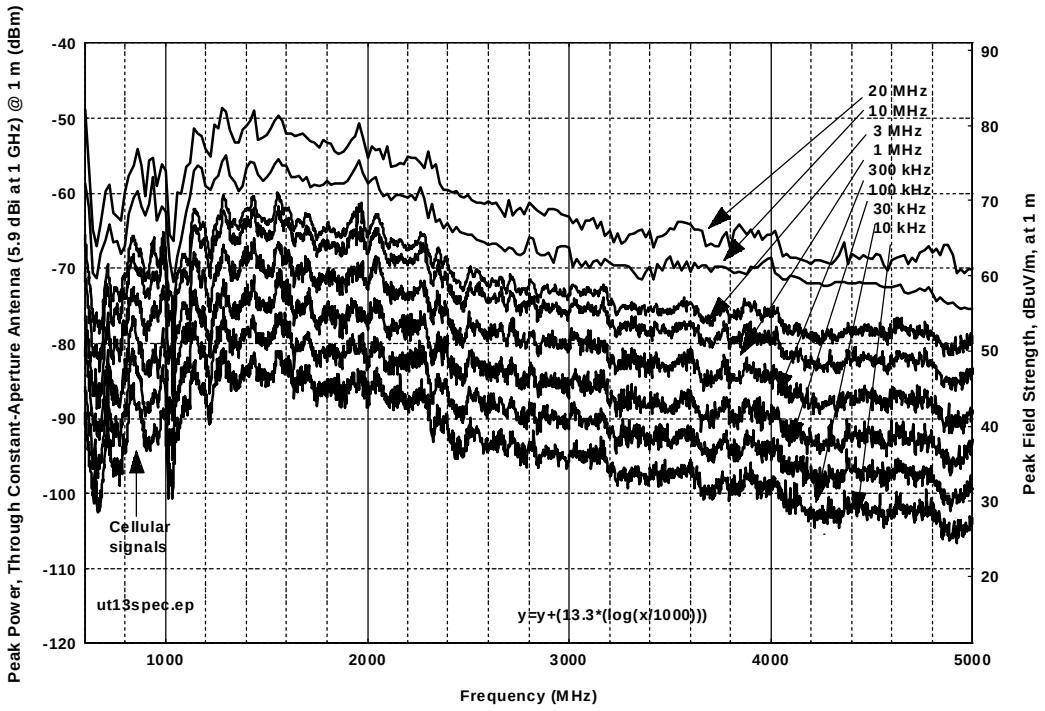

Figure D.D.8. Device D, absolute dither, 10-MHz nominal PRR, no gating.

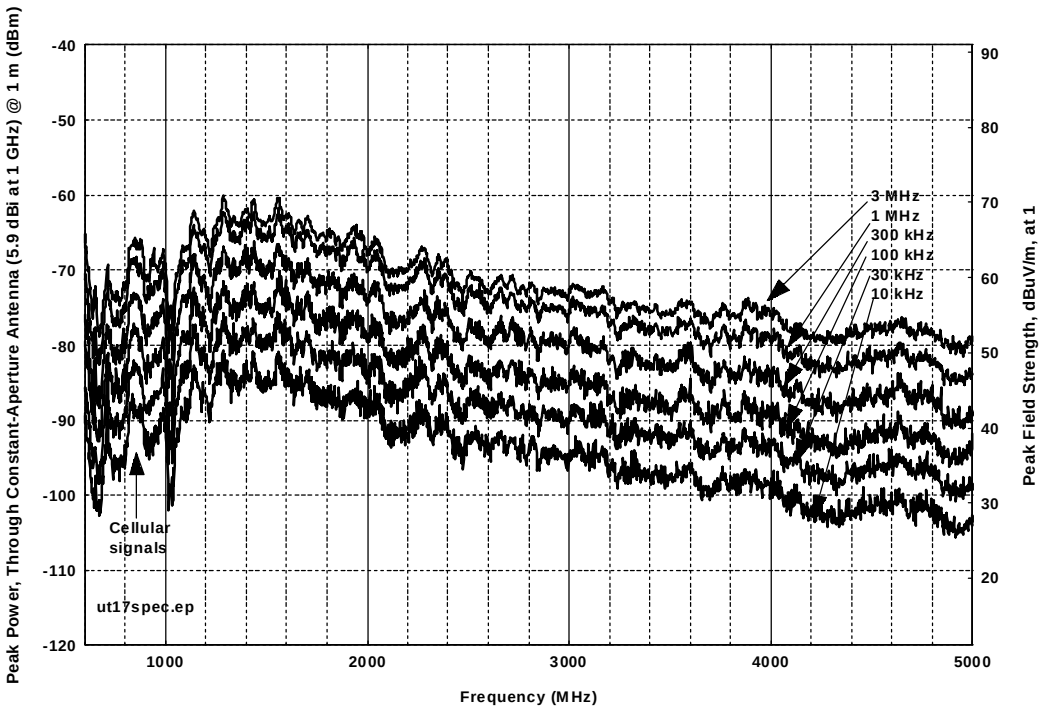

Figure D.D.9. Device D, absolute dither, 10-MHz nominal PRR, 25% gating.

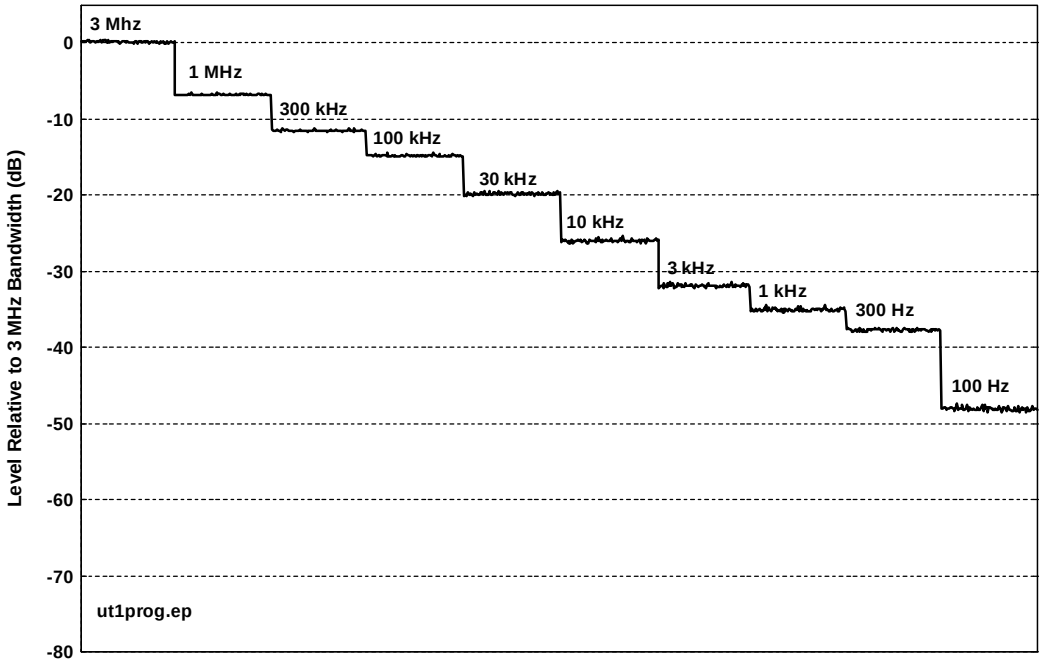

Figure D.D.10. Device D, 1-MHz nominal PRR, no gating, 25% dither (absolute time base).

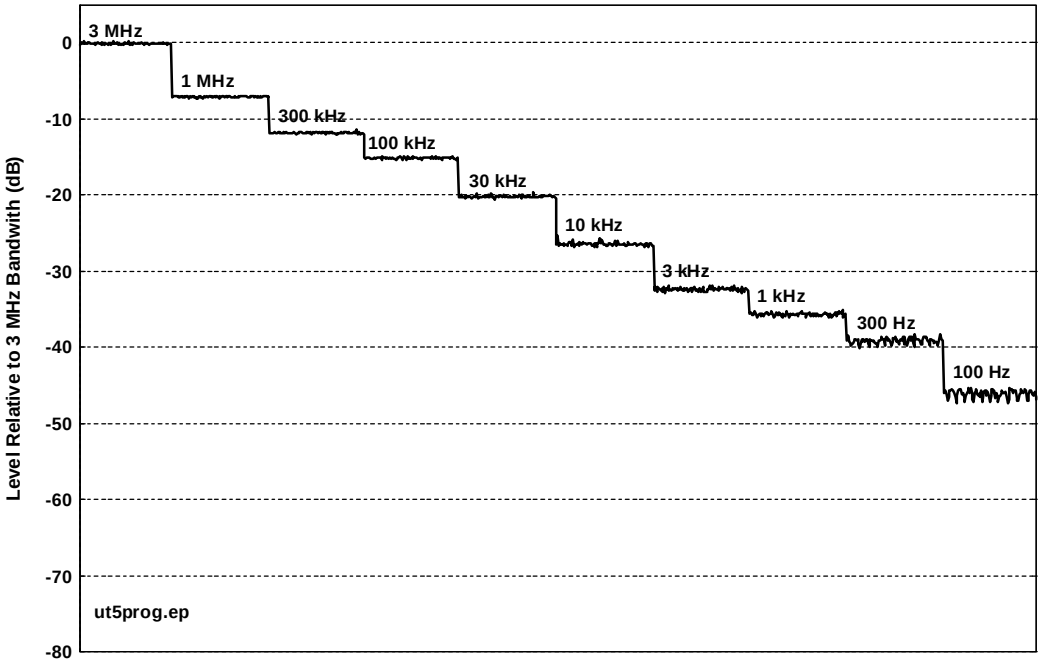

Figure D.D.11. Device D, 1-MHz nominal PRR, 25% gating, 25% dither (absolute time base) stairstep.

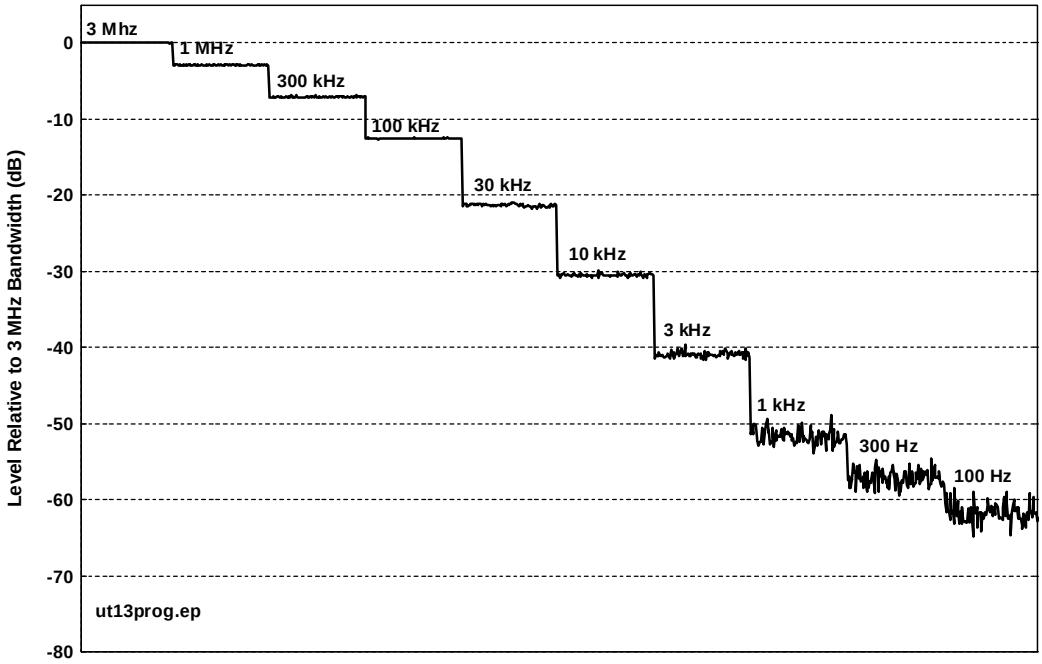

Figure D.D.12. Device D, 10-MHz nominal PRR, no gating, 25% dither (absolute time base) stairstep.

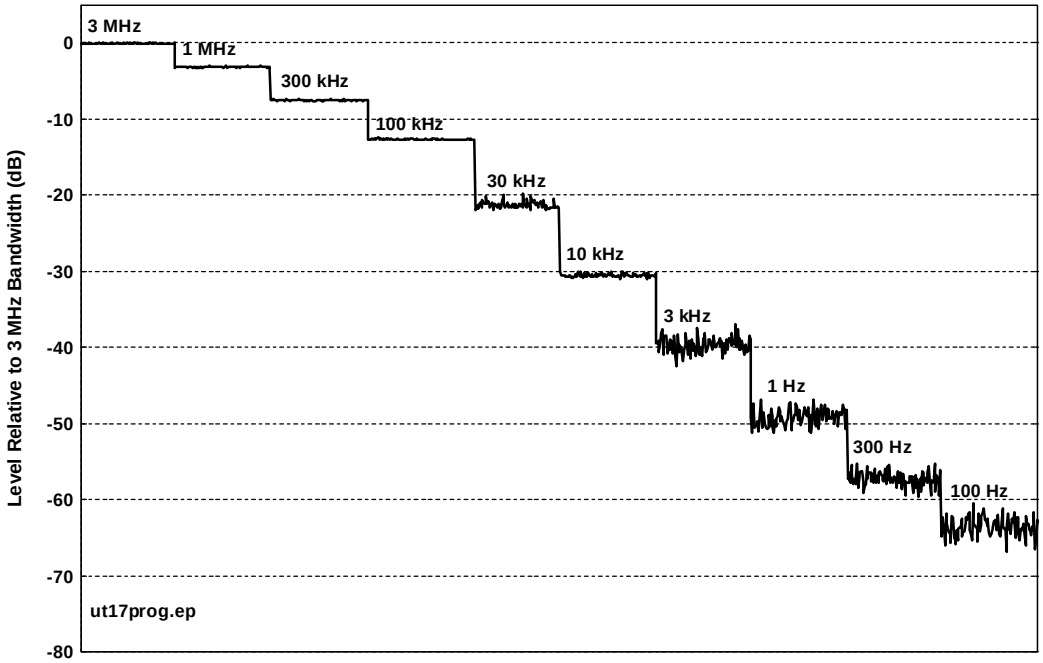

Figure D.D.13. Device D, 10-MHz nominal PRR, 25% gating, 25% dither (absolute time base) stairstep.

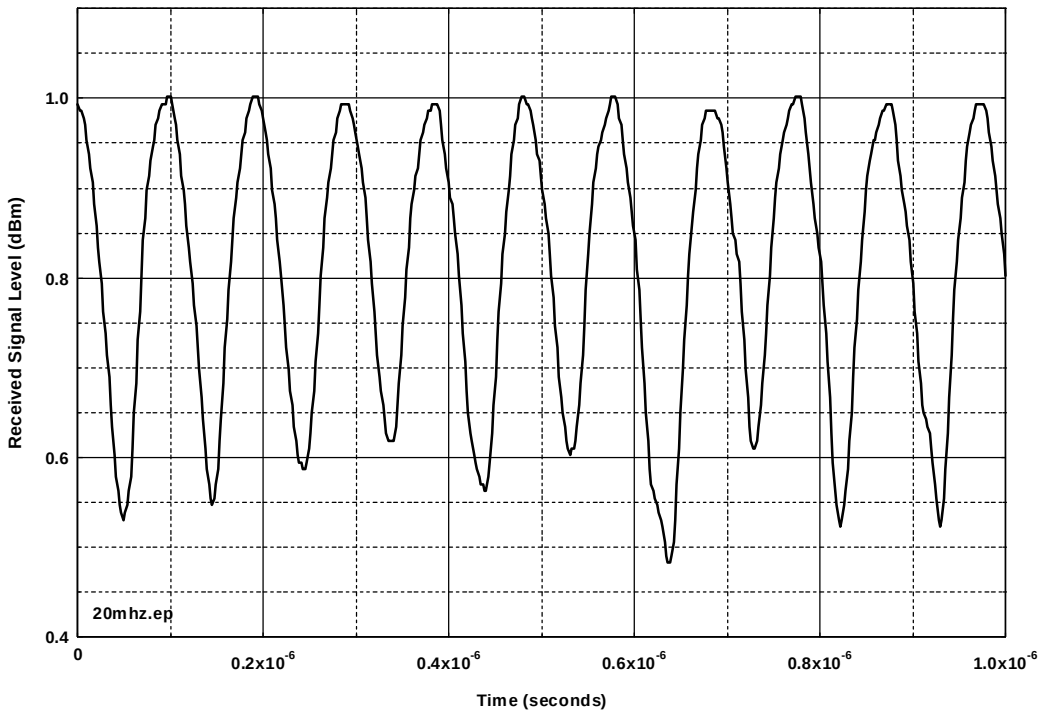

Figure D.D.14. Device D, 10-MHz nominal PRR, no gating, 25% dither, 20-MHz measurement bandwidth.

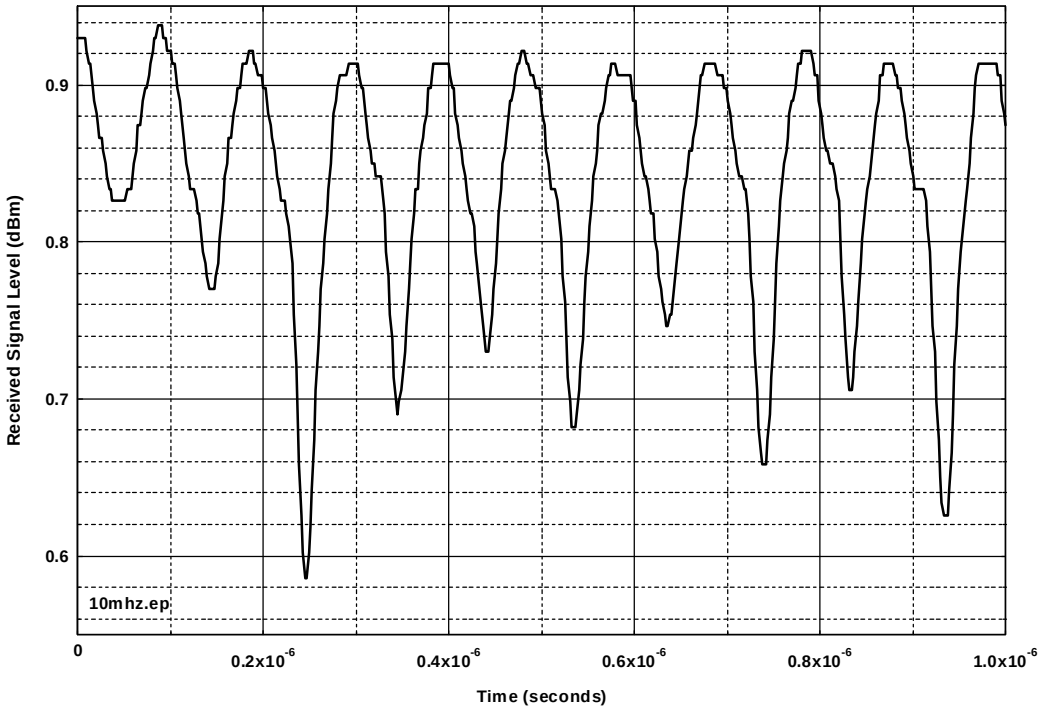

Figure D.D.15. Device D, 10-MHz nominal PRR, no gating, 25% dither, 10-MHz measurement bandwidth.

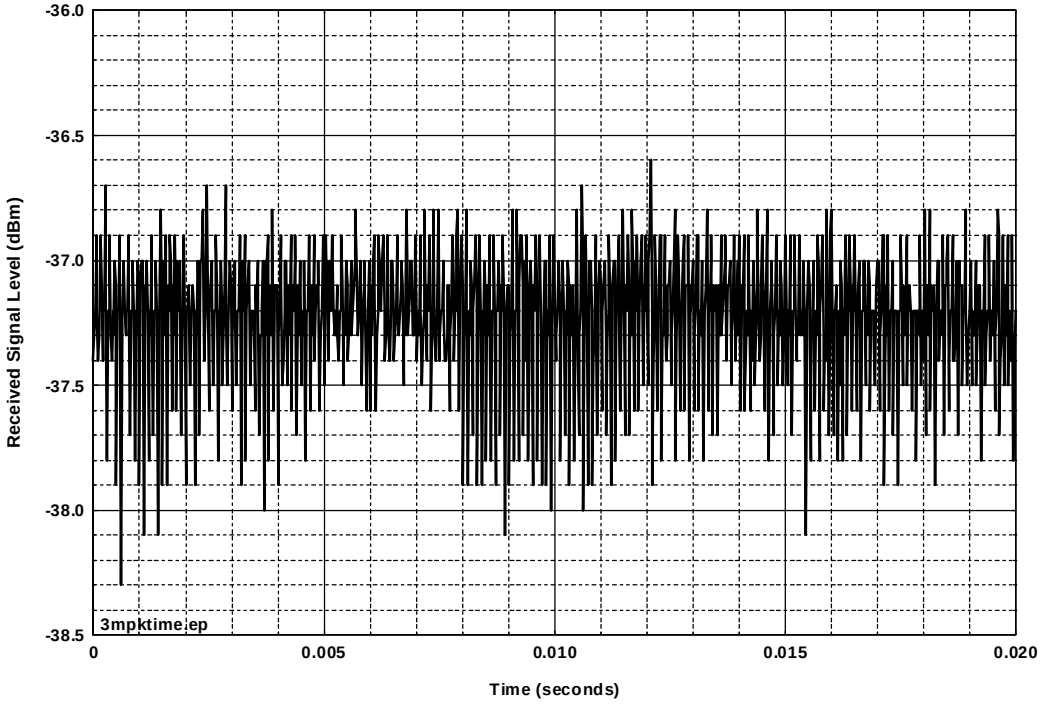

Figure D.D.16. Device D, 10-MHz nominal PRR, no gating, 25% dither, 3-MHz measurement bandwidth.

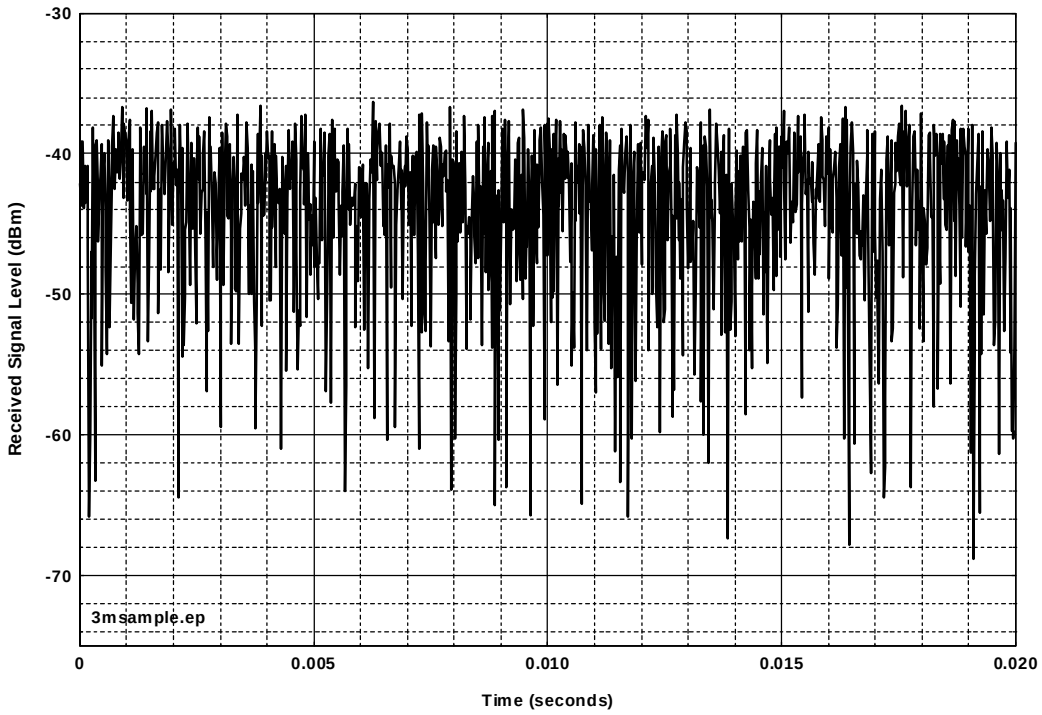

Figure D.D.17. Device D, 10-MHz nominal PRR, no gating, 25% dither, 3-MHz bandwidth, sample detector.

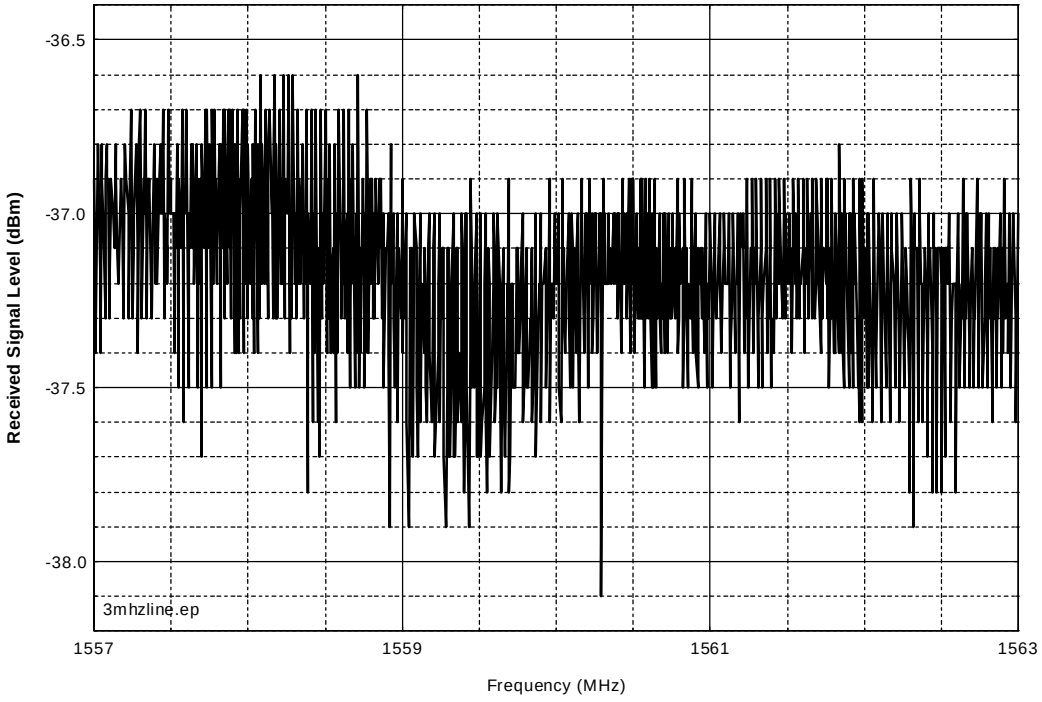

Figure D.D.18. Device D, 10-MHz nominal PRR, no gating, 25% dither, 3-MHz bandwidth.

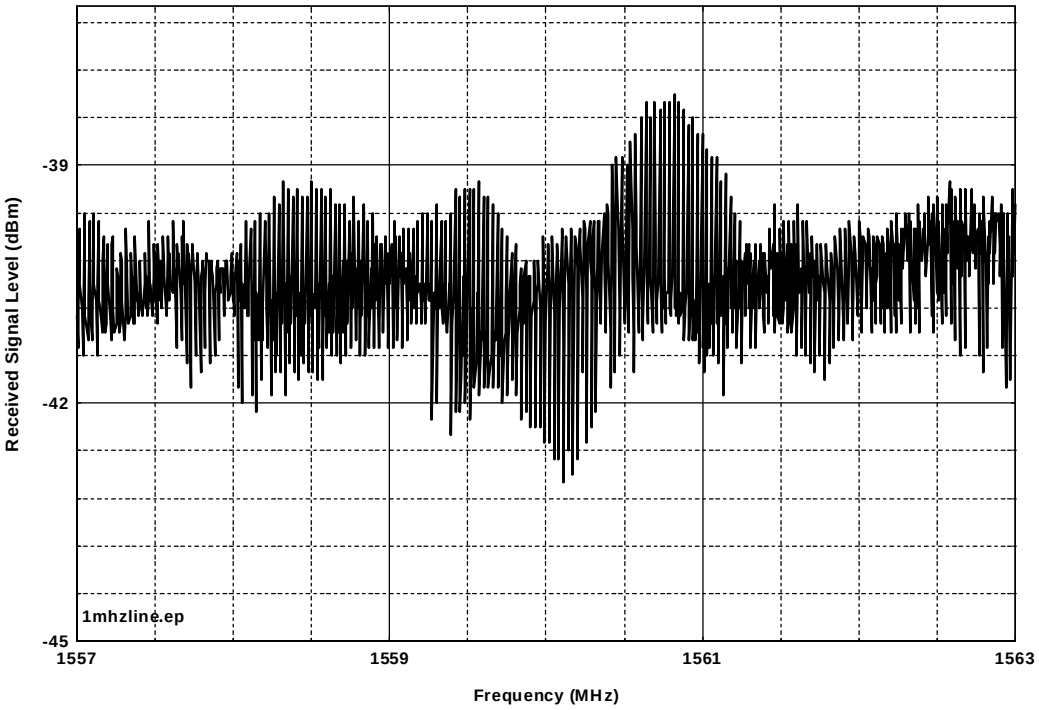

Figure D.D.19. Device D, 10-MHz nominal PRR, no gating, 25% dither, 1-MHz measurement bandwidth..

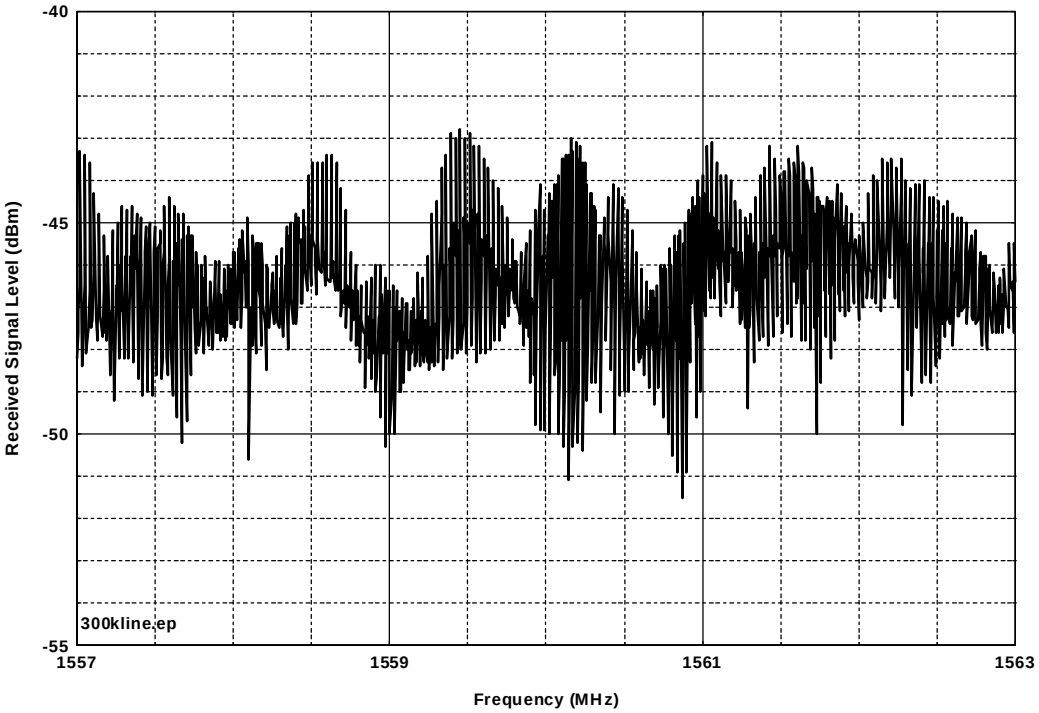

Figure D.D.20. Device D, 10-MHz nominal PRR, no gating, 25% dither, 300-kHz measurement bandwidth.

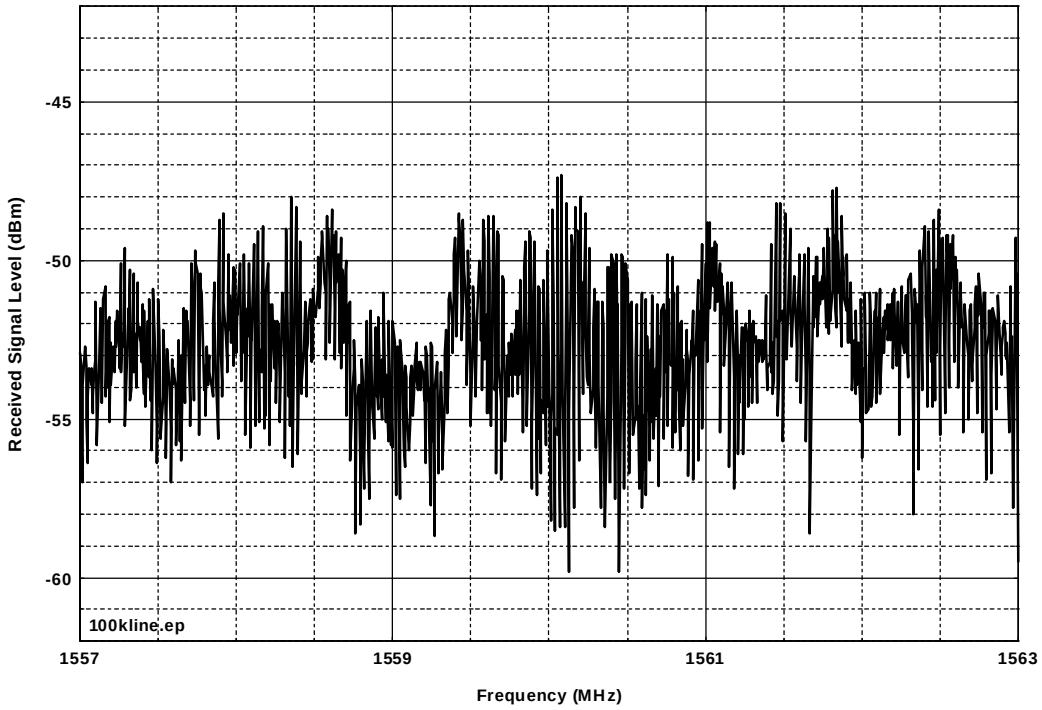

Figure D.D.21. Device D, 10-MHz nominal PRR, no gating, 25% dither, 100-kHz measurement bandwidth.

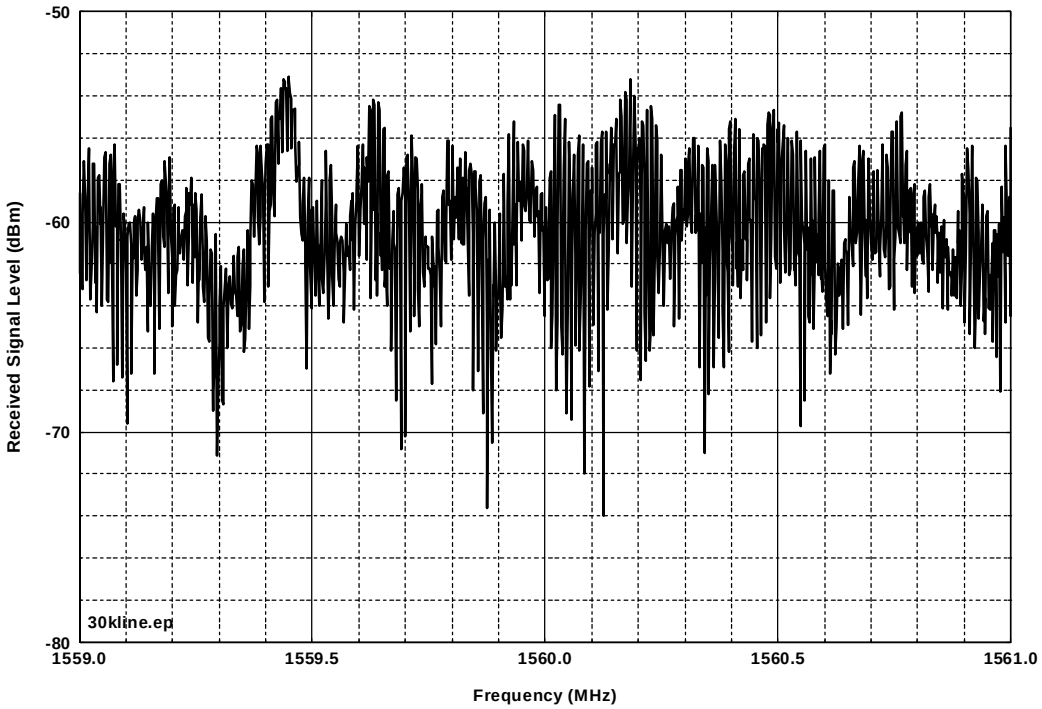

Figure D.D.22. Device D, 10-MHz nominal PRR, no gating, 25% dither, 30-kHz measurement bandwidth.

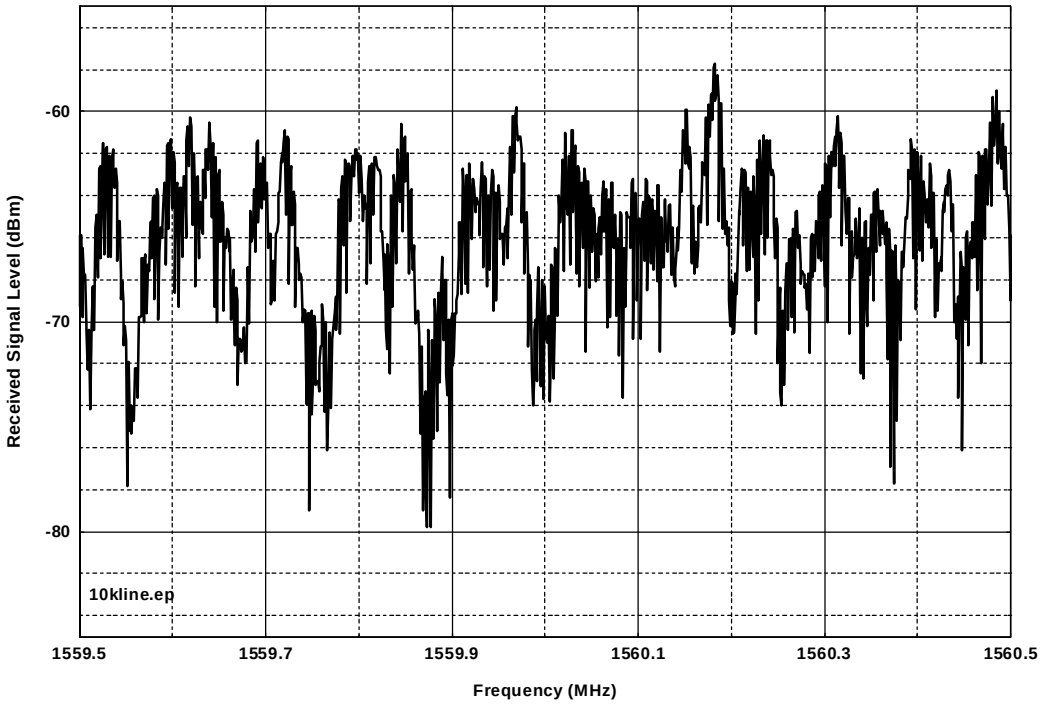

Figure D.D.23. Device D, 10-MHz nominal PRR, no gating, 25% dither, 10-kHz measurement bandwidth.

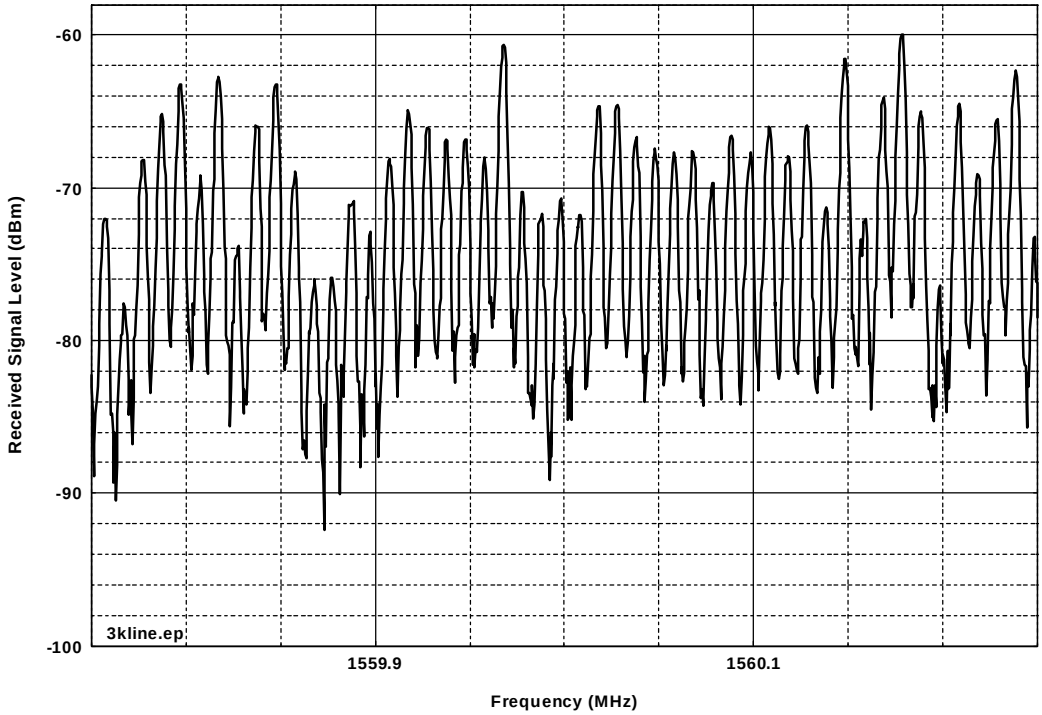

Figure D.D.24. Device D, 10-MHz nominal PRR, no gating, 25% dither, 3-kHz measurement bandwidth.

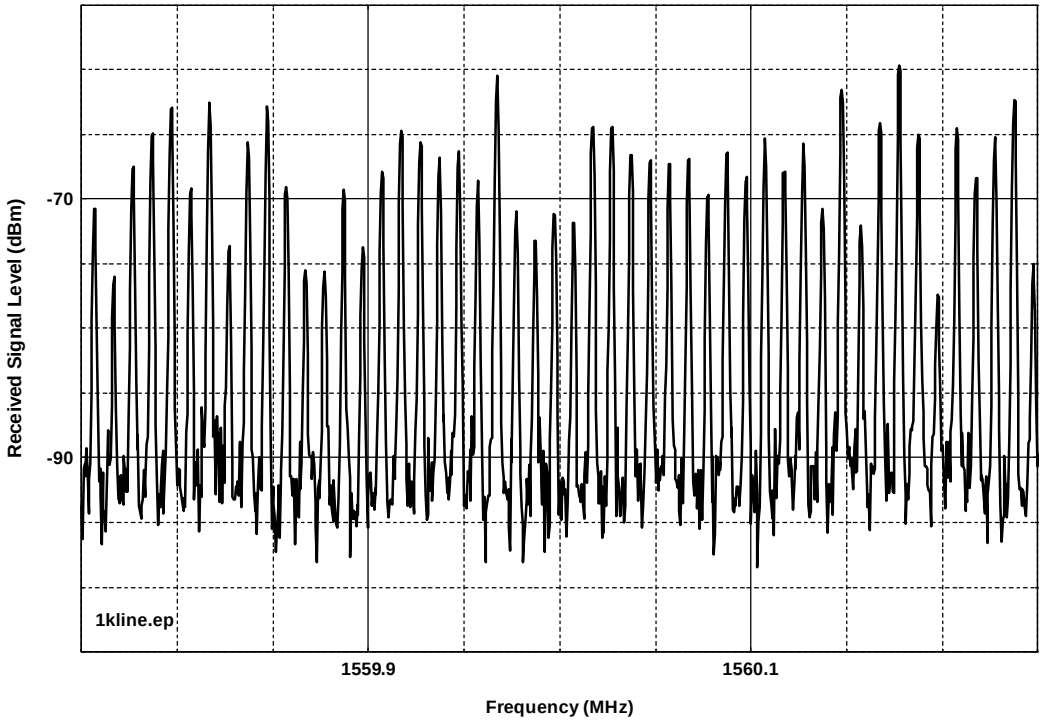

Figure D.D.25. Device D, 10-MHz nominal PRR, no gating, 25% dither, 1-kHz measurement bandwidth.

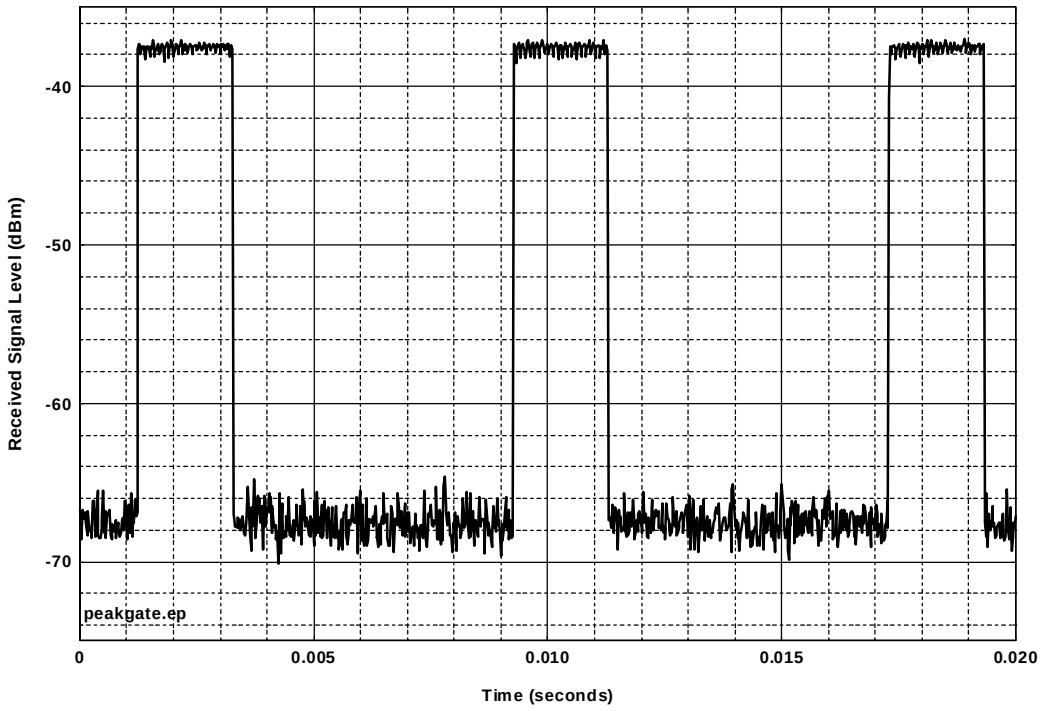

Figure D.D.26. Device D, 10-MHz nominal PRR, 25% gating, 25% dither, 3-MHz peak-detected bandwidth.

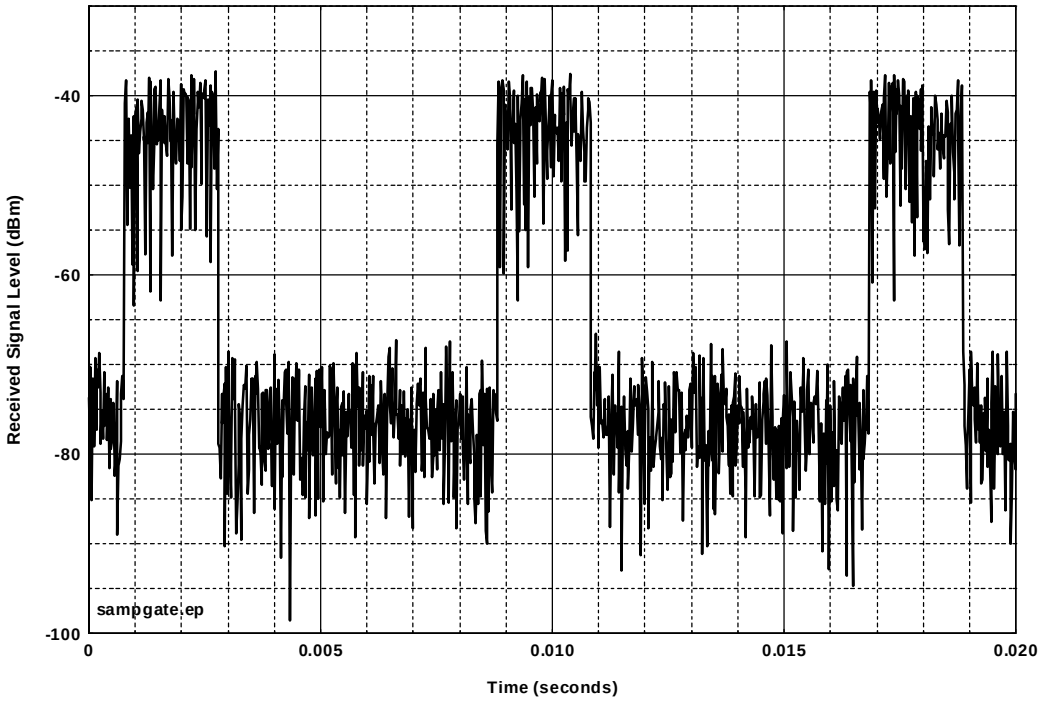

Figure D.D.27. Device D, 10-MHz nominal PRR, 25% gating, 25% dither, 3-MHz sample-detected bandwidth.

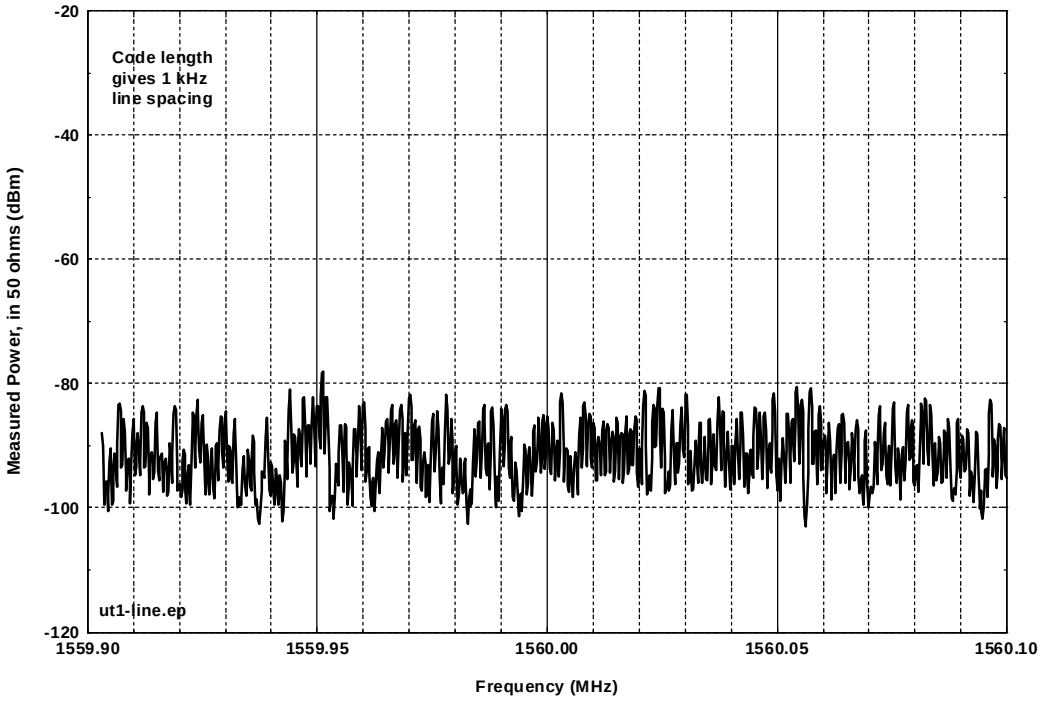

Figure D.D.28. Device D, 1-kHz emission lines with 1-MHz nominal PRR, no gating, 25% dither.

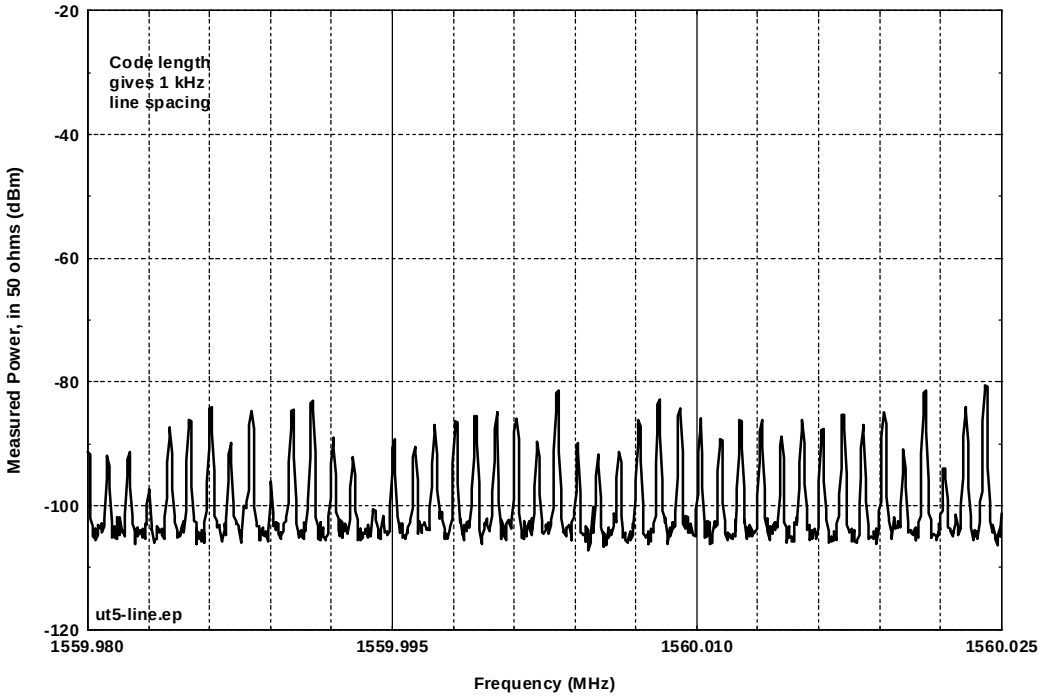

Figure D.D.29. Device D, 1-kHz emission lines with 1-MHz nominal PRR, 25% gating, 25% dither.

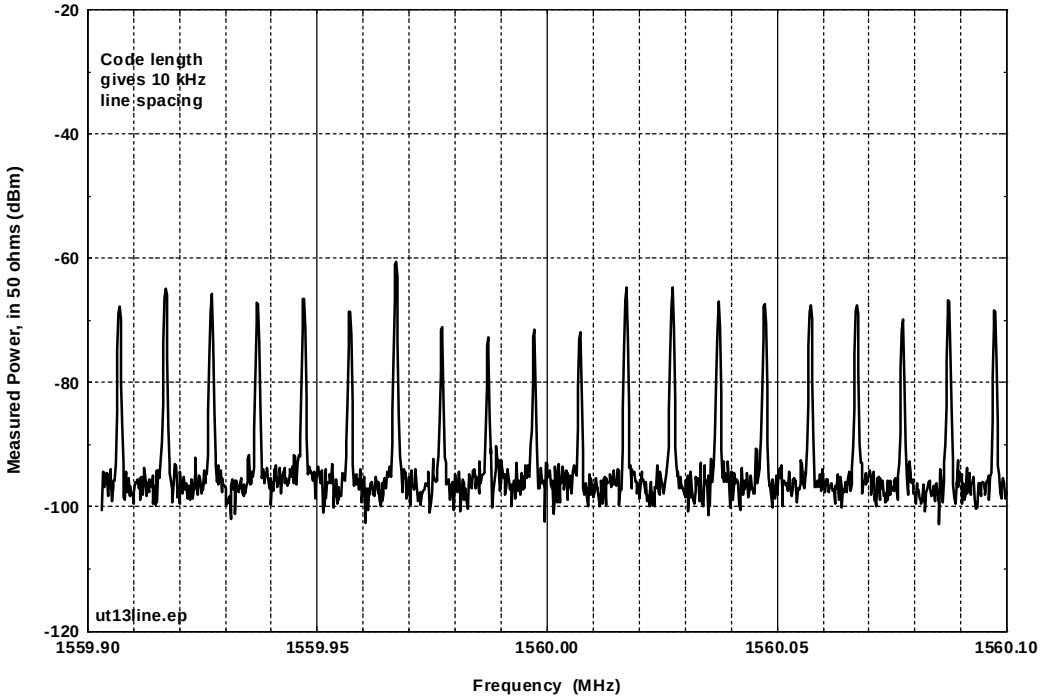

Figure D.D.30. Device D, 10-kHz emission lines with 10-MHz nominal PRR, no gating, 25% dither.

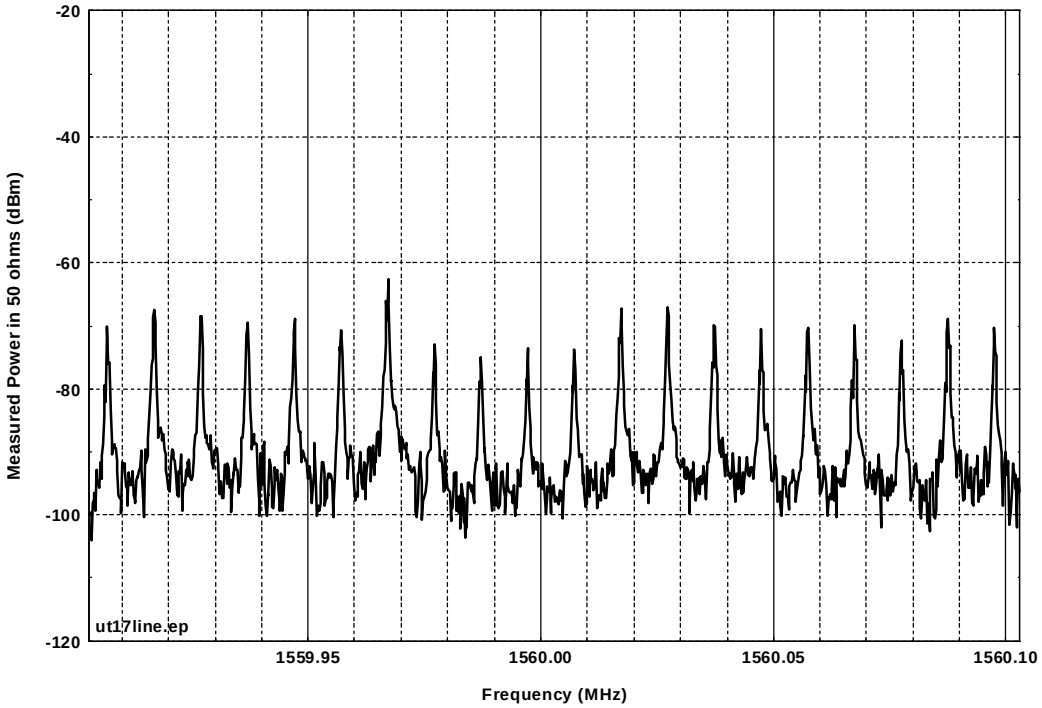

Figure D.D.31. Device D, 10-kHz emission line with 10-MHz nominal PRR, 25% gating, 25% dither.

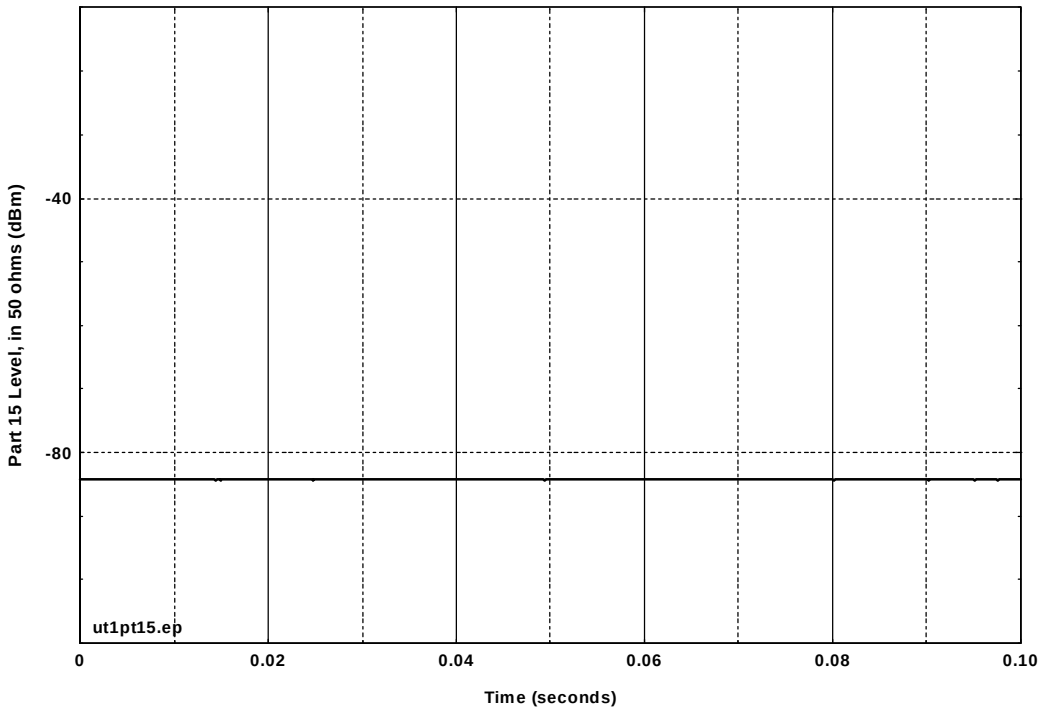

Figure D.D.32. Device D, Part 15, 1-MHz nominal PRR, no gating, 25% dither, 10-Hz video bandwidth.

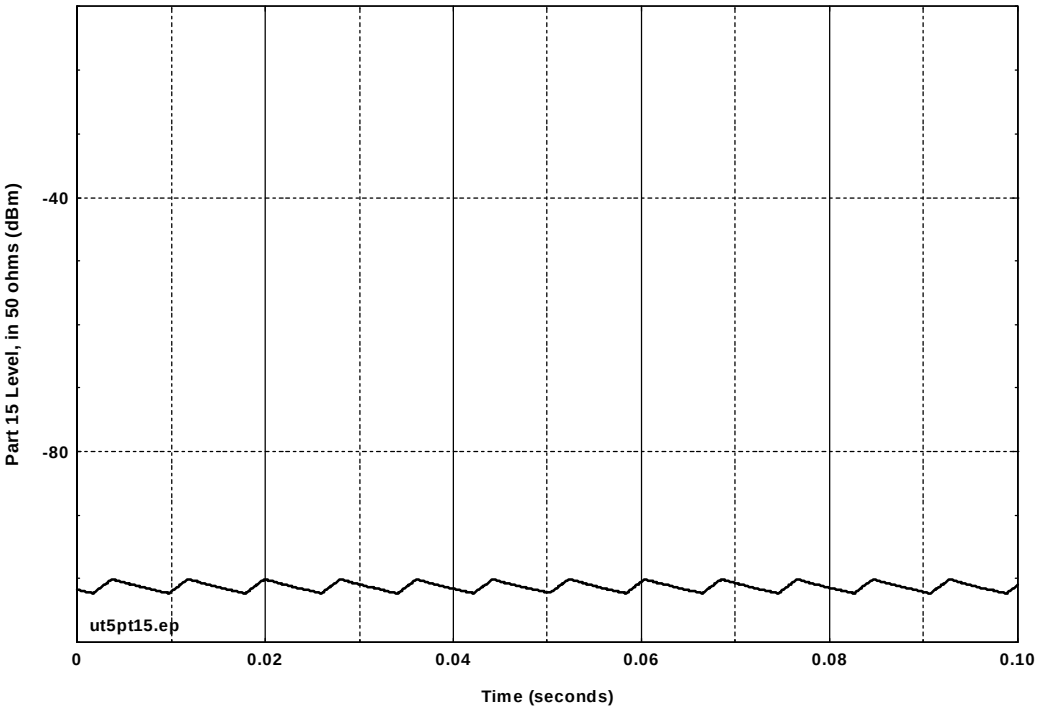

Figure D.D.33. Device D, Part 15, 1-MHz nominal PRR, 25% gating, 25% dither, 10-Hz video bandwidth.

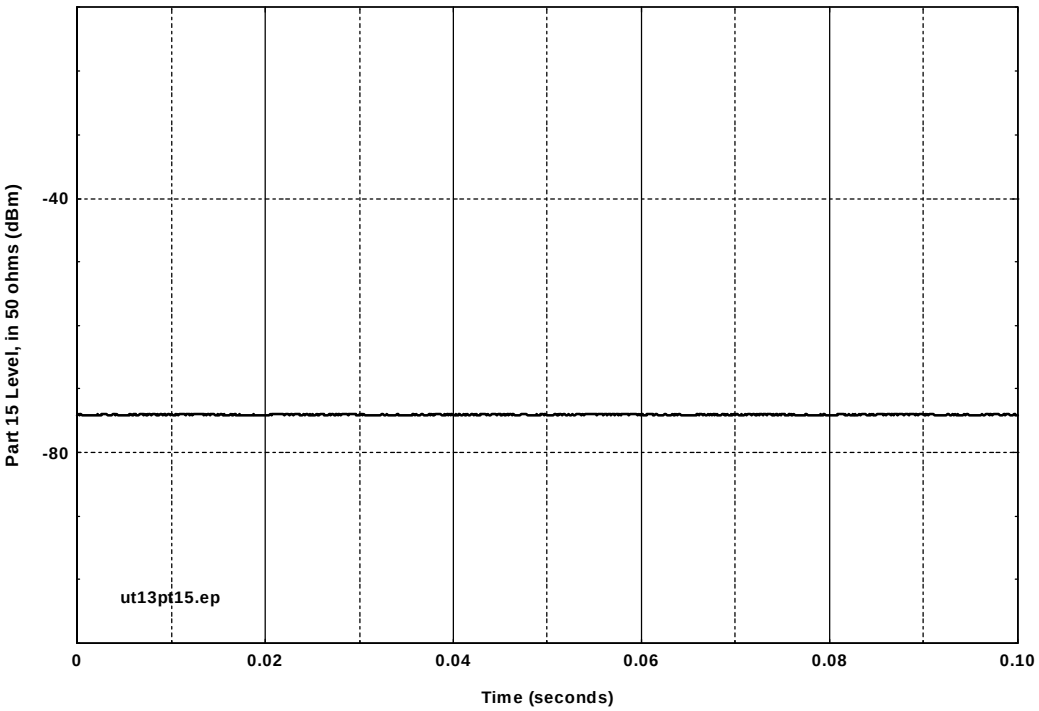

Figure D.D.34. Part 15, 10-MHz nominal PRR, no gating, 25% dither, 10-Hz video bandwidth.

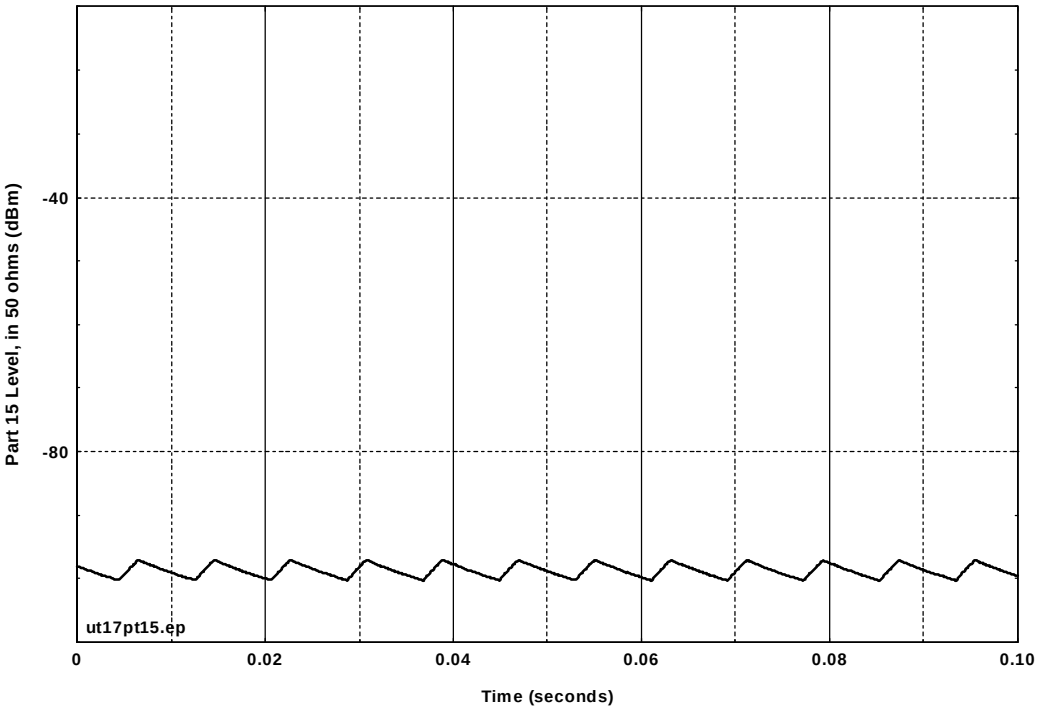

Figure D.D.35. Device D, Part 15, 10-MHz nominal PRR, 25% gating, 25% dither, 10-Hz video bandwidth.

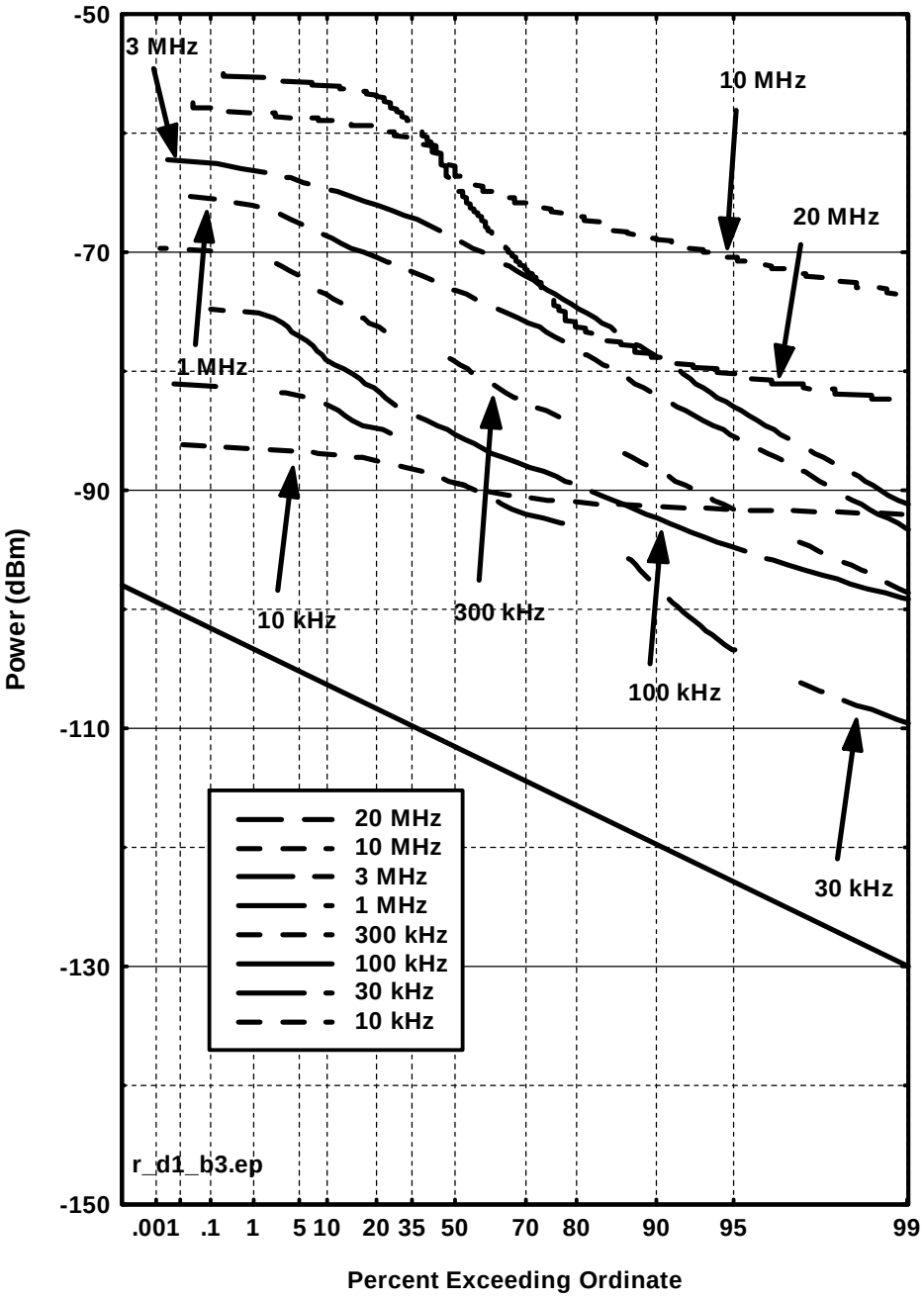

Figure D.D.36. Device D, 10-MHz PRR, 100% gating, APDs.

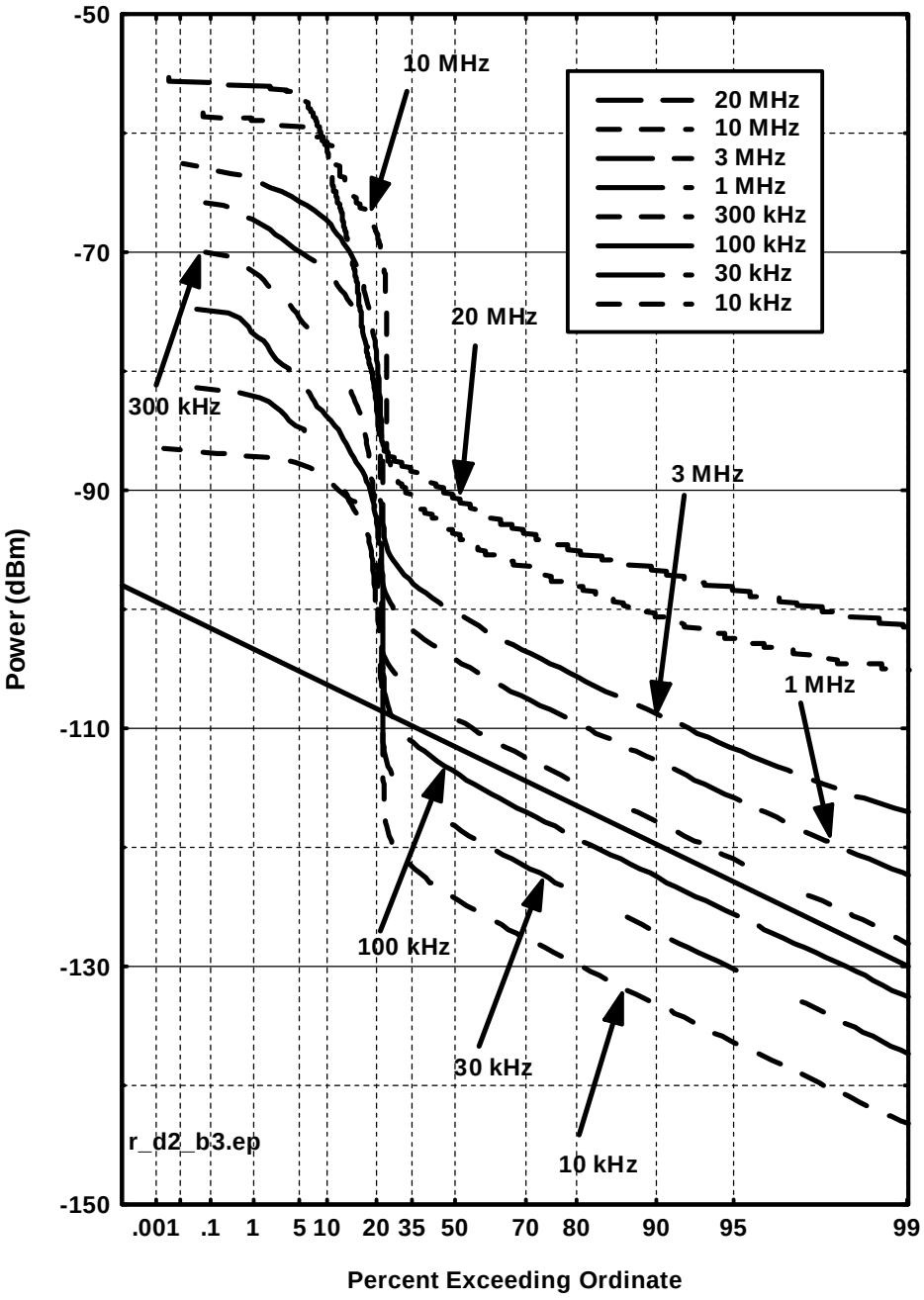

Figure D.D.37. Device D, 10-MHz PRR, 25% gating, APDs.

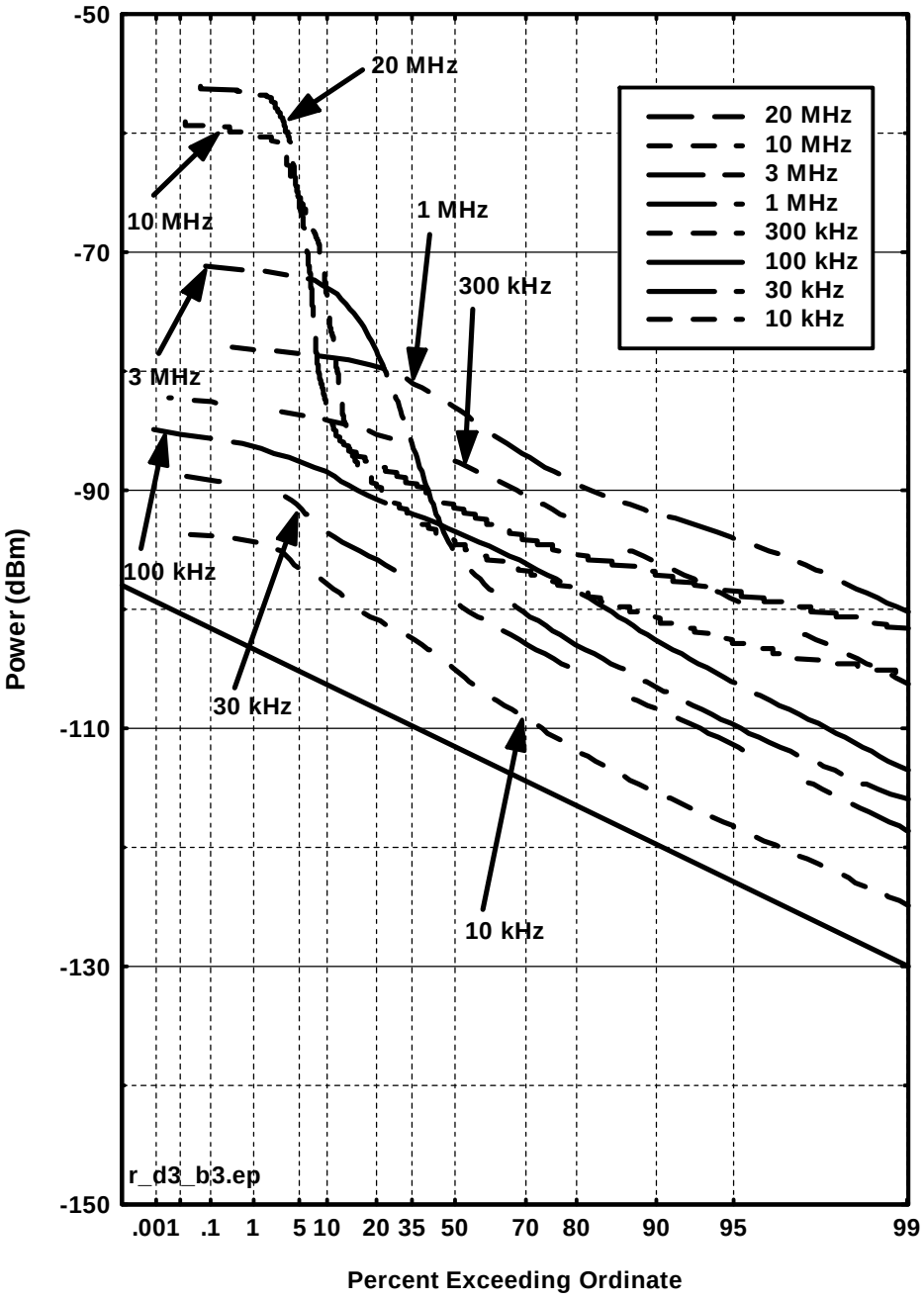

Figure D.D.38. Device D, 1-MHz PRR, 100% gating, APDs.

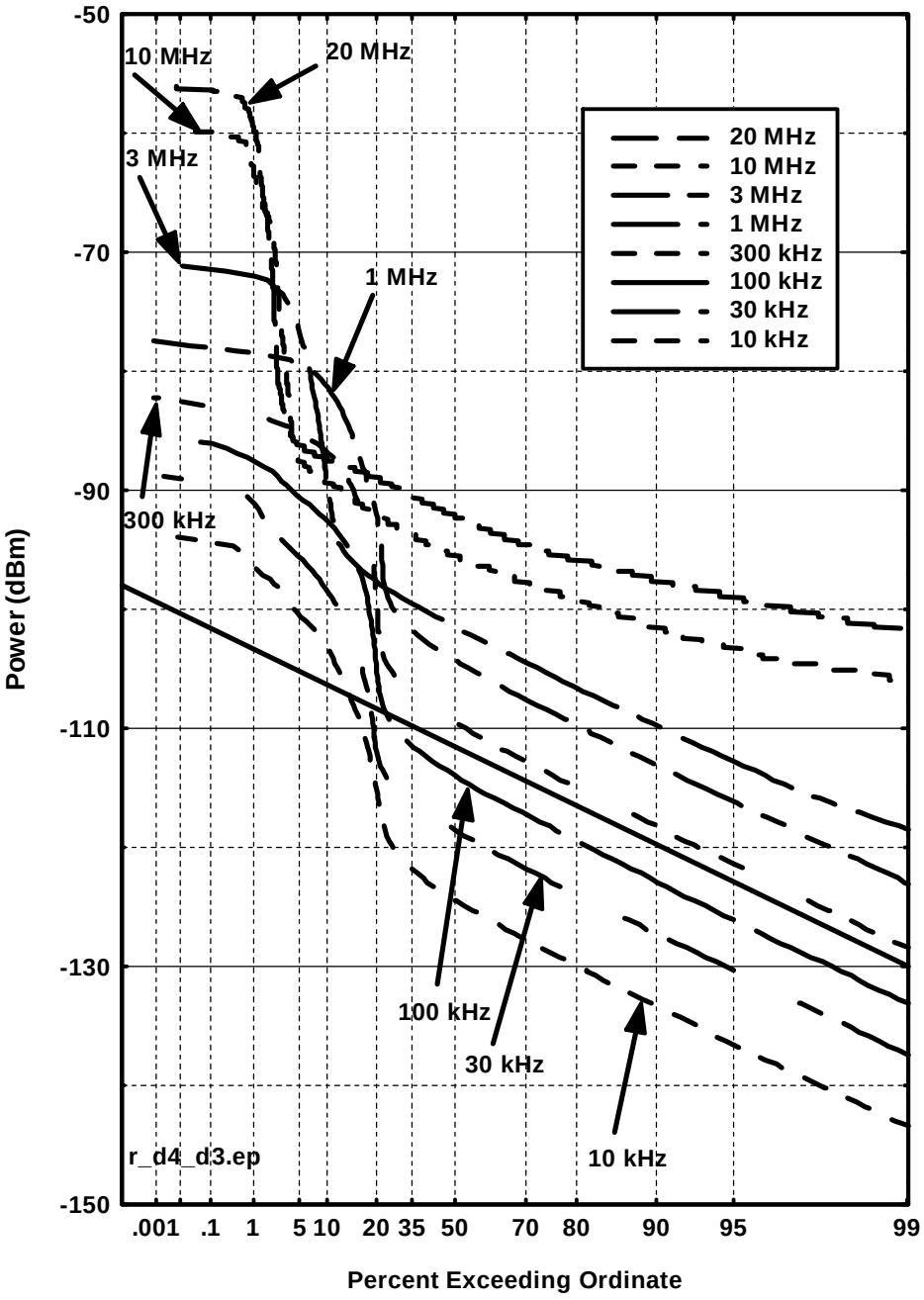

Figure D.D.39. Device D, 1-MHz PRR, 25% gating, APDs.

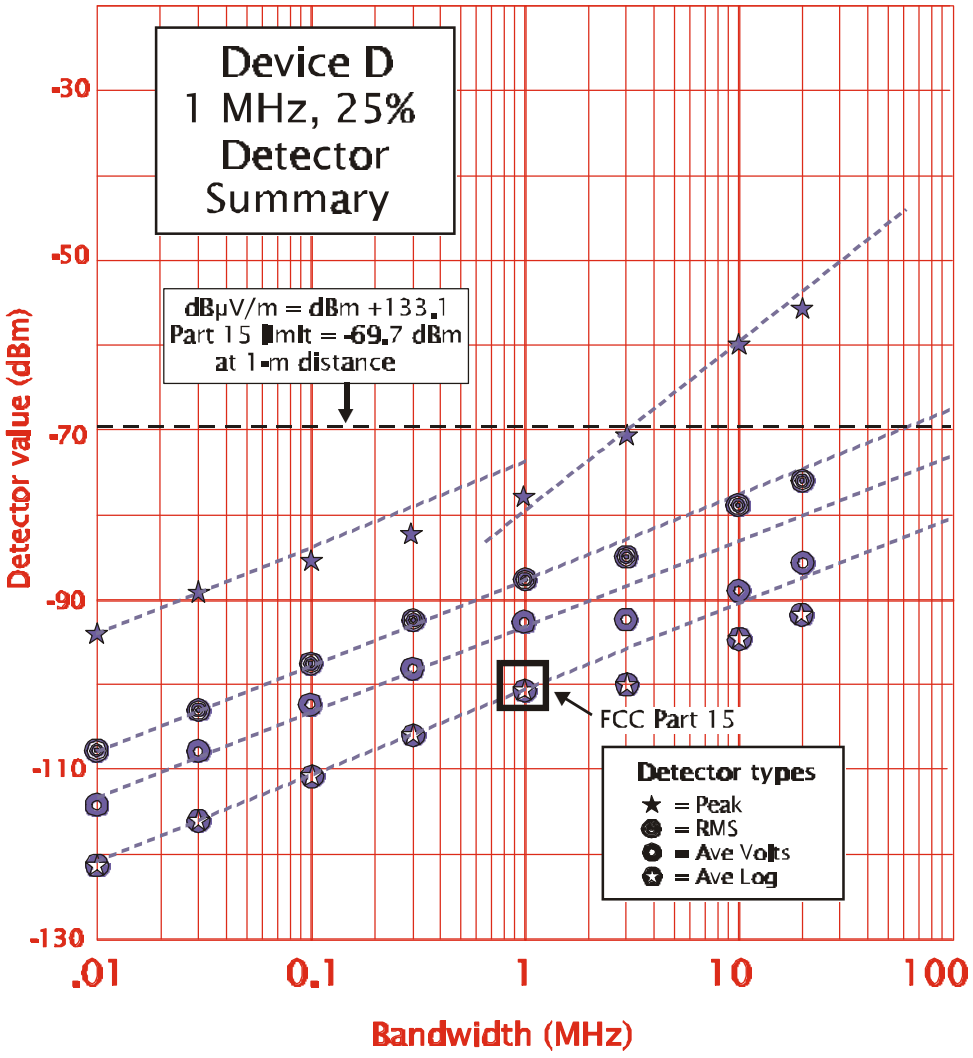

Figure D.D.40. Device D, 1-MHz PRR, 25% gating, detector summary.

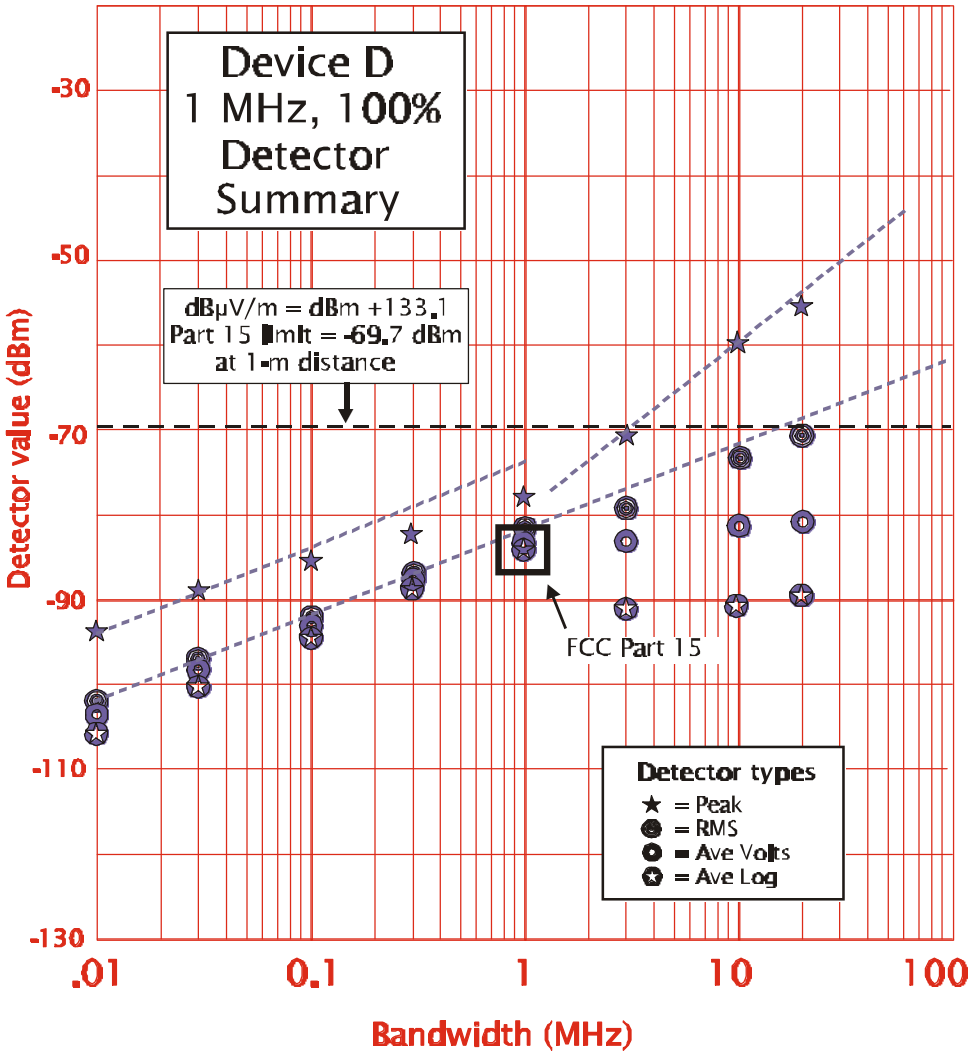

Figure D.D.41. Device D, 1-MHz PRR, 100% gating, detector summary.

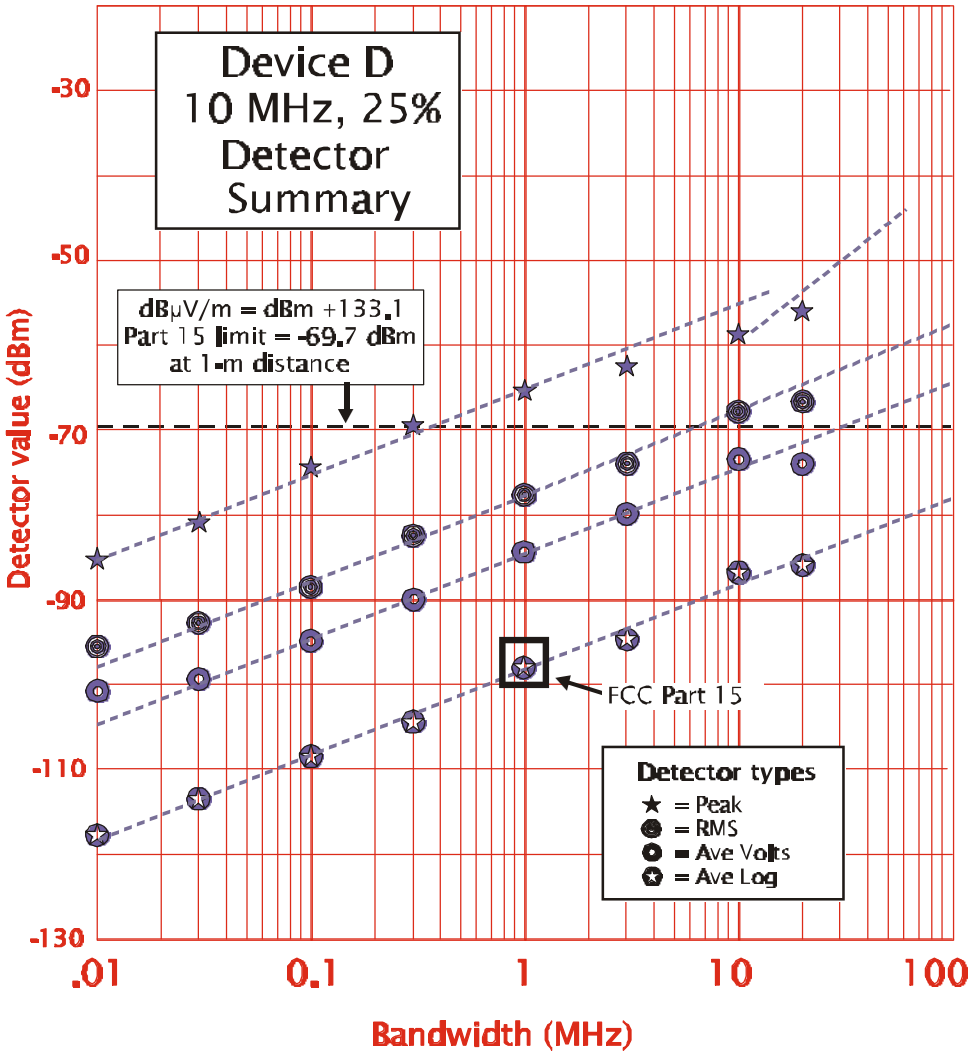

Figure D.D.42. Device D, 10-MHz PRR, 25% gating, detector summary.

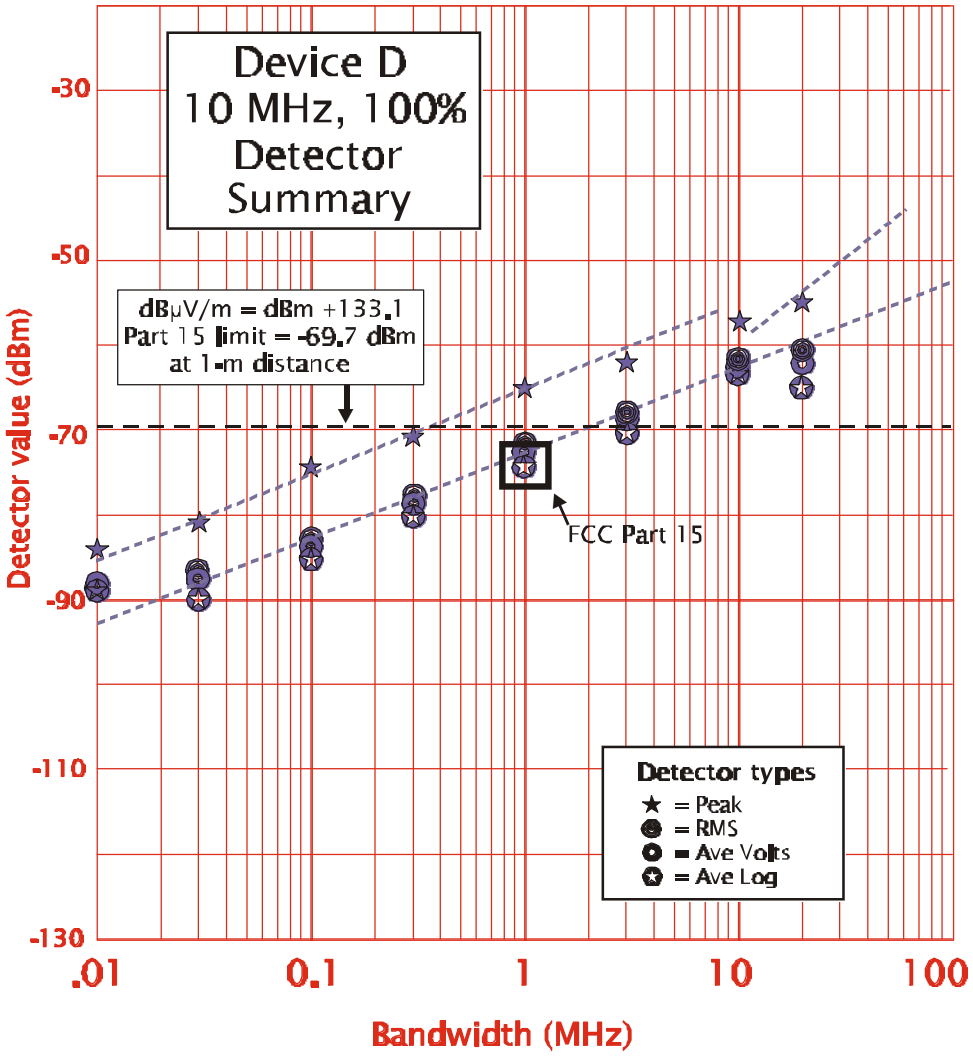

Figure D.D.43. Device D, 10-MHz PRR, 100% gating, detector summary.

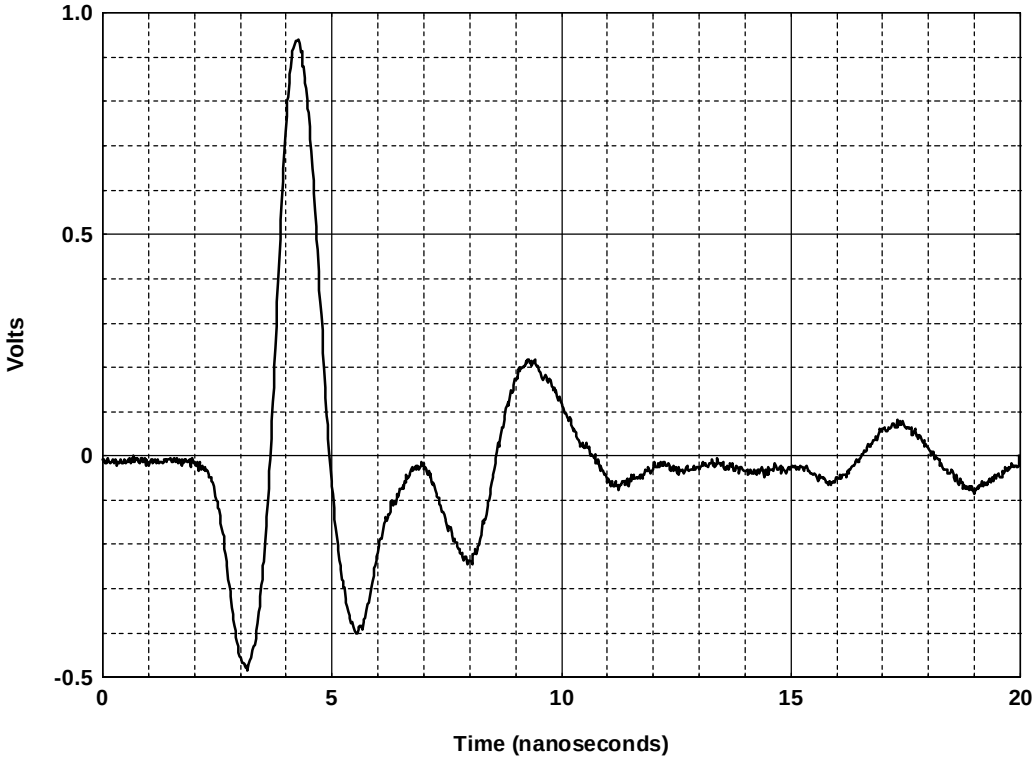

Figure D.E.1. Device E, (300 MHz) radiated time-domain waveform.

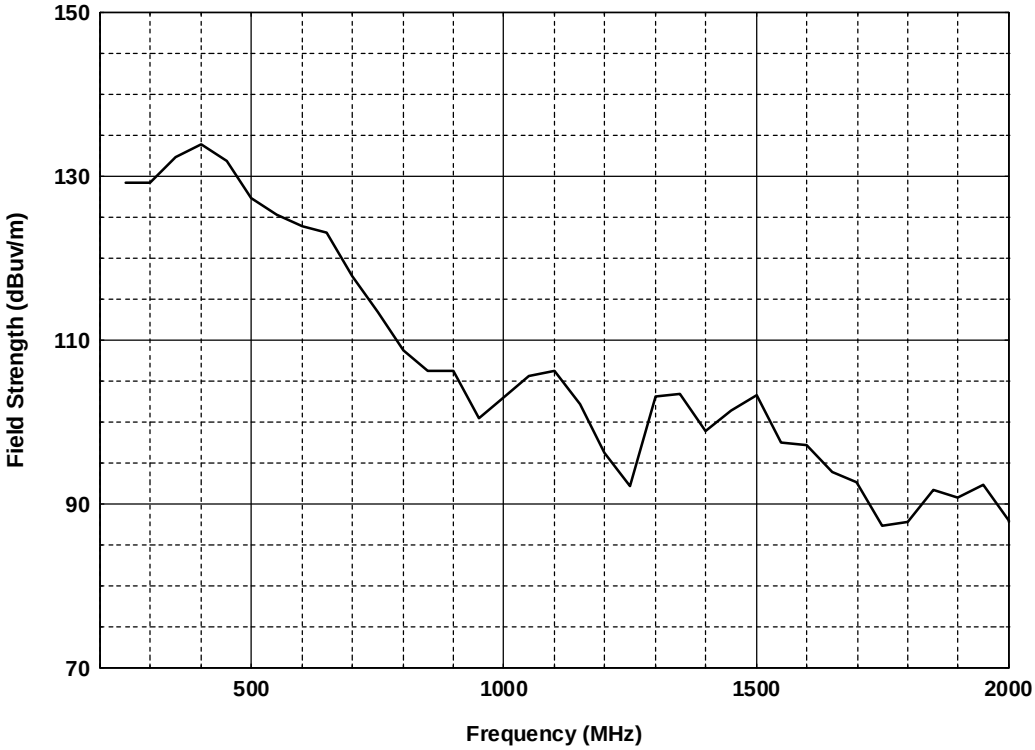

Figure D.E.2. Device E, (300 MHz) radiated peak field strength at 1 m,
) f = 49.99 MHz.

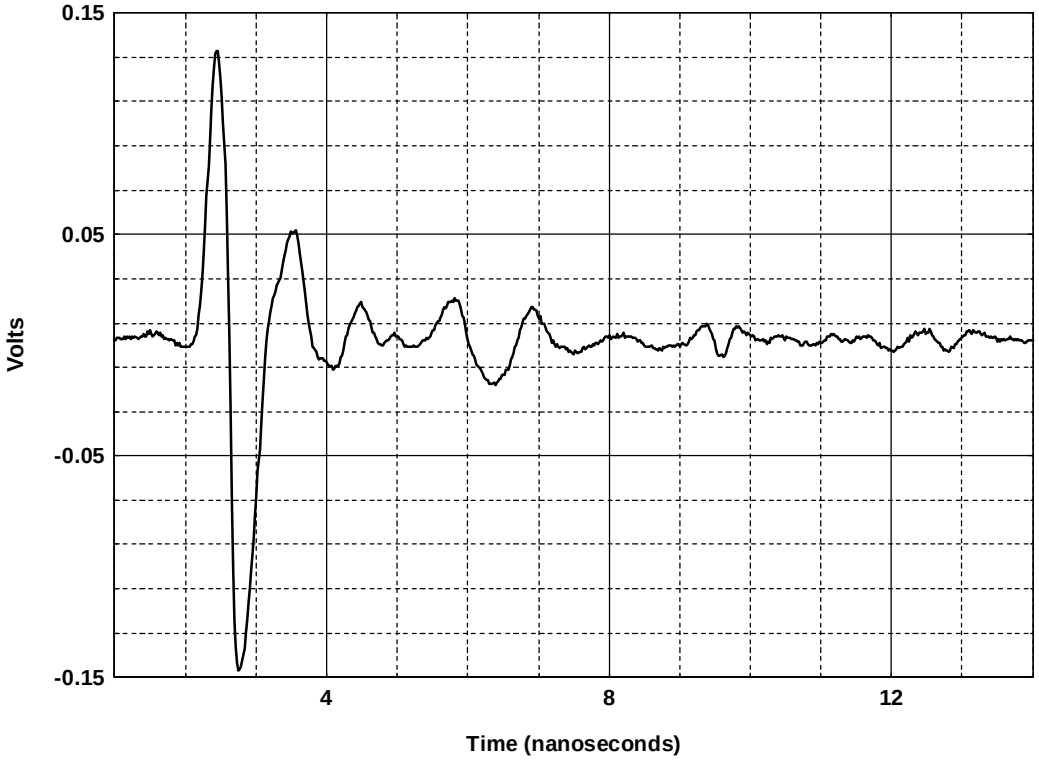

Figure D.E.3. Device E, (900 MHz) radiated time-domain waveform.

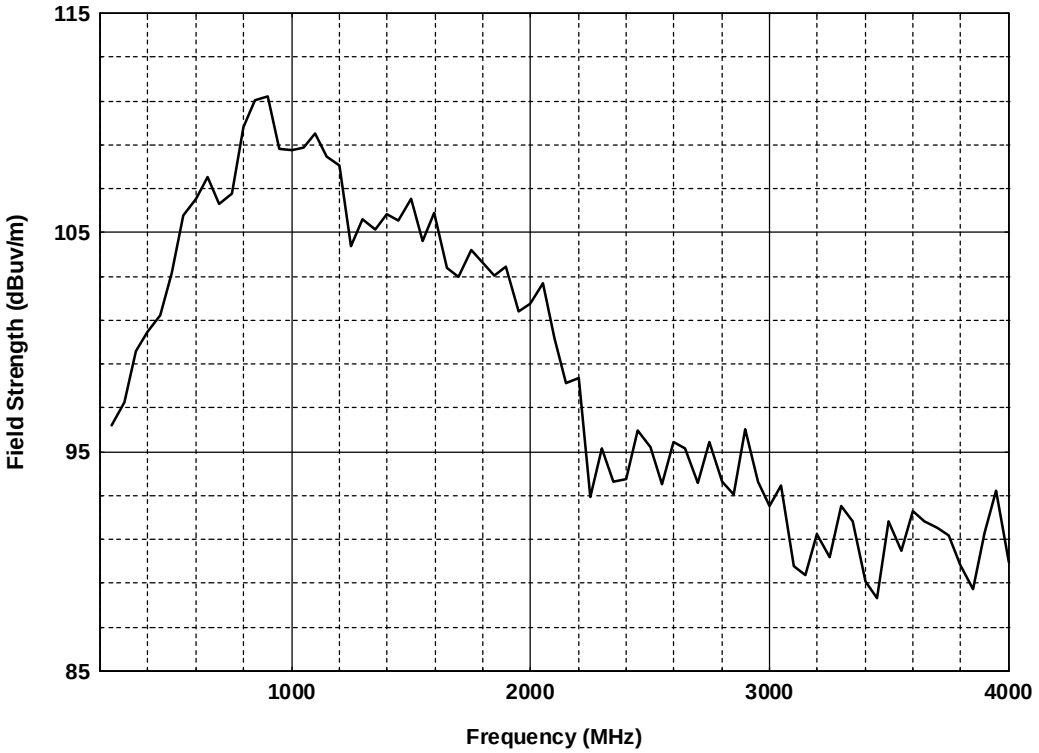

Figure D.E.4. Device E, (900 MHz) radiated peak field strength at 1 m,
) f = 49.99 MHz.

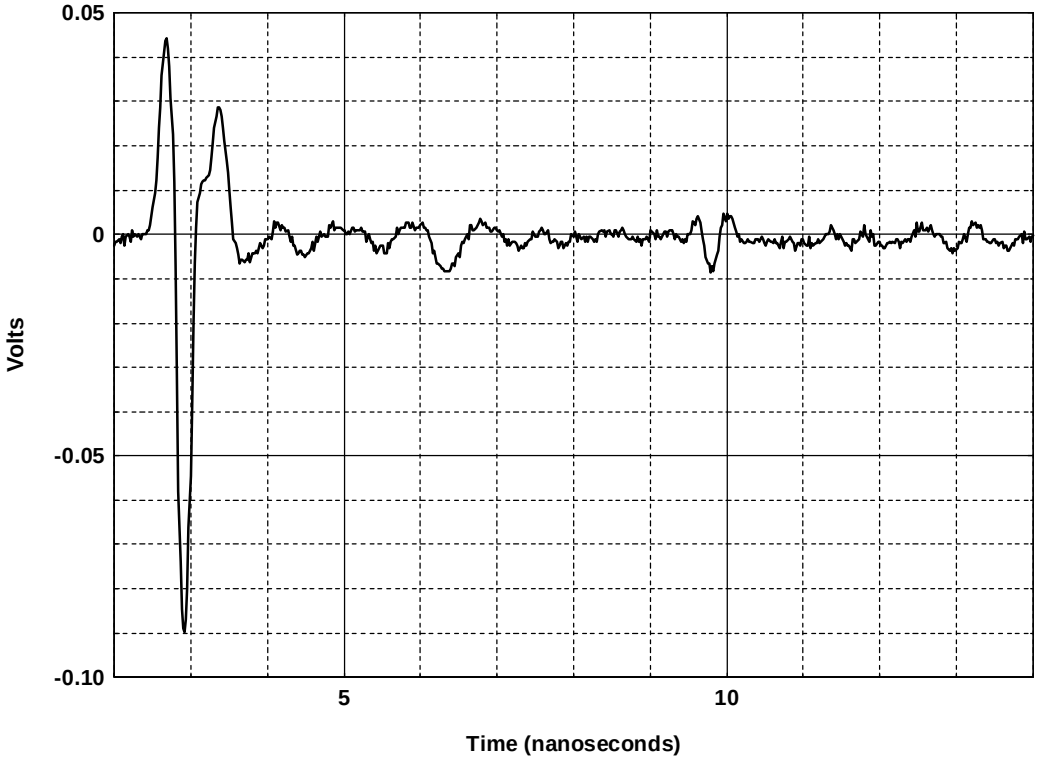

Figure D.E.5. Device E, (1500 MHz) radiated time-domain waveform.

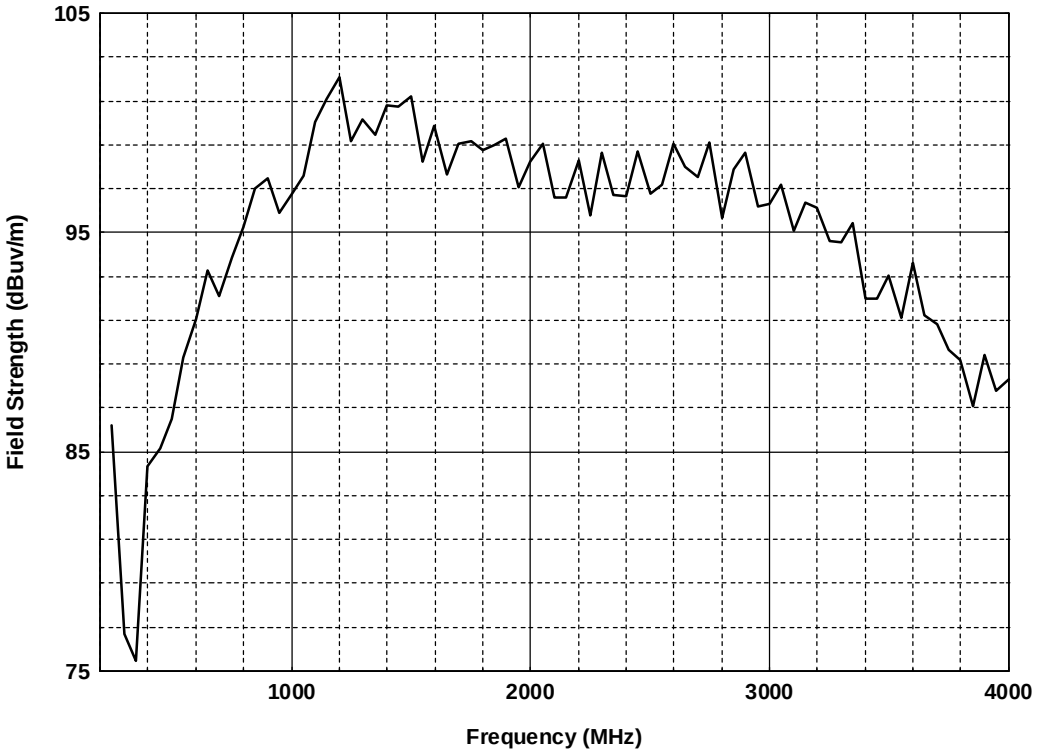

Figure D.E.6. Device E, (1500 MHz) radiated peak field strength at 1 m,) f = 49.99 MHz.

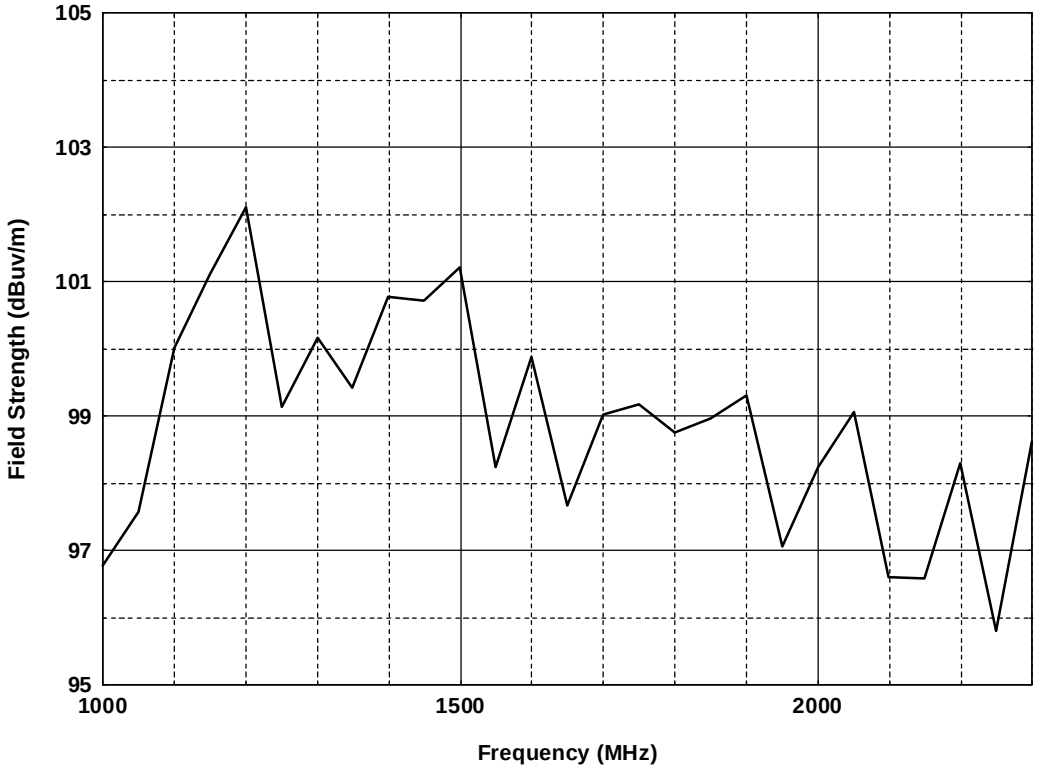

Figure D.E.7. Device E, (1500 MHz) radiated peak field strength at 1 m,) f = 49.99 MHz.

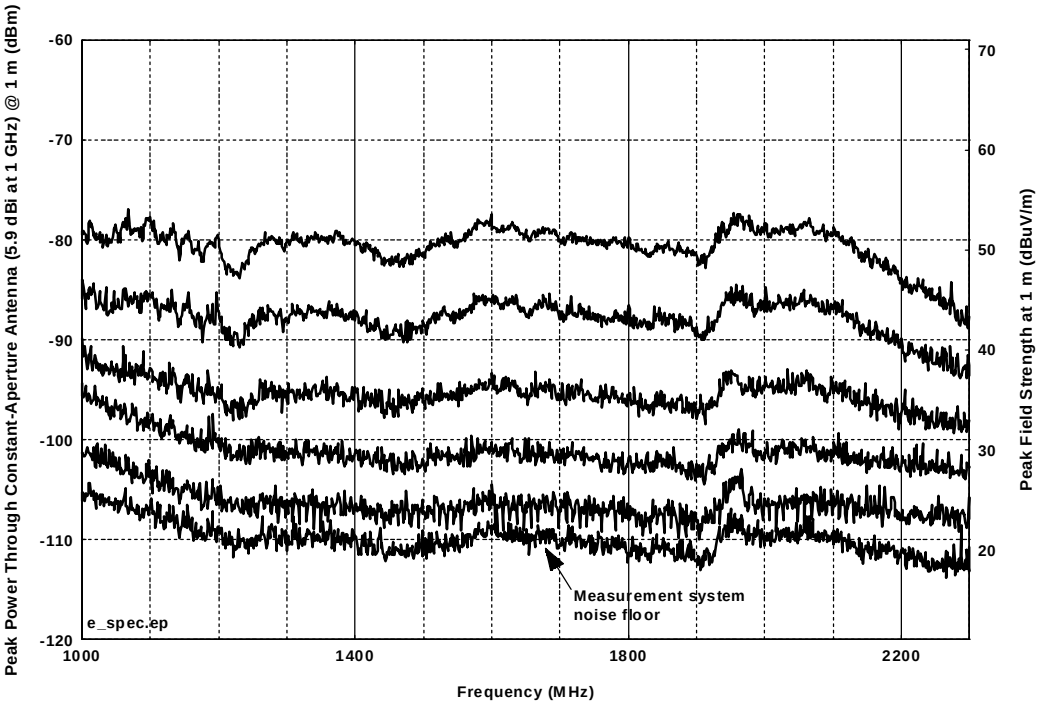

Figure D.E.8. Device E, (1500 MHz head) spectra as a function of measurement bandwidth.

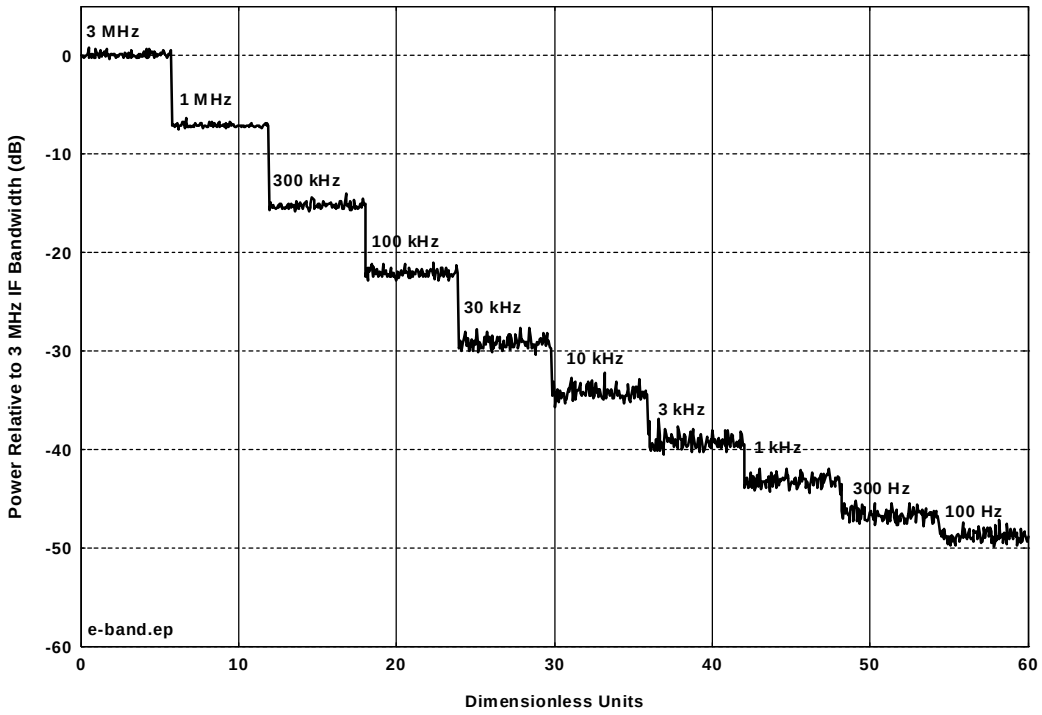

Figure D.E.9. Device E, power as a function of measurement bandwidth stairstep.

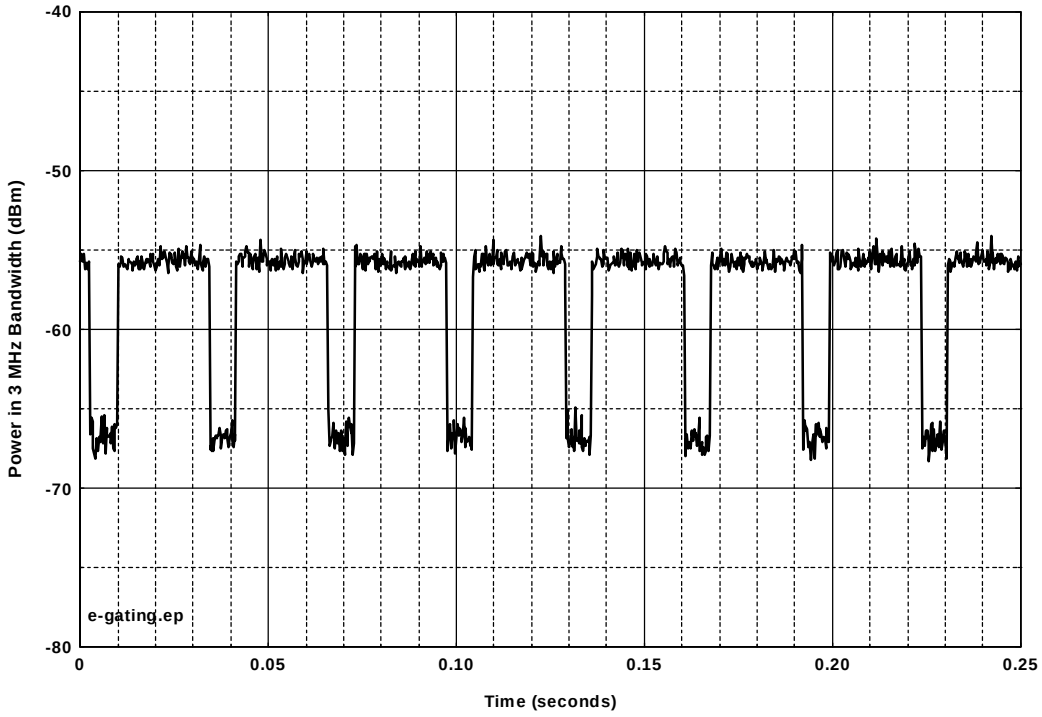

Figure D.E.10. Device E, gating behavior.

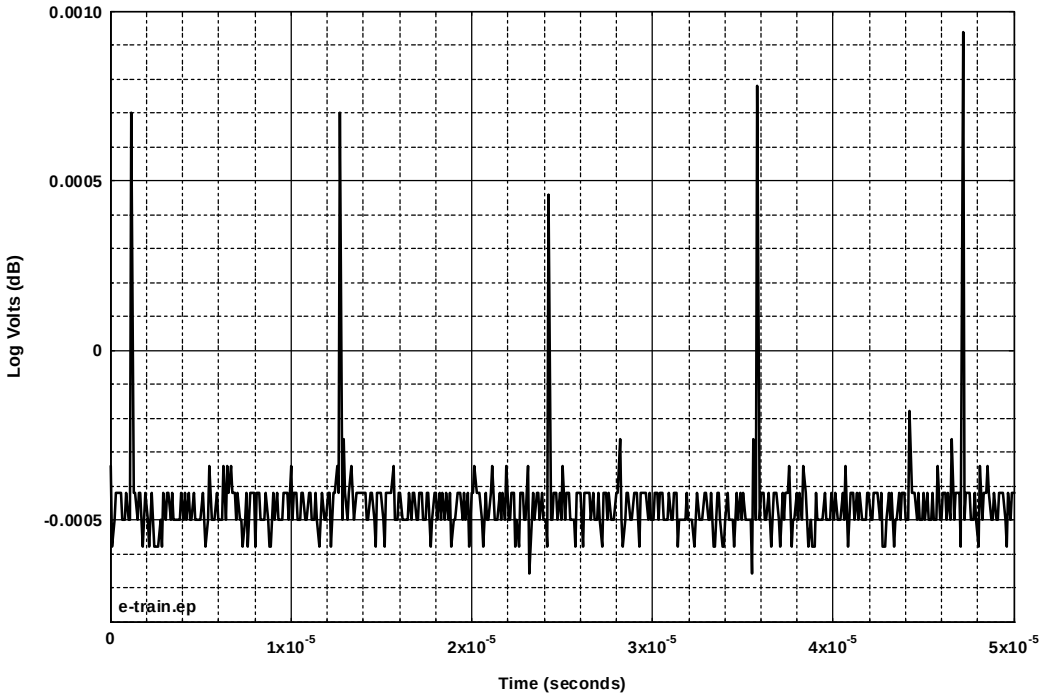

Figure D.E.11. Device E, pulse train.

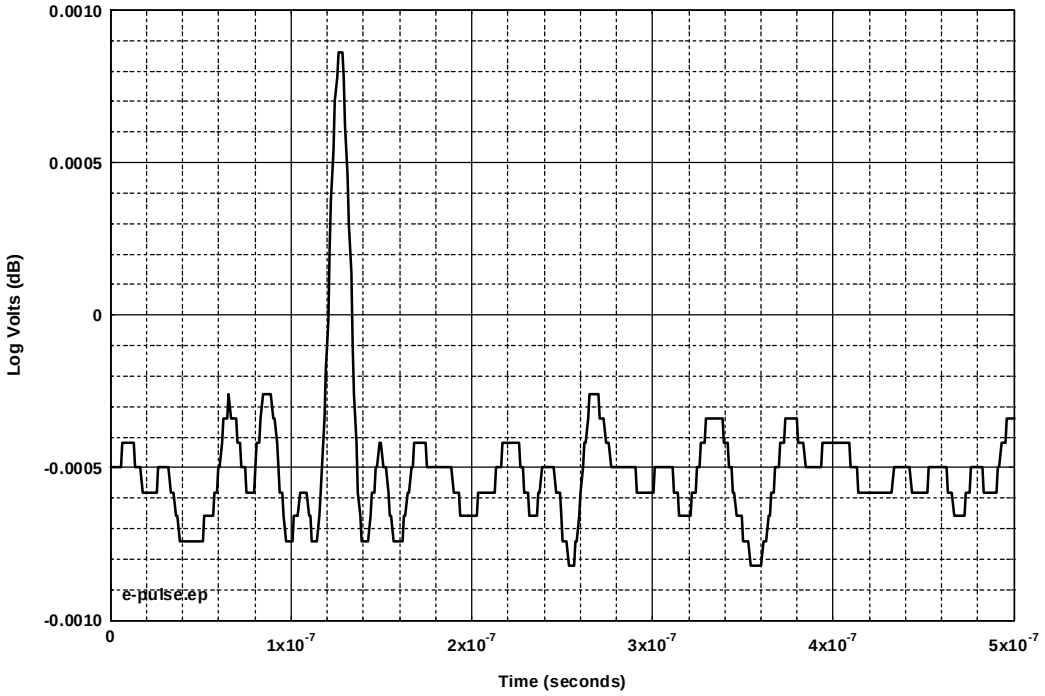

Figure D.E.12. Device E, individual pulse (bandwidth-limited at 50 MHz).

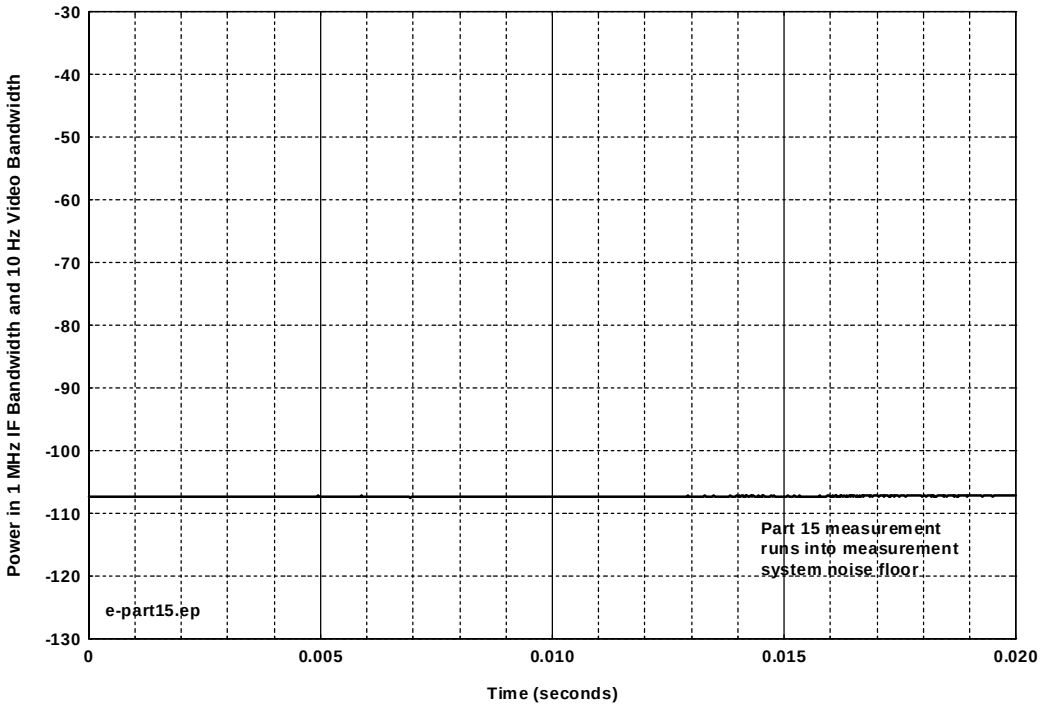

Figure D.E.13. Device E, Part 15 measurement.

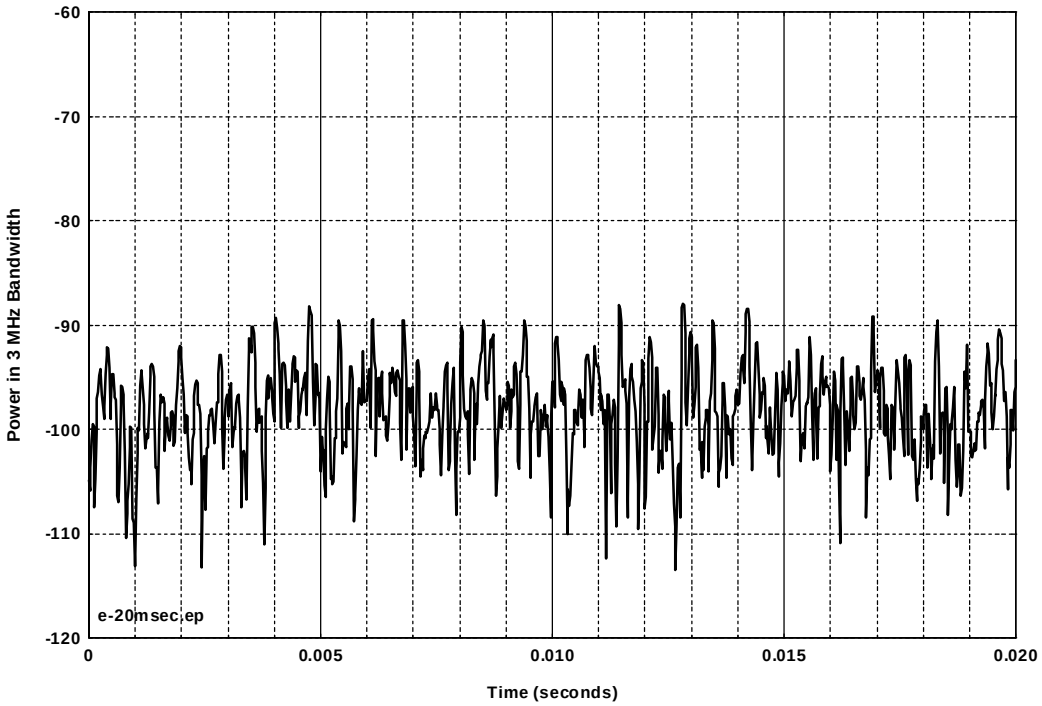

Figure D.E.14. Device E, 20-msec time waveform.

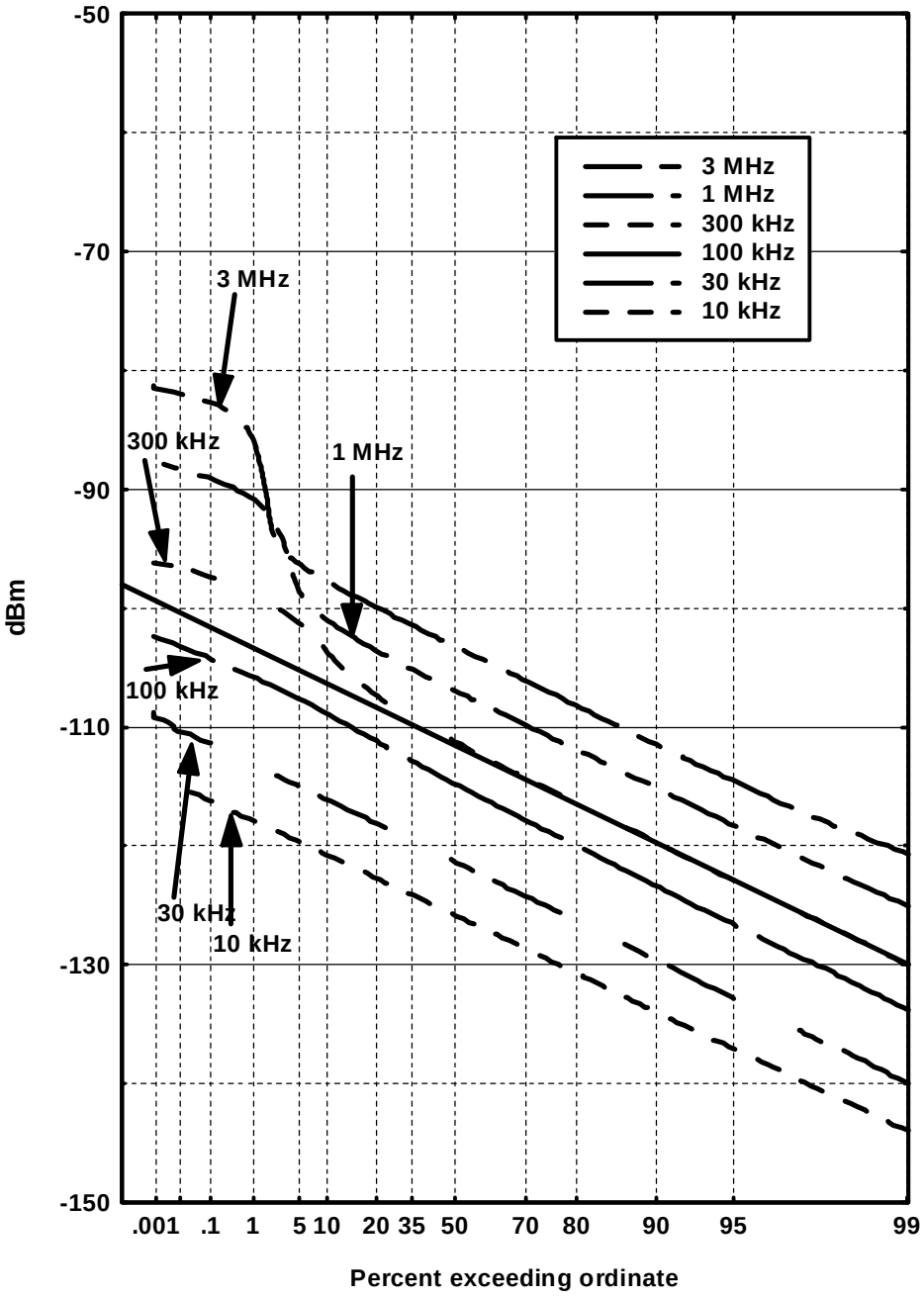

Figure D.E.15. Device E, APDs.

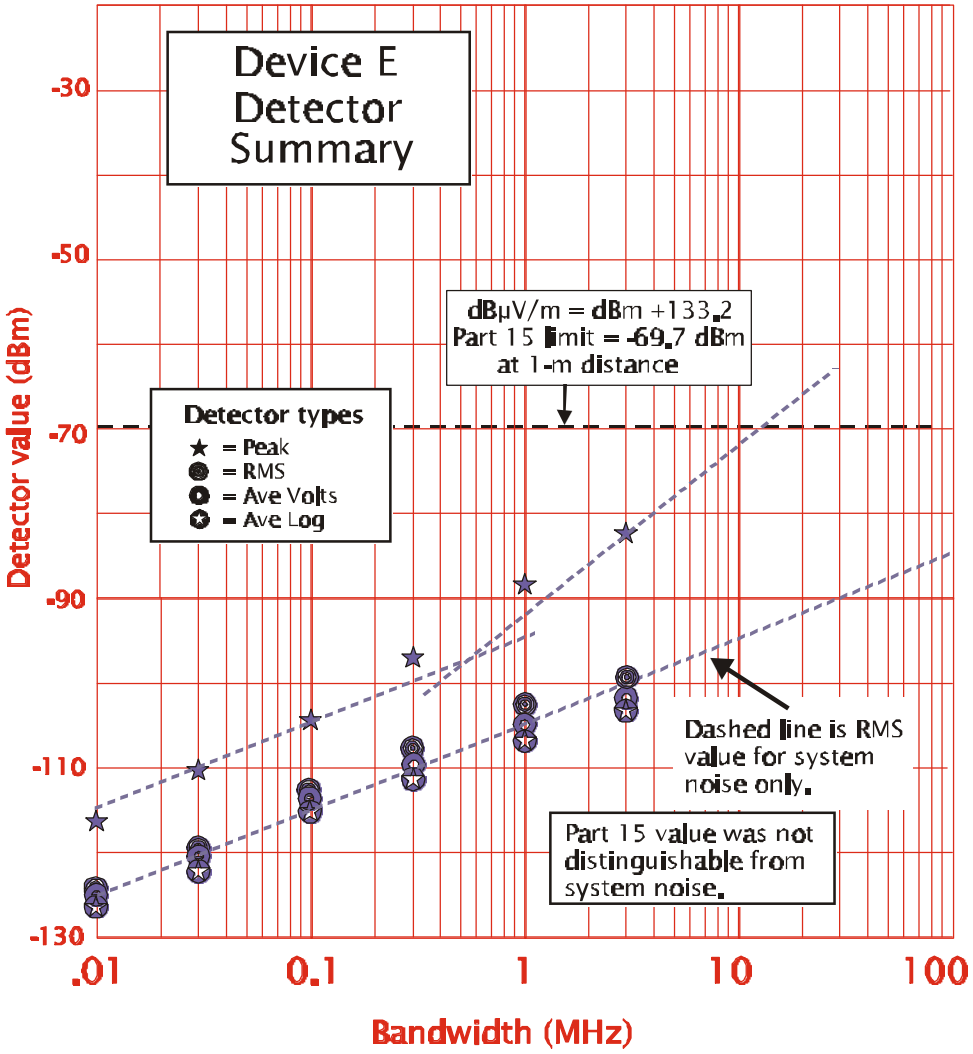

Figure D.E.16. Device E, detector summary.

This Page Intentionally Left Blank

This Page Intentionally Left Blank

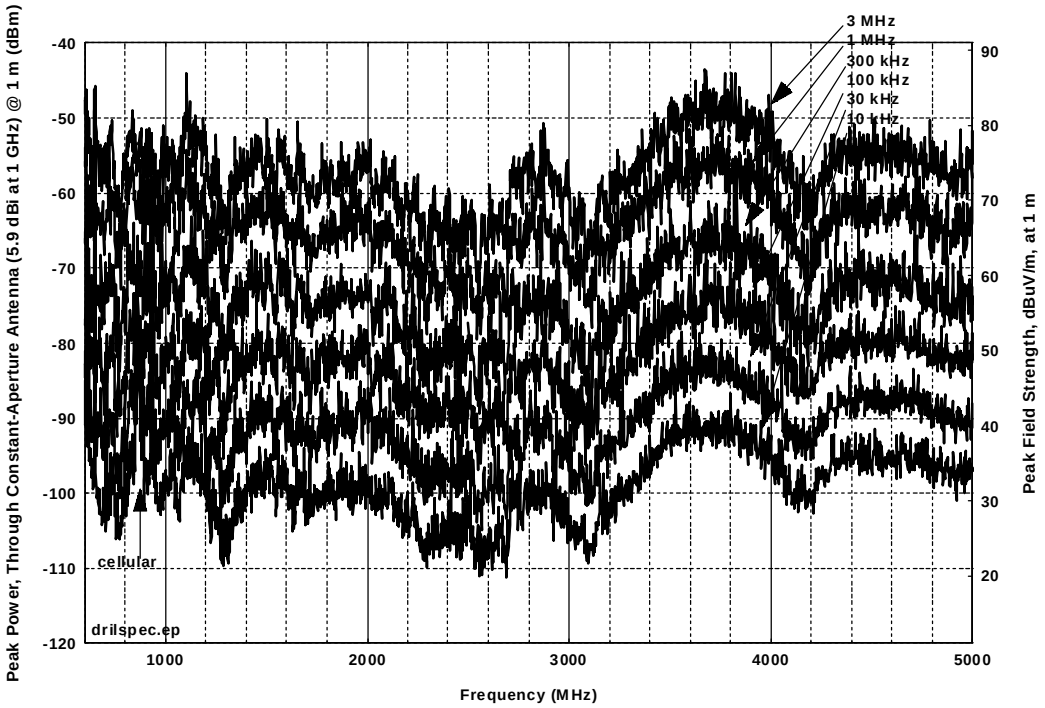

Figure D.F.1. Electric drill, emission spectrum as a function of bandwidth.

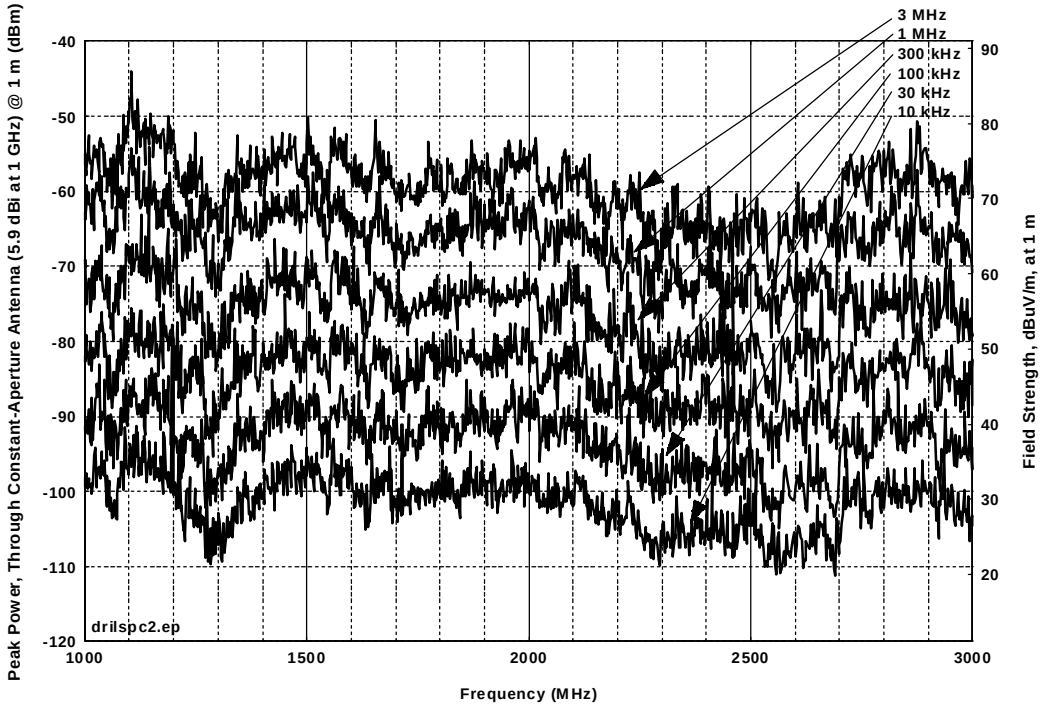

Figure D.F.2. Electric drill, emission spectrum from 1-3 GHz as a function of bandwidth.

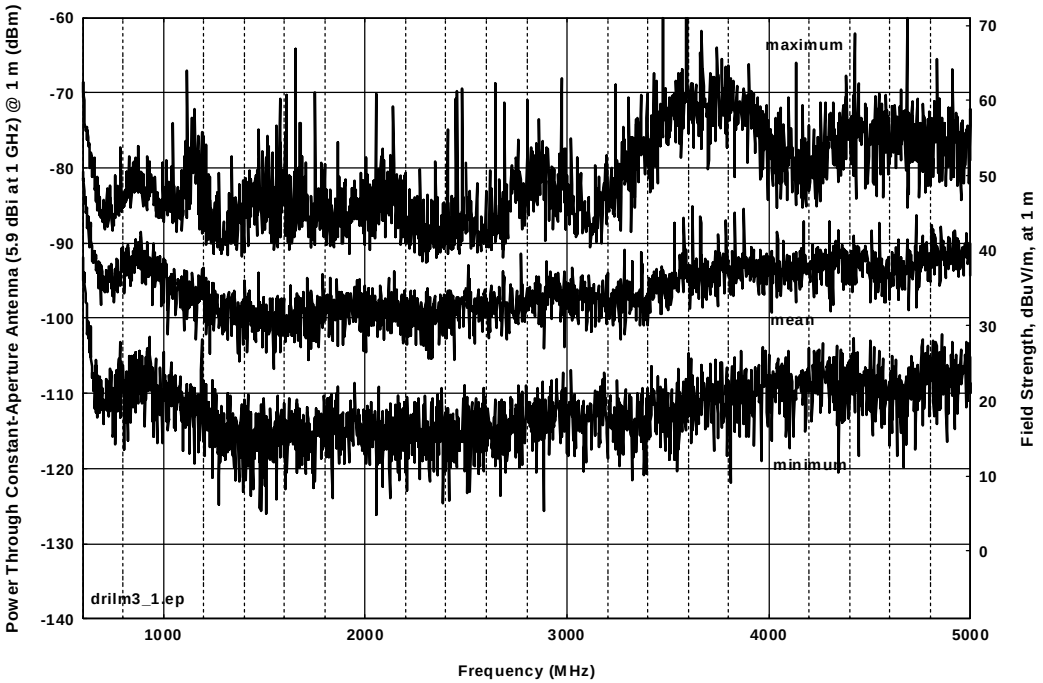

Figure D.F.3. Electric drill, sample-detected electric drill spectrum, 3 MHz bandwidth, max, mean, and min curves.

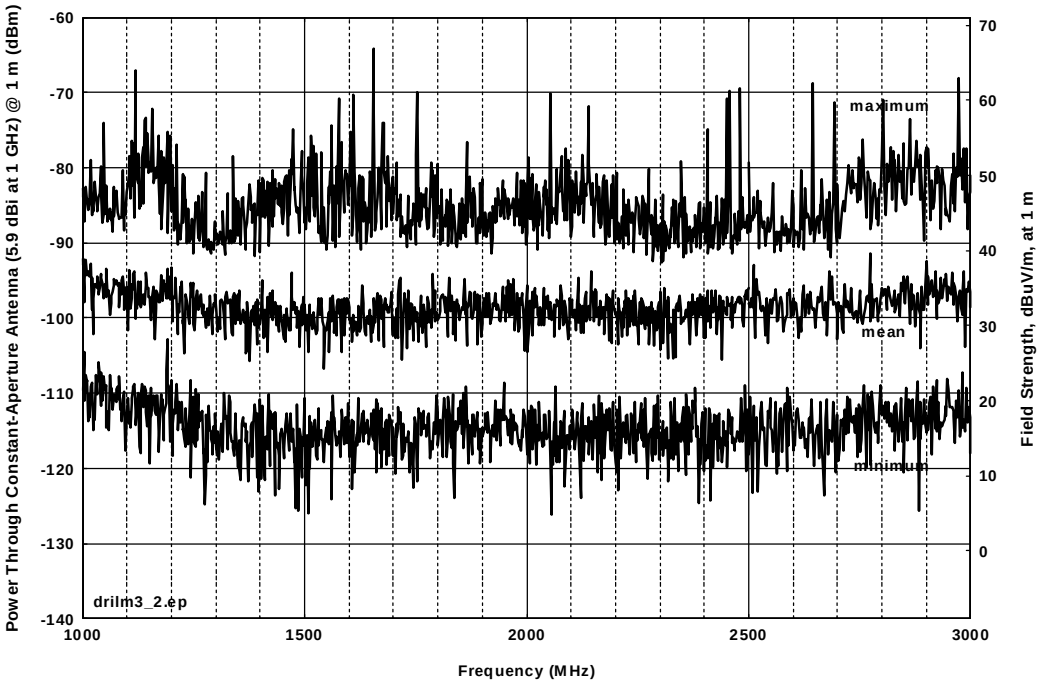

Figure D.F.4. Electric drill, sample-detected electric drill spectrum, 3 MHz bandwidth, max, mean, and min curves.

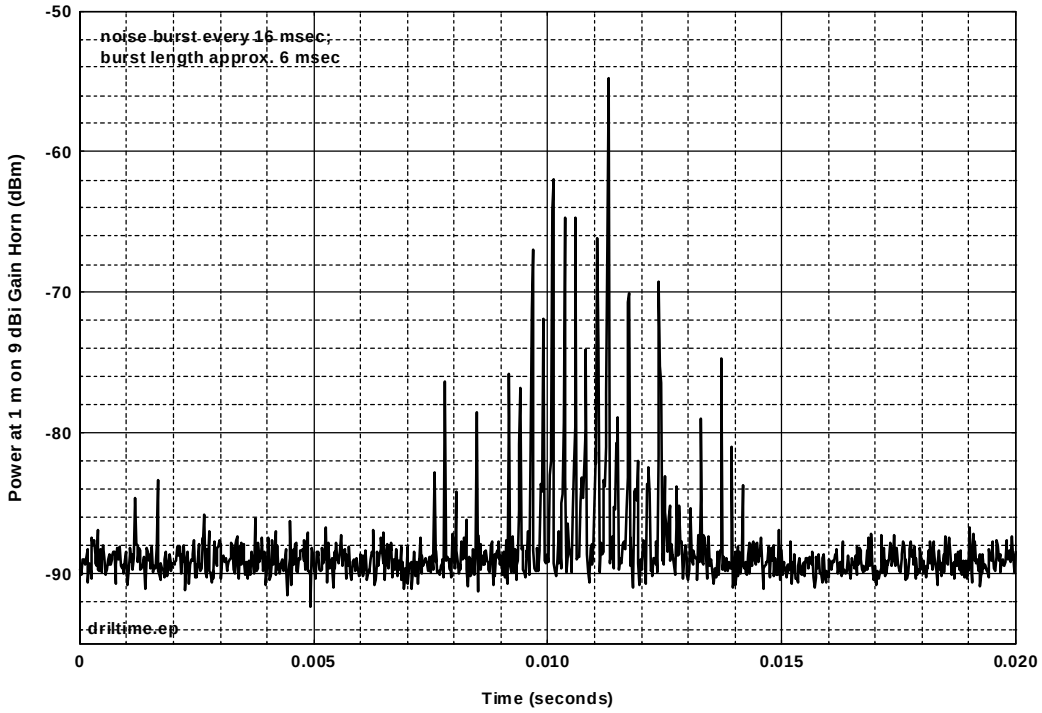

Figure D.F.5. Electric drill, time waveform in 3 MHz bandwidth, sample detected, for 20 msec.

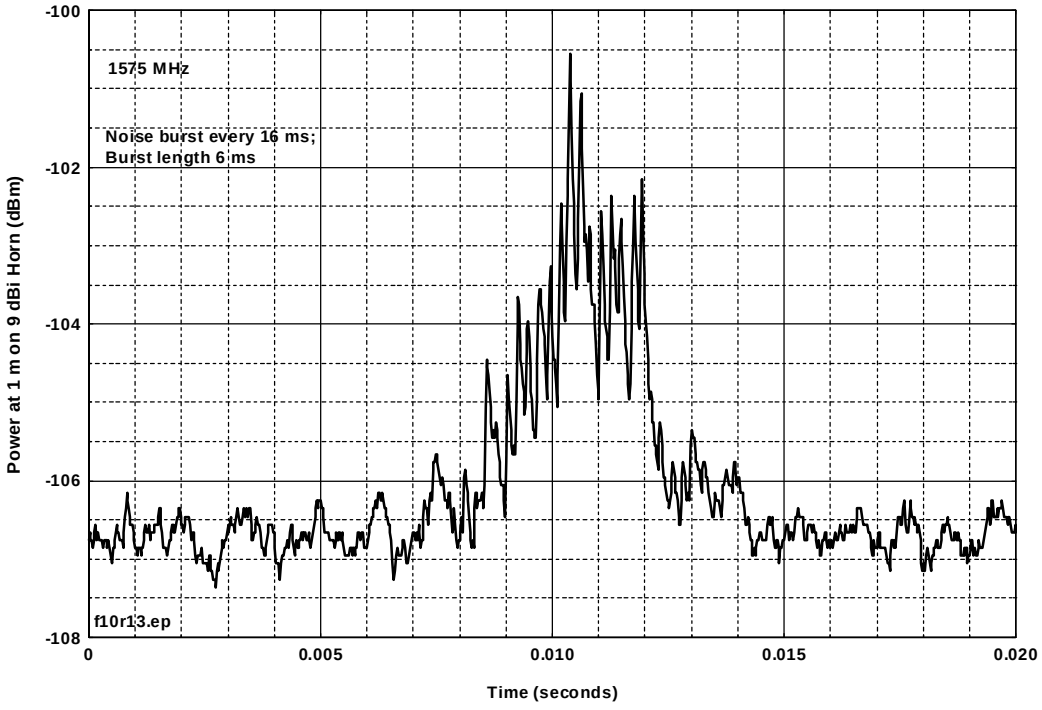

Figure D.F.6. Electric drill, Part 15 measurement, 1-MHz IF bandwidth, 1-kHz video bandwidth.

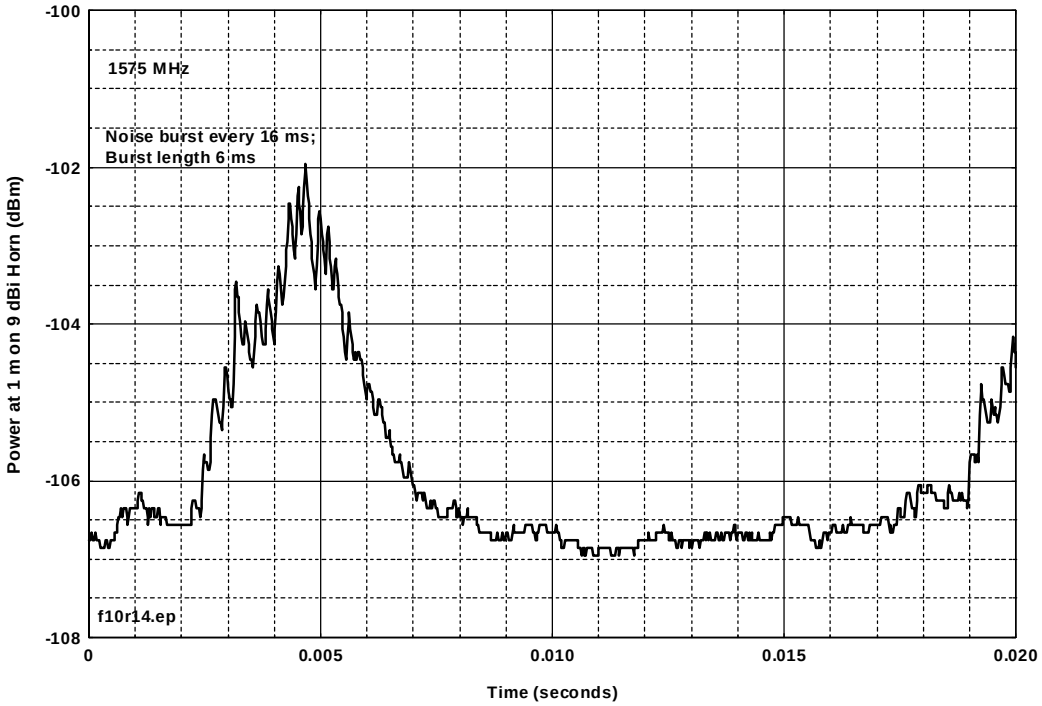

Figure D.F.7. Electric drill, Part 15 measurement, 1-MHz IF bandwidth, 300-Hz video bandwidth.

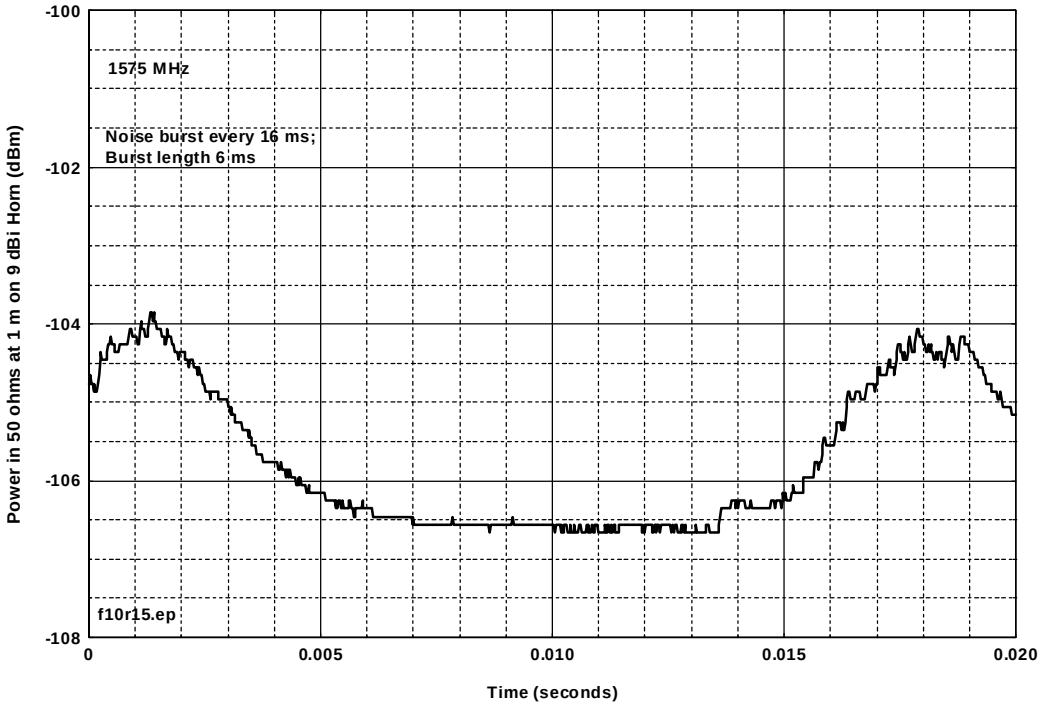

Figure D.F.8. Electric drill, Part 15 measurement, 1-MHz IF bandwidth, 100-Hz video bandwidth.

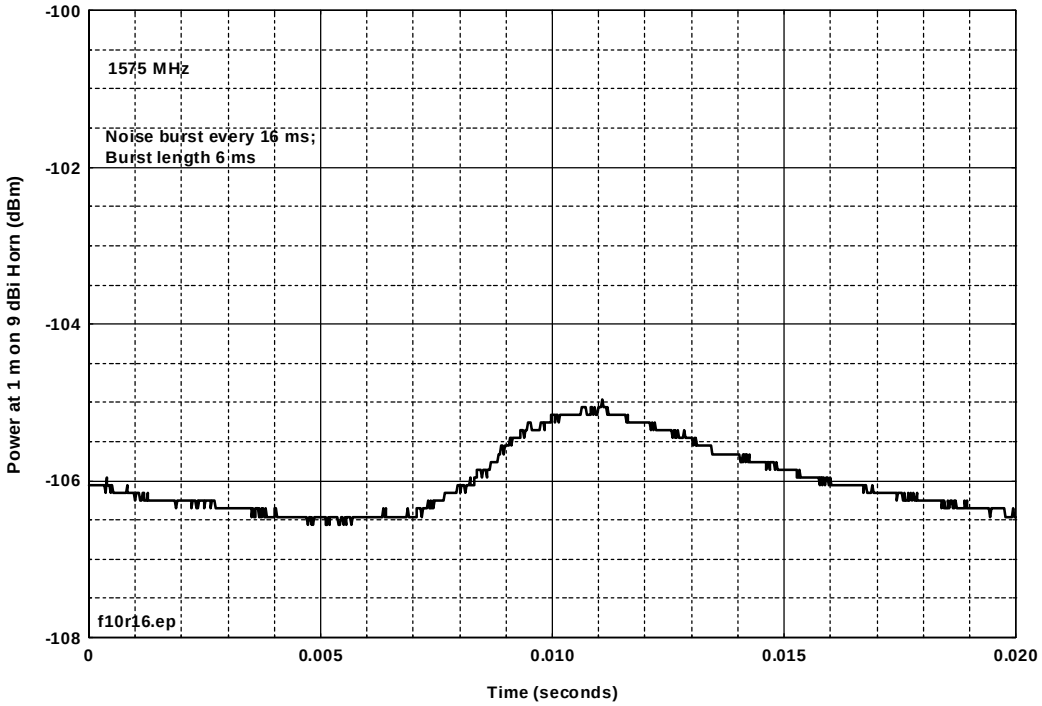

Figure D.F.9. Electric drill, Part 15 measurement, 1-MHz IF bandwidth, 30-Hz video bandwidth.

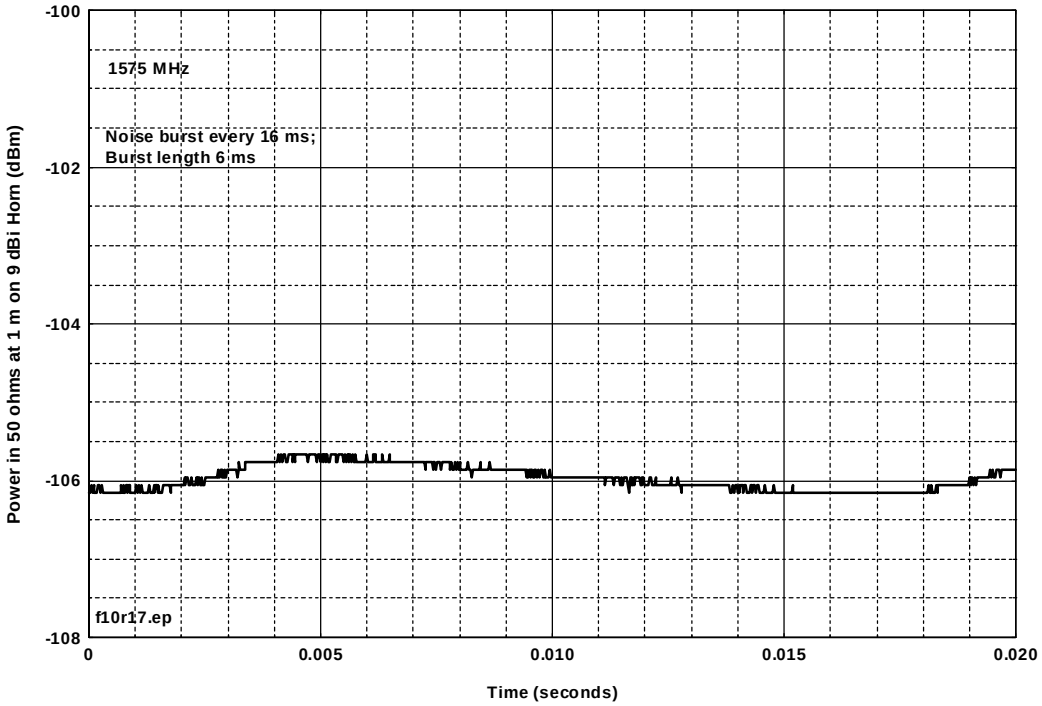

Figure D.F.10. Electric drill, Part 15 measurement, 1-MHz IF bandwidth, 10-Hz video bandwidth.

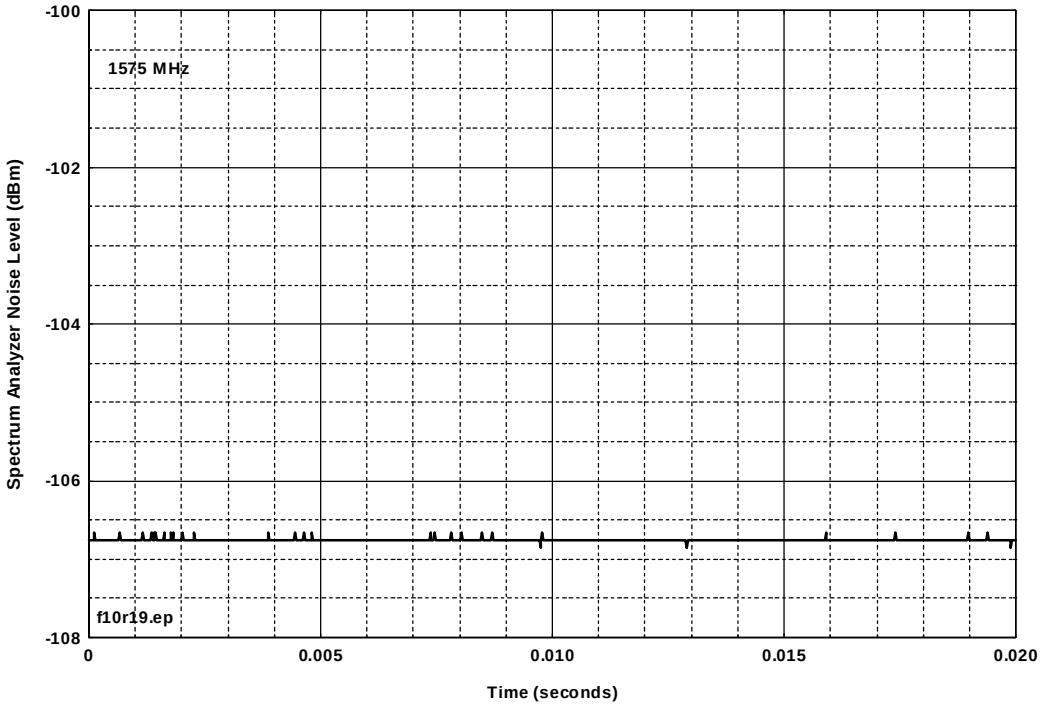

Figure D.F.11. Electric drill, terminated spectrum analyzer input with 1-MHz IF bandwidth, 10-Hz video bandwidth.

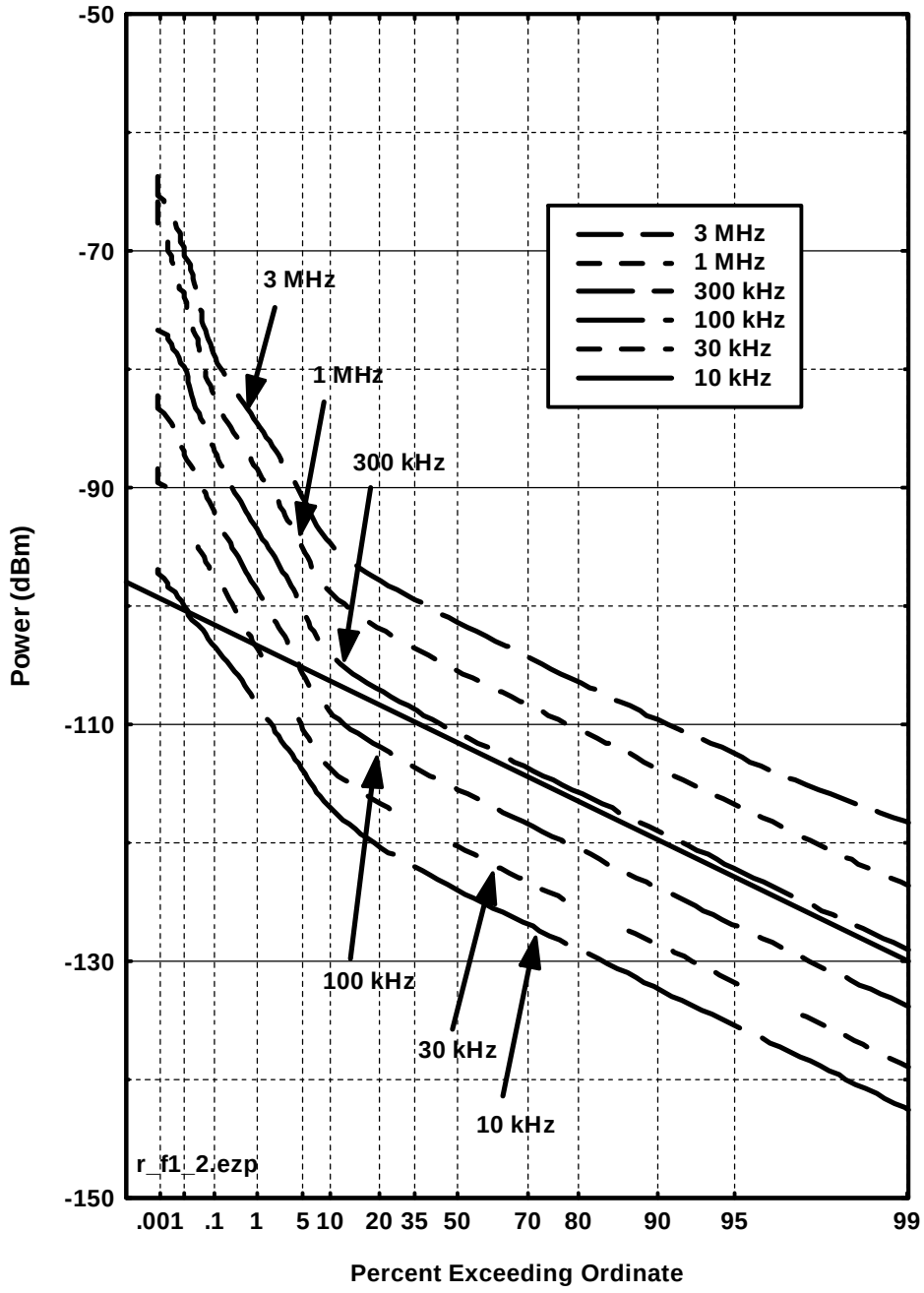

Figure D.F.12. Electric Drill, APDs.

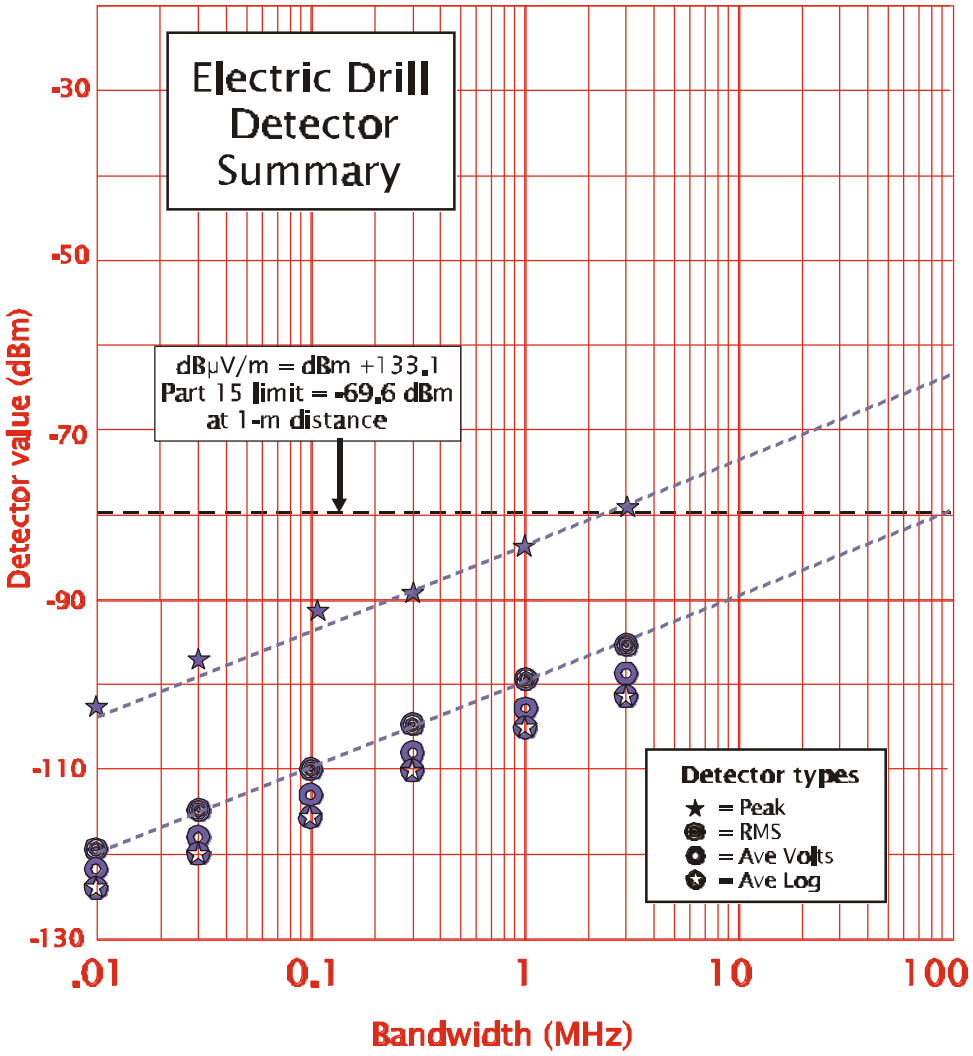

Figure D.F.13. Electric Drill, detector summary.

APPENDIX E. SUMMARY OF AGGREGATE MEASUREMENTS

Frank Sanders[1]

Device description. A pair of UWB pulsers were procured by ITS and operated for the purpose of assessing the emission levels in various IF bandwidths as a function of nominal pulse repetition rate (PRR), dither, and the number of pulsers in an aggregate. These pulsers produce UWB impulses at times precisely controlled by signals from an arbitrary waveform generator. Therefore, these pulsers can be controlled to provide a wide range of PRR, dither, and gating combinations, depending on the programming of the arbitrary waveform generators. An independent (and non-synchronized) generator was used to control each pulser.

Figure E.1 shows the measurement system used for the aggregate measurements.

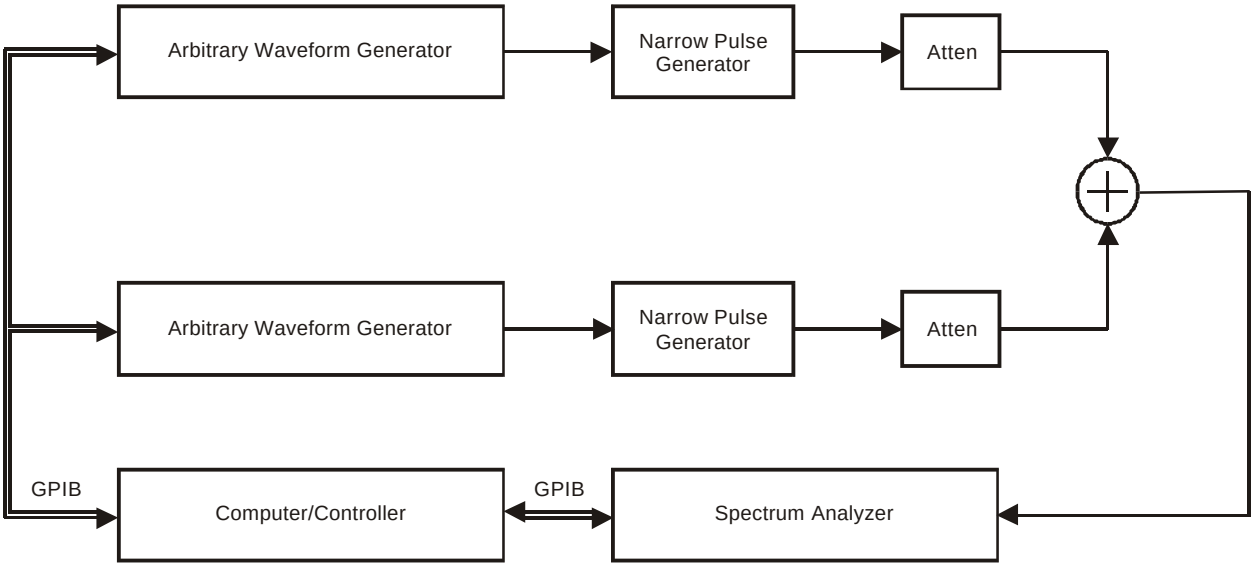

Figure E.1. Aggregate measurements block diagram.

Arbitrary waveform generators were programmed to give average PRRs of 100 kHz and 10 MHz, 50% dithered or non-dithered. This dithering is based on delay relative to a fixed time base. When both pulsers were in use, their respective wideband peak amplitudes were matched to within 0.2 dB.

---

[1]The author is with the Institute for Telecommunication Sciences, National Telecommunications and Information Administration, U.S. Department of Commerce, Boulder, CO 80305.

Measurement comments. The general technique for investigating aggregate UWB signals was to independently measure APDs from each of two UWB sources, then combine the UWB sources and measure an APD from the combined sources. This technique was followed for all of the aggregate measurements, with the only variable being the modulation parameters of two UWB signals.

Figures E.2 and E.3 show the wide range peak emission spectra of single pulsers using a 100-kHz PRR and 50% dithering, and a 10-MHz PRR and 50% dithering, respectively. Figure E.4 shows the peak bandwidth progression for a pulser with 10 MHz PRR and 50% dithering.

Figure E.5 shows video-averaged measurements for a single dithered pulser (10 MHz PRR, 50% dither) and for two such pulsers. The measured signal for two pulsers increased 2.6 dB over the level for a single pulser. This falls within the precision of the measurement for the expected 3-dB increase.

Figure E.6 shows APDs measured in a 1-MHz bandwidth for a single pulser and two pulsers. Each pulser produced a signal with10-MHz PRR and 50% dither. The APDs for the individual pulsers appeared Gaussian. The APD for the two pulsers also appeared Gaussian, but was raised about 3 dB from the individual pulser APD, as theory predicts.

Figure E.7 shows APDs measured in a 1-MHz bandwidth for a single pulser and two pulsers. Each pulser produced a non-dithered signal with 100-kHz PRR. The two-pulser APD shows a stepped high-amplitude plateau, where the lower step is equal in amplitude to the single pulser APD, but with about 1.5-2 times the percentage duration (depending on what amplitude is used to compare the duration). In addition, there is a very-small-percentage step that is about 6 dB higher than the single pulser maximum amplitude, which is consistent with impulses from the two pulsers occasionally overlapping and combining coherently.

Figure E.8 shows a 1-MHz APD that was derived from the combination of one pulser with 10-MHz PRR (dithered) and one pulser with 100-kHz PRR (non-dithered). The APD shows an approximately Gaussian character, which should be expected considering that the non-dithered 100-kHz pulser produced only 1% as many impulses as the 10-MHz dithered pulser.

Figure E.9 shows APDs measured in a 1-MHz bandwidth for a single pulser and two pulsers. Each pulser produced a signal with 100-kHz PRR and 50% dithering. Since the UWB pulses remain non-overlapping in the 1-MHz bandwidth, the resulting APDs are identical to the APDs measured in Figure E.7.

Table E.1 shows the detector values for the various APDs.

Table E.1 - Detector Values for Aggregate Tests

Figure	Source	PRR	Dither	Avg Log	Avg volt	RMS	Peak
Figure E.6	#1	10 MHz	50%	-49.2	-47.9	-46.9	-39
	#2	10 MHz	50%	-49.2	-47.9	-46.9	-39
	#1 & #2	- - -	- - -	-46.5	-45.1	-44.1	-36.5
Figure E.7	#1	100 kHz	none	-87.2	-76.6	-67.9	-54
	#2	100 kHz	none	-87.2	-76.6	-67.9	-54
	#1 & #2	- - -	- - -	-84.1	-72.1	-65.2	-49
Figure E.8	#1	10 MHz	50%	-49.2	-47.9	-46.9	-39
	#2	100 kHz	none	-87.2	-76.6	-67.9	-54
	#1 & #2	- - -	- - -	-49.2	-47.9	-46.9	-39
Figure E.9	#1	100 kHz	50%	-86.9	-76.6	-67.9	-54
	#2	100 kHz	50%	-86.9	-76.6	-67.9	-54
	#1 & #2	- - -	- - -	-84.0	-72.1	-65.2	-49

The measurement results can be summarized as follows:

1. Noise-like signals with Gaussian APD characteristics (10-MHz PRR, 50% dither) add together to give noise-like signals with Gaussian APD characteristics (Figure E.6). All detector values increased by approximately 3 dB when two equal UWB Gaussian signals were added.

2. A noise-like signal with Gaussian APD characteristics added to a weaker (20 dB weaker) impulsive signal produced a signal with a Gaussian APD characteristic (Figure E.8). The difference in detector values was not apparent, though this may have been caused by limited measurement system resolution.

3. Impulsive signals added to impulsive signals (Figures E.7 and E.8) produced APDs that were less impulsive that the original signals. Dithering of signals in an impulse environment (i.e., measurement bandwidth greater than the combined PRR) produced similar results to non-dithered signals. The combined signals produced APDs with approximately twice the total percentage pulse duration as the original pulses at the same amplitude, as well as a small percentage of pulses with amplitudes as much as 6 dB higher than the original pulses. The detector values were generally about 3 dB higher for the combined signals (except 6 dB increase for peak).

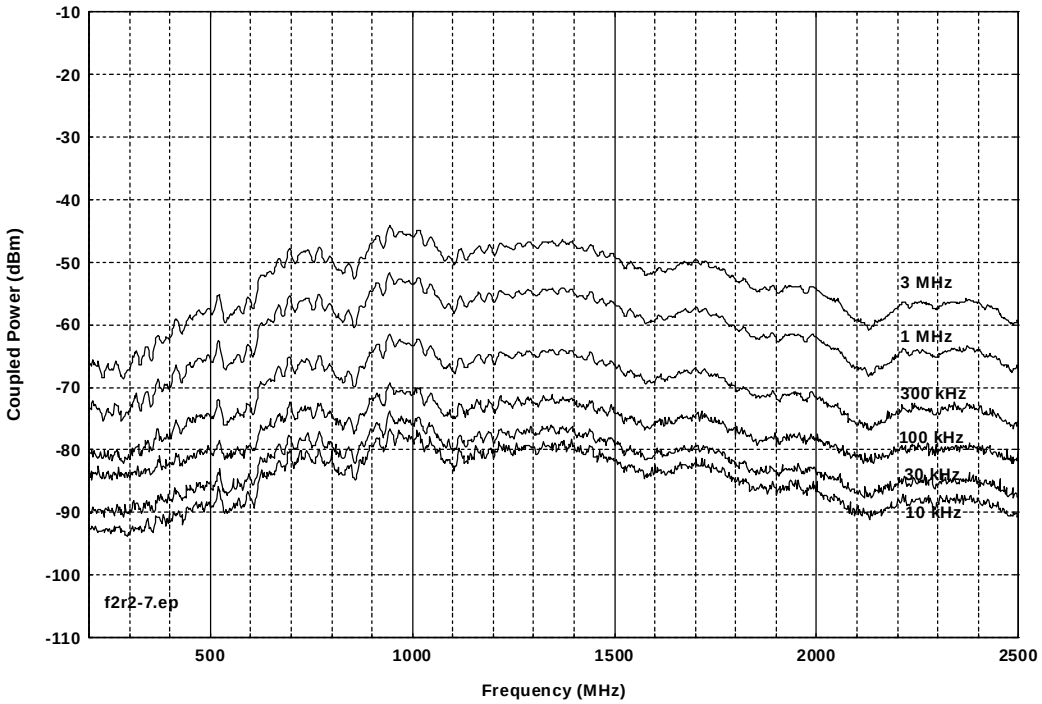

Figure E.2. Spectrum analyzer emissions spectra from 100-kHz PRR, 50% dither pulser.

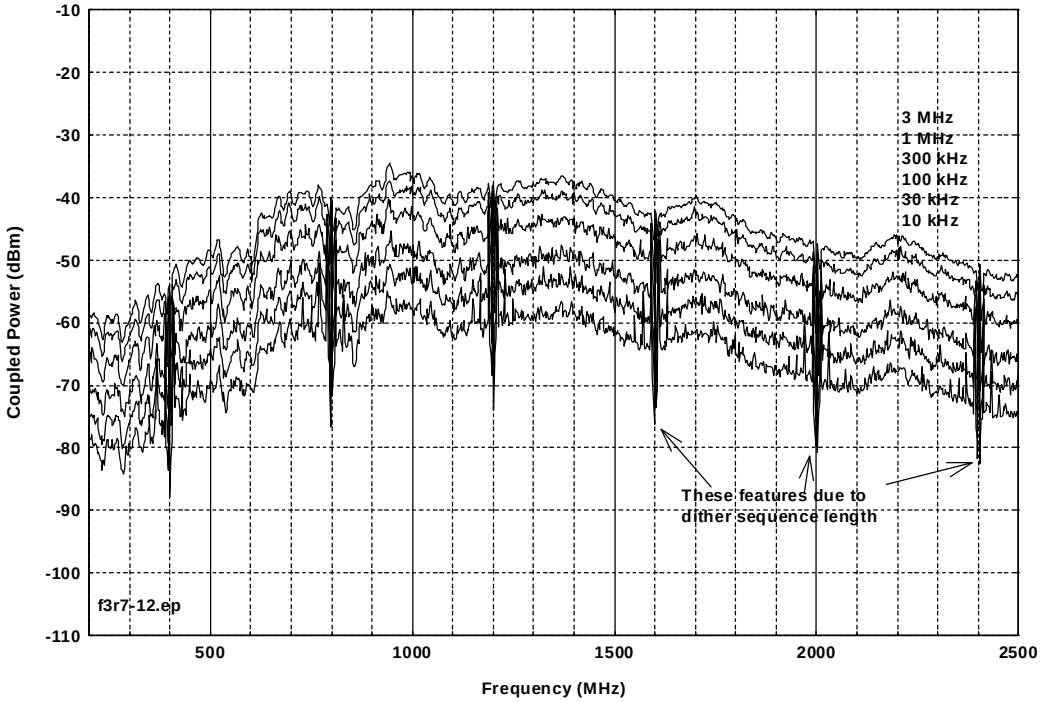

Figure E.3. Spectrum analyzer emission spectra from 10-MHz PRR, 50% dither pulser.

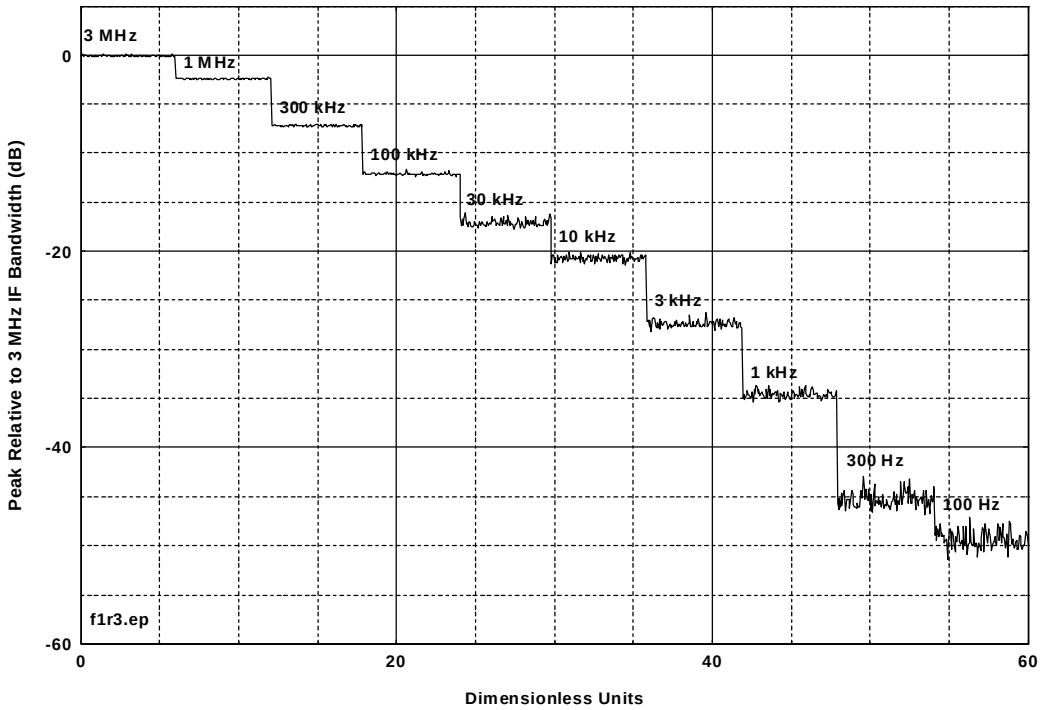

Figure E.4. Peak bandwidth progression stairstep for 10-MHz PRR, 50% dither pulser.

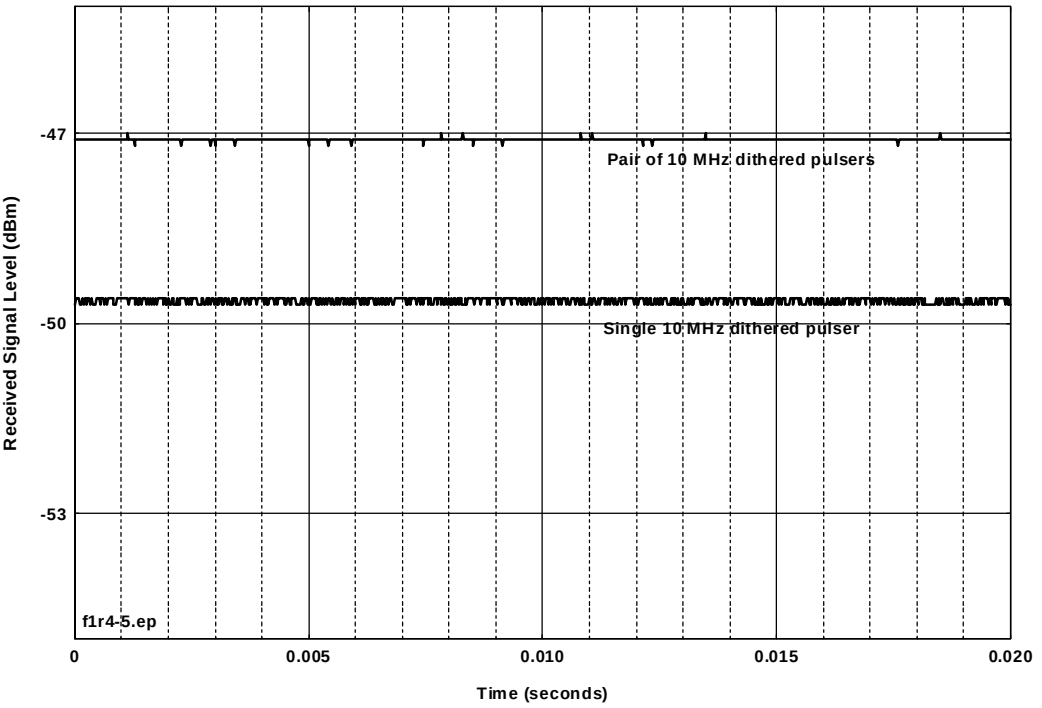

Figure E.5. Video signal from single and double pulsers, each at 10 MHz PRR, 50% dither.

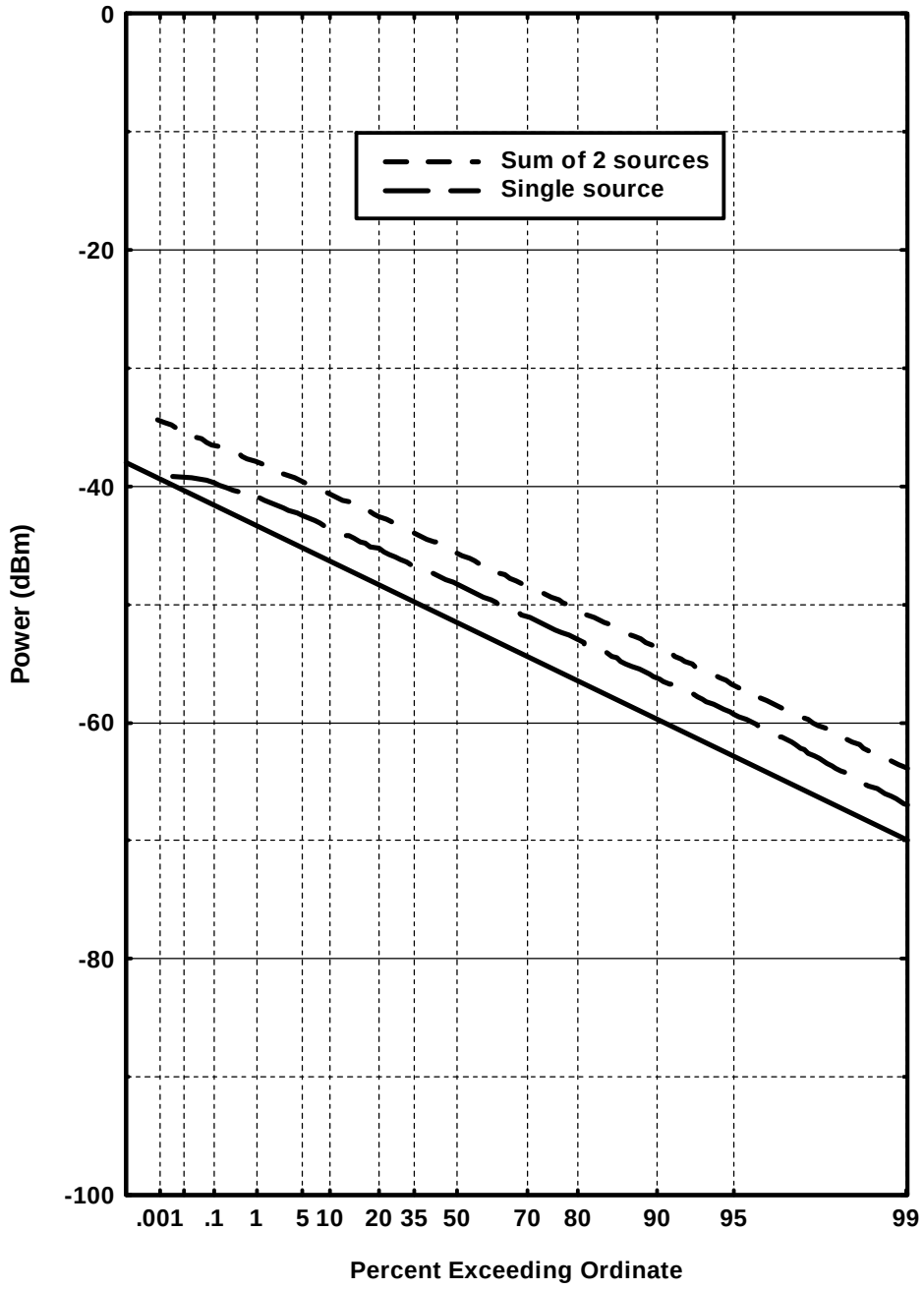

Figure E.6. 1-MHz APD for single and double 10-MHz, 50% dither pulser.

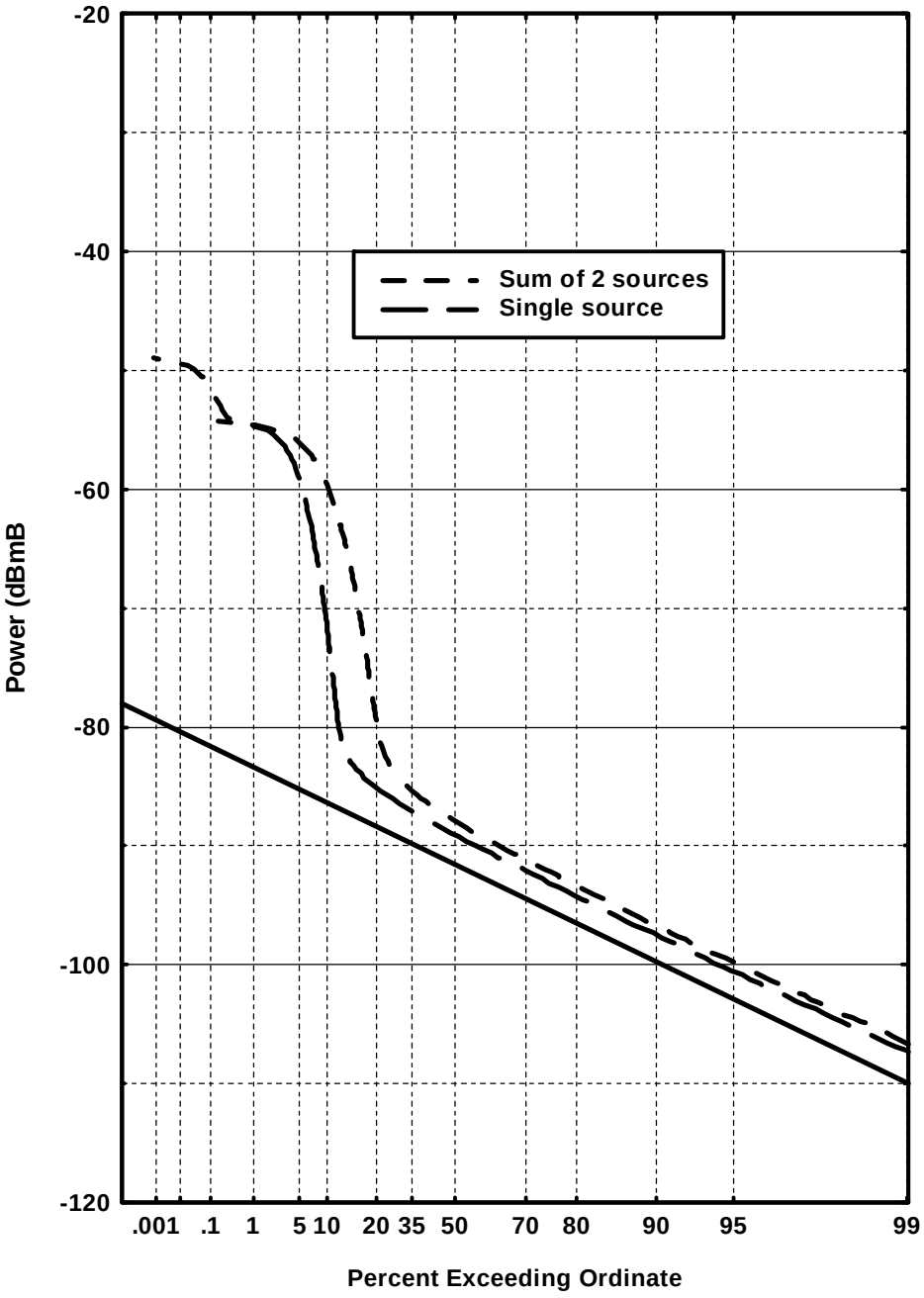

Figure E.7. 1-MHz APD for single and double 100-kHz PRR, non-dither pulsers.

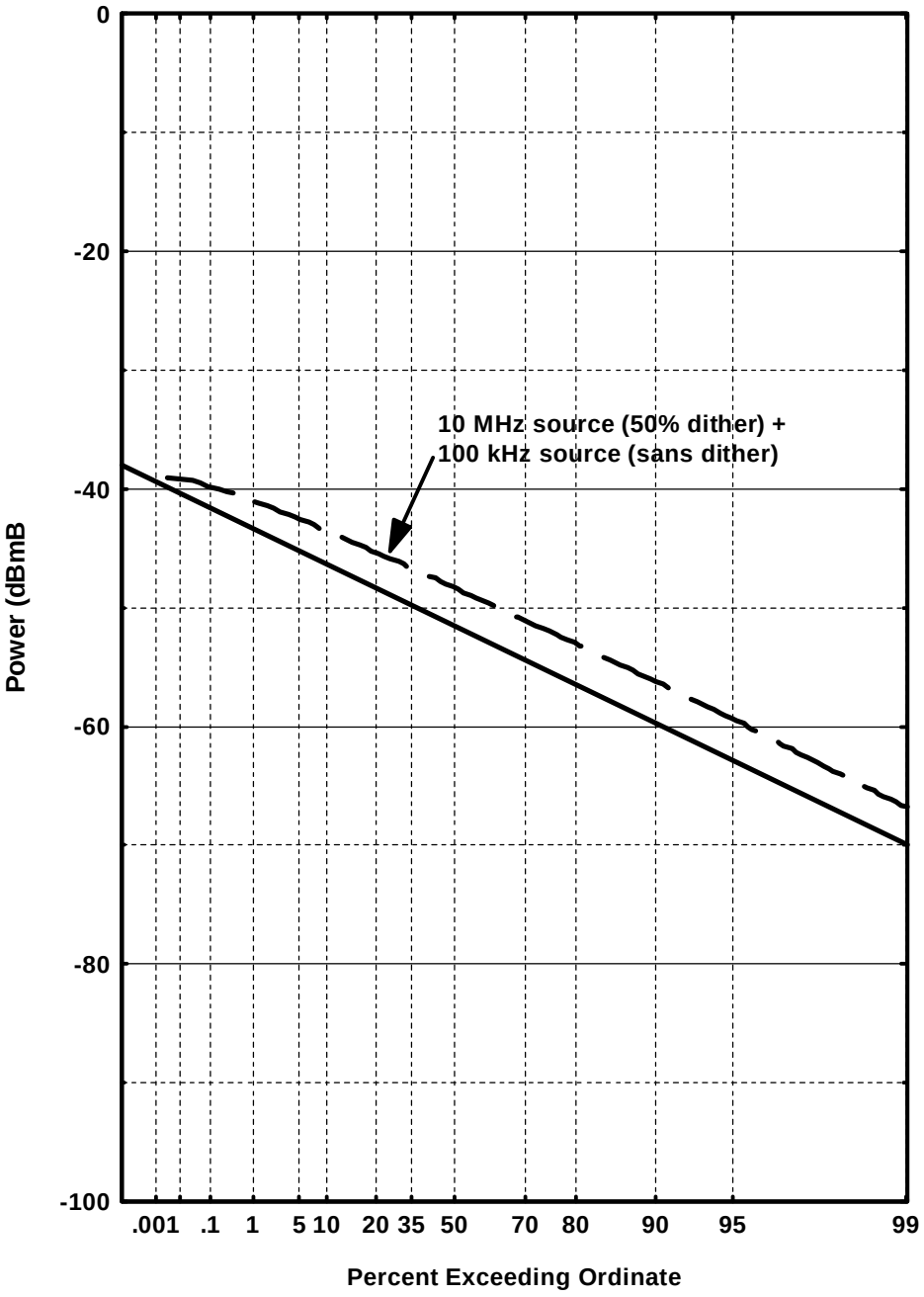

Figure E.8. 1-MHz APD for a 10-MHz PRR, 50% dither pulser and a 100-kHz, non-dithered pulser.

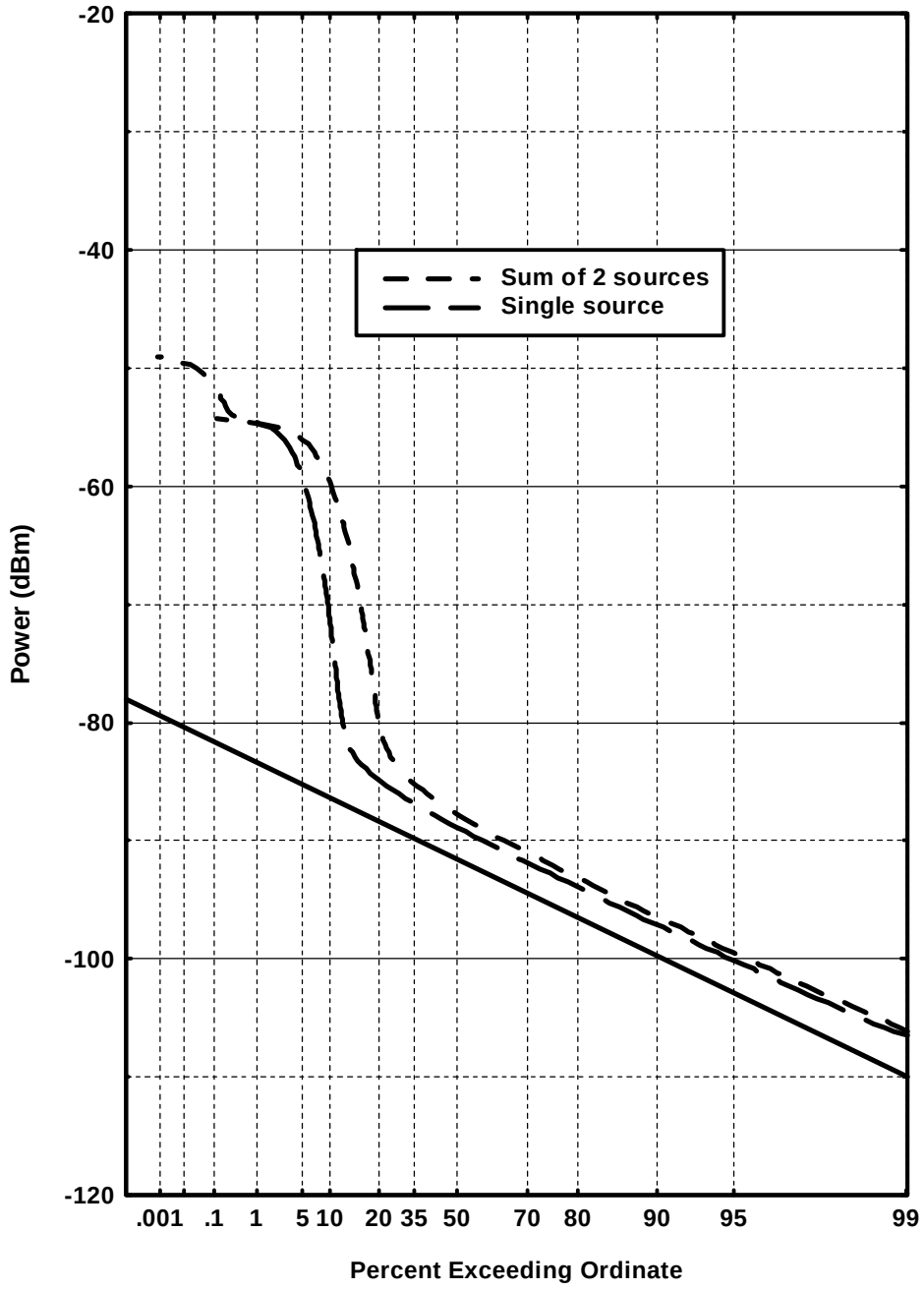

Figure E.9. 1-MHz APDs for single and double 100-kHz PRR 50% dithered pulsers.